INVESTIGATING THE ROLES OF DISTINCT MACROPHAGE PHENOTYPES IN CARDIOVASCULAR DISEASE

Caitlin Vanessa Lewis

Bachelor of Biomedical Science (Honours)

A thesis submitted for the degree of *Doctor of Philosophy* at

Monash University in 2017

Cardiovascular Disease Program, Biomedicine Discovery Institute,

Department of Pharmacology

Table of Contents

COPYRIGHT NOTICE **5**

SUMMARY **6**

GENERAL DECLARATION **8**

ACKNOWLEDGEMENTS **10**

PUBLICATIONS FROM PHD CANDIDATURE **12**

LIST OF ABBREVIATIONS **14**

CHAPTER 1: **20**

GENERAL INTRODUCTION **20**

1.1 Introduction ***21***

1.2 Macrophage biology ***22***

1.2.1 Macrophage origin *22*

1.2.2 Monocyte heterogeneity *23*

1.2.2.1 Functions of monocyte subsets *26*

1.2.2.2 Monocyte differentiation *27*

1.2.3 Macrophage subset activation and function *28*

1.2.3.1 M1 macrophages *30*

1.2.3.2 M2 macrophages *31*

1.2.3.3 Current limitations of macrophage markers *36*

1.2.4 NADPH oxidases and reactive oxygen species in M1 and M2 function *36*

1.2.4.1 Superoxide dismutase isoforms *40*

1.3 Macrophage polarisation in cardiovascular disease ***42***

1.3.1 Obesity and Diabetes *43*

1.3.2 Atherosclerosis *45*

1.3.2.1 Macrophage phenotypes in atherosclerotic plaques *48*

1.3.2.2 Differential roles for IL-4 and IL-13 in atherosclerosis *49*

1.3.2.3 The Apolipoprotein E-deficient ($ApoE^{-/-}$) mouse model of atherosclerosis *56*

1.3.3 Hypertension *57*

1.3.3.1 Pro-fibrotic processes in the vessel wall *60*

1.3.3.2 Pro-fibrotic actions of M2 macrophages *63*

1.3.3.3 M2 macrophage-derived ROS in the pro-fibrotic response *63*

1.3.3.4 CCL18 as a potential M2 macrophage-derived mediator of aortic stiffening *64*

1.3.3.5 Angiotensin II model of hypertension *66*

1.4 Conclusions and therapeutic implications ***68***

1.5 Hypothesis and aims of thesis ***69***

References ***70***

CHAPTER 2: **103**

GENERAL METHODS **103**

2.1 Animals ***104***

2.2 Models of cardiovascular disease ***104***

2.2.1 Angiotensin II infusion model of hypertension in mice *104*

2.2.1.1 Tail-cuff plethysmography *105*

2.2.2 ApoE$^{-/-}$ model of atherosclerosis in mice *106*

2.3 Cell culture ***106***

2.3.1 THP-1 monocytes *106*

2.3.1.1 Differentiation of THP-1 cells into macrophages and treatment with M1 or M2 polarising stimuli *107*

2.3.1.2 siRNA knockdown of NOX2 in THP-1 macrophages *107*

2.3.2 Human primary macrophages from donor blood *108*

2.3.2.1 Treatment with M1 or M2 polarising stimuli *111*

2.3.2.2 IL-4 and IL-13 concentration response curves and treatment in the presence of signalling inhibitors *111*

2.3.2.3 Treatment of unpolarised or M2-polarised macrophages with angiotensin II *112*

2.3.3 Human aortic adventitial fibroblasts *113*

2.3.3.1 Hydrogen Peroxide treatment *113*

2.3.3.2 Co-culture with polarised THP-1 macrophages *113*

2.3.3.3 CCL18 treatment *114*

2.3.4 Human cardiac fibroblasts *114*

2.4 Assessment of gene expression ***115***

2.4.1 RNA extraction from cell culture lysates *115*

2.4.2 RNA extraction from aortae *115*

2.4.3 cDNA conversion and RT-PCR *116*

2.5 Assessment of protein expression ***117***

2.6 Detection of reactive oxygen species ***118***

2.6.1 Superoxide detection via L-012-enhanced chemiluminescence *118*

2.6.2 Hydrogen peroxide detection via Amplex Red assay *119*

2.6.3 DCF ROS detection via Flow cytometry *120*

2.7 Quantification of CCL18 secreted into culture media via ELISA ***120***

2.8 Quantification of MMP-2 and MMP-9 secreted into culture media via gelatin zymography ***122***

2.9 Immunohistochemistry ***123***

2.9.1 Localisation of M2 macrophages, CCR8 and CCL8 in thoracic aortae from normotensive vs angiotensin II-treated hypertensive mice *123*

2.9.2 Detection and localisation of F4/80 and IFIT1 in the aortic sinus and brachiocephalic arteries ApoE-/- mice *124*

2.10 Statistical Analysis ***124***

References ***126***

CHAPTER 3: **128**

PROTEOMIC IDENTIFICATION OF INTERFERON-INDUCED PROTEINS WITH TETRATRICOPEPTIDE REPEATS (IFITs) AS MARKERS OF M1 MACROPHAGE POLARIZATION **128**

Abstract ***130***

Introduction ***131***

Materials and Methods ***133***

Results ***141***

Discussion ***146***

References ***151***

Figures and tables ***158***

CHAPTER 4: **174**

M1 AND M2 MACROPHAGE PHENOTYPES ARE ASSOCIATED WITH DISTINCT REDOX SIGNALLING: IMPACTS ON FIBROSIS **174**

Abstract ***176***

Introduction ***177***

Materials and Methods ***180***

Results ***187***

Figures ***192***

Discussion ***202***

References ***210***

CHAPTER 5: **220**

THE ROLE OF IL-4 AND IL-13 IN THE MODULATION OF MACROPHAGE PHENOTYPE AND REACTIVE OXYGEN SPECIES GENERATION **220**

Abstract ***224***

Introduction ***225***

Materials and Methods *229*
Results *234*
Figures and tables *238*
Discussion *250*
References *258*
CHAPTER 6: **267**
CCL18 AS A POTENTIAL MEDIATOR OF THE PRO-FIBROTIC ACTIONS OF M2 MACROPHAGES IN THE VESSEL WALL DURING HYPERTENSION **267**
Abstract *269*
Introduction *270*
Materials and Methods *273*
Results *279*
Figures *283*
Discussion *291*
References *299*
CHAPTER 7: **306**
GENERAL DISCUSSION **306**
7.1 Summary of key findings ***307***
7.2 Identifying M1 and M2 macrophages in disease settings ***308***
7.3 M2 macrophages: friend or foe? ***311***
7.3.1 Oxidative stress and inflammation *312*
7.3.2 Roles in atherosclerosis *315*
7.3.3 Roles in hypertension and aortic fibrosis *319*
7.4 Limitations and future directions ***322***
7.5 Conclusions and therapeutic implications ***325***
References *326*

SUMMARY

Macrophages are central to the pathophysiology of hypertension and atherosclerosis and exist in a multitude of phenotypes dependent on local micro-environmental cues. Pro-inflammatory M1, and reparative M2 macrophages, are at opposite ends of a phenotypic spectrum. Given the potential anti-inflammatory properties of M2 macrophages, in contrast to M1 macrophages, studies propose that promoting M2 polarisation is protective. However, M2 macrophages are reported to display some atherogenic actions and to promote aortic fibrosis. Identifying the macrophage-derived effector molecules implicated in disease, rather than attempting to skew towards a particular macrophage phenotype, represents a more targeted approach to modulate macrophage function in cardiovascular pathologies.

Despite a large body of research exploring macrophage phenotypes, there remains a lack of robust markers to distinguish them, particularly *in vivo.* In **Chapter 3** we characterised the global proteomes of M1 and M2 macrophages and identified a large number of differentially regulated proteins. In particular, we reported upregulation of a family of anti-viral proteins, interferon-induced proteins with tetratricopeptide repeats (IFITs), in M1 macrophages, and validated the use of IFIT1 as an M1 marker *in vivo,* identifying its expression in atherosclerotic plaque macrophages of $ApoE^{-/-}$ mice.

To further characterise M1 and M2 macrophage phenotypes, we sought to compare the nature and levels of reactive oxygen species (ROS) they produce. Although ROS generation is widely recognised as a function of M1 macrophages, in **Chapter 4**, we identified robust superoxide and hydrogen peroxide generation in M2 macrophages polarised with IL-4. Furthermore, we revealed that M2 macrophage-derived hydrogen peroxide can target aortic fibroblasts to promote fibrosis, suggesting it may contribute to the pro-fibrotic actions of M2

macrophages in the vessel wall. Given these findings, it was tempting to speculate that enhanced ROS generation from IL-4-polarised macrophages may also explain the atherogenic role reported for IL-4, in contrast to the atheroprotective effects observed with IL-13. Therefore in **Chapter 5** we compared the ROS generating capacities, and M2 phenotypes, induced by IL-4 and IL-13, yet did not detect any major differences in their effects on macrophage function. Rather the opposing roles of IL-4 and IL-13 in atherosclerosis, may reflect their ability to modulate other vascular cell types

As our lab has recently identified a crucial role for M2 macrophages in aortic stiffening during hypertension, we wanted to investigate the potential mechanisms underlying these effects. In **Chapter 6**, the role of the M2 macrophage-derived pro-fibrotic chemokine, CCL18, in vascular fibrosis was explored. We found that its expression in the aorta was localised to M2 macrophages and enhanced in hypertensive mice and that the chemokine could promote fibrosis *in vitro*. Given we also identified the expression of its receptor, CCR8, in the vessel wall, we propose that the CCL18-CCR8 axis could be targeted to limit aortic stiffening and the major cardiovascular events associated with chronic hypertension.

In conclusion, this thesis has advanced our understanding of M1 and M2 macrophage function, contributing to the growing characterisation of macrophage polarisation in cardiovascular disease. We highlight the importance of the polarising stimulus in dictating the potential protective or pathogenic properties of macrophages and suggest advantages of targeting their effector molecules over altering the macrophage phenotype *per se*. We reveal that hydrogen peroxide and CCL18 may mediate the pro-fibrotic effects of M2 macrophages in the vessel wall during hypertension, and could be explored as therapeutic targets in the future.

GENERAL DECLARATION

In accordance with Monash University Doctorate Regulation 17.2 Doctor of Philosophy Research Master's regulations the following declarations are made:

I hereby declare that this thesis contains no material which has been accepted for the award of any other degree or diploma at any university or equivalent institution and that, to the best of my knowledge and belief, this thesis contains no material previously published or written by another person, except where due reference is made in the text of the thesis.

This thesis includes 1 submitted publication and 3 unpublished publications. The core theme of the thesis is "Investigating the distinct roles of macrophage phenotypes in cardiovascular disease". The ideas, development and writing up of all the papers in the thesis were the principal responsibility of myself, the student, working within the Department of Pharmacology under the supervision of Dr Barbara Kemp-Harper (main supervisor) and Professor Grant Drummond (co-supervisor). (The inclusion of co-authors reflects the fact that the work came from active collaboration between researchers and acknowledges input into team-based research.)

Chapter 3 has been submitted to the Journal of Proteome Research and Mr Cheng Huang (Monash Student) and I made equal contributions to this work (co-first authors, 40% contribution each). It provides a global proteomic characterization of distinct macrophage phenotypes, which are then explored further in Chapters 4-6 and was hence included in this thesis. In terms of contributions, I performed the immunohistochemistry, cell culture and PCR experiments, whilst Mr Cheng Huang performed the proteomics experiments. We both analysed data, prepared figures, and contributed to the design of the experiments and drafting of the manuscript. This was performed under the guidance of our supervisors, Associate Professor Martin Stone (5% contribution) and Dr Barbara Kemp-Harper (5% contribution). Some PCR experiments were performed by Ms Mingyu Zhu (<1% contribution; Monash Student) and the animal tissue was provided by Mr Henry Diep (<1% contribution). A number of additional authors provided intellectual advice and technical assistance. These authors together make up the remaining ~10% and are, in no particular order: Dr Natalie Borg,

Dr Meritxell Canals, Dr Robert Goode, Dr Ralf Schittenhelm, Dr Antony Vinh, Professor Grant Drummond and Dr Oded Kleifeld.

I have renumbered sections of submitted or published papers in order to generate a consistent presentation within the thesis.

Student signature: [redacted] **Date: 28/11/17**

The undersigned hereby certify that the above declaration correctly reflects the nature and extent of the student's and co-authors' contributions to this work. In instances where I am not the responsible author I have consulted with the responsible author to agree on the respective contributions of the authors.

Main Supervisor signature: [redacted] **Date: 28/11/17**

ACKNOWLEDGEMENTS

There are many people I would like to express my sincere thanks to for the contributions and support they have provided to make the completion of this thesis possible.

Most importantly, I would like to thank my supervisor, Dr Barbara Kemp-Harper for her endless encouragement and support over the last 6 years. From my third year project to now, you have always made time for me despite an increasingly busy schedule and your enthusiasm and confidence in me has never failed to raise my spirits. You have been a huge inspiration to me both as a scientist and as a person and I look forward to staying in touch for many years to come. I will forever be grateful for your guidance over these years and for making this chapter of my life such a fulfilling and enjoyable one. I have been incredibly lucky to have you as my supervisor. I would also like to extend my gratitude to my co-supervisor Prof Grant Drummond who has been another infinite source of inspiration. Your enthusiasm for science is infectious and as a co-head of the Vascular Biology and Immunopharmacology (VBIG) lab you helped to create the fun, friendly working environment that I will always associate with VBIG and the Department of Pharmacology at Monash as a whole. I would also like to thank all members of the department and the VBIG and Cardiovascular and Pulmonary Pharmacology Group (CPPG) labs in particular, who have provided invaluable assistance and support to my research.

In particular I would like to thank the head of the Department of Pharmacology, Prof Robert Widdop, the co-head of VBIG, Prof Chris Sobey, as well as Dr Bradley Broughton, Dr Antony Vinh, A/Prof Chrishan Samuel, Mr Henry Diep, Ms Dorota Forens, Dr Chris Chan, Dr Shalini Krishnan, Ms Maggie Lieu, Ms Yan Wang, Mr John Ling and Mr Chao Wang for their technical advice and intellectual input to my work. I am also very grateful to Ms Mingyu Zhu and Ms

Tara McConaghy who assisted me with a large number of experiments presented in this thesis, and to our collaborators Prof Martin Stone and Mr Cheng Huang. There are many more members of the Department of Pharmacology who I would like to thank for making my time here so enjoyable and for getting me through it with jokes and encouragement, especially Megan, Quynh, Shalini, John, Henry, Chris and Maggie. I will hold on to many fond memories of our trips away, nights out and catch ups. You all helped make coming in to work every day something to really look forward to. I would also like to thank all of my friends outside of Monash who have and continue to be a constant source of joy and support and have helped and encouraged me through the ups and downs of PhD life.

Finally, I would like to thank my family, Mum, Dad and Emma for their love, help and patience over this time. I am so lucky to have such a beautiful family, Mum and Dad, you have always encouraged and motivated me and your constant support and guidance have greatly helped me to achieve this.

PUBLICATIONS FROM PHD CANDIDATURE

Co-authored publications

1. Chan, C. T., Sobey, C. G., Lieu, M., Ferens, D., Kett, M. M., Diep, H., Kim, H. A., Krishnan S. M., **Lewis, C. V.,** Salimova, E., Tipping, P., Vinh, A., Samuel, C. S., Peter, K., Guzik, T. J., Kyaw, T. S., Toh, B. H., Bobik, A., Drummond, G. R. (2015). Obligatory role for B cells in the development of angiotensin II-dependent hypertension. *Hypertension* 66 (5): 1023-33

2. Sobey, C. G., Judkins, C. P., Rivera, J., **Lewis, C. V.**, Diep, H., Lee, H. W., Kemp-Harper, B. K., Broughton, B. R., Selemidis, S., Gaspari, T. A., Samuel, C. S., Drummond, G. R. (2015). NOX1 deficiency in apolipoprotein E-knockout mice is associated with elevated plasma lipids and enhanced atherosclerosis. *Free Radical Research* 49 (2): p186-98

Conference Abstracts

Oral presentations

1. **Lewis C.V**., Zhu M., Lieu M., Moodley S., Wang Y., McConaghy T.E., Larner B., Widdop R.E., Sobey C.G., Drummond G.R., Kemp-Harper B.K. (2016). CCL18 as a mediator of the pro-fibrotic actions of M2 macrophages in the vessel wall during hypertension. Joint Annual Scientific Meeting of AAS, HBPRCA and AVBS December 2016, Hobart, Tasmania, Australia

2. **Lewis C.V**., Zhu M., McConaghy T.E., Larner B., Wang Y., Vinh A., Widdop R.E., Sobey C.G., Drummond G.R., Kemp-Harper B.K. (2016). CCL18 and reactive oxygen species are potential mediators of the pro-fibrotic actions of M2 macrophages. ASCEPT-MPGPCR Joint Scientific Meeting November 2016, Melbourne, Victoria, Australia **(Finalist for ASCEPT Garth McQueen PhD Oral Communication Prize)**

Poster presentations

1. **Lewis C.V**., Zhu M., Lieu M., Moodley S., Wang Y., McConaghy T.E., Larner B., Widdop R.E., Sobey C.G., Drummond G.R., Kemp-Harper B.K. (2016). CCL18 as a mediator of the pro-fibrotic actions of M2 macrophages in the vessel wall during hypertension. *Experimental Biology, April 2017, Chicago, Illinois, United States of America*

2. **Lewis C.V**., Zhu M., McConaghy T.E., Larner B., Wang Y., Vinh A., Widdop R.E., Sobey C.G., Drummond G.R., Kemp-Harper B.K. (2016). CCL18 and reactive oxygen species are potential mediators of the pro-fibrotic actions of M2 macrophages. *ASCEPT-MPGPCR Joint Scientific Meeting November 2016, Melbourne, Victoria, Australia.* **(Finalist for ASCEPT Neville Percy PhD Poster Prize, Awarded Cardiovascular Special Interest Group Poster Prize)**

3. **Lewis C.V.,** Huang, C., Canals M, Ludeman J, Stone M, Sobey C.G, Drummond G. R., Kemp-Harper B., K. (2015). Monocyte chemoattractant proteins differentially affect macrophage polarisation. *23rd Annual Scientific Meeting of the Australian Vascular Biology Society, November 2015, Kiama, New South Wales, Australia*

4. **Lewis C.V.,** McConaghy T.E., Sobey C.G, Drummond G. R., Kemp-Harper B., K. (2015). The role of Th2 cytokines in the modulation of macrophages phenotype and reactive oxygen species generation. *23rd Annual Scientific Meeting of the Australian Vascular Biology Society, November 2015, Kiama, New South Wales, Australia*

5. **Lewis C.V.,** Canals M, Ludeman J, Stone M, Sobey C.G, Drummond G. R., Kemp-Harper B., K. (2015). Monocyte chemoattractant proteins differentially affect macrophage polarisation. *4th European Congress of Immunology, September 2015, Vienna, Austria*

6. **Lewis C.V.,** Canals M, Ludeman J, Stone M, Sobey C.G, Drummond G. R., Kemp-Harper B., K. (2015). Monocyte chemoattractant proteins differentially affect macrophage polarisation. *The Australian-European Consortium on Immune Mechanisms in Vascular Disease and Stroke, September 2015, Krakow, Poland*

7. **Lewis C.V.,** Firth D, McConaghy T.E., Peshavariya H.M, Diep H, Sobey C.G, Drummond G. R., Kemp-Harper B., K. (2014). Interleukin-4 activates NOX2 and NOX5 oxidase to increase macrophage reactive oxygen species generation. *22nd Annual Scientific Meeting of The Society of Free Radical Research Australasia, December 2014, Melbourne, Victoria, Australia*

8. **Lewis C.V.,** Canals M, Stone M, Sobey C.G, Ludeman J, Drummond G. R., Kemp-Harper B., K. (2014). Monocyte chemoattractant proteins differentially affect macrophage polarisation. *State of the Heart Conference, November 2014, Adelaide, South Australia, Australia*

LIST OF ABBREVIATIONS

4-PL	4 parameter logistic
A2R	adenosine A2A receptor
ACE	angiotensin converting enzyme
Ang II	angiotensin II
ANOVA	analysis of variance
AP-1	activator protein 1
ApoE	apolipoprotein E
Arg1	arginase 1
α-SMA	alpha-smooth muscle actin
AT_1R	angiotensin II receptor type 1
BCA	bicinchoninic acid
BMDM	bone marrow derived macrophage
BP	blood pressure
BSA	bovine serum albumin
CAD	coronary artery disease
CCL	C-C motif chemokine ligand
CCR	C-C motif chemokine receptor
CD	cluster of differentiation
cDNA	complementary DNA
cMOP	common monocyte progenitor
CMP	common myeloid progenitor
CREB	cAMP response element binding protein
CRP	C-reactive protein
CSFR1	colony-stimulating factor receptor 1
Ct	cycle threshold
CXCL	C-X-C motif chemokine ligand
CXCR	C-X-C motif chemokine receptor

CX_3CL	C-X_3-C motif chemokine ligand
CX_3CR	C-X_3-C motif chemokine receptor
DAMP	damage-associated molecular pattern
DAPI	4’,6-diamidino-2-phenylindole
DBP	diastolic blood pressure
DDA	data-dependent acquisition
dH_2O	distilled water
DMSO	dimethyl sulphoxide
DNA	deoxyribonucleic acid
DOCA	deoxycorticosterone-acetate
dsRNA	double stranded RNA
DUOX	dual oxidase
ECL	enhanced chemiluminescence
ECM	extracellular matrix
EDTA	ethylenediaminetetraacetic acid
ELISA	enzyme linked immunosorbent assay
EndMT	endothelial-mesenchymal transition
ER	endoplasmic reticulum
ET_A	endothelin receptor type A
FBS	fetal bovine serum
FCγR	Fc gamma receptor
FDR	false discovery rate
GAPDH	glyceraldehyde 3-phophate dehydrogenase
gDNA	genomic DNA
GM-CSF	granulocyte-macrophage colony-stimulating factor
GMP	granulocyte-macrophage progenitor
GPx	gluthione peroxidase
Gr-1	granulocyte differentiation antigen-1
HFD	high fat diet

HSC	haematopoietic stem cell
HLA	human leukocyte antigen
HRP	horseradish peroxidase
HSP	heat shock protein
ICAM-1	intracellular adhesion molecule-1
IFIT	interferon-induced protein with tetratricopeptide repeats
IFN	interferon
Ig	immunoglobulin
IGF-1	insulin-like growth factor-1
IL	interleukin
iNOS	inducible nitric oxide synthase
int	intermediate
IRF	interferon-regulatory factor
IRS2	insulin receptor substrate 2
ISG	interferon-stimulated gene
JAK	janus kinase
JAM	junctional adhesion molecule
LC-MS/MS	liquid chromatography–tandem mass spectrometry
LDL	low density lipoprotein
LDLR	low density lipoprotein receptor
LFA1	lymphocyte function-associated antigen 1
LF PVDF	low fluorescence polyvinylidene fluoride
LFQ	label-free quantification
LPS	lipopolysaccharide
Ly6C	lymphocyte antigen 6C
MAPK	mitogen-activated protein kinase
MARCO	macrophage receptor with collagenous structure
M-CSF	macrophage colony-stimulating factor
MDA5	melanoma differentiation associated protein 5

MDP	macrophage and dendritic cell progenitor
MerTK	Mer tyrosine kinase
MHC II	major histocompatibility complex II
MIP	macrophage inflammatory protein
MMP	matrix metalloproteinase
MR	mineralocorticoid receptor
mRNA	messenger ribonucleic acid
MRC-1	mannose receptor C-type 1
Myd88	myeloid differentiation primary response protein 88
NADPH oxidase	NOX
NEAA	non-essential amino acids
NFκB	nuclear factor kappa-light-chain-enhancer of activated B cells
NOD	non-obese diabetic
NR4A1	nuclear receptor subfamily 4 group A member 1
OASL	oligoadenylate synthetase-like protein
OCT	optimal cutting temperature compound
OD	optic density
Opti-MEM	opti-minimum essential medium
ox-LDL	oxidised low density lipoproteins
PAMP	pathogen-associated molecular pattern
PARC	pulmonary and activation-regulated chemoline
PBMCs	peripheral blood mononuclear cells
PBS	phosphate-buffered saline
PCR	polymerase chain reaction
PDBu	phorbol-12,13-dibutyrate
PDGF	platelet-derived growth factor
PECAM1	platelet endothelial cell adhesion molecule 1
PFA	paraformaldehyde
PI3K	phosphoinositide 3-kinase

PKC	protein kinase C
PMSF	phenylmethanesulfonyl fluoride
POLDIP2	polymerase-δ-intreracting protein 2
PPARγ	peroxisome proliferator-activated receptor γ
PSGL1	p-selectin glycoprotein ligand 1
PRM	parallel reaction monitoring
Prxs	peroxiredoxins
PWV	pulse wave velocity
RAAS	renin angiotensin aldosterone system
RELB	rel-like domain-containing protein B
RIG-1	retinoic acid-inducible gene-1
RLU	relative light units
ROS	reactive oxygen species
RPMI	Roswell Park Memorial Institute 1640 medium
RT-PCR	real-time polymerase chain reaction
SBP	systolic blood pressure
s.c	subcutaneous
SCGM	stromal cell growth medium
SEM	standard error of the mean
SOD	superoxide dismutase
SR-A1	scavenger receptor type 1
STAT	signal transducer and activator of transcription
S1PR5	sphingosine 1 phosphate receptor 5
TAM	tumour-associated macrophage
TBS	tris-buffered saline
TGF-β	transforming growth factor beta
Th	T helper cell
TIMP	tissue inhibitor of matrix metalloproteinases
Tip-DC	TNFα and iNOS-producing dendritic cells

TLR	toll like receptor
TNF	tumour necrosis factor
Treg	T regulatory cell
T1D	type 1 diabetes
T2D	type 2 diabetes
UAP	unstable angina pectoris
VCAM-1	vascular cell adhesion molecule-1
VEGF	vascular endothelial growth factor
VLA4	very late antigen 4
VSMC	vascular smooth muscle cell
vWF	von Willebrand factor

CHAPTER 1:

GENERAL INTRODUCTION

1.1 Introduction

Chronic inflammation underlies many cardiovascular diseases including atherosclerosis, hypertension and diabetes. Macrophages are a central immune cell implicated in the pathology of these diseases (38, 54, 124, 213). Far from being a homogenous population, macrophages can adopt different phenotypes dependent on the microenvironment such that they can exert inflammatory, fibrotic, reparative and anti-inflammatory properties in different physiological situations (165). Activated macrophages can be broadly classified into the pro-inflammatory M1 macrophage (classically activated) or the tissue remodelling, anti-inflammatory M2 macrophage (alternatively activated) (220). Interestingly, macrophages are highly plastic and can be skewed from one polarisation state to another (112). In fact, it has been proposed that rather than forming stable subsets within tissues, macrophages will respond to a combination of local, interacting factors to adopt complex or mixed phenotypes (149). Hence macrophage phenotype and function can be readily manipulated and this holds promise for the treatment of cardiovascular and inflammatory diseases. In the settings of atherosclerosis, obesity and type II diabetes, increasing the proportion of M2 macrophages over M1 appears to confer protection (85, 168, 174) while in hypertension a pathogenic role for both M1 (119), and M2 macrophages is evident (161). Hence the disease context and specific polarising stimuli are likely to be important in understanding the roles of different macrophage subsets in cardiovascular disease and how they can best be targeted to limit major cardiovascular events. This chapter will provide an overview of the current theory regarding macrophage ontogeny and polarisation and the biological functions of different macrophage subsets. Furthermore existing evidence for the roles of both M1 and M2 macrophages in the development of atherosclerosis and hypertension will be outlined.

Finally, the potential contributions of reactive oxygen species (ROS) and other macrophage-derived mediators to these diseases will be examined.

1.2 Macrophage biology

1.2.1 Macrophage origin

Central to the mononuclear phagocyte system, and to the innate immune system as a whole, macrophages are a diverse population of cells that play a range of roles in homeostasis and disease. They are crucial to effective host defense, key regulators of adaptive immunity and play important roles in wound healing, tissue remodeling and metabolic function (70). In recent years both the developmental origin of macrophages and the phenomenon of monocyte and macrophage phenotypic heterogeneity have been the subject of much research and debate. It was long accepted that the macrophages present in adulthood are derived from haematopoietic precursors in the bone marrow (Shown in Figure 1.1) and hence that tissue-resident macrophages were solely derived, and replenished from, circulating bone marrow-derived monocytes (162, 217). However, whilst it is true that circulating monocytes can be a major source for the expansion of the macrophage population in tissues, particularly during inflammation and infection (203), recent studies have provided evidence that in homeostasis, tissue-resident macrophage populations such as those in the heart, lung, spleen, liver and peritoneum, are established early in development from foetal-derived 'primitive' macrophages and are maintained throughout adulthood independent of blood monocytes (69, 81, 236). The level to which the expanding population of macrophages in an inflammatory state is derived from local proliferation of resident macrophages or through enhanced monocyte infiltration has not been fully elucidated and is likely to depend both on the disease and tissue in question. Of particular interest in a cardiovascular setting, the existence of a

unique population of macrophage progenitor cells in the aortic adventitia of mice was recently discovered (181) and this population was increased in hyperlipidaemic ($ApoE^{-/-}$ and $LDLR^{-/-}$) mice (181). These findings suggest that in addition to the infiltration and differentiation of circulating monocytes, some vessel wall macrophages which accumulate in cardiovascular disease may also be locally-derived. Nonetheless, many studies have demonstrated the importance of monocyte infiltration to the development of atherosclerosis (21, 39, 45) and hypertension (46, 116, 225). Prevention of monocyte infiltration results in marked reductions in atherosclerotic lesion size (21, 39) and attenuates increases in blood pressure in multiple models of hypertension (46, 116, 161, 225). To add further complexity to this system, like macrophages, monocytes exist in distinct phenotypes, with implications on their relative contributions to both the macrophage population and disease progression.

1.2.2 Monocyte heterogeneity

Perhaps not surprising given the complexity of macrophage phenotype, monocytes too are subject to a large degree of heterogeneity. Two main subsets of monocytes have been identified in mice (classical and non-classical), with three populations observed in humans (classical, intermediate and non-classical). Lymphocyte antigen 6C (Ly6C) expression (also known as Gr-1: granulocyte differentiation antigen 1) is most commonly used to differentiate between murine subsets with CCR2 and CX_3CR1 also commonly used as cell surface markers. Classical monocytes are identified as being $Ly6C^{high}/CCR2^{+}/CX_3CR1^{int}$ while non-classical monocytes are $Ly6C^{low}/CCR2^{-}/CX_3CR1^{high}$ (Table 1.1) (67). Transcriptional profiling of human and murine monocyte subsets show that the human counterparts to murine classical and non-classical subtypes express CD14 and CD16 on their cell surface, respectively, with a third 'intermediate' subset expressing both markers (94, 227) (Table 1.1). While some studies have

suggested a similar 'intermediate' monocyte population in mice, less is known about the existence and potential roles of these cells (209). In humans the classical subset make up approximately 80-90% of the circulating monocyte population, while in mice the proportion of classical to non-classical circulating monocytes appears to be more even (99, 242).

While it was initially thought that classical and non-classical monocytes may give rise to classical and alternative macrophage subsets respectively, studies have now indicated that, at least in mice, 'classical' Ly-6C^{high} monocytes differentiate into macrophages of various subsets and 'non-classical' monocytes may not be a major precursor for tissue macrophages (187, 236). Indeed in a mouse model of myocardial infarction, Ly-6C^{low} monocytes were not required for the presence of Ly-6C^{low} macrophages in the infarcted heart (84). Classical monocytes will exit the bone marrow into the circulation in response to several stimuli including pro-inflammatory chemokines such as CCL2 (39), while Ly6C^{low} monocytes emigrate in response to a separate set of signals including nuclear receptor subfamily 4 group A member 1 (NR4A1) (77) (Figure 1.1). Circulating non-classical monocytes can also be derived (perhaps primarily) from the transformation of circulating classical monocytes (236). Though both subsets can reportedly infiltrate into tissue in response to local cues (222), the classical subset are the predominant group which undergo extravasation and differentiate into macrophages (243). A summary of the current theory of monocyte maturation and infiltration into the vessel wall is shown in Figure 1.1.

Figure 1.1 Sources of macrophages in tissues. Monocytes are originally derived from haematopoietic stem cells (HSC) which develop into macrophage and dendritic cell progenitor (MDP) and common monocyte progenitor (cMoP) cells giving rise to classical (Lymphocyte antigen 6C [Ly6C]^{high} in mice) and non-classical (Ly6C^{low} in mice) monocytes in the bone marrow or spleen. In response to specific inflammatory cues these subsets will emigrate into the blood and can then patrol blood vessels or infiltrate into tissues in response to adhesion molecules such as vascular cell adhesion protein 1 (VCAM1). Within tissues, both resident macrophages (derived from yolk sac and foetal liver precursors during development), and monocyte-derived macrophages will respond to local signals such as cytokines and damage-associated molecular patterns (DAMPs) to polarise cells into a spectrum of macrophage phenotypes. Dotted lines show hypothesised or unknown pathways. AGTR1A, type 1A angiotensin II receptor; Ang II, angiotensin II; CCL2, C-C motif chemokine 2; CD11b, cluster of differentiation molecule 11b; CD115, cluster of differentiation molecule 115; CD43, cluster of differentiation molecule 43; CD62L, L-selectin; CMP, common myeloid progenitor; CCR2, C-C chemokine receptor type 2; CX_3CL1, C-X_3-C-chemokine ligand 1; CX_3CR1, C-X_3-C-chemokine receptor 1; CXCR4, C-X-C chemokine receptor type 4; GMP, granulocyte–macrophage progenitor; ICAM, intercellular adhesion molecule; int, intermediate; JAM, junctional adhesion molecule; LFA1, lymphocyte function-associated antigen 1; miR-146, microRNA 146; NR4A1, nuclear receptor subfamily 4 group A member 1; PAMPs, pathogen-associated molecular patterns; PECAM1, platelet endothelial cell adhesion molecule; PSGL1, P-selectin glycoprotein ligand 1; RELB, rel-like domain-containing protein B; S1PR5, sphingosine 1-phosphate receptor 5; VLA4, very late antigen 4. From Rahman *et al.* (2017) (187).

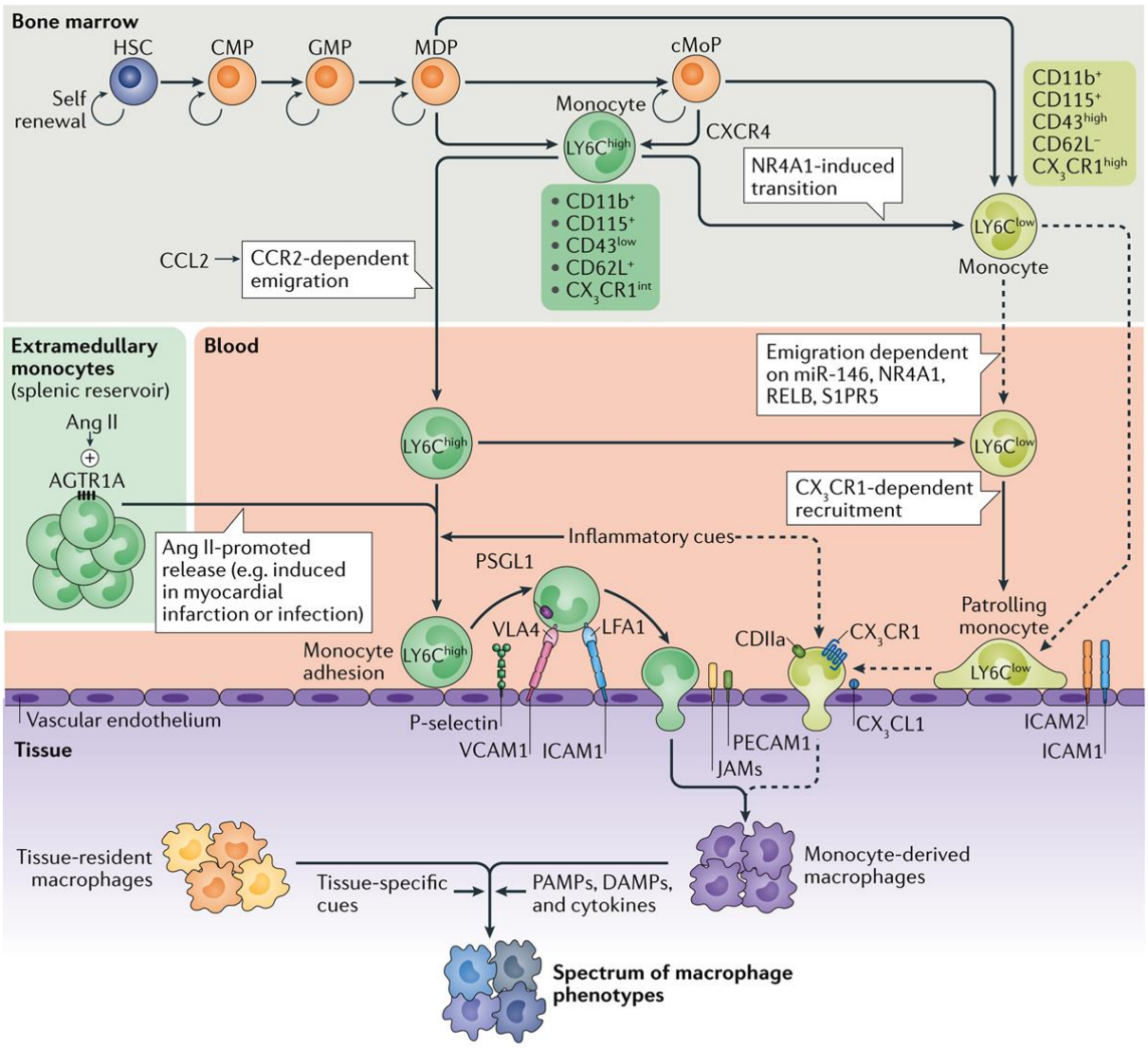

Nature Reviews | Cardiology

1.2.2.1 Functions of monocyte subsets

Although the precise functions of the different monocyte populations remain to be fully elucidated, classical monocytes are short-lived with a half-life of approximately 20 hours (236) and are rapidly recruited to sites of inflammation where they can further generate inflammatory cytokines and will extravasate into tissues and differentiate into macrophages (243). They have also been shown to play a role in antigen presentation and can themselves act as phagocytes (100). The main identified function of non-classical monocytes is surveillance, with several studies indicating that these monocytes, with a longer half-life from 2 days to 2 weeks (236), 'patrol' blood vessels where they survey endothelial integrity and can respond to viral infections (41, 209). Hence in an inflammatory setting, most, if not all, infiltrating monocytes will be of the classical phenotype and once in the tissue microenvironment will respond to local factors which will determine their polarisation and function. A summary of the markers of human and murine monocyte subsets and their functions is provided in Table 1.1.

Table 1.1 Classification and function of monocyte subsets

Subset	Human markers	Murine markers	Key functions
Classical	$CD14^{high}$ $CD16^{low}$	$Ly6C^{high}$ $CCR2^{+}$ CX_3CR1^{int}	• Inflammatory cytokine production • Phagocytosis • Extravasation and macrophage differentiation • Antigen presentation
Intermediate	$CD14^{high}$ $CD16^{high}$	$Ly6C^{int}$	• Display characteristics of classical and non-classical monocytes • Expand in inflammatory conditions
Non-classical	$CD14^{low}$ $CD16^{high}$	$Ly6C^{low}$ $CCR2^{-}$ CX_3CR1^{high}	• 'Patrolling' of endothelium

int=intermediate

1.2.2.2 Monocyte differentiation

Upon recruitment into tissues, monocytes can rapidly differentiate to macrophages or dendritic cells dependent on local signals. Their most common fate during inflammation appears to be differentiation to macrophages, which mostly occurs via activation of colony-stimulating factor 1 receptor (CSF1R) by macrophage colony-stimulating factor (M-CSF) (36, 42, 95), or, less commonly, by IL-34 (223). Other factors such as granulocyte-macrophage colony-stimulating factor (GM-CSF), IL-3 and other inflammatory stimuli such as IL-1β can promote differentiation (196), as well as influencing the macrophage phenotype. However, unlike M-CSF, they are not required for normal monocyte to macrophage differentiation (42, 229). An additional role for monocytes as precursors for non-lymphoid dendritic cells is now well recognised and can also be induced by a range of stimuli. GM-CSF, together with IL-4, can promote dendritic cell differentiation of blood monocytes (192) and Th1 stimuli can also promote TNF-α and inducible nitric oxide synthase (iNOS)-producing dendritic cells, known

as Tip-DCs (93). There is also some evidence to suggest that in the steady state monocytes will extravasate and persist undifferentiated in tissues for a limited time. These 'tissue monocytes' are shown to perform functions such as antigen surveillance and transport to draining lymph nodes (100), rather than differentiating to macrophages or dendritic cells, as is most common during an inflammatory response. Nonetheless, contribution to the macrophage population during inflammation is an important function of monocytes. Furthermore, factors within the local tissue environment will not only determine whether monocytes differentiate to macrophages, but can also influence the macrophage phenotype generated (56).

1.2.3 Macrophage subset activation and function

It has long been established that macrophages adopt a range of phenotypes dependent on local micro-environmental stimuli. These stimuli are generally derived from recruited or resident immune cells such as monocytes and macrophages, T helper cells (Th1/Th2/Th17/Treg) and granulocytes, depending on the tissue. In addition to immune cell-derived cytokines, chemokines, bacterial or viral proteins, and lipids such as oxidized-low density lipoproteins (ox-LDL) in atherosclerosis (12), can also directly stimulate pathways in the monocyte or macrophage for activation towards distinct phenotypes (229).

The theory of macrophage 'polarisation' in which macrophage phenotype can be skewed towards an inflammatory M1 or an alternatively activated M2 phenotype, first emerged in 1992 (207). In this study, treatment of macrophages with interleukin-4 (IL-4) enhanced cell surface mannose receptor expression while, in contrast to interferon-γ (IFN-γ) treatment, it did not up-regulate the pro-inflammatory cytokine tumour necrosis factor-α (TNF-α) (207). Subsequently, M1 and M2 macrophages, defined to reflect the Th1 and Th2 cytokines which

activate them, were proposed as two opposing macrophage subsets and began to be identified and characterized in various disease settings. Since then a more complex 'spectrum' of polarisation has been proposed with many additional subsets and activation stimuli observed. It is now recognised that rather than forming two distinct populations, these two macrophage subsets are likely to be at opposing ends of this spectrum. Despite the inherent complexity in macrophage phenotype and function, an improved understanding of the roles of M1 and M2 macrophages and their effector molecules in specific disease settings may shed light on new therapeutic targets.

Over the years, many different macrophage phenotypes have been characterised based on activation stimuli, cell surface markers and cytokine profiles. Terminology and nomenclature of these macrophage subsets has been varied and a lack of general consensus on the appropriate reporting and definition of macrophage subsets both *in vitro* and *in vivo* was recently acknowledged (164). Of particular importance is the definition of both the original source of the macrophage (including differentiation stimulus if monocyte-derived) as well as the 'polarisation' or 'activation' stimuli. The two most well researched and defined subsets of macrophage are the pro-inflammatory M1 or "classically activated" macrophage and the tissue-reparative M2 or "alternatively activated" macrophage. Importantly, in recent years many subtle differences in activation states within these two broadly defined macrophage subsets have come to light. Additional subsets within the M2 classification (eg. M2a, M2b, M2c and M2d) (38) as well as tissue (eg. alveolar macrophages, Kupffer cells of the liver, microglia)- and disease (eg. tumor-associated macrophages (TAM) in cancer, haemoglobin-stimulated macrophage (MHb) in atherosclerosis)-specific subsets, are evident (55, 165).

It has been proposed that rather than simply giving the terms M1 and M2, that macrophage phenotypes should be defined by their specific activation stimulus i.e. M(IFN-γ + LPS) and M(IL-4) (164). While previous studies have defined GM-CSF and M-CSF differentiated macrophages as being 'M1' and 'M2', the field has moved away from this classification and these are not considered true stimuli of the M1 or M2 response (164). The characteristics, stimuli and common markers of M1 macrophages and the several subsets of M2 macrophages will be discussed in detail below.

1.2.3.1 M1 macrophages

Although TNFα and several toll like receptor (TLR) ligands can be used to polarise macrophages to an M1 phenotype *in vitro*, the most widely recognised method of M1 polarisation is via stimulation with the Th1 cytokine IFN-γ and the bacterial component lipopolysaccharide (LPS), either alone or in combination. The key pathways driven by these stimuli are i) IFN-γ stimulation of the transcription factors, signal transducer and activator of transcription 1 (STAT1) (43) and interferon-regulatory factor 5 (IRF5) (125), ii) induction of myeloid differentiation primary response protein 88 (Myd88)-dependent toll-like receptor 4 (TLR4) signalling by LPS which activates IRF-3 (110) and iii) activation of the pro-inflammatory transcription factor, nuclear factor κ-light-chain-enhancer of activated B cells (NFκB) (193). These pathways lead to the generation of pro-inflammatory cytokines (eg. IL-1β, TNF-α, IL-12, IL-23) and chemokines (eg. CXCL9, CXCL10 and CXCL11). M1 macrophages also have increased expression of the chemokine receptor CCR7 and other M1 markers such as iNOS, the co-stimulatory molecules, cluster of differentiation 80 (CD80) and CD86, major histocompatibility complex II (MHCII) and macrophage receptor with collagenous structure (MARCO) (Table 1.2) (38).

The main function of M1 macrophages is to respond to microbial infection. As such, typical characteristics of M1 macrophages are pro-inflammatory cytokine secretion, leading to inflammatory cell recruitment and the activation and expansion of the Th1 and Th17 T cell populations. Nitric oxide and reactive nitrogen and oxygen species (RNS/ROS) generation are key mediators of M1 responses and M1 macrophages can also generate matrix metalloproteinases (MMPs) (49), which, in addition to ROS, can lead to tissue damage. All of these functions make M1 macrophages ideal for microbial and tumour cell killing (38), but also contribute to the pathogenesis of inflammatory diseases.

1.2.3.2 M2 macrophages

M2 macrophages, although traditionally stimulated with the Th2 cytokine IL-4, can be polarised with a range of alternative stimuli associated with immune-regulatory and wound healing responses (eg. IL-13, IL-10, TGF-β, glucocorticoids, immune complex) resulting in different sub-classes of M2 macrophages. While markers for these subsets can differ, increased expression of mannose receptor C-type 1 (MRC-1; also known as CD206) is most commonly used to identify M2 macrophages and its upregulation is observed in all M2 subsets with the exception of the M2d subtype (38, 148).

M2a- 'wound healing' macrophages

The first identified M2 macrophage was that induced by the Th2 cytokines IL-4 and IL-13 (207). This subset is now also known as the M2a macrophage and STAT6, IRF-4 and peroxisome proliferator-activated receptor γ (PPARγ) signalling pathways are involved in its activation (83, 210). These macrophages are central to immune responses to metazoan parasite, and drive Th2 immunity. Often referred to as 'wound healing', M2a macrophages secrete pro-fibrotic factors such as transforming growth factor-β (TGF-β) and insulin-like growth factor 1 (IGF-1)

as well as fibronectin, collagen, and other extracellular matrix (ECM) proteins involved in tissue remodelling and repair (70, 162). IL-4- or IL-13-activated macrophages also produce large amounts of chitinase and chitinase-like molecules (YM1, YM2) (185) which can have a role in response to parasitic infection as well as remodelling of the ECM (20). Although upregulation of the anti-inflammatory cytokine IL-10 can be observed in M2a macrophages, these macrophages are less associated with immune regulatory responses and more associated with the Th2 immune response. Given their roles in wound healing they have particularly potent remodelling and pro-fibrotic effects, which when left unchecked can contribute to fibrosis. M2b-d subtypes of macrophages are considered to be more 'regulatory' in phenotype compared to the wound healing M2a, a comparison of their different polarising stimuli, markers and functions is provided in Table 1.2.

M2b-d- 'regulatory' macrophages

In contrast to M2a macrophages, M2b, c and d macrophages lack strong tissue remodelling capacities. M2b macrophages can be induced by stimulation with IgG immune complexes (which will activate FCγR) in combination with TLR or IL-1R agonists (64). These macrophages generate large amounts of IL-10 and have reduced IL-12 production as a result of Fc gamma receptor (FCγR) binding, therefore exhibiting some anti-inflammatory effects. However, their generation of other pro-inflammatory cytokines (IL-1β, TNFα, IL-6) in response to TLR/IL-1R activation remains intact (64). Increased expression of co-stimulatory molecules CD80 and CD86 is also evident as part of their immunoregulatory activity, thus enhancing antigen presentation and allowing for regulation of T cell activation (162). M2b cells therefore are not entirely anti-inflammatory and, in addition to M2a macrophages, can mediate Th2 responses.

Playing a clearer role in immunosuppression, the M2c macrophage is induced by the anti-inflammatory stimuli IL-10, TGF-β and glucocorticoids. Through activation of STAT3 and inactivation of NFκB signalling, M2c macrophages will dampen the inflammatory response. These macrophages also exhibit enhanced efferocytosis via increased expression of Mer receptor tyrosine kinase (MerTK) (245), aiding in the clearance of cell debris at wounds or sites of inflammation. A key marker for M2c macrophages, in addition to MRC-1, is the cell surface protein CD163 (38). Finally, M2d macrophages are induced by co-stimulation with TLR and adenosine receptor (A2R) agonists. They produce high levels of IL-10 and vascular endothelial growth factor (VEGF) and decreased pro-inflammatory cytokine production. This production of VEGF is linked to their pro-angiogenic actions and is a property commonly observed in tumour associated macrophages (52, 71). Unlike the other M2 subtypes, M2d do not upregulate MRC-1 and additional common M2 markers Fizz1, and Ym1 are also not induced in this subtype (52). A summary of the processes involved in determining macrophage polarisation in the vessel wall is outlined in Figure 1.2.

Table 1.2 Macrophage subsets and functions

Subset	Stimuli	Key markers and mediators	Key functions
M1	**IFN-γ + LPS** TNFα TLR agonists	IL-1β, TNF-α, IL-12, IL-23, CXCL9-11, iNOS/NOS2, ROS/RNS, MHCII, CD86, CD80, MARCO	Microbial killing Th1/Th17 immunity ECM breakdown
M2a	**IL-4** IL-13	MRC-1/CD206, TGF-β, IGF-1 CCL17, CCL18, CCL22, Arg1, Fizz1, Ym1/Chi3l3	Wound healing/tissue remodelling Th2 immunity
M2b	IC + TLR/IL-1R agonists	MRC-1/CD206, IL-10, MHCII, CD86	Immunoregulation Th2 immunity
M2c	IL-10 Glucocorticoids TGF-β	MRC-1/CD206, CD163, IL-10, TGF-β	Efferocytosis Anti-inflammatory response
M2d	TLR + A2R agonists	VEGF, IL-10	Promotion of angiogenesis

Figure 1.2 Spectrum of macrophage polarisation in the vessel wall. Monocyte-derived and tissue resident macrophages respond to local signals to polarise towards different phenotypes such as the pro-inflammatory M1, wound healing M2a and resolving M2c macrophages. The plasticity of macrophages enable alterations throughout this spectrum in response to different stimuli. Inflammatory stimuli such as interferon-γ (IFN-γ), lipopolysaccharide (LPS), tumour necrosis factor-α (TNF-α) and interleukin-1β (IL-1β) will promote macrophages towards an M1 phenotype characterised by expression of cell surface markers such as macrophage receptor with collagenous structure (MARCO), cluster of differentiation 80 (CD80) and C-C chemokine receptor type 7 (CCR7) and the release of cytokines and chemokines such as IL-1β, TNFα, IL-12 and C-X-C motif chemokine 11 (CXCL11) through signal transducer and activator 1 (STAT1)-, interferon regulatory factor 5 (IRF5)- and nuclear factor κ-light-chain-enhancer of activated B cells (NFκB)-driven pathways. Th2 cytokines will promote M2a macrophages, expressing the cell surface marker mannose receptor C-type 1 (MRC-1), and releasing pro-fibrotic mediators such as insulin-like growth factor-1 (IGF-1), platelet derived growth factor (PDGF), C-C motif chemokine 18 (CCL18) and CCL22 through STAT6 and peroxisome proliferator-activated receptor γ (PPARγ) signalling. The presence of anti-inflammatory stimuli such as IL-10 and glucocorticoids can signal through STAT3 and polarise macrophages towards an anti-inflammatory phenotype expressing CD163 in addition to MRC-1 and releasing IL-10 and transforming growth factor-β (TGF-β) to resolve inflammation. It should be noted that this is a simplification of the complex environment and mixed phenotypes and, although not shown, the M2b and M2d phenotypes are also likely to be present. Macrophages can be polarised from one phenotype to another, indicated by dotted arrows and are likely to fit somewhere along a spectrum of phenotypes indicated by the red (inflammatory)/green (anti-inflammatory) gradient.

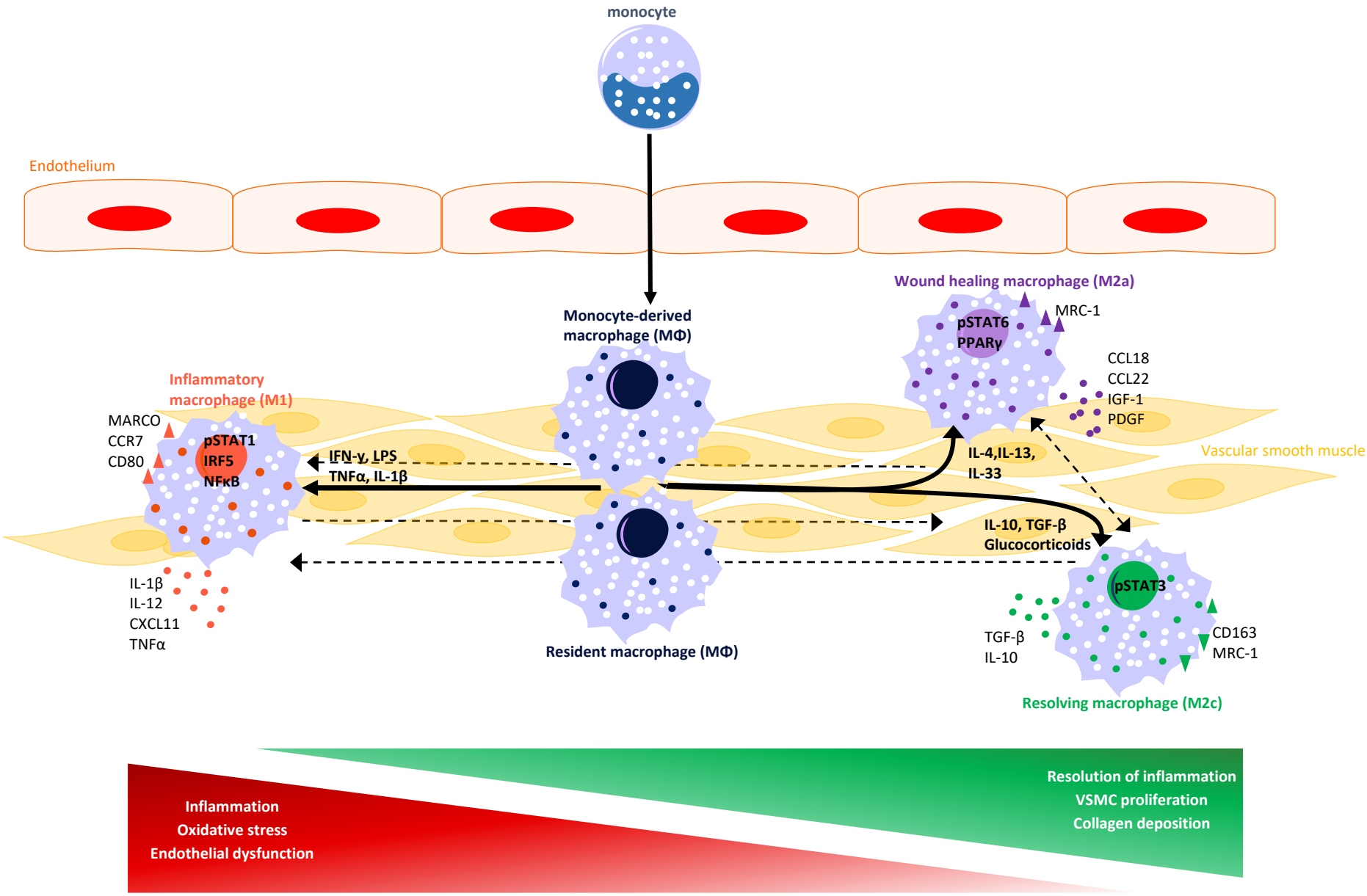
monocyte
Endothelium
Monocyte-derived
macrophage (MΦ)
Inflammatory
macrophage (M1)
MARCO
CCR7
CD80
pSTAT1
IRF5
NFκB
IFN-γ, LPS
TNFα, IL-1β
IL-1β
IL-12
CXCL11
TNFα
Resident macrophage (MΦ)
Wound healing macrophage (M2a)
pSTAT6
PPARγ
MRC-1
CCL18
CCL22
IGF-1
PDGF
IL-4,IL-13,
IL-33
Vascular smooth muscle
IL-10, TGF-β
Glucocorticoids
pSTAT3
TGF-β
IL-10
CD163
MRC-1
Resolving macrophage (M2c)
Inflammation
Oxidative stress
Endothelial dysfunction
Resolution of inflammation
VSMC proliferation
Collagen deposition

1.2.3.3 Current limitations of macrophage markers

Whilst several markers of M1 and M2 macrophage phenotypes are currently established (Table 1.2), limitations in consistency between *in vitro* and *in vivo* macrophages and translation between mice and humans exist (204). Some markers that are commonly used *in vitro* are not expressed highly enough *in vivo* for reliable detection of protein and differences between *in vivo* and *in vitro* macrophages are evident (164, 204). Furthermore, while the properties of M1 and M2 subsets are generally consistent across mammalian species, some human markers are lacking in the rodent genome and some differences in macrophage properties are also observed between mice and humans (164). An important example of this is arginine metabolism. Whilst robustly used as an M2 marker in mice, Arg1 upregulation is not observed in human M2 macrophages (150, 186). Therefore there remains a need for new M1 and M2 markers which are consistently upregulated in immortalized and primary cell lines and can be translated *in vivo* in both mice and humans to aid in the investigation of the differing roles of macrophage phenotypes in disease.

1.2.4 NADPH oxidases and reactive oxygen species in M1 and M2 function

The NADPH oxidases (NOXs) are a family of enzymes whose primary function is the generation of the ROS, superoxide (O_2·-) and hydrogen peroxide (H_2O_2). These ROS are abundantly produced by macrophages as a key mechanism in host defense but have also been shown to contribute to the pathogenesis of cardiovascular diseases (88). The NOX family consists of NOX isoforms 1-5 and dual oxidases (DUOX) 1 and 2. Each of these catalytic subunits (with the exception of NOX5) are associated with several regulatory subunits which must be assembled together for activation of the complex. NOX1, NOX2, NOX4 and NOX5 have been

identified in the cardiovascular system and are increased in disease (11, 50), however NOX5 is absent from the rodent genome.

NOX2 is the most highly expressed NOX in macrophages and is responsible for the oxidative burst for microbial killing. Also expressed in endothelial cells and adventitial fibroblasts, NOX2 is elevated in both human atherosclerotic plaques (206) and animal models of atherosclerosis (106) as well as being implicated in hypertension, stroke, and diabetes (50). Interestingly, NOX-derived ROS have not only been implicated in the inflammatory contribution to diseases such as atherosclerosis, hypertension, diabetes and stroke (50), but also contribute to pro-fibrotic and remodelling responses in the cardiovascular system (8, 145). Hence an upregulation of NOX activity may contribute to both the inflammatory actions of M1 macrophages and the tissue remodelling pro-fibrotic actions of M2 macrophages, but this remains to be investigated.

In terms of structure and activation, the NOX2 catalytic subunit constitutively associates with p22phox and activation of the NOX2/p22phox heterodimer requires translocation of activator (p67phox) and organiser (p47phox) cytosolic subunits to the complex (Figure 1.3), initiated by phosphorylation of p47phox. The role of p40phox, a small subunit which binds to p67phox, is not well established with evidence for both inhibitory (195) and enhancer (127) roles. Whilst NOX2 is most commonly associated with macrophage function, the additional expression of NOX1, NOX4 and NOX5 has been reported in macrophages (113, 130, 146). Like NOX2, NOX1 associates with p22phox, an activator subunit (NOXA1) and a regulatory subunit (NOXO1 or p47phox) (Figure 1.3). Although several studies have failed to detect NOX1 in macrophages (11, 130), one study of RAW264.7 and bone marrow derived (BMDM) murine macrophages reported its expression and upregulation through TLR activation (113). The NOX4 isoform

requires association with p22phox, while polymerase-δ-intreracting protein 2 (POLDIP2) is thought to regulate its activity (50) (Figure 1.3). Unlike other NOXs, the ROS produced by NOX4 is primarily hydrogen peroxide. NOX4 expression in human primary macrophages was first demonstrated in 2010, predominantly localised to the endoplasmic reticulum (130). Its expression and release of intracellular ROS increased following treatment with oxLDL and was associated with oxLDL cytotoxicity (130). Furthermore, expression of NOX4 has been observed in mouse BMDMs where it was shown to play a role in macrophage inflammasome activation (160). Finally, two recent studies have reported NOX5 expression in human macrophages (146, 151). Although Marzaioli *et al.* (151) demonstrate its association with p22phox in monocytes, in contrast to the other NOXs, NOX5 does not require activation through regulatory subunits. Instead it contains a Ca^{2+}-binding EF-hand domain on its intracellular NH_2 terminus (Figure 1.3). Hence NOX5 is activated by increased intracellular calcium (6), although it has also been shown to be activated through protein kinase C (200). The precise roles that these three additional NOXs have in macrophage function and whether they may be differentially regulated in macrophage polarisation has not been thoroughly investigated. However it should be noted that NOX1 and NOX5 upregulation was observed in response to LPS- and IFN-γ-treatment of macrophages, respectively (113, 146), suggesting potential for roles in pro-inflammatory macrophage phenotypes. The structure of these four NOX complexes are shown in Figure 1.3.

While it has generally been assumed that M1 macrophages generate more ROS than M2 macrophages (148, 204, 220), no studies have fully characterized or compared the activity and expression of NOXs and their regulatory subunits in different macrophage phenotypes. Interestingly, early studies showed that IL-4 could inhibition LPS-stimulated ROS production

but enhance the signal with IFN-γ (10, 15). Furthermore, a potential role for ROS in the activity of alternatively activated macrophages, particularly M-CSF differentiated macrophages, has recently come to light (120, 121, 240). Contrary to the theory that pro-inflammatory macrophages produce the greatest amount of ROS, Kraaij et al., (2010) found that M-CSF-differentiated human macrophages produced significantly more superoxide *in vitro* than their GM-CSF-differentiated pro-inflammatory counterparts. Although this comparison of differentiation stimuli doesn't properly represent the M1/M2 states, it did demonstrate ROS generation across several alternative macrophage subsets, suggesting ROS production may not simply be an M1 function. Interestingly, treatment with IL-4 after M-CSF differentiation (M2a macrophages) appeared to reduce ROS, but the anti-inflammatory cytokine IL-10 (M2c) maintained high levels of ROS (120). That macrophage ROS can drive T-regulatory (Treg) cell activation (121, 122), further suggests there could be a role for NOX2 oxidase in resolution of inflammation in addition to its well-recognised roles in inflammation and tissue damage (90).

In addition to its contribution to macrophage function, a role for NOX2 oxidase in the polarisation of macrophages has also been identified, however there is evidence for its involvement in both M1 and M2 activation. A role in M1 polarisation has been observed in non-obese diabetic (NOD) mice deficient in the p47phox subunit of the NOX2 oxidase complex, where an increase in the proportion of M2 over M1 macrophages was observed, suggesting that effective M1 polarisation required functional NOX2 oxidase expression (174). This is in agreement with a second study of p47phox$^{-/-}$ mice in the setting of *Listeria monocytogenes* infection, in which deficiency in functional NOX2 oxidase enhanced M2, and limited M1, polarisation (234). However, at odds with these studies, several groups have demonstrated the opposite effects of NOX2 on macrophage polarisation, showing that its

expression is critical to M2 polarisation. For example, deficiency in p47phox enhanced inflammatory responses to LPS (199, 239) and resulted in hyper-activation of inflammatory responses in auto-immune arthritis (89), suggesting NOX2 function would actually limit pro-inflammatory M1 function. Moreover, lack of NOX1 and NOX2 expression prevented M2 polarisation *in vitro* (240) and attenuated M2 accumulation and wound healing responses *in vivo* (232), suggesting a requirement for functional NOX for M2 polarisation. Taken together, these findings point to a role for macrophage ROS not just in driving pro-inflammatory M1 processes but also in M2 function. Whether the NOX isoform, or ROS end product, differs between these two phenotypes to mediate their responses remains to be fully elucidated.

1.2.4.1 Superoxide dismutase isoforms

Superoxide dismutases (SODs) are antioxidant enzymes that rapidly convert superoxide to hydrogen peroxide, for further conversion to water by catalase, peroxiredoxins (Prxs) or glutathione peroxidases (GPx). Thus SODs are thought to protect cells against the damaging effects of oxidative stress and are shown be protective in vascular disease (60). There are three mammalian isoforms of SOD: SOD1 or Cu,Zn-SOD, SOD2 or Mn-SOD, and SOD3 or extracellular (EC)-SOD. Each isoform can convert superoxide (NOX-derived or from additional sources) to hydrogen peroxide and they mainly differ in terms of cellular localisation. SOD1 is the main isoform expressed intracellularly and is located within the cytosol, while SOD2 is expressed only in the mitochondria. By contrast, SOD3 is secreted from cells, hence also known as extracellular SOD (60). Interestingly, SOD2 upregulation has been observed in pro-inflammatory macrophages (177, 188), and increased SOD1 expression is reported in M2 macrophages during pro-fibrotic responses (82), suggesting there may be differential roles for these isoforms in macrophage polarisation.

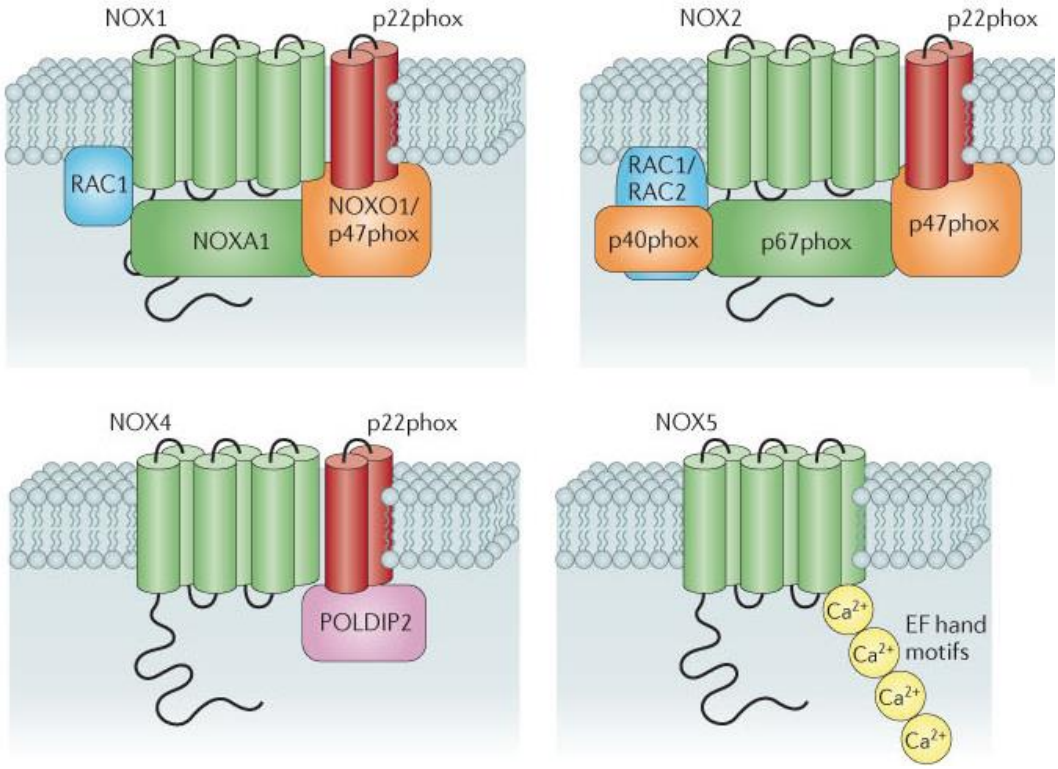

Figure 1.3. Subunit compositions of NOX1,2,4 and 5 NADPH oxidases. Catalytic subunits shown in green and p22phox in red. Activator subunits (NOXA1 and p67phox) shown in green and organiser complexes (NOXO1, p47phox and p40phox) shown in orange. POLDIP2= polymerase-δ-interacting protein 2, shown in pink. Adapted from Drummond *et al.* (2011) (50).

1.3 Macrophage polarisation in cardiovascular disease

The polarisation state of macrophages has been shown to influence the progression of many diseases, particularly those affecting the cardiovascular system. M1 macrophages will often accumulate and contribute to the early stages of disease, exacerbating inflammation and tissue damage (119, 132). M2 macrophages by contrast form part of the 'reparative' phase clearing cell debris, promoting healing and regeneration, and dampening down the immune response. However, hyper-activation of this response can become pathological and contribute to excessive ECM deposition and remodelling (70). The presence of both M1 and M2 macrophages is observed in diabetes, atherosclerosis and hypertension (85, 161, 168). A shift in the polarisation of adipose tissues macrophages from an M2 to an M1 phenotype occurs in obesity and is associated with insulin resistance and the development of type II diabetes (29). In addition, M1 macrophages contribute to the destruction of the β-cells of the pancreas (29). Thus, in obesity and diabetes, protective and pathological roles are evident for M2 and M1 macrophages, respectively (Table 1.3). While M1 macrophages are also implicated in atherosclerosis and hypertension (112, 119), the role of M2 macrophages in these settings is less definitive. It appears that whilst reducing M1 macrophage accumulation at the early stages of these diseases is protective (45, 225), M2 macrophages can also contribute to pathology, particularly in the remodelling and stiffening of blood vessels (161) (Table 1.3).

Table 1.3 Roles of macrophage subsets in cardiovascular diseases

Disease	Role of macrophage phenotype	Reference
Type 1 Diabetes	• ↓M1:M2 delayed and reduced onset of disease in mice • adoptive transfer of M2 macrophages protective	Padgett *et al*., 2014 Parsa *et al.,* 2012
Obesity and Type 2 Diabetes	• ↑M1:M2 in obese adipose tissue associated with development of T2D • ↓M1:M2 protects from insulin resistance and fatty liver in mice	Calderon *et al.,* 2006 Nio *et al*., 2012
Atherosclerosis	• ↓M1:M2 associated with plaque stabilisation and reduced lesion size in mice • ↓M1:M2 associated with reduced coronary plaque in humans	Khallou-Laschet *et al*., 2010 Hirata *et al*., 2011
	• M2 macrophages ↑cholesterol uptake, ↑ER stress	Oh *et al.,* 2012
	• Additional phenotypes involved: eg. M4, MHb, Mox, Mhem	Tabas and Bornfeldt, 2016
Hypertension	• M1 macrophages ↑inflammation-associated organ damage in early stages	Kossmann *et al.,* 2014
	• M2 macrophages promote vascular remodelling and stiffening	Moore *et al.,* 2015

1.3.1 Obesity and Diabetes

Obesity is thought to induce a state of chronic low grade inflammation, which is implicated in associated conditions such as type 2 diabetes (T2D). Adipose tissue macrophages are a key immune cell involved in this inflammatory response (124). In healthy lean individuals, macrophages comprise approximately 10% of the cells found in white adipose tissue and these are predominantly M2-polarised. In obesity, both the number and polarisation state of these macrophages is altered such that there is an accumulation of M1 macrophages (124). Through the production of pro-inflammatory cytokines this leads to further inflammation and

contributes to insulin resistance in adipocytes (5, 124). Protection from the development of type II diabetes in mice has been associated with skewing polarisation back towards the M2 phenotype (168) (Table 1.3). Further evidence for a benefit of increasing M2 polarisation is observed in humans as inflammatory markers correlate with high glycaemia and the M2 markers, TGF-β, CD163 and MRC-1 are all increased with exercise and associated with enhanced insulin sensitivity (54).

Although the mechanisms involved in the development of type 1 diabetes (T1D) differ to type 2 and are independent of obesity, M1 macrophages are also implicated in this form of the disease with protection observed when macrophage infiltration is prevented (91). Infiltrating pro-inflammatory macrophages can be identified in the islets of the pancreas in the prediabetic stage of the disease (78, 131). Here they can directly induce β-cell death and enhance the activation of autoreactive T cells (29). A protective role for M2 macrophages has been demonstrated in several studies whereby adoptive transfer of immune regulatory alternatively activated macrophages (stimulated with a combination of IL-4, IL-10 and TGF-β) delays the onset of T1D (175) and infiltration of M2 macrophages, rather than M1, into islets is associated with protection (28) (Table 1.3). Finally, a recent study demonstrated that skewing the macrophage phenotype towards an M2 state, through the deletion of NOX activity, protected against the development of T1D in NOD mice (174) (Table 1.3). Hence, unlike atherosclerosis and hypertension where there appear to be pathogenic roles for both subsets, in the setting of diabetes the protective and pathogenic roles of M2 and M1 macrophages, respectively, appear to be more definitive. Based upon these observations, this thesis will focus predominantly on the function of M1 and M2 macrophages in the context of atherosclerosis and hypertension.

1.3.2 Atherosclerosis

Atherosclerosis is a chronic inflammatory disease affecting the vascular wall and remains a leading cause of death worldwide (163). It is the underlying cause of much of the morbidity and mortality associated with cardiovascular disease. Rupture of atherosclerotic plaques and subsequent thrombus formation can lead to blockage of smaller vessels: the cause of ischemic heart disease, ischemic stroke and peripheral artery disease (13). The primary treatment currently available to patients is cholesterol lowering drugs such as statins. However, two thirds of patients on this medication are still at risk of a major cardiovascular event (158). Much research in recent years has focussed on targeting the immune component of the disease, in addition to the dyslipidemia, in an attempt to improve this outcome (201).

An important aspect of atherosclerosis and its potential consequences, is plaque instability. While they remain stable, atherosclerotic plaques pose less of a threat to cardiovascular health. However the rupture of vulnerable plaques and subsequent thrombosis results in the acute cardiovascular events described above. Vulnerable plaques are characterised by a large lipid-rich necrotic core and a thin fibrous cap (235). By contrast, stable plaques have a smaller lipid pool, greater density of vascular smooth muscle cells (VSMCs) and ECM, and a thick, protective fibrous cap (235). As the most abundant immune cell in atherosclerotic lesions, macrophages play a central role in both plaque progression and instability.

A role of macrophages is evident in both the early and advanced stages of atherosclerosis, as illustrated in Figure 1.4. Endothelial dysfunction is a major initiating factor of atherosclerosis (136) and leads to the recruitment of macrophages into the arterial wall. Endothelial dysfunction can be triggered by vessel injury or disturbed blood flow as well as a number of cardiovascular risk factors such as hypertension and hypercholesterolaemia (61, 214).

Associated with endothelial dysfunction is an up-regulation of adhesion molecules such as VCAM-1, and P and E selectins promoting entry of circulating monocytes into the intima for maturation into macrophages (61, 65, 136) (Figure 1.4b). Here, macrophages further amplify endothelial cell activation and lesion inflammation via secretion of ROS and pro-inflammatory cytokines (136, 184). Importantly, endothelial dysfunction also alters endothelial permeability allowing entry of cholesterol-containing low density lipoproteins (LDLs) into the intima. These become oxidised (oxLDL) and are taken up by residing macrophages which, via ROS production, can themselves oxidise LDL (14, 191). These lipid-rich macrophages are known as foam cells and as more lipid and foam cells accumulate these cells can undergo apoptosis. This releases lipids, cholesterol and cellular debris into the plaque producing a fatty necrotic core (Figure 1.4c), characteristic of an unstable plaque (235). Infiltrating macrophages can further contribute to plaque destabilisation via the release of MMPs which degrade the ECM, increasing the likelihood of rupture (35, 48, 138). Finally, macrophages promote expression of the coagulant, tissue factor, promoting thrombosis and increasing the likelihood of plaque disruption (Figure 1.4d) (138). Given their many roles in atherogenesis, limiting or manipulating the properties and effector molecules of the macrophage population in atherosclerotic plaques, remains a promising therapeutic target.

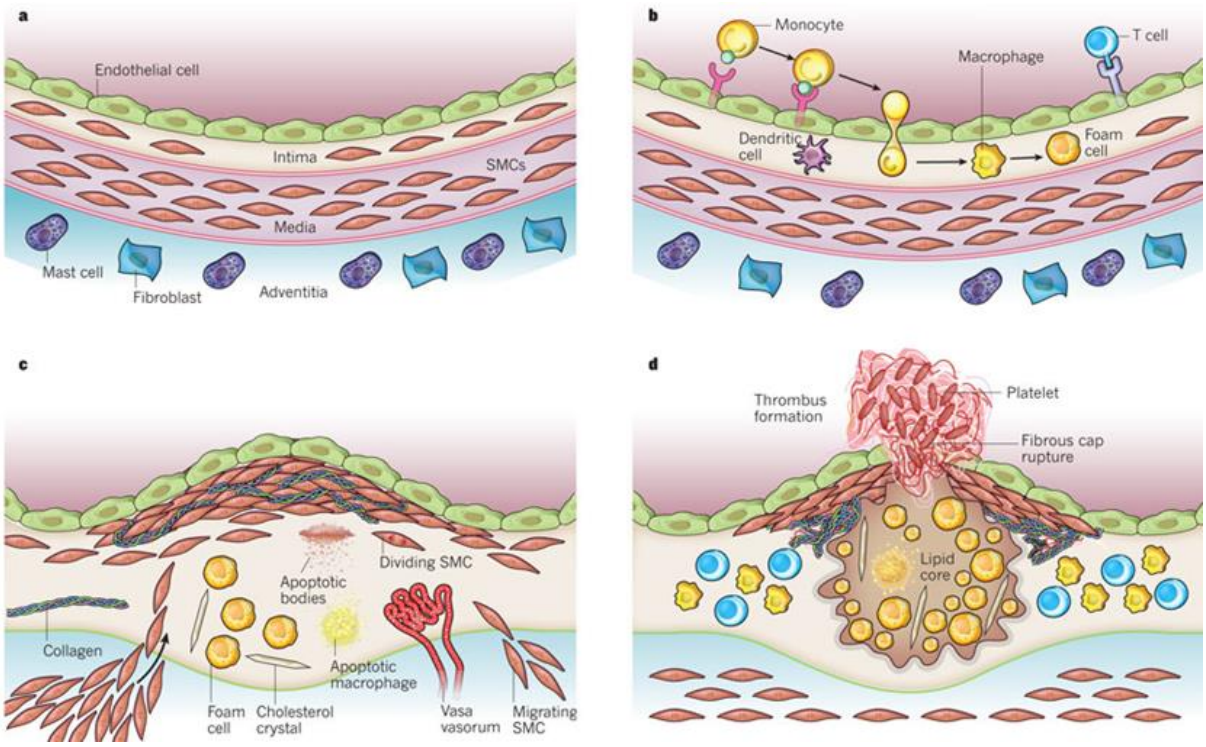

Libby *et al.*, (2011). *Nature* 473 (7347): 317-325

Figure 1.4 Macrophages plays a key roles in the progression of atherosclerosis. a. The normal arterial wall consists of three layers; the intima lined by an endothelial monolayer in contact with the blood; the media containing vascular smooth muscle cells (VSMC) in extracellular matrix (ECM); and the adventitia containing mast cells, fibroblasts, microvessels and nerve endings. **b.** endothelial dysfunction leads to monocyte recruitment lipid entry. Monocytes mature to macrophages, which engulf lipids and can transdifferentiate into foam cells. **c.** As the plaque progresses, VSMCs migrate, proliferate and produce collagen and ECM to form a fibrous cap. Both VSMCs and accumulated foam cells can undergo apoptosis at the centre of the plaque, forming a lipid-rich necrotic core. **d.** A large lipid core with a thin overlying fibrous cap characterises a vulnerable plaque. These are likely to rupture exposing blood coagulants to tissue factors in the plaque and triggering thrombosis (138).

1.3.2.1 Macrophage phenotypes in atherosclerotic plaques

The macrophages present within atherosclerotic lesions are a highly heterogeneous population of cells, not necessarily limited to simply M1 or M2 in phenotype (147, 176, 226). Several other macrophage populations have been suggested to contribute to atherosclerosis such as haemoglobin(Mhb)- and haem(Mhem)-stimulated, Mox (oxidised phospholipid-stimulated), M4 (CXCL4-stimulated) and IL-17A-stimulated macrophages (48, 211) (Table 1.3). Nonetheless both M1 and M2 macrophages have been identified in plaques (135), and many of the atherogenic actions of plaque macrophages such as cytokine and ROS release, MMP generation and activation of the Th1/Th17 response, are characteristic of an M1 phenotype. Hence it has long been believed that therapeutics which can skew macrophages towards the M2 phenotype may be atheroprotective. Thus M2 macrophages would supress inflammation and promote plaque stabilisation through the release of growth factors and ECM. Indeed, a reduction in the M1:M2 ratio within lesions has been associated with protection from atherosclerosis in both mice (112) and humans (85) (Table 1.3). A separate study of human plaques demonstrated that, while markers of both subsets increase as the plaques progress, they demonstrate differential distribution within the plaque. While M1 macrophages were shown to be most prevalent in the unstable 'shoulder' regions the balance of M1 and M2 was more even in the protective fibrous cap and M2-markers were predominant in the adventitia (208). An additional study by Chinetti-Gbaduidi *et al.* identified M2 macrophages and high expression of the M2-polarising cytokine IL-4, in more stable areas of human plaques. These macrophages were found to have reduced cholesterol handling and enhanced phagocytic properties (34), suggesting that the M2 phenotype could limit foam cell formation and enhance clearance of cell debris. Hence an ability to skew macrophage polarisation towards

an M2 phenotype, which is anti-inflammatory and reparative, remains a promising target to prevent the progression, and even promote regression, of atherosclerotic plaques.

However while M1 macrophages are strongly implicated in the pathogenesis of atherosclerosis, there is some evidence to suggest that the M2 phenotype can also display atherogenic properties (115, 133, 134, 171) (Table 1.3) and protection may depend on the precise polarisation stimulus involved. This is evident in the opposing roles which have been observed for the M2-polarising stimuli, IL-4 and IL-13, in animal models of atherosclerosis. Specifically, IL-4 has been associated with atherogenesis, yet atheroprotective actions of IL-13 have been identified (31, 115, 133, 134).

1.3.2.2 Differential roles for IL-4 and IL-13 in atherosclerosis

IL-4 and IL-13 are closely related Th2 cytokines whose roles in allergy, asthma and pulmonary fibrosis are well recognised (152). Both cytokines are secreted by Th2-polarised T cells, as well as many other leukocytes including granulocytes, natural killer (NK) T cells and macrophages (152). An important function of both IL-4 and IL-13 is to inhibit type I inflammatory responses (i.e IFN-γ induced) (228). However, rather than being purely anti-inflammatory, IL-4 and IL-13 drive a type II immune response characterised by eosinophil and mast cell recruitment, B cell production of IgG1 and IgE antibodies, and expansion and activation of Th2 cells and M2a macrophages (118). In the setting of atherosclerosis, this activation of M2 macrophages is thought to promote the stabilisation of atherosclerotic plaques (208), however IL-4 and IL-13 appear to have opposing roles in the disease.

Although the majority of CD4+ T cells in atherosclerotic lesions are Th1-polarised (87), Th2 T cells (111), mast cells (4) and eosinophils (167) also contribute to atherogenesis and can be sources of IL-4 and IL-13 within plaques. Thus Th2 cytokines are present in atherosclerotic

plaques, but are generally found to be less abundant than typical pro-inflammatory cytokines such as IFN-γ and IL-6 (34, 58, 62, 142). Although there has been limited investigation of IL-4 and IL-13 levels in patients with atherosclerosis, two studies of patients with coronary artery disease (CAD) report both IL-4 and IL-13 to be among the cytokines whose levels were elevated with disease, while the anti-inflammatory cytokine IL-10 was decreased (104, 183). Interestingly, reduced plasma IL-13 was associated with coronary artery calcification suggesting a protective role (182), while peripheral blood mononuclear cells (PBMCs) from patients with subclinical femoral artery atherosclerosis show strongly elevated IL-4 expression, in support of a pathogenic role (143). However it should be noted that in a correlative study of patients with periodontitis, increased C-reactive protein (CRP) and IL-18 were associated with a greater risk for atherosclerosis yet, by contrast, IL-4 was decreased in this setting (26). Collectively, studies in patients with CAD have provided evidence of differing roles of the Th2 cytokines,IL-4 and IL-13, and this is further supported by investigations utilising cultured macrophages and murine models of atherosclerosis (31, 115).

There is a growing body of *in vitro* evidence which suggests that IL-4 may be atherogenic. It has been shown to enhance foam cell formation (171) and, due to increased expression of the scavenger receptors CD36 and scavenger receptor type 1 (SR-A1), IL-4-polarised M2 macrophages exhibit a greater propensity to uptake cholesterol and a greater susceptibility to endoplasmic reticulum (ER) stress than IFN-γ-treated macrophages (171). These findings suggest that M2a macrophages may contribute to the development of the necrotic core of unstable plaques. Furthermore, treatment of macrophages with IL-4 increases proliferation (102), and induces fusion of macrophages into multinucleated giant cells that degrade elastic lamina (18), which would also contribute to an expanding necrotic core. Importantly, IL-4 has

also been implicated in the progression of atherosclerosis in murine studies. King *et al*. (115), demonstrated reductions in atherosclerotic lesion area in the aortic arch and thoracic aorta of female low density lipoprotein receptor $(LDLR)^{-/-}$ mice following IL-$4^{-/-}$ bone marrow transplantation. This is supported by a second study of global IL-4 deficiency in which aortic lesion area in apolipoprotein E $(ApoE)^{-/-}$ mice was reduced (44). Furthermore, fatty streak formation is attenuated in IL-4 deficient mice placed on a high fat diet and immunised against heat shock protein (HSP)-65 or *mycobacterium tuberculosis* to induce atherosclerosis (63). Finally, a recent study in mice with allergic asthma found that increased IL-4 and IL-17 expression was associated with accelerated development of atherosclerosis (219). Importantly, treatment with monoclonal antibodies against IL-4 reduced this effect (219). It should be noted however, that one study has reported no impact of IL-4 deficiency on atherosclerotic lesion development in hypercholesterolaemic or angiotensin II treated $ApoE^{-/-}$ or $LDLR^{-/-}$ mice (114) and another demonstrated that IL-4 treatment was atheroprotective in $ApoE^{-/-}$ mice fed a high fat diet and treated with ox-LDL (241). These opposing findings, with regard to IL-4, may be indicative of the nature of the murine model of atherosclerosis used. Collectively however, the evidence to date suggests that IL-4 promotes atherosclerosis.

In contrast to IL-4, although the study of IL-13 in atherosclerosis has been more limited, IL-13 has shown atheroprotective properties. Th2-derived IL-13 contributed to the beneficial effects of malon-dialdehyde-modified LDL immunisation in $LDLR^{-/-}$ mice with atherosclerosis (17). Here mice were immunised with MDA-LDL to induce antigen-specific Th2 responses involving the production of IgM antibodies specific for oxLDL. This treatment lead to reductions in lesion size and was characterised by increased production of IL-5 and IL-13, but only small quantities of IL-4, suggesting only a minor contribution of IL-4 to this protective

response (17). Recently, more direct evidence for IL-13 as an atheroprotective cytokine has come to light in a study by Cardilo-Reis *et al*., in which both IL-13 deficiency and IL-13 intervention treatment was investigated in mice (31). In this study, IL-13 treatment was administered to $LDLR^{-/-}$ mice with established atherosclerosis (fed on a high fat diet for 16 weeks). Treatment with IL-13 for 5 weeks did not reduce overall lesion size, but did lead to characteristics of plaque stabilisation with increased collagen content, reduced M1:M2 marker expression and an overall reduction in macrophage content (31). To further support these findings, a separate cohort of mice with bone marrow-specific deletion of IL-13, demonstrated increased aortic lesion size which was associated with a larger necrotic core and reduced M2 macrophage content (31). Although it should be noted that, as with IL-4, IL-13-polarised M2 macrophages have been shown to be susceptible to oxLDL-induced apoptosis via enhanced ER stress (96), overall the available evidence suggests an atheroprotective role for IL-13. This effect appears to be, at least in part, via its ability to increase the activation of M2 macrophages.

Whilst both IL-4 and IL-13 promote an M2 phenotype, their disparate effects in atherosclerosis may be related to differences in their potency and efficacy to promote M2 polarisation and ability to modulate M2 macrophage function. Interestingly, both types of IL-4 receptors (type I and type II) are expressed on macrophages and this could be a potential point of difference. Thus via activation of different receptors and downstream signalling pathways, IL-4 and IL-13 may induce the expression of distinct macrophage effector molecules, a concept which remains to be investigated.

Distinct signalling pathways employed by IL-4 and IL-13

IL-4 can activate two different heterodimeric receptor complexes (known as type I and type II IL-4 receptors), the type II IL-4 receptor being shared with IL-13. Macrophages are one of a small number of cell types which express both type I and II receptors with type I receptor expression is mainly limited to haematopoietic cells (152). While levels of expression can differ between cell lines, it is reported that macrophages express more type I, than type II, receptors (107). The type I receptor consists of the IL-4Rα subunit complexed with the IL-2Rγ (also known as the γC chain) and is specific for IL-4. The type II receptor also requires IL-4Rα, but instead complexes with the IL-13Rα1 subunit and is activated by both IL-4 and IL-13 (Figure 1.5). Despite the involvement of the IL-4Rα subunit in both complexes, the activation and assembly of the type II receptor differs between the two cytokines. IL-4 binds the IL-4Rα subunit, which will then associate with either the IL-2Rγ or IL-13Rα1 subunit to form the receptor complex. IL-13 on the other hand does not bind to IL-4Rα, but instead binds to IL-13Rα1 which subsequently forms the type II receptor by associating with IL-4Rα (202). Thus as IL-4 has two receptor targets on macrophages, compared to a single receptor target for IL-13, this may underlie its distinct actions. Indeed, several studies of monocytes and macrophages have reported greater sensitivity to IL-4 than IL-13, attributed in part to lower expression of the type II receptor and preferential activation of the type I receptor by IL-4 (80, 83, 107). Of note, IL-13 exhibits high affinity for a 'decoy' receptor, IL-13Rα2 (144), which is not constitutively expressed on macrophages. Interestingly, one study has reported that its expression can be induced in macrophages by treatment with IL-4 or IL-13, in combination with TNFα, and that it could play a signalling role in these cells (53).

The involvement of divergent downstream signalling pathways in response to these cytokines is also evident. Although both receptors recruit STAT6 and STAT3 (16), key differences in signalling include the recruitment of PI3K/Akt and cAMP response element binding protein (CREB) (83, 101) via the type I receptor by IL-4, and STAT1 recruitment by IL-13 via the type II receptor (16). Although STAT1 activation was absent in monocytes treated with IL-4 (16), it should be noted that this is due to its preference for the type I receptor and hence it too can recruit STAT1 if the type II receptor predominates (218). Interestingly, PI3K inhibition is protective against plaque rupture (237) and CREB signalling can regulate NADPH oxidase activity (59), a key driver of ROS production. Although ROS production has generally been regarded as a function of M1 macrophages, IL-4 has previously been shown to promote vascular oxidative stress (133). There is hence potential for a role of IL-4 in stimulating NOX expression and activity in macrophages, while the distinct signalling of IL-13 suggests it may not have such an effect. Therefore the distinctive signalling pathways employed by the type I and II receptors (outlined in Figure 1.5), may underlie their differential effects of these Th2 cytokines on macrophage function and atherogenesis.

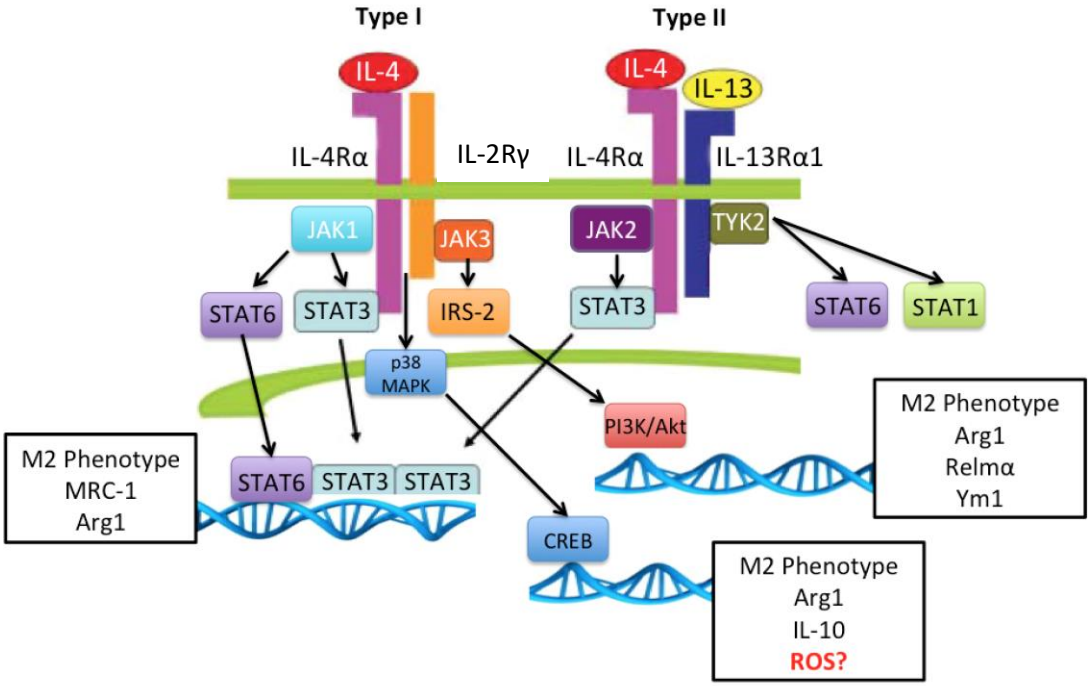

Figure 1.5 Signalling pathways associated with IL-4 and IL-13 receptors. The Type I IL-4 receptor comprises the IL-4Rα subunit linked to JAK1/STAT3/STAT6 (16) and IL-2Rγ subunit linked to JAK3/IRS-2/PI3K/Akt pathways (216). In addition, IL-4 may stimulate the p38 MAPK/CREB pathway (101). The type II IL-4 receptor comprises the IL-13Rα1 subunit (arrows to M2 phenotype omitted for clarity) linked to TYK2/STAT1/STAT6 and the IL-4Rα linked to the JAK2/STAT3 (16).Figure adapted from Oh *et al* (2010) (170).

1.3.2.3 The Apolipoprotein E-deficient (ApoE$^{-/-}$) mouse model of atherosclerosis

The ApoE deficient mouse is a well accepted model of atherosclerosis and is used in this thesis to explore macrophage phenotypes during atherogenesis. ApoE is a glycoprotein involved in plasma lipoprotein transport. As a high affinity ligand for several receptors of the LDLR family it allows for specific uptake of bound lipoproteins by the liver for metabolism (238). Thus deficiency in ApoE results in the accumulation of cholesterol in the circulation which leads to the development of atherosclerosis (238). The ApoE$^{-/-}$ mouse, as a model for atherosclerosis, emerged in 1992 with two laboratory groups in the United States characterising inactivation of the ApoE gene by homologous recombination in murine embryonic stem cells (178, 179). These mice were shown to have elevated plasma cholesterol levels, which were exacerbated on a high fat Western-type diet, and atherosclerotic lesions were reported at 10 weeks of age (179). Since then ApoE$^{-/-}$ mice have been widely used to study the development of atherosclerotic plaques and to assess the effects of genetic (21, 106) or pharmacological interventions (9) on the disease.

The progression of atherosclerotic lesions in ApoE$^{-/-}$ mice has been well characterised. By 8-10 weeks of age on a normal diet, fatty streaks containing smooth muscle and foam cells are evident and develop into more advanced fibrous plaques between 15-20 weeks with almost total vessel occlusion observed in old mice (~70 weeks) (156). This process is accelerated on a high fat diet with 90% or more of the vessel occluded by 32 weeks (37). Lesions are predominantly observed in the aortic root, aortic arch, and the common carotid and innominate (brachiocephalic) arteries (155, 156). An important aspect of the pathogenesis of atherosclerosis is the loss of stability of lesions and hence susceptibility to rupture resulting in vascular complications (137). There is debate as to whether plaque rupture occurs in the

ApoE$^{-/-}$ model however, given that the development of an acellular necrotic core, loss of fibrous cap, and intraplaque haemorrhage can all be observed in advanced lesions from these mice, they do appear to parallel human atherosclerosis (155, 156). This, in addition to the hypercholesterolemia, enhanced oxidative stress and endothelial dysfunction, which are also common to human disease (156), makes them an appropriate model for the study of human atherosclerosis.

1.3.3 Hypertension

Hypertension is defined as a systolic blood pressure (SBP) of at least 140 mmHg and/or a diastolic blood pressure (DBP) of more than 90 mmHg. It is a major risk factor for cardiovascular events such as myocardial infarction, stroke and kidney disease (23) and it affects approximately one third of the Western population (57). A contributor and major complication of the disease is stiffening of the aorta (108) which occurs via fibrotic mechanisms in the vessel wall and can contribute to end organ damage. Hence pulse wave velocity (PWV), a measure of aortic stiffening, is strongly correlated with the incidence of major cardiovascular events (19, 129, 154, 159). Vascular inflammation is shown to contribute to these processes (157). Importantly, current treatments for hypertension which include angiotensin converting enzyme (ACE) inhibitors, beta blockers, calcium channel blockers and diuretics (172) do not directly target the inflammatory or pro-fibrotic mechanisms implicated in the disease. Furthermore a need for new therapies is evident as a large cohort of patients taking two or more classes of these traditional antihypertensives are resistant to treatment and/or remain at high risk of cardiovascular events (1, 51, 109).

In the setting of hypertension, leukocytes infiltrate into the vessel wall, as well as the heart (76) and kidneys (105), where they can contribute to vessel and organ damage. Vessel

stiffening, which involves the accumulation of collagen and loss of elastin in the vessel wall, can be promoted both in response to inflammation-associated vascular injury and directly via the release of pro-fibrotic factors from immune cells (189, 230). Therefore, inflammation during hypertension may be central to the collagen accumulation and vessel stiffening which ultimately increases the likelihood of major cardiovascular events. Macrophages are an important immune cell involved in vascular inflammation and remodelling. They accumulate in the vessel wall throughout hypertension, predominantly in the adventitia and perivascular adipose tissue (7, 246), and are major generators of ROS, inflammatory cytokines and pro-fibrotic factors, all of which can contribute to the development of hypertension (213). An important role for macrophages was demonstrated by De Ciuceis *et al*. in a study of mice deficient in M-CSF. The loss of M-CSF, and subsequent reduction in macrophage accumulation in the vessel wall, protected mice against angiotensin II-induced hypertension and resistance artery remodelling (46). These effects were later replicated in the one kidney/deoxycorticosterone acetate(DOCA)-salt model of hypertension (116). Furthermore, Wenzel *et al.* showed that selective depletion of circulating monocytes markedly reduced macrophage numbers in the vessel wall and attenuated angiotensin II-induced hypertension and vascular dysfunction (225). Hypertension was restored with adoptive transfer of Ly6C^{high} monocytes, suggesting a key role for monocytes and macrophages in this hypertensive response (225). While the accumulation of macrophages is reported in many studies of hypertension, the activation state of these macrophages has only recently begun to be reported.

In the context of hypertension and arterial stiffening, roles for both macrophage phenotypes have been identified (Table 1.3). Through the release of pro-inflammatory cytokines and ROS,

M1 macrophages are likely to play a role in the early stages of the disease. Increased M1 marker expression was reported in the aorta of hypertensive mice following 7 days of angiotensin II treatment and was associated with the development of endothelial dysfunction (119). Further evidence for a role for M1 macrophages is observed in mice lacking the mineralcorticoid receptor (MR) on myeloid cells, with a reduction in blood pressure associated with an attenuation in M1 macrophage marker expression (215). However, in mice deficient in monocyte/macrophage-specific MR, protection from cardiac fibrosis and hypertension was observed despite no change in inflammatory marker expression or macrophage number. In this study, the protective effects correlated with reduced TGF-β expression, a pro-fibrotic cytokine known to be produced by M2 macrophages (190). Indeed, a definitive role for M2 macrophages in vascular fibrosis and hypertension, has recently emerged. Our laboratory has shown that following 28 days of angiotensin II-induced hypertension in mice, a large increase in aortic M2 macrophages is observed (161). This was associated with enhanced collagen deposition, vascular remodelling and aortic stiffening; effects that were prevented when Ly6C^{high} monocyte infiltration was blocked using a CCR2 inhibitor, in turn reducing the M2 macrophage population in the aorta (161). The mechanisms via which M2 macrophages promote fibrosis in the vessel wall have not been fully elucidated. However, given that M2 macrophages generate TGF-β and platelet derived growth factor (PDGF), which promote differentiation of fibroblasts to collagen generating myofibroblasts (68, 72), it may be anticipated that these factors contribute to vascular fibrosis and stiffening in hypertension. Excitingly, a recently identified pro-fibrotic chemokine, CCL18, is abundantly produced by M2 macrophages (198) and may represent be a novel therapeutic target in the treatment of cardiovascular diseases, particularly hypertension.

1.3.3.1 Pro-fibrotic processes in the vessel wall

Pro-fibrotic mediators such as TGF-β can directly stimulate the production and release of collagen from multiple cell types in the vessel wall (eg. endothelial cells, VSMCs and fibroblasts) leading to vessel stiffening (86). As part of this response, some mediators can also promote fibroblast differentiation into collagen-producing myofibroblasts. This effect can be identified by induction of the expression of the VSMC marker alpha-smooth muscle actin (α-SMA) in fibroblasts (103, 140).

Several different types of collagen are found in the vessel wall including the fibrillary collagen types I, III and V, as well as the basement membrane collagen type IV. Collagen I fibrils are the most abundant, making up approximately 67% of total collagen in the aorta (173). Collagen I, III, and to a lesser extent V, are produced by VSMCs and myofibroblasts in the media and adventitia and are the major contributors to the mechanical strength of the artery wall (173). These collagens are characterised by a triple helical structure and are subject to much processing both intra- and extra-cellularly (Figure 1.6A).

Collagen generation begins with the synthesis of pro-collagen chains which are folded together in a triple helix with N- and C-propeptides at either end. In the case of collagen I, this consists of two collagen 1a1 and a single collagen 1a2 chain (30). These pro-collagen chains are secreted and their N- and C-propeptide domains are then cleaved by specific N- or C-proteinases to generate collagen fibrils. These fibrils aggregate and assemble into collagen fibers in the vessel wall (30) (Figure 1.6A). Proteolytic enzymes, predominantly but not limited to MMPs, can then cleave collagen fibrils into fragments, leading to degradation (Figure 1.6B). However this process can also be involved in ECM remodelling and hence MMPs can be identified as playing pro- and anti-fibrotic roles in different settings (66). Collagen fibrils can

be cleaved by a subset of MMPs including MMP1, MMP8, MMP13, MMP14, MMP16 and MMP18, as well as the lysosomal cysteine protease cathepsin K, which can cleave collagen I. The resultant collagen fragments can then be further cleaved by the gelatinases MMP2 and MMP9 (Figure 1.6B) (153). Though clearly a complex process, increased collagen deposition in the vessel wall is associated with aortic remodelling and stiffening, an important contributor to hypertension (161). Stimuli which increase myofibroblast differentiation and stimulate collagen synthesis are therefore likely to be detrimental in this setting.

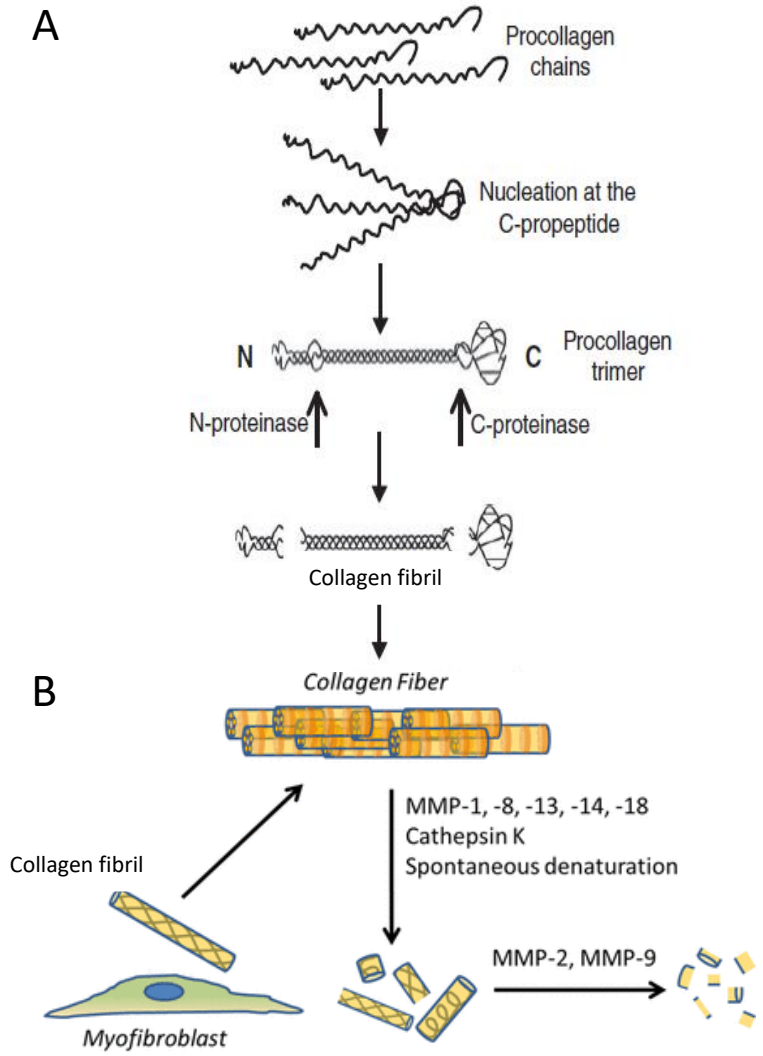

Figure 1.6 Collagen synthesis and processing. A. Adapted from Canty and Kadler (2005) (30). Pro-collagen chains form a triple helical structure flanked by N- and C-propeptides. These pro-collagen trimers can be released from the cell and cleaved into collagen fibrils by N- and C-proteinases. B. Adapted from McKleroy *et al.* (2013) (153). Collagen fibrils aggregate to form fibers but can be cleaved by MMPs in two steps; first into 1/4 and 3/4 fragments by several MMPs (eg. MMP1 and MMP8) and then further degraded by MMP2 and MMP9.

1.3.3.2 Pro-fibrotic actions of M2 macrophages

While the wound healing response, involving recruitment of M2a macrophages is vital to repair tissues and resolve inflammation, chronic or dysregulated activation of these macrophages can lead to fibrosis. This response is driven by the production of growth factors such as PDGF, TGF-β1, IGF-1 and VEGF-α promoting local cell proliferation, angiogenesis, and myofibroblast differentiation leading to increased synthesis of ECM components such as collagen (231). In the setting of hypertension, these actions of M2 macrophages are likely to be detrimental, as remodelling of the vessel wall and increased deposition of collagen leads to vessel stiffening, an important contributor to the disease. In addition to the secretion of growth factors, other potential mediators of these responses include ROS, particularly hydrogen peroxide, and the pro-fibrotic chemokine CCL18 which is highly expressed in M2a macrophages (198). The potential roles of these mediators are discussed below.

1.3.3.3 M2 macrophage-derived ROS in the pro-fibrotic response

Oxidative stress, an abundance of cellular oxidants over antioxidants, has long been associated with cardiovascular disease and ROS are implicated in hypertension, cardiac fibrosis and cardiac hypertrophy. Key components of these conditions are tissue remodelling and overproduction of ECM, typically from fibroblasts and smooth muscle cells. A role for reactive oxygen species and redox signalling in pro-fibrotic pathways is well recognised (8, 25) and ROS can induce upregulation of ECM proteins as well as TGF-β (74, 92, 169). In a cardiovascular setting, both superoxide (139, 141) and hydrogen peroxide (74, 221) have been shown to stimulate cardiac fibrosis and to be involved in angiotensin II signalling to promote myofibroblast differentiation and collagen production in cardiac and adventitial fibroblasts (194, 233).

Macrophages are a major source of ROS and there is some evidence to suggest ROS are generated by M2 macrophages (120). Although it remains to be thoroughly investigated, it is possible that M2 macrophage-derived ROS, particularly hydrogen peroxide, could contribute to their pro-fibrotic actions. While it is true that superoxide can be involved in intracellular signalling to induce fibrosis, as a more stable ROS, hydrogen peroxide is a more likely paracrine mediator of these responses (2). NOX-derived superoxide can be rapidly converted to hydrogen peroxide, via SOD, which can directly stimulate collagen production and myofibroblast differentiation *in vitro* (221). Evidence for a direct role of macrophage NOX-derived ROS in promoting fibrosis has been observed in pulmonary fibroblasts, where co-culture with alveolar macrophages lead to increases in collagen and α-SMA expression, an effect which was attenuated in the presence of the NOX inhibitor apocynin (33). Given that M2 macrophage accumulation is observed in the vessel wall during hypertension and contributes to aortic stiffening (161), it is plausible that hydrogen peroxide release from these macrophages may in part mediate these effects, though this remains to be investigated.

1.3.3.4 CCL18 as a potential M2 macrophage-derived mediator of aortic stiffening

CCL18, also known as pulmonary and activation-regulated chemokine (PARC) or macrophage inflammatory protein-4 (MIP-4) is another novel candidate which could mediate the M2 pro-fibrotic response in the vessel wall. It is produced by myeloid cells and is particularly abundant in alveolar and M2 macrophages (198). Its expression from macrophages and monocytes is highly induced by Th2 cytokines and can also be upregulated by IFN-γ and IL-10 (197, 198). Dendritic cells, eosinophils, chondrocytes and leukemia cells are a further source of CCL18 (198). The main recognised functions of CCL18 to date are chemoattraction of T and B

lymphocytes (particularly Th2 cells) and immature dendritic cells (98, 198), stimulation of collagen generation from pulmonary fibroblasts (3), and induction of M2 polarisation (197).

The receptor activated by CCL18 was recently identified to be the G-protein coupled receptor, CCR8 (98); the predominant chemokine receptor expressed on Th2 cells (244). However, CCL18 can also antagonise CCR3 (126) to limit leukocyte infiltration during allergic inflammation (166). As CCR3 activation has been shown to promote pulmonary fibrosis (117), it should be acknowledged that the potential pro-fibrotic actions of CCL18, through CCR8, may be tempered by its antagonism of CCR3 if both receptors are present. As CCL18 is not expressed in the rodent genome, the finding that it could activate CCR8 lead to the identification of murine CCL8 (mCCL8) as the functional analogue for human CCL18 (hCCL18) (97). Human CCL18 and murine CCL8 induce chemotactic responses via CCR8, most commonly on Th2-polarised T cells, sharing this receptor with the chemokine CCL1 (97, 98). Interestingly, CCL18 is highly expressed during inflammation and thus is likely to drive activation of CCR8 in inflammatory disease settings to a greater extent than CCL1 (126). Myeloid and dendritic cell-derived CCL18 was recently implicated in crescentic glomerulonephritis with increased serum CCL18, but not CCL1, observed in patients suffering from renal relapses (22). To complement these findings, genetic deletion of CCR8 in a mouse model of crescentic glomerulonephritis was shown to confer protection. Whilst modest CCL1 upregulation was observed in this model, its levels were far inferior to those of CCL8 (22). In addition to its expression on immune cells, CCR8 expression has also been reported on VSMCs, endothelial cells, and fibroblasts (22, 79). Whilst there is some evidence linking CCL18 to the development of cardiovascular disease, whether CCL18 may target some or all of these cell types to promote vascular fibrosis remains to be investigated.

A role for CCL18 in tissue remodelling and fibrosis is evident in the lung with its expression increased in patients with pulmonary disease and associated with collagen deposition (3, 180). This effect has not been directly investigated in hypertension, yet there is growing evidence implicating CCL18 in cardiovascular disease. The risk of a fatal cardiovascular event in patients suffering from acute coronary syndrome is 3 times greater in patients with high serum CCL18 (47). Furthermore, CCL18 was identified as a potential biomarker for refractory unstable angina pectoris (UAP), increasing in expression during episodes of UAP (123). Additionally, increased CCL18 levels in aneurysm patients lead to the suggestion that it could serve as a marker for aneurysm rupture risk (40). Expression of CCL18 is also abundant in human carotid atherosclerotic plaques (75). Interestingly, in patients with systemic sclerosis, Gunther *et al.* reported increased CCL18 expression from peripheral blood mononuclear cells (PBMCs) following autoantibody activation of the angiotensin II receptor type 1 (AT_1R), a receptor implicated in hypertension (73). This increase in CCL18 correlated with the incidence of vascular complications in these patients (73). Further evidence for the potential involvement of CCL18 in hypertension is evident in angiotensin II-induced hypertensive mice, with increased aortic CCL8 mRNA associated with vascular stiffening (161). Taken together, these findings suggest that CCL18 may be upregulated in a hypertensive setting and associated with vascular fibrosis. Therefore CCL18, and its receptor CCR8, could represent novel therapeutic targets to reduce cardiovascular complications associated with diseases such as hypertension.

1.3.3.5 Angiotensin II model of hypertension

The angiotensin II-infusion model of hypertension is commonly used to examine the mechanisms involved in the pathogenesis of hypertension and is utilised in this thesis. Over-

activation of the renin angiotensin aldosterone system (RAAS) has long been recognised as a major contributor to the development of hypertension and key regulator of systemic blood pressure (224). Angiotensin II plays a central role in this system. Thus via the activation of AT_1R on cells of the blood vessels, kidney and nervous system, it serves as a potent vasoconstrictor, increases sodium reabsorption and enhances sympathetic neurotransmission all of which contribute to elevations in blood pressure. Additional effects to increase oxidative stress, inflammation and endothelial dysfunction and thrombosis are also evident and implicated in hypertension (224). As such, angiotensin II-induced hypertension, in which animals are chronically treated with angiotensin II, has become a widely used model of experimental hypertension.

An important finding in the development of this model of hypertension was that chronic administration of low 'subpressor' doses of angiotensin II could induce a gradual rise in blood pressure in rodents (24, 128, 205). This lead to a commonly used 2 week model of low dose angiotensin II infusion, often delivered subcutaneously via osmotic mini-pump. In mice, angiotensin II is typically infused at a dose of approximately 0.7 mg/kg/day for 1-4 weeks (27, 32, 161, 225). This model is particularly attractive as hypertension can be easily induced without the need for additional surgery or manipulations (eg. removal of a kidney, addition of salt to drinking water) and can be used across many species (128). This model is known to involve multiple neuroendocrine, vascular and immunological mechanisms which can be readily studied. Relevance to human disease is evident with RAAS upregulation observed in human hypertension and inhibitors of this pathway in common therapeutic use (212). Hence the angiotensin II infusion model of hypertension is a valuable tool in assessing the mechanisms underlying hypertension development in humans.

1.4 Conclusions and therapeutic implications

In summary, macrophages play important and diverse roles in cardiovascular disease and can exist in a range of different phenotypes including but not limited to, the pro-inflammatory M1 and regulatory and reparative M2 macrophages. Many studies have investigated ways of skewing the macrophage population towards the M2 phenotype to limit inflammation and alleviate cardiovascular disease, particularly in atherosclerosis and diabetes (85, 112, 174, 235). Whilst preventing monocyte infiltration, and suppressing inflammatory responses, is effective in mouse models of disease, treatments which promote systemic immunosuppression are likely to be detrimental in humans in the long term as they would compromise host defence. Hence therapies which alter macrophage phenotype would need to be targeted to appropriate tissues (eg. atherosclerotic plaques). A further limitation of treatments designed to promote one macrophage phenotype over another is that the population of macrophages in tissues is highly varied and phenotypes are often mixed. Furthermore, as has been discussed, both M1 and M2 macrophages can contribute to the pathophysiology of cardiovascular disease. In atherosclerosis, the M2 phenotype may be favourable over M1, yet the actions of these macrophages are not exclusively. Conversely, in hypertension both macrophage phenotypes play pathogenic roles, with M2 macrophages particularly central to hypertension and fibrosis due to their tissue remodelling properties. Investigating, and targeting, the potential mediators involved in the pathogenic effects of these macrophages may therefore be more efficacious in treating the disease, allowing for more specific targeting of the mechanisms implicated in both atherosclerosis and hypertension.

1.5 Hypothesis and aims of thesis

As has been discussed, both M1 and M2 macrophages contribute to the pathogenesis of hypertension and atherosclerosis. Identification of novel markers of either phenotype would aid in a more thorough investigation and identification of these cells in human disease. From a therapeutic perspective, it is important to understand the mechanisms, and effector molecules, involved in the pathological actions of these macrophage phenotypes and we are particularly interested in the potential atherogenic and pro-fibrotic actions of M2 macrophages in the vessel wall. We hypothesise that the generation of ROS may be an important, previously unrecognised, property of M2 macrophages which would make them less protective in atherosclerosis and could underpin the differential effects of IL-4 and IL-13 in this setting. Furthermore, M2 macrophage-derived ROS could play a role in the pro-fibrotic actions of M2 macrophages in hypertension. Given its association with human cardiovascular disease, and its role as a pro-fibrotic chemokine in the lung, we hypothesise that the M2 macrophage-derived chemokine, CCL18 may also have an important role to play in aortic remodelling and stiffening in hypertension. Therefore the specific aims of this thesis were to:

1. Identify novel markers of M1 and M2 macrophage polarisation via global proteomics and validate a novel marker in a mouse model of atherosclerosis (Chapter 3).

2. Characterise the ROS generating capacity of M1 and M2 macrophages and investigate the potential pro-fibrotic effects of M2 macrophage-derived ROS (Chapter 4).

3. Compare the effects of different Th2 cytokines on macrophage function (Chapter 5).

4. Determine whether CCL18 mediates the pro-fibrotic actions of M2 macrophages in hypertension by targeting CCR8 in vascular cells (Chapter 6).

References

1. Achelrod D, Wenzel U, and Frey S. Systematic review and meta-analysis of the prevalence of resistant hypertension in treated hypertensive populations. *American journal of hypertension* 28: 355-361, 2015.

2. Ardanaz N, and Pagano PJ. Hydrogen peroxide as a paracrine vascular mediator: regulation and signaling leading to dysfunction. *Experimental biology and medicine (Maywood, NJ)* 231: 237-251, 2006.

3. Atamas SP, Luzina IG, Choi J, Tsymbalyuk N, Carbonetti NH, Singh IS, Trojanowska M, Jimenez SA, and White B. Pulmonary and activation-regulated chemokine stimulates collagen production in lung fibroblasts. *Am J Respir Cell Mol Biol* 29: 743-749, 2003.

4. Atkinson JB, Harlan CW, Harlan GC, and Virmani R. The association of mast cells and atherosclerosis: a morphologic study of early atherosclerotic lesions in young people. *Human pathology* 25: 154-159, 1994.

5. Bai Y, and Sun Q. Macrophage recruitment in obese adipose tissue. *Obesity reviews : an official journal of the International Association for the Study of Obesity* 16: 127-136, 2015.

6. Banfi B, Tirone F, Durussel I, Knisz J, Moskwa P, Molnar GZ, Krause KH, and Cox JA. Mechanism of Ca2+ activation of the NADPH oxidase 5 (NOX5). *Journal of Biological Chemistry* 279: 18583-18591, 2004.

7. Barhoumi T, Kasal DA, Li MW, Shbat L, Laurant P, Neves MF, Paradis P, and Schiffrin EL. T regulatory lymphocytes prevent angiotensin II-induced hypertension and vascular injury. *Hypertension* 57: 469-476, 2011.

8. Barnes JL, and Gorin Y. Myofibroblast differentiation during fibrosis: role of NAD(P)H oxidases. *Kidney international* 79: 944-956, 2011.

9. Bea F, Blessing E, Bennett B, Levitz M, Wallace EP, and Rosenfeld ME. Simvastatin promotes atherosclerotic plaque stability in apoE-deficient mice independently of lipid lowering. *Arterioscler Thromb Vasc Biol* 22: 1832-1837, 2002.

10. Becker S, and Daniel EG. Antagonistic and additive effects of IL-4 and interferon-gamma on human monocytes and macrophages: effects on Fc receptors, HLA-D antigens, and superoxide production. *Cell Immunol* 129: 351-362, 1990.

11. Bedard K, and Krause K-H. The NOX family of ROS-generating NADPH oxidases: Physiology and pathophysiology. *Physiological Reviews* 87: 245-313, 2007.

12. Bekkering S, Quintin J, Joosten LA, van der Meer JW, Netea MG, and Riksen NP. Oxidized low-density lipoprotein induces long-term proinflammatory cytokine production and foam cell formation via epigenetic reprogramming of monocytes. *Arterioscler Thromb Vasc Biol* 34: 1731-1738, 2014.

13. Bentzon JF, Otsuka F, Virmani R, and Falk E. Mechanisms of plaque formation and rupture. *Circ Res* 114: 1852-1866, 2014.

14. Bey EA, and Cathcart MK. In vitro knockout of human p47phox blocks superoxide anion production and LDL oxidation by activated human monocytes. *Journal of Lipid Research* 41: 489-495, 2000.

15. Bhaskaran G, Nii A, Sone S, and Ogura T. DIFFERENTIAL-EFFECTS OF INTERLEUKIN-4 ON SUPEROXIDE ANION PRODUCTION BY HUMAN ALVEOLAR MACROPHAGES STIMULATED WITH LIPOPOLYSACCHARIDE AND INTERFERON-GAMMA. *Journal of Leukocyte Biology* 52: 218-223, 1992.

16. Bhattacharjee A, Shukla M, Yakubenko VP, Mulya A, Kundu S, and Cathcart MK. IL-4 and IL-13 employ discrete signaling pathways for target gene expression in alternatively activated monocytes/macrophages. *Free radical biology & medicine* 54: 1-16, 2013.

17. Binder CJ, Hartvigsen K, Chang MK, Miller M, Broide D, Palinski W, Curtiss LK, Corr M, and Witztum JL. IL-5 links adaptive and natural immunity specific for epitopes of oxidized LDL and protects from atherosclerosis. *J Clin Invest* 114: 427-437, 2004.

18. Binder F, Hayakawa M, Choo MK, Sano Y, and Park JM. Interleukin-4-induced beta-catenin regulates the conversion of macrophages to multinucleated giant cells. *Molecular immunology* 54: 157-163, 2013.

19. Blacher J, Asmar R, Djane S, London GM, and Safar ME. Aortic pulse wave velocity as a marker of cardiovascular risk in hypertensive patients. *Hypertension* 33: 1111-1117, 1999.

20. Bleau G, Massicotte F, Merlen Y, and Boisvert C. Mammalian chitinase-like proteins. *Exs* 87: 211-221, 1999.

21. Boring L, Gosling J, Cleary M, and Charo IF. Decreased lesion formation in CCR2-/- mice reveals a role for chemokines in the initiation of atherosclerosis. *Nature* 394: 894-897, 1998.

22. Brix SR, Stege G, Disteldorf E, Hoxha E, Krebs C, Krohn S, Otto B, Klatschke K, Herden E, Heymann F, Lira SA, Tacke F, Wolf G, Busch M, Jabs WJ, Ozcan F, Keller F, Beige J, Wagner K, Helmchen U, Noriega M, Wiech T, Panzer U, and Stahl RA. CC Chemokine Ligand 18 in ANCA-Associated Crescentic GN. *Journal of the American Society of Nephrology : JASN* 26: 2105-2117, 2015.

23. Bromfield S, and Muntner P. High blood pressure: the leading global burden of disease risk factor and the need for worldwide prevention programs. *Curr Hypertens Rep* 15: 134-136, 2013.

24. Brown AJ, Casals-Stenzel J, Gofford S, Lever AF, and Morton JJ. Comparison of fast and slow pressor effects of angiotensin II in the conscious rat. *The American journal of physiology* 241: H381-388, 1981.

25. Brown DI, and Griendling KK. Regulation of signal transduction by reactive oxygen species in the cardiovascular system. *Circ Res* 116: 531-549, 2015.

26. Buhlin K, Hultin M, Norderyd O, Persson L, Pockley AG, Rabe P, Klinge B, and Gustafsson A. Risk factors for atherosclerosis in cases with severe periodontitis. *Journal of clinical periodontology* 36: 541-549, 2009.

27. Bush E, Maeda N, Kuziel WA, Dawson TC, Wilcox JN, DeLeon H, and Taylor WR. CC chemokine receptor 2 is required for macrophage infiltration and vascular hypertrophy in angiotensin II-induced hypertension. *Hypertension* 36: 360-363, 2000.

28. Calderon B, Suri A, Pan XO, Mills JC, and Unanue ER. IFN-gamma-dependent regulatory circuits in immune inflammation highlighted in diabetes. *J Immunol* 181: 6964-6974, 2008.

29. Calderon B, Suri A, and Unanue ER. In CD4+ T-cell-induced diabetes, macrophages are the final effector cells that mediate islet beta-cell killing: studies from an acute model. *The American journal of pathology* 169: 2137-2147, 2006.

30. Canty EG, and Kadler KE. Procollagen trafficking, processing and fibrillogenesis. *Journal of cell science* 118: 1341-1353, 2005.

31. Cardilo-Reis L, Gruber S, Schreier SM, Drechsler M, Papac-Milicevic N, Weber C, Wagner O, Stangl H, Soehnlein O, and Binder CJ. Interleukin-13 protects from atherosclerosis and modulates plaque composition by skewing the macrophage phenotype. *EMBO molecular medicine* 4: 1072-1086, 2012.

32. Chan CT, Sobey CG, Lieu M, Ferens D, Kett MM, Diep H, Kim HA, Krishnan SM, Lewis CV, Salimova E, Tipping P, Vinh A, Samuel CS, Peter K, Guzik TJ, Kyaw TS, Toh BH, Bobik A, and Drummond GR. Obligatory Role for B Cells in the Development of Angiotensin II-Dependent Hypertension. *Hypertension* 66: 1023-1033, 2015.

33. Chen C, Yang S, Zhang M, Zhang Z, Hong J, Han D, Ma J, Zhang SB, Okunieff P, and Zhang L. Triptolide mitigates radiation-induced pulmonary fibrosis via inhibition of axis of alveolar macrophages-NOXes-ROS-myofibroblasts. *Cancer biology & therapy* 17: 381-389, 2016.

34. Chinetti-Gbaguidi G, Baron M, Bouhlel MA, Vanhoutte J, Copin C, Sebti Y, Derudas B, Mayi T, Bories G, Tailleux A, Haulon S, Zawadzki C, Jude B, and Staels B. Human Atherosclerotic Plaque Alternative Macrophages Display Low Cholesterol Handling but High Phagocytosis Because of Distinct Activities of the PPAR gamma and LXR alpha Pathways. *Circulation Research* 108: 985-995, 2011.

35. Chinetti-Gbaguidi G, Colin S, and Staels B. Macrophage subsets in atherosclerosis. *Nature reviews Cardiology* 12: 10-17, 2015.

36. Chitu V, and Stanley ER. Colony-stimulating factor-1 in immunity and inflammation. *Curr Opin Immunol* 18: 39-48, 2006.

37. Coleman R, Hayek T, Keidar S, and Aviram M. A mouse model for human atherosclerosis: long-term histopathological study of lesion development in the aortic arch of apolipoprotein E-deficient (E0) mice. *Acta histochemica* 108: 415-424, 2006.

38. Colin S, Chinetti-Gbaguidi G, and Staels B. Macrophage phenotypes in atherosclerosis. *Immunological reviews* 262: 153-166, 2014.

39. Combadiere C, Potteaux S, Rodero M, Simon T, Pezard A, Esposito B, Merval R, Proudfoot A, Tedgui A, and Mallat Z. Combined inhibition of CCL2, CX3CR1, and CCR5 abrogates Ly6C(hi) and Ly6C(lo) monocytosis and almost abolishes atherosclerosis in hypercholesterolemic mice. *Circulation* 117: 1649-1657, 2008.

40. Courtois A, Nusgens BV, Hustinx R, Namur G, Gomez P, Kuivaniemi H, Defraigne JO, Colige AC, and Sakalihasan N. Gene expression study in positron emission tomography-

positive abdominal aortic aneurysms identifies CCL18 as a potential biomarker for rupture risk. *Molecular medicine (Cambridge, Mass)* 20: 697-706, 2014.

41. Cros J, Cagnard N, Woollard K, Patey N, Zhang SY, Senechal B, Puel A, Biswas SK, Moshous D, Picard C, Jais JP, D'Cruz D, Casanova JL, Trouillet C, and Geissmann F. Human CD14dim monocytes patrol and sense nucleic acids and viruses via TLR7 and TLR8 receptors. *Immunity* 33: 375-386, 2010.

42. Dai XM, Ryan GR, Hapel AJ, Dominguez MG, Russell RG, Kapp S, Sylvestre V, and Stanley ER. Targeted disruption of the mouse colony-stimulating factor 1 receptor gene results in osteopetrosis, mononuclear phagocyte deficiency, increased primitive progenitor cell frequencies, and reproductive defects. *Blood* 99: 111-120, 2002.

43. Darnell JE, Kerr IM, and Stark GR. JAK-STAT PATHWAYS AND TRANSCRIPTIONAL ACTIVATION IN RESPONSE TO IFNS AND OTHER EXTRACELLULAR SIGNALING PROTEINS. *Science* 264: 1415-1421, 1994.

44. Davenport P, and Tipping PG. The role of interleukin-4 and interleukin-12 in the progression of atherosclerosis in apolipoprotein E-deficient mice. *The American journal of pathology* 163: 1117-1125, 2003.

45. Dawson TC, Kuziel WA, Osahar TA, and Maeda N. Absence of CC chemokine receptor-2 reduces atherosclerosis in apolipoprotein E-deficient mice. *Atherosclerosis* 143: 205-211, 1999.

46. De Ciuceis C, Amiri F, Brassard P, Endemann DH, Touyz RM, and Schiffrin EL. Reduced Vascular Remodeling, Endothelial Dysfunction, and Oxidative Stress in Resistance Arteries of Angiotensin II–Infused Macrophage Colony-Stimulating Factor–Deficient Mice. *Aterioslcerosis, Thrombosis and Vascular Biology* 25: 2106-2113, 2005.

47. de Jager SC, Bongaerts BW, Weber M, Kraaijeveld AO, Rousch M, Dimmeler S, van Dieijen-Visser MP, Cleutjens KB, Nelemans PJ, van Berkel TJ, and Biessen EA. Chemokines CCL3/MIP1alpha, CCL5/RANTES and CCL18/PARC are independent risk predictors of short-term mortality in patients with acute coronary syndromes. *PLoS One* 7: e45804, 2012.

48. De Paoli F, Staels B, and Chinetti-Gbaguidi G. Macrophage phenotypes and their modulation in atherosclerosis. *Circulation journal : official journal of the Japanese Circulation Society* 78: 1775-1781, 2014.

49. de Pinho RT, da Silva WS, de Castro Cortes LM, da Silva Vasconcelos Sousa P, de Araujo Soares RO, and Alves CR. Production of MMP-9 and inflammatory cytokines by Trypanosoma cruzi-infected macrophages. *Experimental parasitology* 147: 72-80, 2014.

50. Drummond GR, Selemidis S, Griendling KK, and Sobey CG. Combating oxidative stress in vascular disease: NADPH oxidases as therapeutic targets. *Nature Reviews Drug Discovery* 10: 453-471, 2011.

51. Egan BM, Zhao Y, Axon RN, Brzezinski WA, and Ferdinand KC. Uncontrolled and apparent treatment resistant hypertension in the United States, 1988 to 2008. *Circulation* 124: 1046-1058, 2011.

52. Ferrante CJ, Pinhal-Enfield G, Elson G, Cronstein BN, Hasko G, Outram S, and Leibovich SJ. The adenosine-dependent angiogenic switch of macrophages to an M2-like phenotype is independent of interleukin-4 receptor alpha (IL-4Ralpha) signaling. *Inflammation* 36: 921-931, 2013.

53. Fichtner-Feigl S, Strober W, Kawakami K, Puri RK, and Kitani A. IL-13 signaling through the IL-13alpha2 receptor is involved in induction of TGF-beta1 production and fibrosis. *Nat Med* 12: 99-106, 2006.

54. Fink LN, Oberbach A, Costford SR, Chan KL, Sams A, Bluher M, and Klip A. Expression of anti-inflammatory macrophage genes within skeletal muscle correlates with insulin sensitivity in human obesity and type 2 diabetes. *Diabetologia* 56: 1623-1628, 2013.

55. Finn AV, Nakano M, Polavarapu R, Karmali V, Saeed O, Zhao X, Yazdani S, Otsuka F, Davis T, Habib A, Narula J, Kolodgie FD, and Virmani R. Hemoglobin directs macrophage differentiation and prevents foam cell formation in human atherosclerotic plaques. *J Am Coll Cardiol* 59: 166-177, 2012.

56. Fleetwood AJ, Lawrence T, Hamilton JA, and Cook AD. Granulocyte-macrophage colony-stimulating factor (CSF) and macrophage CSF-dependent macrophage phenotypes display differences in cytokine profiles and transcription factor activities: Implications for CSF blockade in inflammation. *Journal of Immunology* 178: 5245-5252, 2007.

57. Franklin SS, Gustin Wt, Wong ND, Larson MG, Weber MA, Kannel WB, and Levy D. Hemodynamic patterns of age-related changes in blood pressure. The Framingham Heart Study. *Circulation* 96: 308-315, 1997.

58. Frostegard J, Ulfgren AK, Nyberg P, Hedin U, Swedenborg J, Andersson U, and Hansson GK. Cytokine expression in advanced human atherosclerotic plaques: dominance of pro-inflammatory (Th1) and macrophage-stimulating cytokines. *Atherosclerosis* 145: 33-43, 1999.

59. Fu X, Beer DG, Behar J, Wands J, Lambeth D, and Cao W. cAMP-response element-binding protein mediates acid-induced NADPH oxidase NOX5-S expression in Barrett esophageal adenocarcinoma cells. *Journal of Biological Chemistry* 281: 20368-20382, 2006.

60. Fukai T, and Ushio-Fukai M. Superoxide dismutases: role in redox signaling, vascular function, and diseases. *Antioxidants & redox signaling* 15: 1583-1606, 2011.

61. Galkina E, and Ley K. Leukocyte influx in atherosclerosis. *Current Drug Targets* 8: 1239-1248, 2007.

62. Geng YJ, Holm J, Nygren S, Bruzelius M, Stemme S, and Hansson GK. Expression of the macrophage scavenger receptor in atheroma. Relationship to immune activation and the T-cell cytokine interferon-gamma. *Arterioscler Thromb Vasc Biol* 15: 1995-2002, 1995.

63. George J, Shoenfeld Y, Gilburd B, Afek A, Shaish A, and Harats D. Requisite role for interleukin-4 in the acceleration of fatty streaks induced by heat shock protein 65 or Mycobacterium tuberculosis. *Circ Res* 86: 1203-1210, 2000.

64. Gerber JS, and Mosser DM. Reversing lipopolysaccharide toxicity by ligating the macrophage Fc gamma receptors. *J Immunol* 166: 6861-6868, 2001.

65. Gerhardt T, and Ley K. Monocyte trafficking across the vessel wall. *Cardiovasc Res* 107: 321-330, 2015.

66. Giannandrea M, and Parks WC. Diverse functions of matrix metalloproteinases during fibrosis. *Disease models & mechanisms* 7: 193-203, 2014.

67. Ginhoux F, and Jung S. Monocytes and macrophages: developmental pathways and tissue homeostasis. *Nat Rev Immunol* 14: 392-404, 2014.

68. Glim JE, Niessen FB, Everts V, van Egmond M, and Beelen RH. Platelet derived growth factor-CC secreted by M2 macrophages induces alpha-smooth muscle actin expression by dermal and gingival fibroblasts. *Immunobiology* 218: 924-929, 2013.

69. Gomez Perdiguero E, Klapproth K, Schulz C, Busch K, Azzoni E, Crozet L, Garner H, Trouillet C, de Bruijn MF, Geissmann F, and Rodewald HR. Tissue-resident macrophages originate from yolk-sac-derived erythro-myeloid progenitors. *Nature* 518: 547-551, 2015.

70. Gordon S, and Martinez FO. Alternative Activation of Macrophages: Mechanism and Functions. *Immunity* 32: 593-604, 2010.

71. Grinberg S, Hasko G, Wu D, and Leibovich SJ. Suppression of PLCbeta2 by endotoxin plays a role in the adenosine A(2A) receptor-mediated switch of macrophages from an

inflammatory to an angiogenic phenotype. *The American journal of pathology* 175: 2439-2453, 2009.

72. Guimaraes DA, Rizzi E, Ceron CS, Martins-Oliveira A, Gerlach RF, Shiva S, and Tanus-Santos JE. Atorvastatin and sildenafil decrease vascular TGF-beta levels and MMP-2 activity and ameliorate arterial remodeling in a model of renovascular hypertension. *Redox biology* 6: 386-395, 2015.

73. Gunther J, Kill A, Becker MO, Heidecke H, Rademacher J, Siegert E, Radic M, Burmester GR, Dragun D, and Riemekasten G. Angiotensin receptor type 1 and endothelin receptor type A on immune cells mediate migration and the expression of IL-8 and CCL18 when stimulated by autoantibodies from systemic sclerosis patients. *Arthritis research & therapy* 16: R65, 2014.

74. Guo JL, Yu Y, Jia YY, Ma YZ, Zhang BY, Liu PQ, Chen SR, and Jiang JM. Transient receptor potential melastatin 7 (TRPM7) contributes to H2O2-induced cardiac fibrosis via mediating Ca(2+) influx and extracellular signal-regulated kinase 1/2 (ERK1/2) activation in cardiac fibroblasts. *Journal of pharmacological sciences* 125: 184-192, 2014.

75. Hagg DA, Olson FJ, Kjelldahl J, Jernas M, Thelle DS, Carlsson LM, Fagerberg B, and Svensson PA. Expression of chemokine (C-C motif) ligand 18 in human macrophages and atherosclerotic plaques. *Atherosclerosis* 204: e15-20, 2009.

76. Haller H, Behrend M, Park JK, Schaberg T, Luft FC, and Distler A. Monocyte infiltration and c-fms expression in hearts of spontaneously hypertensive rats. *Hypertension* 25: 132-138, 1995.

77. Hanna RN, Carlin LM, Hubbeling HG, Nackiewicz D, Green AM, Punt JA, Geissmann F, and Hedrick CC. The transcription factor NR4A1 (Nur77) controls bone marrow differentiation and the survival of Ly6C- monocytes. *Nat Immunol* 12: 778-785, 2011.

78. Hanninen A, Jalkanen S, Salmi M, Toikkanen S, Nikolakaros G, and Simell O. Macrophages, T cell receptor usage, and endothelial cell activation in the pancreas at the onset of insulin-dependent diabetes mellitus. *J Clin Invest* 90: 1901-1910, 1992.

79. Haque NS, Fallon JT, Pan JJ, Taubman MB, and Harpel PC. Chemokine receptor-8 (CCR8) mediates human vascular smooth muscle cell chemotaxis and metalloproteinase-2 secretion. *Blood* 103: 1296-1304, 2004.

80. Hart PH, Bonder CS, Balogh J, Dickensheets HL, Donnelly RP, and Finlay-Jones JJ. Differential responses of human monocytes and macrophages to IL-4 and IL-13. *J Leukoc Biol* 66: 575-578, 1999.

81. Hashimoto D, Chow A, Noizat C, Teo P, Beasley MB, Leboeuf M, Becker CD, See P, Price J, Lucas D, Greter M, Mortha A, Boyer SW, Forsberg EC, Tanaka M, van Rooijen N, Garcia-Sastre A, Stanley ER, Ginhoux F, Frenette PS, and Merad M. Tissue-resident macrophages self-maintain locally throughout adult life with minimal contribution from circulating monocytes. *Immunity* 38: 792-804, 2013.

82. He C, Ryan AJ, Murthy S, and Carter AB. Accelerated development of pulmonary fibrosis via Cu,Zn-superoxide dismutase-induced alternative activation of macrophages. *J Biol Chem* 288: 20745-20757, 2013.

83. Heller NM, Qi X, Junttila IS, Shirey KA, Vogel SN, Paul WE, and Keegan AD. Type I IL-4Rs Selectively Activate IRS-2 to Induce Target Gene Expression in Macrophages. *Science Signaling* 1: 2008.

84. Hilgendorf I, Gerhardt LM, Tan TC, Winter C, Holderried TA, Chousterman BG, Iwamoto Y, Liao R, Zirlik A, Scherer-Crosbie M, Hedrick CC, Libby P, Nahrendorf M, Weissleder R, and Swirski FK. Ly-6Chigh monocytes depend on Nr4a1 to balance both inflammatory and reparative phases in the infarcted myocardium. *Circ Res* 114: 1611-1622, 2014.

85. Hirata Y, Tabata M, Kurobe H, Motoki T, Akaike M, Nishio C, Higashida M, Mikasa H, Nakaya Y, Takanashi S, Igarashi T, Kitagawa T, and Sata M. Coronary Atherosclerosis Is Associated With Macrophage Polarization in Epicardial Adipose Tissue. *Journal of the American College of Cardiology* 58: 248-255, 2011.

86. Hori D, Dunkerly-Eyring B, Nomura Y, Biswas D, Steppan J, Henao-Mejia J, Adachi H, Santhanam L, Berkowitz DE, Steenbergen C, Flavell RA, and Das S. miR-181b regulates vascular stiffness age dependently in part by regulating TGF-beta signaling. *PLoS One* 12: e0174108, 2017.

87. Huber SA, Sakkinen P, David C, Newell MK, and Tracy RP. T helper-cell phenotype regulates atherosclerosis in mice under conditions of mild hypercholesterolemia. *Circulation* 103: 2610-2616, 2001.

88. Hulsmans M, and Holvoet P. The vicious circle between oxidative stress and inflammation in atherosclerosis. *Journal of Cellular and Molecular Medicine* 14: 70-78, 2010.

89. Hultqvist M, Olofsson P, Holmberg J, Backstrom BT, Tordsson J, and Holmdahl R. Enhanced autoimmunity, arthritis, and encephalomyelitis in mice with a reduced oxidative burst due to a mutation in the Ncf1 gene. *Proc Natl Acad Sci U S A* 101: 12646-12651, 2004.

90. Hultqvist M, Olofsson P, Wallner FK, and Holmdahl R. Pharmacological Potential of NOX2 Agonists in Inflammatory Conditions. *Antioxidants & redox signaling* 2014.

91. Hutchings P, Rosen H, O'Reilly L, Simpson E, Gordon S, and Cooke A. Transfer of diabetes in mice prevented by blockade of adhesion-promoting receptor on macrophages. *Nature* 348: 639-642, 1990.

92. Iglesias-De La Cruz MC, Ruiz-Torres P, Alcami J, Diez-Marques L, Ortega-Velazquez R, Chen S, Rodriguez-Puyol M, Ziyadeh FN, and Rodriguez-Puyol D. Hydrogen peroxide increases

extracellular matrix mRNA through TGF-beta in human mesangial cells. *Kidney international* 59: 87-95, 2001.

93. Iijima N, Mattei LM, and Iwasaki A. Recruited inflammatory monocytes stimulate antiviral Th1 immunity in infected tissue. *Proc Natl Acad Sci U S A* 108: 284-289, 2011.

94. Ingersoll MA, Spanbroek R, Lottaz C, Gautier EL, Frankenberger M, Hoffmann R, Lang R, Haniffa M, Collin M, Tacke F, Habenicht AJ, Ziegler-Heitbrock L, and Randolph GJ. Comparison of gene expression profiles between human and mouse monocyte subsets. *Blood* 115: e10-19, 2010.

95. Irvine KM, Burns CJ, Wilks AF, Su S, Hume DA, and Sweet MJ. A CSF-1 receptor kinase inhibitor targets effector functions and inhibits pro-inflammatory cytokine production from murine macrophage populations. *The FASEB Journal* 20: 1921-1923, 2006.

96. Isa SA, Ruffino JS, Ahluwalia M, Thomas AW, Morris K, and Webb R. M2 macrophages exhibit higher sensitivity to oxLDL-induced lipotoxicity than other monocyte/macrophage subtypes. *Lipids in Health and Disease* 10: 2011.

97. Islam SA, Chang DS, Colvin RA, Byrne MH, McCully ML, Moser B, Lira SA, Charo IF, and Luster AD. Mouse CCL8, a CCR8 agonist, promotes atopic dermatitis by recruiting IL-5+ T(H)2 cells. *Nat Immunol* 12: 167-177, 2011.

98. Islam SA, Ling MF, Leung J, Shreffler WG, and Luster AD. Identification of human CCR8 as a CCL18 receptor. *J Exp Med* 210: 1889-1898, 2013.

99. Italiani P, and Boraschi D. From Monocytes to M1/M2 Macrophages: Phenotypical vs. Functional Differentiation. *Frontiers in immunology* 5: 514, 2014.

100. Jakubzick C, Gautier EL, Gibbings SL, Sojka DK, Schlitzer A, Johnson TE, Ivanov S, Duan Q, Bala S, Condon T, van Rooijen N, Grainger JR, Belkaid Y, Ma'ayan A, Riches DW, Yokoyama WM, Ginhoux F, Henson PM, and Randolph GJ. Minimal differentiation of classical monocytes

as they survey steady-state tissues and transport antigen to lymph nodes. *Immunity* 39: 599-610, 2013.

101. Jang YS, Kim HA, Park SR, Lee MR, Park JB, and Kim PH. IL-4 stimulates mouse macrophages to express APRIL through p38MAPK and two different downstream molecules, CREB and Stat6. *Cytokine* 47: 43-47, 2009.

102. Jenkins SJ, Ruckerl D, Thomas GD, Hewitson JP, Duncan S, Brombacher F, Maizels RM, Hume DA, and Allen JE. IL-4 directly signals tissue-resident macrophages to proliferate beyond homeostatic levels controlled by CSF-1. *J Exp Med* 210: 2477-2491, 2013.

103. Jester JV, Barry-Lane PA, Cavanagh HD, and Petroll WM. Induction of alpha-smooth muscle actin expression and myofibroblast transformation in cultured corneal keratocytes. *Cornea* 15: 505-516, 1996.

104. Jha HC, Divya A, Prasad J, and Mittal A. Plasma circulatory markers in male and female patients with coronary artery disease. *Heart & lung : the journal of critical care* 39: 296-303, 2010.

105. Johnson RJ, Alpers CE, Yoshimura A, Lombardi D, Pritzl P, Floege J, and Schwartz SM. Renal injury from angiotensin II-mediated hypertension. *Hypertension* 19: 464-474, 1992.

106. Judkins CP, Diep H, Broughton BRS, Mast AE, Hooker EU, Miller AA, Selemidis S, Dusting GJ, Sobey CG, and Drummond GR. Direct evidence of a role for Nox2 in superoxide production, reduced nitric oxide bioavailability, and early atherosclerotic plaque formation in ApoE(-/-) mice. *American Journal of Physiology-Heart and Circulatory Physiology* 298: H24-H32, 2010.

107. Junttila IS, Mizukami K, Dickensheets H, Meier-Schellersheim M, Yamane H, Donnelly RP, and Paul WE. Tuning sensitivity to IL-4 and IL-13: differential expression of IL-4Ralpha, IL-

13Ralpha1, and gammac regulates relative cytokine sensitivity. *J Exp Med* 205: 2595-2608, 2008.

108. Kaess BM, Rong J, Larson MG, and et al. Aortic stiffness, blood pressure progression, and incident hypertension. *JAMA* 308: 875-881, 2012.

109. Kannel WB. Hypertension: reflections on risks and prognostication. *The Medical clinics of North America* 93: 541-558, Table of Contents, 2009.

110. Kayama H, Ramirez-Carrozzi VR, Yamamoto M, Mizutani T, Kuwata H, Iba H, Matsumoto M, Honda K, Smale ST, and Takeda K. Class-specific regulation of pro-inflammatory genes by MyD88 pathways and I kappa B zeta. *Journal of Biological Chemistry* 283: 12468-12477, 2008.

111. Ketelhuth DF, and Hansson GK. Cellular immunity, low-density lipoprotein and atherosclerosis: break of tolerance in the artery wall. *Thromb Haemost* 106: 779-786, 2011.

112. Khallou-Laschet J, Varthaman A, Fornasa G, Compain C, Gaston A-T, Clement M, Dussiot M, Levillain O, Graff-Dubois S, Nicoletti A, and Caligiuri G. Macrophage plasticity in experimental atherosclerosis. *PLoS ONE [Electronic Resource]* 5: e8852, 2010.

113. Kim JS, Yeo S, Shin DG, Bae YS, Lee JJ, Chin BR, Lee CH, and Baek SH. Glycogen synthase kinase 3beta and beta-catenin pathway is involved in toll-like receptor 4-mediated NADPH oxidase 1 expression in macrophages. *The FEBS journal* 277: 2830-2837, 2010.

114. King VL, Cassis LA, and Daugherty A. Interleukin-4 does not influence development of hypercholesterolemia or angiotensin II-induced atherosclerotic lesions in mice. *The American journal of pathology* 171: 2040-2047, 2007.

115. King VL, Szilvassy SJ, and Daugherty A. Interleukin-4 deficiency decreases atherosclerotic lesion formation in a site-specific manner in female LDL receptor-/- mice. *Arterioscler Thromb Vasc Biol* 22: 456-461, 2002.

116. Ko EA, Amiri F, Pandey NR, Javeshghani D, Leibovitz E, Touyz RM, and Schiffrin EL. Resistance artery remodeling in deoxycorticosterone acetate-salt hypertension is dependent on vascular inflammation: evidence from m-CSF-deficient mice. *American journal of physiology Heart and circulatory physiology* 292: H1789-1795, 2007.

117. Komai M, Tanaka H, Nagao K, Ishizaki M, Kajiwara D, Miura T, Ohashi H, Haba T, Kawakami K, Sawa E, Yoshie O, Inagaki N, and Nagai H. A novel CC-chemokine receptor 3 antagonist, Ki19003, inhibits airway eosinophilia and subepithelial/peribronchial fibrosis induced by repeated antigen challenge in mice. *Journal of pharmacological sciences* 112: 203-213, 2010.

118. Kopf M, Le Gros G, Bachmann M, Lamers MC, Bluethmann H, and Kohler G. Disruption of the murine IL-4 gene blocks Th2 cytokine responses. *Nature* 362: 245-248, 1993.

119. Kossmann S, Hu H, Steven S, Schonfelder T, Fraccarollo D, Mikhed Y, Brahler M, Knorr M, Brandt M, Karbach SH, Becker C, Oelze M, Bauersachs J, Widder J, Munzel T, Daiber A, and Wenzel P. Inflammatory monocytes determine endothelial nitric-oxide synthase uncoupling and nitro-oxidative stress induced by angiotensin II. *J Biol Chem* 289: 27540-27550, 2014.

120. Kraaij MD, Koekkoek KM, van der Kooij SW, Gelderman KA, and van Kooten C. Subsets of human type 2 macrophages show differential capacity to produce reactive oxygen species. *Cell Immunol* 284: 1-8, 2013.

121. Kraaij MD, Savage ND, van der Kooij SW, Koekkoek K, Wang J, van den Berg JM, Ottenhoff TH, Kuijpers TW, Holmdahl R, van Kooten C, and Gelderman KA. Induction of regulatory T cells by macrophages is dependent on production of reactive oxygen species. *Proc Natl Acad Sci U S A* 107: 17686-17691, 2010.

122. Kraaij MD, van der Kooij SW, Reinders ME, Koekkoek K, Rabelink TJ, van Kooten C, and Gelderman KA. Dexamethasone increases ROS production and T cell suppressive capacity by anti-inflammatory macrophages. *Molecular immunology* 49: 549-557, 2011.

123. Kraaijeveld AO, de Jager SC, de Jager WJ, Prakken BJ, McColl SR, Haspels I, Putter H, van Berkel TJ, Nagelkerken L, Jukema JW, and Biessen EA. CC chemokine ligand-5 (CCL5/RANTES) and CC chemokine ligand-18 (CCL18/PARC) are specific markers of refractory unstable angina pectoris and are transiently raised during severe ischemic symptoms. *Circulation* 116: 1931-1941, 2007.

124. Kraakman MJ, Murphy AJ, Jandeleit-Dahm K, and Kammoun HL. Macrophage polarization in obesity and type 2 diabetes: weighing down our understanding of macrophage function? *Frontiers in immunology* 5: 470, 2014.

125. Krausgruber T, Blazek K, Smallie T, Alzabin S, Lockstone H, Sahgal N, Hussell T, Feldmann M, and Udalova IA. IRF5 promotes inflammatory macrophage polarization and T(H)1-T(H)17 responses. *Nature Immunology* 12: 231-U266, 2011.

126. Krohn SC, Bonvin P, and Proudfoot AE. CCL18 exhibits a regulatory role through inhibition of receptor and glycosaminoglycan binding. *PLoS One* 8: e72321, 2013.

127. Kuribayashi F, Nunoi H, Wakamatsu K, Tsunawaki S, Sato K, Ito T, and Sumimoto H. The adaptor protein p40(phox) as a positive regulator of the superoxide-producing phagocyte oxidase. *EMBO Journal* 21: 6312-6320, 2002.

128. Kuroki MT, Fink GD, and Osborn JW. Comparison of arterial pressure and plasma ANG II responses to three methods of subcutaneous ANG II administration. *American journal of physiology Heart and circulatory physiology* 307: H670-679, 2014.

129. Laurent S, Boutouyrie P, Asmar R, Gautier I, Laloux B, Guize L, Ducimetiere P, and Benetos A. Aortic Stiffness Is an Independent Predictor of All-Cause and Cardiovascular Mortality in Hypertensive Patients. *Hypertension* 37: 1236-1241, 2001.

130. Lee CF, Qiao M, Schroder K, Zhao Q, and Asmis R. Nox4 is a novel inducible source of reactive oxygen species in monocytes and macrophages and mediates oxidized low density lipoprotein-induced macrophage death. *Circ Res* 106: 1489-1497, 2010.

131. Lee KU, Kim MK, Amano K, Pak CY, Jaworski MA, Mehta JG, and Yoon JW. Preferential infiltration of macrophages during early stages of insulitis in diabetes-prone BB rats. *Diabetes* 37: 1053-1058, 1988.

132. Lee S, Huen S, Nishio H, Nishio S, Lee HK, Choi BS, Ruhrberg C, and Cantley LG. Distinct macrophage phenotypes contribute to kidney injury and repair. *Journal of the American Society of Nephrology : JASN* 22: 317-326, 2011.

133. Lee YW, Kim PH, Lee WH, and Hirani AA. Interleukin-4, Oxidative Stress, Vascular Inflammation and Atherosclerosis. *Biomolecules & therapeutics* 18: 135-144, 2010.

134. Lee YW, Lee WH, and Kim PH. Role of NADPH oxidase in interleukin-4-induced monocyte chemoattractant protein-1 expression in vascular endothelium. *Inflammation research : official journal of the European Histamine Research Society [et al]* 59: 755-765, 2010.

135. Libby P. Inflammation in atherosclerosis. *Arterioscler Thromb Vasc Biol* 32: 2045-2051, 2012.

136. Libby P. Inflammation in atherosclerosis. *Nature* 420: 868-874, 2002.

137. Libby P. The molecular mechanisms of the thrombotic complications of atherosclerosis. *Journal of Internal Medicine* 263: 517-527, 2008.

138. Libby P, Ridker PM, and Hansson GK. Progress and challenges in translating the biology of atherosclerosis. *Nature* 473: 317-325, 2011.

139. Lijnen P, Papparella I, Petrov V, Semplicini A, and Fagard R. Angiotensin II-stimulated collagen production in cardiac fibroblasts is mediated by reactive oxygen species. *J Hypertens* 24: 757-766, 2006.

140. Lijnen P, and Petrov V. Transforming growth factor-beta 1-induced collagen production in cultures of cardiac fibroblasts is the result of the appearance of myofibroblasts. *Methods and findings in experimental and clinical pharmacology* 24: 333-344, 2002.

141. Lijnen P, Petrov V, van Pelt J, and Fagard R. Inhibition of superoxide dismutase induces collagen production in cardiac fibroblasts. *American journal of hypertension* 21: 1129-1136, 2008.

142. Lindeman JH, Abdul-Hussien H, Schaapherder AF, Van Bockel JH, Von der Thusen JH, Roelen DL, and Kleemann R. Enhanced expression and activation of pro-inflammatory transcription factors distinguish aneurysmal from atherosclerotic aorta: IL-6- and IL-8-dominated inflammatory responses prevail in the human aneurysm. *Clinical science (London, England : 1979)* 114: 687-697, 2008.

143. Llorente-Cortes V, de Gonzalo-Calvo D, Orbe J, Paramo JA, and Badimon L. Signature of subclinical femoral artery atherosclerosis in peripheral blood mononuclear cells. *European journal of clinical investigation* 44: 539-548, 2014.

144. Lupardus PJ, Birnbaum ME, and Garcia KC. Molecular basis for shared cytokine recognition revealed in the structure of an unusually high affinity complex between IL-13 and IL-13Ralpha2. *Structure (London, England : 1993)* 18: 332-342, 2010.

145. Madamanchi NR, and Runge MS. Redox signaling in cardiovascular health and disease. *Free radical biology & medicine* 61: 473-501, 2013.

146. Manea A, Manea SA, Gan AM, Constantin A, Fenyo IM, Raicu M, Muresian H, and Simionescu M. Human monocytes and macrophages express NADPH oxidase 5; a potential source of reactive oxygen species in atherosclerosis. *Biochem Biophys Res Commun* 461: 172-179, 2015.

147. Mantovani A, Garlanda C, and Locati M. Macrophage Diversity and Polarization in Atherosclerosis A Question of Balance. *Arteriosclerosis Thrombosis and Vascular Biology* 29: 1419-1423, 2009.

148. Mantovani A, Sica A, Sozzani S, Allavena P, Vecchi A, and Locati M. The chemokine system in diverse forms of macrophage activation and polarization. *Trends in immunology* 25: 677-686, 2004.

149. Martinez FO, and Gordon S. The M1 and M2 paradigm of macrophage activation: time for reassessment. *F1000prime reports* 6: 13, 2014.

150. Martinez FO, Gordon S, Locati M, and Mantovani A. Transcriptional profiling of the human monocyte-to-macrophage differentiation and polarization: New molecules and patterns of gene expression. *Journal of Immunology* 177: 7303-7311, 2006.

151. Marzaioli V, Hurtado-Nedelec M, Pintard C, Tlili A, Marie JC, Monteiro RC, Gougerot-Pocidalo MA, Dang PM, and El-Benna J. NOX5 and p22phox are 2 novel regulators of human monocytic differentiation into dendritic cells. *Blood* 130: 1734-1745, 2017.

152. McCormick SM, and Heller NM. Commentary: IL-4 and IL-13 receptors and signaling. *Cytokine* 75: 38-50, 2015.

153. McKleroy W, Lee TH, and Atabai K. Always cleave up your mess: targeting collagen degradation to treat tissue fibrosis. *American journal of physiology Lung cellular and molecular physiology* 304: L709-721, 2013.

154. Meaume S, Benetos A, Henry OF, Rudnichi A, and Safar ME. Aortic pulse wave velocity predicts cardiovascular mortality in subjects >70 years of age. *Arterioscler Thromb Vasc Biol* 21: 2046-2050, 2001.

155. Meir KS, and Leitersdorf E. Atherosclerosis in the apolipoprotein-E-deficient mouse: a decade of progress. *Arterioscler Thromb Vasc Biol* 24: 1006-1014, 2004.

156. Meyrelles SS, Peotta VA, Pereira TM, and Vasquez EC. Endothelial dysfunction in the apolipoprotein E-deficient mouse: insights into the influence of diet, gender and aging. *Lipids Health Dis* 10: 211, 2011.

157. Mian MO, Paradis P, and Schiffrin EL. Innate immunity in hypertension. *Curr Hypertens Rep* 16: 413, 2014.

158. Mihaylova B, Emberson J, Blackwell L, Keech A, Simes J, Barnes EH, Voysey M, Gray A, Collins R, and Baigent C. The effects of lowering LDL cholesterol with statin therapy in people at low risk of vascular disease: meta-analysis of individual data from 27 randomised trials. *Lancet* 380: 581-590, 2012.

159. Mitchell GF, Hwang SJ, Vasan RS, Larson MG, Pencina MJ, Hamburg NM, Vita JA, Levy D, and Benjamin EJ. Arterial stiffness and cardiovascular events: the Framingham Heart Study. *Circulation* 121: 505-511, 2010.

160. Moon JS, Nakahira K, Chung KP, DeNicola GM, Koo MJ, Pabon MA, Rooney KT, Yoon JH, Ryter SW, Stout-Delgado H, and Choi AM. NOX4-dependent fatty acid oxidation promotes NLRP3 inflammasome activation in macrophages. *Nat Med* 22: 1002-1012, 2016.

161. Moore JP, Vinh A, Tuck KL, Sakkal S, Krishnan SM, Chan CT, Lieu M, Samuel CS, Diep H, Kemp-Harper BK, Tare M, Ricardo SD, Guzik TJ, Sobey CG, and Drummond GR. M2 macrophage accumulation in the aortic wall during angiotensin II infusion in mice is

associated with fibrosis, elastin loss, and elevated blood pressure. *American journal of physiology Heart and circulatory physiology* 309: H906-917, 2015.

162. Mosser DM, and Edwards JP. Exploring the full spectrum of macrophage activation. *Nature Reviews Immunology* 8: 958-969, 2008.

163. Mozaffarian D, Benjamin EJ, Go AS, Arnett DK, Blaha MJ, Cushman M, de Ferranti S, Despres JP, Fullerton HJ, Howard VJ, Huffman MD, Judd SE, Kissela BM, Lackland DT, Lichtman JH, Lisabeth LD, Liu S, Mackey RH, Matchar DB, McGuire DK, Mohler ER, 3rd, Moy CS, Muntner P, Mussolino ME, Nasir K, Neumar RW, Nichol G, Palaniappan L, Pandey DK, Reeves MJ, Rodriguez CJ, Sorlie PD, Stein J, Towfighi A, Turan TN, Virani SS, Willey JZ, Woo D, Yeh RW, and Turner MB. Heart disease and stroke statistics--2015 update: a report from the American Heart Association. *Circulation* 131: e29-322, 2015.

164. Murray PJ, Allen JE, Biswas SK, Fisher EA, Gilroy DW, Goerdt S, Gordon S, Hamilton JA, Ivashkiv LB, Lawrence T, Locati M, Mantovani A, Martinez FO, Mege JL, Mosser DM, Natoli G, Saeij JP, Schultze JL, Shirey KA, Sica A, Suttles J, Udalova I, van Ginderachter JA, Vogel SN, and Wynn TA. Macrophage activation and polarization: nomenclature and experimental guidelines. *Immunity* 41: 14-20, 2014.

165. Murray PJ, and Wynn TA. Protective and pathogenic functions of macrophage subsets. *Nat Rev Immunol* 11: 723-737, 2011.

166. Nibbs RJ, Salcedo TW, Campbell JD, Yao XT, Li Y, Nardelli B, Olsen HS, Morris TS, Proudfoot AE, Patel VP, and Graham GJ. C-C chemokine receptor 3 antagonism by the beta-chemokine macrophage inflammatory protein 4, a property strongly enhanced by an amino-terminal alanine-methionine swap. *J Immunol* 164: 1488-1497, 2000.

167. Niccoli G, and Cosentino N. Eosinophils: a new player in coronary atherosclerotic disease. *Hypertension research : official journal of the Japanese Society of Hypertension* 35: 269-271, 2012.

168. Nio Y, Yamauchi T, Iwabu M, Okada-Iwabu M, Funata M, Yamaguchi M, Ueki K, and Kadowaki T. Monocyte chemoattractant protein-1 (MCP-1) deficiency enhances alternatively activated M2 macrophages and ameliorates insulin resistance and fatty liver in lipoatrophic diabetic A-ZIP transgenic mice. *Diabetologia* 55: 3350-3358, 2012.

169. Novitskiy G, Potter JJ, Wang L, and Mezey E. Influences of reactive oxygen species and nitric oxide on hepatic fibrogenesis. *Liver international : official journal of the International Association for the Study of the Liver* 26: 1248-1257, 2006.

170. Oh CK, Geba GP, and Molfino N. Investigational therapeutics targeting the IL-4/IL-13/STAT-6 pathway for the treatment of asthma. *Eur Respir Rev* 19: 46-54, 2010.

171. Oh J, Riek AE, Weng S, Petty M, Kim D, Colonna M, Cella M, and Bernal-Mizrachi C. Endoplasmic reticulum stress controls M2 macrophage differentiation and foam cell formation. *J Biol Chem* 287: 11629-11641, 2012.

172. Oparil S, Zaman M, and Calhoun DA. Pathogenesis of hypertension. *Annals of Internal Medicine* 139: 761-776, 2003.

173. Osidak MS, Osidak EO, Akhmanova MA, Domogatsky SP, and Domogatskaya AS. Fibrillar, fibril-associated and basement membrane collagens of the arterial wall: architecture, elasticity and remodeling under stress. *Current pharmaceutical design* 21: 1124-1133, 2015.

174. Padgett LE, Burg AR, Lei W, and Tse HM. Loss of NADPH Oxidase-Derived Superoxide Skews Macrophage Phenotypes to Delay Type 1 Diabetes. *Diabetes* 2014.

175. Parsa R, Andresen P, Gillett A, Mia S, Zhang XM, Mayans S, Holmberg D, and Harris RA. Adoptive transfer of immunomodulatory M2 macrophages prevents type 1 diabetes in NOD mice. *Diabetes* 61: 2881-2892, 2012.

176. Pello OM, Silvestre C, De Pizzol M, and Andres V. A glimpse on the phenomenon of macrophage polarization during atherosclerosis. *Immunobiology* 216: 1172-1176, 2011.

177. Peterman EM, Sullivan C, Goody MF, Rodriguez-Nunez I, Yoder JA, and Kim CH. Neutralization of mitochondrial superoxide by superoxide dismutase 2 promotes bacterial clearance and regulates phagocyte numbers in zebrafish. *Infection and immunity* 83: 430-440, 2015.

178. Piedrahita JA, Zhang SH, Hagaman JR, Oliver PM, and Maeda N. Generation of mice carrying a mutant apolipoprotein E gene inactivated by gene targeting in embryonic stem cells. *Proc Natl Acad Sci U S A* 89: 4471-4475, 1992.

179. Plump AS, Smith JD, Hayek T, Aalto-Setala K, Walsh A, Verstuyft JG, Rubin EM, and Breslow JL. Severe hypercholesterolemia and atherosclerosis in apolipoprotein E-deficient mice created by homologous recombination in ES cells. *Cell* 71: 343-353, 1992.

180. Pochetuhen K, Luzina IG, Lockatell V, Choi J, Todd NW, and Atamas SP. Complex regulation of pulmonary inflammation and fibrosis by CCL18. *The American journal of pathology* 171: 428-437, 2007.

181. Psaltis PJ, Puranik AS, Spoon DB, Chue CD, Hoffman SJ, Witt TA, Delacroix S, Kleppe LS, Mueske CS, Pan S, Gulati R, and Simari RD. Characterization of a resident population of adventitial macrophage progenitor cells in postnatal vasculature. *Circ Res* 115: 364-375, 2014.

182. Raaz-Schrauder D, Klinghammer L, Baum C, Frank T, Lewczuk P, Achenbach S, Cicha I, Stumpf C, Wiltfang J, Kornhuber J, Daniel WG, and Garlichs CD. Association of systemic

inflammation markers with the presence and extent of coronary artery calcification. *Cytokine* 57: 251-257, 2012.

183. Raaz-Schrauder D, Schrauder MG, Stumpf C, Lewczuk P, Kilian T, Dietel B, Garlichs CD, Schlundt C, Achenbach S, and Klinghammer L. Plasma levels of sRANKL and OPG are associated with atherogenic cytokines in patients with intermediate cardiovascular risk. *Heart and vessels* 32: 1304-1313, 2017.

184. Rader DJ, and Daugherty A. Translating molecular discoveries into new therapies for atherosclerosis. *Nature* 451: 904-913, 2008.

185. Raes G, De Baetselier P, Noel W, Beschin A, Brombacher F, and Hassanzadeh Gh G. Differential expression of FIZZ1 and Ym1 in alternatively versus classically activated macrophages. *J Leukoc Biol* 71: 597-602, 2002.

186. Raes G, Van den Bergh R, De Baetselier P, Ghassabeh GH, Scotton C, Locati M, Mantovani A, and Sozzani S. Arginase-1 and Ym1 are markers for murine, but not human, alternatively activated myeloid cells. *J Immunol* 174: 6561; author reply 6561-6562, 2005.

187. Rahman MS, Murphy AJ, and Woollard KJ. Effects of dyslipidaemia on monocyte production and function in cardiovascular disease. *Nature reviews Cardiology* 14: 387-400, 2017.

188. Rakkola R, Matikainen S, and Nyman TA. Proteome analysis of human macrophages reveals the upregulation of manganese-containing superoxide dismutase after toll-like receptor activation. *Proteomics* 7: 378-384, 2007.

189. Rekhter MD. Collagen synthesis in atherosclerosis: too much and not enough. *Cardiovasc Res* 41: 376-384, 1999.

190. Rickard AJ, Morgan J, Tesch G, Funder JW, Fuller PJ, and Young MJ. Deletion of mineralocorticoid receptors from macrophages protects against deoxycorticosterone/salt-induced cardiac fibrosis and increased blood pressure. *Hypertension* 54: 537-543, 2009.

191. Rosenblat M, and Aviram M. Oxysterol-induced activation of macrophage NADPH-oxidase enhances cell-mediated oxidation of LDL in the atherosclerotic apolipoprotein E deficient mouse: inhibitory role for vitamin E. *Atherosclerosis* 160: 69-80, 2002.

192. Sallusto F, and Lanzavecchia A. Efficient presentation of soluble antigen by cultured human dendritic cells is maintained by granulocyte/macrophage colony-stimulating factor plus interleukin 4 and downregulated by tumor necrosis factor alpha. *J Exp Med* 179: 1109-1118, 1994.

193. Sanjabi S, Hoffmann A, Liou HC, Baltimore D, and Smale ST. Selective requirement for c-Rel during IL-12 P40 gene induction in macrophages. *Proc Natl Acad Sci U S A* 97: 12705-12710, 2000.

194. Sano M, Fukuda K, Sato T, Kawaguchi H, Suematsu M, Matsuda S, Koyasu S, Matsui H, Yamauchi-Takihara K, Harada M, Saito Y, and Ogawa S. ERK and p38 MAPK, but not NF-kappaB, are critically involved in reactive oxygen species-mediated induction of IL-6 by angiotensin II in cardiac fibroblasts. *Circ Res* 89: 661-669, 2001.

195. Sathyamoorthy M, deMendez I, Adams AG, and Leto TL. p40(phox) down-regulates NADPH oxidase activity through interactions with its SH3 domain. *Journal of Biological Chemistry* 272: 9141-9146, 1997.

196. Schenk M, Fabri M, Krutzik SR, Lee DJ, Vu DM, Sieling PA, Montoya D, Liu PT, and Modlin RL. Interleukin-1beta triggers the differentiation of macrophages with enhanced capacity to present mycobacterial antigen to T cells. *Immunology* 141: 174-180, 2014.

197. Schraufstatter IU, Zhao M, Khaldoyanidi SK, and Discipio RG. The chemokine CCL18 causes maturation of cultured monocytes to macrophages in the M2 spectrum. *Immunology* 135: 287-298, 2012.

198. Schutyser E, Richmond A, and Van Damme J. Involvement of CC chemokine ligand 18 (CCL18) in normal and pathological processes. *J Leukoc Biol* 78: 14-26, 2005.

199. Segal BH, Han W, Bushey JJ, Joo M, Bhatti Z, Feminella J, Dennis CG, Vethanayagam RR, Yull FE, Capitano M, Wallace PK, Minderman H, Christman JW, Sporn MB, Chan J, Vinh DC, Holland SM, Romani LR, Gaffen SL, Freeman ML, and Blackwell TS. NADPH oxidase limits innate immune responses in the lungs in mice. *PLoS One* 5: e9631, 2010.

200. Serrander L, Jaquet V, Bedard K, Plastre O, Hartley O, Arnaudeau S, Demaurex N, Schlegel W, and Krause K-H. NOX5 is expressed at the plasma membrane and generates superoxide in response to protein kinase C activation. *Biochimie* 89: 1159-1167, 2007.

201. Shapiro MD, and Fazio S. From Lipids to Inflammation: New Approaches to Reducing Atherosclerotic Risk. *Circ Res* 118: 732-749, 2016.

202. Sheikh F, Dickensheets H, Pedras-Vasconcelos J, Ramalingam T, Helming L, Gordon S, and Donnelly RP. The Interleukin-13 Receptor-alpha1 Chain Is Essential for Induction of the Alternative Macrophage Activation Pathway by IL-13 but Not IL-4. *Journal of innate immunity* 2015.

203. Shi C, and Pamer EG. Monocyte recruitment during infection and inflammation. *Nat Rev Immunol* 11: 762-774, 2011.

204. Sica A, and Mantovani A. Macrophage plasticity and polarization: in vivo veritas. *J Clin Invest* 122: 787-795, 2012.

205. Simon G, Abraham G, and Cserep G. Pressor and subpressor angiotensin II administration. Two experimental models of hypertension. *American journal of hypertension* 8: 645-650, 1995.

206. Sorescu D, Weiss D, Lassegue B, Clempus RE, Szocs K, Sorescu GP, Valppu L, Quinn MT, Lambeth JD, Vega JD, Taylor WR, and Griendling KK. Superoxide production and expression of Nox family proteins in human atherosclerosis. *Circulation* 105: 1429-1435, 2002.

207. Stein M, Keshav S, Harris N, and Gordon S. INTERLEUKIN-4 POTENTLY ENHANCES MURINE MACROPHAGE MANNOSE RECEPTOR ACTIVITY - A MARKER OF ALTERNATIVE IMMUNOLOGICAL MACROPHAGE ACTIVATION. *Journal of Experimental Medicine* 176: 287-292, 1992.

208. Stoger JL, Gijbels MJ, van der Velden S, Manca M, van der Loos CM, Biessen EA, Daemen MJ, Lutgens E, and de Winther MP. Distribution of macrophage polarization markers in human atherosclerosis. *Atherosclerosis* 225: 461-468, 2012.

209. Sunderkotter C, Nikolic T, Dillon MJ, Van Rooijen N, Stehling M, Drevets DA, and Leenen PJ. Subpopulations of mouse blood monocytes differ in maturation stage and inflammatory response. *J Immunol* 172: 4410-4417, 2004.

210. Szanto A, Balint BL, Nagy ZS, Barta E, Dezso B, Pap A, Szeles L, Poliska S, Oros M, Evans RM, Barak Y, Schwabe J, and Nagy L. STAT6 transcription factor is a facilitator of the nuclear receptor PPARgamma-regulated gene expression in macrophages and dendritic cells. *Immunity* 33: 699-712, 2010.

211. Tabas I, and Bornfeldt KE. Macrophage Phenotype and Function in Different Stages of Atherosclerosis. *Circ Res* 118: 653-667, 2016.

212. Te Riet L, van Esch JH, Roks AJ, van den Meiracker AH, and Danser AH. Hypertension: renin-angiotensin-aldosterone system alterations. *Circ Res* 116: 960-975, 2015.

213. Thang LV, Demel SL, Crawford R, Kaminski NE, Swain GM, Van Rooijen N, and Galligan JJ. Macrophage depletion lowers blood pressure and restores sympathetic nerve alpha2-adrenergic receptor function in mesenteric arteries of DOCA-salt hypertensive rats. *American journal of physiology Heart and circulatory physiology* 309: H1186-1197, 2015.

214. Tiwari RL, Singh V, and Barthwal MK. Macrophages: An elusive yet emerging therapeutic target of atherosclerosis. *Medicinal Research Reviews* 28: 483-544, 2008.

215. Usher MG, Duan SZ, Ivaschenko CY, Frieler RA, Berger S, Schutz G, Lumeng CN, and Mortensen RM. Myeloid mineralocorticoid receptor controls macrophage polarization and cardiovascular hypertrophy and remodeling in mice. *J Clin Invest* 120: 3350-3364, 2010.

216. Van Dyken SJ, and Locksley RM. Interleukin-4- and interleukin-13-mediated alternatively activated macrophages: roles in homeostasis and disease. *Annual review of immunology* 31: 317-343, 2013.

217. van Furth R, and Cohn ZA. The origin and kinetics of mononuclear phagocytes. *J Exp Med* 128: 415-435, 1968.

218. Wang IM, Lin H, Goldman SJ, and Kobayashi M. STAT-1 is activated by IL-4 and IL-13 in multiple cell types. *Molecular immunology* 41: 873-884, 2004.

219. Wang L, Gao S, Xu W, Zhao S, Zhou J, Wang N, and Yuan Z. Allergic asthma accelerates atherosclerosis dependent on Th2 and Th17 in apolipoprotein E deficient mice. *Journal of molecular and cellular cardiology* 72: 20-27, 2014.

220. Wang N, Liang H, and Zen K. Molecular mechanisms that influence the macrophage m1-m2 polarization balance. *Frontiers in immunology* 5: 614, 2014.

221. Wang P, Zhou S, Xu L, Lu Y, Yuan X, Zhang H, Li R, Fang J, and Liu P. Hydrogen peroxide-mediated oxidative stress and collagen synthesis in cardiac fibroblasts: blockade by tanshinone IIA. *Journal of ethnopharmacology* 145: 152-161, 2013.

222. Weber C, Belge KU, von Hundelshausen P, Draude G, Steppich B, Mack M, Frankenberger M, Weber KS, and Ziegler-Heitbrock HW. Differential chemokine receptor expression and function in human monocyte subpopulations. *J Leukoc Biol* 67: 699-704, 2000.

223. Wei S, Nandi S, Chitu V, Yeung YG, Yu W, Huang M, Williams LT, Lin H, and Stanley ER. Functional overlap but differential expression of CSF-1 and IL-34 in their CSF-1 receptor-mediated regulation of myeloid cells. *J Leukoc Biol* 88: 495-505, 2010.

224. Weir MR, and Dzau VJ. The renin-angiotensin-aldosterone system: a specific target for hypertension management. *American journal of hypertension* 12: 205s-213s, 1999.

225. Wenzel P, Knorr M, Kossmann S, Stratmann J, Hausding M, Schuhmacher S, Karbach SH, Schwenk M, Yogev N, Schulz E, Oelze M, Grabbe S, Jonuleit H, Becker C, Daiber A, Waisman A, and Munzel T. Lysozyme M-positive monocytes mediate angiotensin II-induced arterial hypertension and vascular dysfunction. *Circulation* 124: 1370-1381, 2011.

226. Wolfs IMJ, Donners MMPC, and de Winther MPJ. Differentiation factors and cytokines in the atherosclerotic plaque micro-environment as a trigger for macrophage polarisation. *Thromb Haemost* 106: 763-771, 2011.

227. Wong KL, Tai JJ, Wong WC, Han H, Sem X, Yeap WH, Kourilsky P, and Wong SC. Gene expression profiling reveals the defining features of the classical, intermediate, and nonclassical human monocyte subsets. *Blood* 118: e16-31, 2011.

228. Wurtz O, Bajenoff M, and Guerder S. IL-4-mediated inhibition of IFN-gamma production by CD4+ T cells proceeds by several developmentally regulated mechanisms. *Int Immunol* 16: 501-508, 2004.

229. Wynn TA, Chawla A, and Pollard JW. Macrophage biology in development, homeostasis and disease. *Nature* 496: 445-455, 2013.

230. Wynn TA, and Ramalingam TR. Mechanisms of fibrosis: therapeutic translation for fibrotic disease. *Nat Med* 18: 1028-1040, 2012.

231. Wynn TA, and Vannella KM. Macrophages in Tissue Repair, Regeneration, and Fibrosis. *Immunity* 44: 450-462, 2016.

232. Xu Q, Choksi S, Qu J, Jang J, Choe M, Banfi B, Engelhardt JF, and Liu ZG. NADPH Oxidases Are Essential for Macrophage Differentiation. *J Biol Chem* 291: 20030-20041, 2016.

233. Yang W, Zhang J, Wang H, Gao P, Singh M, Shen K, and Fang N. Angiotensin II downregulates catalase expression and activity in vascular adventitial fibroblasts through an AT1R/ERK1/2-dependent pathway. *Molecular and cellular biochemistry* 358: 21-29, 2011.

234. Yi L, Liu Q, Orandle MS, Sadiq-Ali S, Koontz SM, Choi U, Torres-Velez FJ, and Jackson SH. p47(Phox) Directs Murine Macrophage Cell Fate Decisions. *American Journal of Pathology* 180: 1049-1058, 2012.

235. Yla-Herttuala S, Bentzon JF, Daemen M, Falk E, Garcia-Garcia HM, Herrmann J, Hoefer I, Jukema JW, Krams R, Kwak BR, Marx N, Naruszewicz M, Newby A, Pasterkamp G, Serruys P, Waltenberger J, Weber C, and Tokgozoglu L. Stabilisation of atherosclerotic plaques: Position Paper of the European Society of Cardiology (ESC) Working Group on Atherosclerosis and Vascular Biology. *Thrombosis and Haemostasis* 106: 1-19, 2011.

236. Yona S, Kim KW, Wolf Y, Mildner A, Varol D, Breker M, Strauss-Ayali D, Viukov S, Guilliams M, Misharin A, Hume DA, Perlman H, Malissen B, Zelzer E, and Jung S. Fate mapping reveals origins and dynamics of monocytes and tissue macrophages under homeostasis. *Immunity* 38: 79-91, 2013.

237. Zhai C, Cheng J, Mujahid H, Wang H, Kong J, Yin Y, Li J, Zhang Y, Ji X, and Chen W. Selective inhibition of PI3K/Akt/mTOR signaling pathway regulates autophagy of macrophage and vulnerability of atherosclerotic plaque. *PLoS One* 9: e90563, 2014.

238. Zhang SH, Reddick RL, Piedrahita JA, and Maeda N. Spontaneous hypercholesterolemia and arterial lesions in mice lacking apolipoprotein E. *Science* 258: 468-471, 1992.

239. Zhang WJ, Wei H, and Frei B. Genetic deficiency of NADPH oxidase does not diminish, but rather enhances, LPS-induced acute inflammatory responses in vivo. *Free radical biology & medicine* 46: 791-798, 2009.

240. Zhang Y, Choksi S, Chen K, Pobezinskaya Y, Linnoila I, and Liu ZG. ROS play a critical role in the differentiation of alternatively activated macrophages and the occurrence of tumor-associated macrophages. *Cell research* 23: 898-914, 2013.

241. Zhao XN, Li YN, and Wang YT. Interleukin-4 regulates macrophage polarization via the MAPK signaling pathway to protect against atherosclerosis. *Genetics and molecular research : GMR* 15: 2016.

242. Ziegler-Heitbrock L, Ancuta P, Crowe S, Dalod M, Grau V, Hart DN, Leenen PJ, Liu YJ, MacPherson G, Randolph GJ, Scherberich J, Schmitz J, Shortman K, Sozzani S, Strobl H, Zembala M, Austyn JM, and Lutz MB. Nomenclature of monocytes and dendritic cells in blood. *Blood* 116: e74-80, 2010.

243. Ziegler-Heitbrock L, and Hofer TP. Toward a refined definition of monocyte subsets. *Frontiers in immunology* 4: 23, 2013.

244. Zingoni A, Soto H, Hedrick JA, Stoppacciaro A, Storlazzi CT, Sinigaglia F, D'Ambrosio D, O'Garra A, Robinson D, Rocchi M, Santoni A, Zlotnik A, and Napolitano M. The chemokine receptor CCR8 is preferentially expressed in Th2 but not Th1 cells. *J Immunol* 161: 547-551, 1998.

245. Zizzo G, Hilliard BA, Monestier M, and Cohen PL. Efficient clearance of early apoptotic cells by human macrophages requires M2c polarization and MerTK induction. *J Immunol* 189: 3508-3520, 2012.

246. Zou L, Wang W, Liu S, Zhao X, Lyv Y, Du C, Su X, Geng B, and Xu G. Spontaneous hypertension occurs with adipose tissue dysfunction in perilipin-1 null mice. *Biochimica et biophysica acta* 1862: 182-191, 2016.

CHAPTER 2:

GENERAL METHODS

2.1 Animals

Male C57BL6/J mice were obtained from Monash Animal Services and ApoE$^{-/-}$ mice of the C57BL6/J background were obtained from the Animal Resources Centre (Canning Vale, WA, Australia). All mice were housed in Animal Research Laboratories (Clayton, VIC, Australia) for use in these studies. Mice were housed under specific pathogen free conditions, maintained at 24°C on a 12 hour light-dark cycle with free access to chow diet and drinking water. All procedures were approved by the Monash University Animal Research Platform Animal Ethics Committee (Monash University, Clayton, Australia) and conducted in accordance with the Australian Code for the Care and Use of Animals for Scientific Purposes. In all experiments, mice were killed by an overdose of isoflurane inhalation (Baxter Healthcare, Australia). The ethics numbers for mice used for the Angiotensin II infusion model and the ApoE$^{-/-}$ model were MARP/2016/077 and MARP/2008/032, respectively.

2.2 Models of cardiovascular disease

2.2.1 Angiotensin II infusion model of hypertension in mice

The angiotensin II infusion model was used to investigate the expression and localisation of CCL8 and CCR8 in the vessel wall during hypertension. Hypertension was induced in 10-12 week-old male wild-type C57BL6/J mice by subcutaneous (*s.c*) infusion of angiotensin II (0.7 mg/kg/d) (8). Once stable baseline measurements of blood pressure were obtained by tail cuff plethysmography, mice were randomly assigned to hypertensive (angiotensin II-treated) and normotensive (saline treated) groups. Mice were placed under general anaesthesia by isoflurane inhalation (0.4 L/min, 2.5%, Baxter, USA) and surgeries performed in a sterile manner. While anaesthetised, mice were monitored for hind paw withdrawal, blink reflexes and respiratory rate. Under anaesthesia, a small incision was made at the nape of the neck

and blunt dissection was then performed to make a subcutaneous pouch for insertion of micro-osmotic minipumps (Model 1004, flow rate 0.11 µl/hr, Alzet, USA) containing either vehicle (0.9% saline) or angiotensin II (0.7 mg/kg/day). The incision was closed using a single wound clip. Immediately following surgery, mice were treated with an antibiotic, Tribactril (Jurox, Australia), applied topically to the site of the wound, and a long-acting analgesic, carprofen (5 mg/kg, *s.c*; Parnell Living Science, Australia). Mice were then allowed to recover on a heating pad and returned to their home cages and monitored daily for 2 days. Mice were maintained on normal chow and drinking water for a total of 28 days. On day 28, systolic blood pressure was measured and then mice were killed and the thoracic aorta harvested with the perivascular fat intact. The top third section was snap frozen in liquid nitrogen for mRNA measurements (see section 2.4), and the bottom third section frozen in Optimal Cutting Temperature compound (OCT; Sakura Finetek, USA) for immunohistochemistry (see section 2.9.1).

2.2.1.1 Tail-cuff plethysmography

Routine blood pressure (BP) measurements in conscious mice were performed by tail cuff plethysmography (MC4000 multi-channel blood pressure analysis system; Hatteras Instruments, USA) (6). Systolic blood pressure was measured prior to surgeries (day 0), and on days 5, 14, 21 and 28 following infusion of saline of angiotensin II. BP was recorded every day for 3 days before surgery to acclimatise mice to the procedure. In brief, mice were removed from their housing cages and placed in a restraint on a heated pad (40°C) and a small inflatable cuff positioned around the base of the tail. BP was determined as the cuff inflation pressure at which blood flow to the tail becomes completely occluded (6).

2.2.2 ApoE$^{-/-}$ model of atherosclerosis in mice

To assess the localisation of a potential novel M1 macrophage marker in atherosclerotic plaques, the ApoE$^{-/-}$ model of atherosclerosis was utilised. Male ApoE$^{-/-}$ mice were weaned at 3 weeks of ages, housed in groups of up to 4 littermates and given access to normal chow and water ad libitum. At 5 weeks of age they were placed on a high fat diet (HFD; 22% fat, 0.15% cholesterol; SFOO-219, Specialty Feeds, WA, Australia) and maintained on this diet for a further 14 weeks. At this time point, mice were killed and hearts and brachiocephalic arteries frozen in OCT for immunohistochemistry (see section 2.9.2).

2.3 Cell culture

2.3.1 THP-1 monocytes

The human monocytic cell line, THP-1, was a kind gift from Dr Meritxell Canals from the Monash Institute of Pharmaceutical Sciences, Parkville, Australia. The cells were cultured in high glucose Roswell Park Memorial Institute 1640 medium (RPMI; Gibco, Life Technologies, USA), supplemented with 10% heat-inactivated foetal bovine serum (FBS; Gibco, Life Technologies, USA). Monocytes were grown in T75 tissue culture flasks in a humidified incubator (Sanyo MCO-18AIC CO_2 incubator, Quantum Scientific, USA), maintained at 37°C with 5% CO_2 and passaged every 3-4 days.

On the day of passaging, cells were either: seeded at 1 x 10^5 cells/ml in a new T75 flask for maintenance of the culture; seeded at 1 x 10^6 cells/well in 6 well plates for RNA (see section 2.4) and protein extraction (see section 2.5) and incubation with the ROS indicator CM-H2DCFDA; or seeded at 5 x 10^4 cells/ well in 96 well plates for ROS detection assays (see section 2.6).

2.3.1.1 Differentiation of THP-1 cells into macrophages and treatment with M1 or M2 polarising stimuli

THP-1 cells were differentiated to macrophages via addition of 100 nM phorbol-12,13-dibutyrate (PDBu; Calbiochem, Germany; 10 mM PDBu dissolved in 100% dimethyl sulphoxide; DMSO, Sigma-Aldrich, USA) for 24 hours. Following differentiation, the media was replaced and THP-1 macrophages were either left untreated (MΦ), treated with a combination of 5 ng/ml IFN-γ (Sigma-Aldrich, USA; reconstituted in sterile dH_2O) and 10 ng/ml LPS (*Escherichia coli* 055:B5 strain Sigma-Aldrich, USA; reconstituted in sterile dH_2O) for M1 polarisation, or treated with 25 ng/ml IL-4 (Sigma-Aldrich, USA; reconstituted in PBS, Sigma-Aldrich, USA) for M2 polarisation. RNA extraction was performed after 6, 24, 48 or 72 hours of polarisation (see section 2.4). Protein extraction (see section 2.5) and ROS detection (see section 2.6) was performed following 72 hours of polarisation.

2.3.1.2 siRNA knockdown of NOX2 in THP-1 macrophages

NOX2 siRNA was used to investigate the contribution of NOX2 to superoxide generation from unpolarised, M1, and M2 THP-1 macrophages. Following differentiation to macrophages with PDBu, cells were rinsed with warm, sterile phosphate buffered saline (PBS; Sigma-Aldrich, USA) and subsequently treated with either vehicle (transfection reagent alone; Lipofectamine RNAiMAX; Invitrogen, ThermoFisher Scientific, USA), NOX2 siRNA (100 nM; Santa-Cruz no. sc-35503) or missense siRNA (100 nM; control siRNA-A; Santa-Cruz no. sc-37007) in opti-minimum essential medium (Opti-MEM, Gibco Life Technologies).

To prepare the treatments, siRNAs were reconstituted in RNase free siRNA diluent (Santa Cruz) and stocks made up to 10 µM for storage at -20°C. On the day of treatment, siRNA and transfection reagent were diluted in separate tubes in Opti-MEM and incubated at 37°C for

20 minutes. Following this incubation, the siRNA was added to the transfection reagent in a one to one ratio and incubated for a further 30 minutes. Treatments were then added to each well for a final siRNA concentration of 100 nM and incubated for 6-8 hours. After incubation with siRNA, cells were again rinsed with warm, sterile PBS and treated with M1 or M2 polarising stimuli in complete RPMI 1640 culture medium as described above. The effectiveness of siRNA knockdown of NOX2 was assessed via measurement of NOX2 mRNA expression via real time-polymerase chain reaction (RT-PCR; see section 2.4).

2.3.2 Human primary macrophages from donor blood

Human monocytes were isolated from the buffy coat of healthy donor blood (Australia Red Cross Blood Bank, Melbourne, Australia), in a sterile Class II laminar flow hood. To first collect all peripheral blood mononuclear cells (PBMCs), buffy coat was aliquoted into 50 ml Falcon tubes so that the total volume did not exceed 20 ml per tube. Tubes were then topped up to 50 mls with MACS buffer (PBS supplemented with 0.5% FBS and 2 mM ethylenediaminetetraacetic acid, EDTA; Sigma-Aldrich) and layered onto Ficoll-Paque PLUS (GE Healthcare no. 17-144; 25 ml buffy coat onto 25 ml Ficoll) for density gradient centrifugation (400 g, 40 minutes, acceleration=1, deceleration=0) at 18-20°C. The plasma layer was then aspirated and the PBMC layer collected (Figure 2) in fresh tubes in MACS buffer.

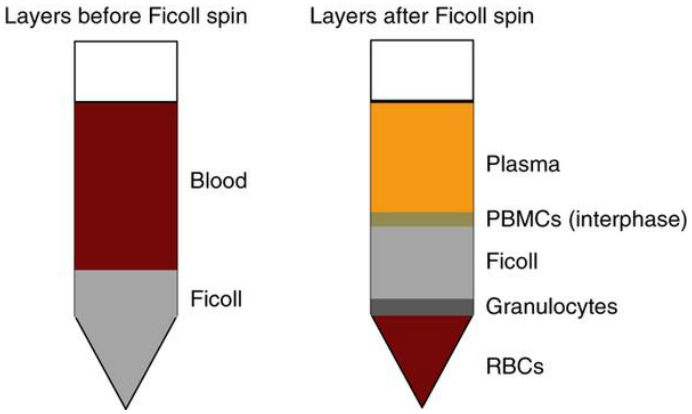

Figure 2.1 Layers before and after Ficoll spin. Adapted from Lin *et al.* (2014)

Platelet depletion was performed by centrifugation at 200 g for 15 minutes at 20°C. Cell pellets were then washed twice by resuspension in 50 ml MACS buffer and subsequent centrifugation at 300g for 10 minutes at room temperature. Any red blood cells (RBC) that may have been present in the pellet after washing were eliminated by incubating with 1 X RBC lysis buffer (10 x BD Pharm lyse; diluted 1 in 10 in sterile dH_2O; BD Biosciences, USA) for 5 minutes at room temperature. Cells were then diluted in a total volume of 50 ml in MACs buffer and an aliquot taken for assessment of cell concentration and viability via trypan blue exclusion. In brief, 10 µl of cell suspension was mixed with 10 µl of trypan blue (0.4%; Invitrogen, ThermoFisher Scientific, USA), loaded into a chamber slide (Countess™ Cell Counting Chamber Slides, Invitrogen, ThermoFisher Scientific, USA) and counted using the Countess™ Automated Cell Counter (Invitrogen, ThermoFisher Scientific, USA).

Monocytes were isolated from the purified PBMCs using the Pan Monocyte Isolation Kit (Miltenyi Biotec, Germany) according to the manufacturer's instructions. This kit allows purification of classical ($CD14^{high}$/ $CD16^{low}$), non-classical ($CD14^{low}$/$CD16^{high}$) and intermediate ($CD14^{high}$/ $CD16^{high}$) monocytes (11). The PBMC cell pellet was resuspended in MACS buffer in a volume of 3 µl per million cells. FcR blocking reagent was added at 1 µl per million cells

to prevent cell-cell attachment, followed by addition of the biotin-antibody cocktail at 1 µl per million cells to bind all non-monocyte leukocytes. Following incubation at 4°C for 5 minutes, MACs buffer (3 µl per million cells) and anti-biotin microbeads (2 µl per million cells) were added and cells were incubated for a further 10 minutes at 4°C. To collect the monocytes, the cell suspension was passed through an LS column (Miltenyi Biotec, Germany) using a MACS magnet (Miltenyi Biotec, Germany). Due to the binding of the biotin antibodies to the anti-biotin beads, all non-monocyte leukocytes were prevented from passing through the column. Hence the collected effluent contained a pure population of monocytes. The purity of the monocyte population was confirmed to be at least 85% as determined by flow cytometry using $CD14^+$ /$CD16^+$ expression and an aliquot was also collected for cell counting. The monocyte suspension was then centrifuged at 300 g for 10 minutes and the cell pellet was resuspended at 1 million cells per ml in RPMI 1640 Glutamax medium (Gibco, Life Technologies, USA) supplemented with 10% FBS, 1 x antibiotic/antimycotic (Gibco, Life Technologies, USA), 1 x sodium pyruvate (Sigma-Aldrich, USA), 1 x non-essential amino acids (NEAA; Gibco, Life Technologies, USA), and 50 ng/ml macrophage-colony stimulating factor (M-CSF; Miltenyi Biotec, Germany). Cells were either seeded in 6 well plates (2 ml per well) for collection of RNA (see section 2.4), protein (see section 2.5) and supernatants or in 96 well plates for ROS detection assays (see section 2.6). For macrophage differentiation, monocytes were maintained in a humidified incubator for 7 days during which the media containing M-CSF was replaced twice. After differentiation, the cell culture media was removed and replaced with standard RPMI Glutamax media and treated in the absence of M-CSF.

2.3.2.1 Treatment with M1 or M2 polarising stimuli

To investigate macrophage polarisation marker and NOX expression over a time course of M1 or M2 activation, macrophages were either left untreated (MΦ), treated with a combination of 20 ng/ml IFN-γ and 100 ng/ml LPS for M1 polarisation, or treated with 25 ng/ml IL-4) for M2 polarisation. RNA extraction was performed after 3, 6 and 24 hours of polarisation. Protein extraction (in 1.5 x Laemmli buffer) and ROS detection was performed following 24 hours of polarisation. In a subset of experiments, the effect of IL-4 or IL-13 on M1 polarisation was examined. In these experiments, macrophages were treated with M1 stimuli for 18 hours before the addition of 50 ng/ml of IL-4 or IL-13 for a further 6 hours. MMP release into the cell culture media was then assessed using gelatin zymography (see section 2.8) and superoxide generation assessed using L-012-enhanced chemiluminescence (see section 2.6.1).

2.3.2.2 IL-4 and IL-13 concentration response curves and treatment in the presence of signalling inhibitors

To compare the effects of different Th2 cytokines on M2 phenotype, macrophages were either left untreated (MΦ) or treated with increasing concentrations of either IL-4 or interleukin-13 (IL-13; Sigma-Aldrich no. I1771; reconstituted in sterile PBS) at concentrations ranging from 0.005 ng/ml to 50 ng/ml for 24 hours. To investigate the signalling pathways utilised by IL-4 and IL-13; a number of signal transduction inhibitors (STAT1, STAT3, STAT6 and p38 MAPK) were employed. The source, concentration and vehicle used for each inhibitor is summarised in Table 2.1. All inhibitors were added 30 minutes prior to treatment with a submaximal concentration (2.5 ng/ml) of IL-4 or IL-13 and remained present for the 24 hour duration of treatment. Inhibitor concentrations were selected based on previous studies in

cell culture and are listed in Table 2.1. As shown in Table 2.1 all inhibitors were dissolved in DMSO and the concentration of DMSO in the cell culture media did not exceed 0.1%.

Table 2.1 Signal transduction inhibitors used in IL-4/IL-13 comparative study (Chapter 5)

Name	Source	Target	[Inhibitor]	Reference	[DMSO]
Fludarabine	Selleckchem, USA	STAT1	100 µM	Cao *et al.*, (2015) (1)	0.1%
Stattic	Selleckchem, USA	STAT3	10 µM	Zhang *et al.,* (2015) (10)	0.1%
AS1517499	Axon MedChem, Netherlands	STAT6	100 nM	Chiba *et al.,* (2010) (2)	0.0001%
SB203580	InvivoGen, USA	p38 MAPK	1 µM	Jarnicki *et al.,* (2008) (4)	0.1%

2.3.2.3 Treatment of unpolarised or M2-polarised macrophages with angiotensin II

To assess the potential effects of angiotensin II on macrophage CCL18 expression, macrophages were either left untreated (MΦ), or treated with angiotensin II (100pM-1µM; AusPep, Australia) or IL-4 (positive control) for 48 hours. In a separate set of experiments, the effects of angiotensin II on IL-4 polarized M2 macrophages were investigated. For these experiments, macrophages were initially polarized to the M2 phenotype with a submaximal concentration of IL-4 (0.5ng/ml) for 24 hours, followed by treatment with 100 pM angiotensin II for a further 24 or 48 hours in the absence or presence of the AT_1R antagonist candesartan (1 µM; 30 minutes pre-treatment; AstraZeneca; reconstituted in DMSO). Angiotensin II was refreshed twice per day. Cell lysates were harvested for RNA and subsequent RT-PCR analysis (see section 2.4) whilst cell culture supernatants were collected for CCL18 detection via ELISA (see section 2.7).

2.3.3 Human aortic adventitial fibroblasts

To assess the potential pro-fibrotic effects of CCL18 and hydrogen peroxide in the vessel wall, human aortic adventitial fibroblasts (AoAF; Lonza no. CC-7014) were cultured from passages 2 to 8 in Stromal Cell Growth Medium (SCGM; Lonza no. CC-3205), containing 5% FBS. Cells were grown in T75 flasks and once confluent, passaged in complete SCGM using Trypsin-EDTA solution (Lonza no. CC-5012) for cell detachment. Cells were seeded at a concentration of 1 x 10^5 cells/ml for 24 hours prior to treatment in serum free SCGM. At the end of the treatment, cells were rinsed with warmed PBS and detached by incubating with Accutase® solution (Sigma-Aldrich, USA) at 37°C for 5 minutes and collected into microcentrifuge tubes for centrifugation (7000 rpm, 5 minutes, 4°C). Supernatants were discarded and cell pellets resuspended in 1 x RIPA Lysis and Extraction buffer for collection of protein. A subset of CCL18-treated cells were set up for RNA extraction (see section 2.4) in which lysis buffer was added directly to the wells for collection.

2.3.3.1 Hydrogen Peroxide treatment

Cells were seeded on 6 well plates (2 ml/well) and either left untreated or treated with transforming growth factor- ß (TGF-ß; 10 ng/mL; R&D systems no. 240-B-002 reconstituted in sterile 4 mM HCl) or hydrogen peroxide (1-10 µM; Invitrogen; diluted in sterile PBS) for 24 hours for collection of protein.

2.3.3.2 Co-culture with polarised THP-1 macrophages

THP-1 macrophages were first polarised to M1 or M2 macrophages (as described in section 2.3.1) or left unpolarised (MΦ) for 72 hours in complete RPMI 1640 medium in 24-well cell culture inserts (0.4 µm pore, <0.85 x 108 pores/cm2; 5 x 10^4 cells/insert; ThermoFisher Scientific). The THP-1 medium was replaced with serum free RPMI 1640 medium and the

inserts were transferred to wells with AoAF (500 µl/well) in serum free SCGM. THP-1 macrophages were stimulated with 10 µM PDBu in the absence or presence of catalase-polyethylene glycol (PEG-catalase; 1000 U/ml; Sigma-Aldrich no. C4963; reconstituted in sterile dH_2O) and the cultures incubated for a further 24 hours before collection of protein (see section 2.5).

2.3.3.3 CCL18 treatment

Cells were seeded on 6 well plates (2 ml/well) and either left untreated or treated with 10 ng/ml TGF-β or CCL18 (3-300 ng/ml; R & D Systems, USA; reconstituted in sterile PBS) for 3, 6, 24, 48 or 72 hours. mRNA was collected after 3, 6 and 24 hours (see section 2.4) and protein collected after 24, 48 and 72 hours (see section 2.5).

2.3.4 Human cardiac fibroblasts

Potential pro-fibrotic effects of CCL18 were also investigated in human cardiac fibroblasts (HCF; ScienCell, USA). HCF were cultured from passages 1 to 6 in Medium 199 (Life Technologies, USA) supplemented with 10% heat inactivated FBS (Life Technologies, USA), 5% penicillin streptomycin (Life Technologies, USA) and 5% fibroblast growth supplement (ScienCell, USA). Cells were grown in T75 flasks and once confluent, passaged in complete medium using Trypsin-EDTA solution (Lonza no. CC-5012) for cell detachment. Cells were seeded at a concentration of 1 x 10^5 cells/ml on 12-well plates (1 ml/well) and immediately treated with either 10 ng/ml TGF-β or CCL18 (3-300 ng/ml) for 72 hours. Untreated fibroblasts were used as a control and cells were collected in 1 x RIPA buffer as described in section 2.5.

2.4 Assessment of gene expression

2.4.1 RNA extraction from cell culture lysates

Total RNA was extracted from cell lysates using the RNeasy Mini Kit (Qiagen, Germany) as per the manufacturer's instructions. On the day of harvest, culture media was removed, cells rinsed with PBS and guanidine thiocynate-based lysis buffer (Buffer RLT; Qiagen, Germany) and 1% β-mercaptoethanol (β-ME; Sigma-Aldrich, USA) was added to each well. Cells were scraped with the base of an RNase-free 1 ml pipette tip and lysates collected in microcentrifuge tubes on ice. Samples were then mixed with 70% ethanol (1:1 volume) and transferred to RNeasy spin columns. RNA samples were purified using a series of wash buffers (Buffer RW1 followed by 2 washes with Buffer RPE) and any contaminating genomic DNA was removed using DNase (Diluted in Buffer RDD; RNase-free DNase Kit; Qiagen, Germany). Purified RNA was then eluted from spin columns with RNase-free water and 2 µl taken for assessment of yield and purity using either the QIAxpert system (Qiagen, Germany) or the Nanodrop 1000D spectrophotometer (ThermoScientific), both of which measure absorbance at 260 nm and 280 nm. An A_{260}:A_{280} ratio of 2 or more was considered sufficiently pure (5).

2.4.2 RNA extraction from aortae

Total RNA was extracted from thoracic aortae using the RNeasy Micro Kit (Qiagen, Germany) as per the manufacturer's instructions. Buffer RLT was added to each frozen aortic sample. Fine scissors were then used to mince the aorta, which was further disrupted by a hand held sonicator (UP50H; Hielscher, Germany). Protein was then digested by incubating samples in proteinase K (Qiagen, Germany) at 55°C for 10 minutes. Samples were then centrifuged (10,000 rpm, 5 minutes) and the supernatant collected into a new tube on ice and mixed with

0.5 volume of 100% ethanol. Purification and subsequent analysis of RNA concentration and purity was performed as described above.

2.4.3 cDNA conversion and RT-PCR

Depending on the RNA yields, 1µg or 0.5µg of RNA samples were converted to cDNA using a high-capacity cDNA reverse transcription kit (as per the manufacturer's instructions; Applied Biosystems, Australia), and a thermal cycler (BioRad MyCycler; BioRad, USA). Reaction conditions on the cycler were set for 4 steps: 25°C for 10min, 37°C for 2h, 85°C for 5min, and 4°C for holding. Resultant cDNA was then used as a template in quantitative real-time PCR (qRT-PCR) with pre-validated Taqman® primers and probes to measure mRNA expression of ACTA2, CCL8, CCL18, CCL22, CCR7, CCR8, COL1A1, COL3A1, COL5A1, CXCL11, IL-1β, IL-13Rα1, IL-4Rα, IL-2γc (γc), IL-6, IL-10, MRC-1, NOX1, NOX2 (CYBB), NOX4, NOX5, p22phox (CYBA), p40phox (NCF4), p47phox (NCF1), p67phox (NCF2), SOD1, SOD2, SOD3, TGF-β, TNFα, or the house keeping genes 18S, β-actin and GAPDH (Taqman Gene Expression Assays, Applied Biosystems, USA). Briefly, cDNA template was loaded in triplicate into the wells of a 96-well plate with Taqman Universal PCR Master Mix (Applied Biosystems, USA) and the Taqman primers and probes. Plates were placed in the Bio-Rad CFX96 RT-PCR Detection System (Bio-Rad Laboratories, Australia) and RT-PCR performed under the following thermal cycle parameters: initial step at 50°C for 2 minutes for optimal AmpErase UNG activity; initial denaturation at 95°C for 10 minutes; followed by 40 cycles of denaturation at 95°C for 15 seconds and annealing and extension at 60°C for 1 minute. Fluorescence was recorded at the end of each PCR cycle, and the threshold cycle (Ct) was defined as the cycle at which a signal was first detected. The ΔCt was defined as the difference between the Ct obtained for each gene marker and the Ct for the corresponding housekeeping gene (18S, β-actin or GAPDH).

ΔΔCt was then calculated as the difference between the ΔCt obtained for the treated sample versus the control sample. Fold change in gene expression was calculated using the following equation (9): Fold change= $2^{-\Delta\Delta Ct}$

2.5 Assessment of protein expression

Protein was extracted from THP-1 and primary macrophages in 1.5 x Laemmli buffer (7.5% glycerol, 3.75% β-ME, 2.25% SDS, 75 mM Tris-HCl pH 6.8, 0.004% bromophenol blue). Cells were disrupted by sonication and cell debris was cleared by centrifugation (13,000 rpm for 30 minutes) and the supernatants stored at -80°C. For aortic and cardiac fibroblasts, cell pellets were resuspended in 1 x RIPA Lysis and Extraction buffer (Cell Signalling Technology, USA), containing 1 mM Phenylmethanesulfonyl Fluoride (PMSF; Cell Signalling Technology, USA) and 1 x Protease/Phosphatase Inhibitor Cocktail (Cell Signalling Technology, USA). The fibroblast cell suspension was then incubated for at least 30 minutes on ice before centrifugation (13,000 rpm, 10 minutes, 4°C) to eliminate cell debris. Supernatants were stored at -20°C for subsequent western blot analysis. Protein concentrations were determined using either a modified Lowry protocol (samples in Laemmli buffer; RCDC colorimetric protein assay kit; BioRad Laboratories) or Bicinchoninic acid (BCA) based colorimetric quantification (Samples in RIPA buffer; PierceTM BCA Protein Assay, ThermoScientific).

Equivalent volumes of protein, loaded with 1.5 x Laemmli buffer, were heated to 95°C for 3 minutes and then loaded into 7.5%, 10% or 4-15% polyacrylamide gels in parallel with a molecular weight marker (Precision Plus Protein Dual Colour Standards, Bio-Rad Laboratories, USA). Proteins were separated according to molecular weight by SDS-PAGE (200 V for up to 1 hour) and transferred onto low fluorescence polyvinylidene fluoride (LF PVDF) membranes

using a semi-dry electroblotting transfer apparatus (Trans Blot Turbo transfer system, Bio-Rad Laboratories). Membranes were blocked with 5% skim milk (Diploma, Australia) in Tris-Buffered Saline (TBS; 200 mM Tris, 150 mM NaCl, pH 7.5) with 0.1 % tween-20 for 1 hour and subsequently probed with primary antibodies against IFIT1 (1:500; OriGene no. TA349041), NOX2 (1:500; Santa-Cruz no. sc-130549 (CL5)), p47phox (1:1000; BD Transduction Laboratories no. 610354), p67phox (1:2000; EMD Millipore no. 07-002), SOD2 (1:1000; EMD Millipore no. 06-984), SOD3 (1:1000; EMD Millipore no. 07-704), α-SMA (1:2500; Abcam no. ab5694), collagen 1 (1:1000; Abcam no. ab34710), IL-4Rα (1:500, Abcam no. ab131058), IL-13Rα1 (1:100, Abcam no. ab140367), IL-2Rγ (γC; 1:500, Abcam no. ab180698) and GAPDH (1:20000; Abcam no. ab8245) overnight at 4 °C. 1 hour incubation with horseradish peroxidase(HRP)-conjugated anti-rabbit (1:10000; Dako) or anti-mouse (1:10000; Jackson ImmunoResearch Laboratories) secondary antibodies was then performed and protein bands visualised using Clarity ECL substrate (BioRad Laboratories) and the ChemiDoc MP system (BioRad Laboratories). Densitometries of protein bands were quantified using Image Lab Software (BioRad Laboratories) and normalised to GAPDH.

2.6 Detection of reactive oxygen species

2.6.1 Superoxide detection via L-012-enhanced chemiluminescence

THP-1 or primary macrophages were seeded and polarised on white 96-well tissue culture plates (Perkin Elmer) at 5 x 10^4 and 2 x 10^5 cells/well respectively. Groups were set up in quintuplicate with a cell free control group, comprising media alone, included to provide a background reference. On the day of experimentation, culture medium was removed and cells were washed and incubated in warmed Krebs-HEPES buffer (118 mM NaCl, 4.7 mM KCl, 1.2 mM KH_2PO_4, 1.2 mM $MgSO_4$·7H2O, 2.5 mM $CaCl_2$, 25 mM $NaHCO_3$, 11.7 mM glucose , 20

mM HEPES; pH 7.4) in the absence or presence of superoxide dismutase-polyethylene glycol (PEG-SOD; Sigma-Aldrich no. S9549; reconstituted in sterile dH_2O) and background chemiluminescence measured for 30 minutes. Chemiluminescence was measured using a Chameleon Luminescence Plate Reader (Hidex Ltd, Turku, Finland) and data acquired using the MicroWin (Mikrotek, Overath, Germany) data acquisition system. 100 µM L-012 (Wako Pure Chemical Industries; reconstituted in distilled water) was then added to each well and basal superoxide levels were monitored for 30 minutes. Finally, the protein kinase C (PKC) activator PDBu (10 µM) was added to each well and superoxide production was then measured for a further 30-60 minutes. Peak PDBu-stimulated superoxide production was quantified as the average of 5 cycles at the peak of the signal for each group with the basal signal (average of the final 5 basal readings) subtracted. In a subset of experiments, cells were treated with superoxide dismutase (SOD; 1000 U/ml; human recombinant, expressed in *E. coli;* Sigma-Aldrich S9076; reconstituted in dH_2O) just prior to the beginning of the assay, to confirm signal specificity for superoxide.

2.6.2 Hydrogen peroxide detection via Amplex Red assay

THP-1 macrophages were seeded and polarised on black 96-well tissue culture plates (Perkin Elmer) at 5 x 10^4 cells/well in quintuplicate. On the day of experimentation, the media was removed, cells rinsed with Krebs-HEPES solution and Krebs-HEPES added to each well in the presence or absence of 1000 U/ml PEG-catalase or SOD. A hydrogen peroxide standard curve (0-5 µM) was constructed on the same plate to be read in parallel with the cell samples. Working amplex Red solution (Invitrogen), comprising of amplex Red (5 µM) and HRP (0.2 U/µl), was then added to sample and standard wells and fluorescence detected over 90 minutes using a Hidex Chameleon Plate Reader at 37 °C (520 nm excitation filter, 590 nm

emission filter). A subset of MΦ, M1 and M2 treatment groups were treated with 10 µM PDBu immediately prior to reading. The final fluorescence measurement from each group was fitted to the standard curve to approximate the hydrogen peroxide concentration. Fold changes in hydrogen peroxide concentration were calculated relative to the MΦ value recorded on the same day.

2.6.3 DCF ROS detection via Flow cytometry

THP-1 macrophages were polarised for 72 hours in complete RPMI 1640 medium on 6-well plates at 1 x 10^6 cells/well. Adherent cells were washed with warmed PBS prior to incubation with a cell permeable ROS-sensitive dye, 5-(and-6)-chloromethyl-2',7'-dichlorodihydrofluorescein diacetate, acetyl ester (CM-H2DCFDA; 1 µM, Sigma-Aldrich no. D6883; reconstituted in DMSO) for 30 minutes at 37°C. Cells were then left unstimulated, or stimulated with 10 µM PDBu for a further 30 minutes. In a subset of experiments, macrophages were incubated with 1000 U/ml PEG-Catalase for 15 minutes prior to PDBu stimulation. Following stimulation, cells were detached with Accutase® solution, centrifuged at 1500 rpm for 5 minutes and resuspended in PBS. Cells were then analysed on a LSR II flow cytometer for (BD Biosciences). Fold changes in DCF fluorescence were calculated relative to the MΦ value recorded on the same day.

2.7 Quantification of CCL18 secreted into culture media via ELISA

A CCL18 ELISA kit (Human CCL18/PARC DuoSet ELISA; R & D Systems, USA) was used to measure the concentration of CCL18 in the culture media from untreated and treated primary macrophages. The kit contained capture antibody, detection antibody, CCL18 standards, and Streptavidin conjugated to horseradish-peroxidase (Streptavidin-HRP). Other reagents (ELISA plates, PBS, 25 x wash buffer, 10 x reagent diluent, substrate solution, and stop solution) were

included in an ancillary kit (DuoSet Ancillary Reagent Kit 2; R & D Systems, USA). The assay was performed according to the manufacturer's instructions with all incubations performed at room temperature. All wash steps were performed 3 times.

Prior to the assay, the capture antibody (specific to CCL18) was reconstituted in 1 ml PBS and subsequently diluted 1:180 in PBS to the working concentration. ELISA plates were coated with the capture antibody (100 µl per well), sealed and incubated overnight. On the day of assay, capture antibody was removed and the plates washed with 1 x wash buffer (diluted in dH_2O; 3 x 300 µl washes). To prevent non-specific binding, the plates were blocked with 1 x reagent diluent (diluted in dH_2O; 300 µl per well) and incubated for 1 hour before washing. During the incubation period, CCL18 standards were prepared (7.81 pg/ml to 1 ng/ml) and samples diluted in reagent diluent to fit in the concentration range (1:1000 dilution for groups with IL-4 or IL-13 treatments, 1:20 for others). Samples and standards were added to the plates in duplicate (100 µl per well), and plates were sealed and incubated for 2 hours.

Following aspiration and washing, detection antibody was diluted 1:180 in reagent diluent to the working concentration and added to the plates (100 µl per well). Plates were sealed and incubated for a further 2 hours before aspiration, washing and subsequent incubation (20 minutes, protected from light) with Streptavidin-HRP (diluted 1:200 in reagent diluent, 100 µl per well). Plates were aspirated and washed and substrate solution (1:1 mixture of hydrogen peroxide and tetramethylbenzidine; 100 µl per well) added and incubated for 20 minutes. In this time the substrate solution was converted by the enzyme to a coloured product. The enzymatic reactions were terminated by the addition of stop solution (50 µl per well), with gentle tapping of the plate for thorough mixing. Finally, the colour density was determined using a micro-plate reader at 450 nm wavelength, and a CCL18 standard curve was created

with a 4 parameter logistic (4-PL) curve-fit. The intensity of the coloured product was directly proportional to the [CCL18] in the sample. The amount of CCL18 was therefore estimated by comparing the optical density (OD) values of the samples with the OD values of the CCL18 standards.

2.8 Quantification of MMP-2 and MMP-9 secreted into culture media via gelatin zymography

Expression of latent (L) MMP-2 and MMP-9 in the primary macrophage culture media following 24 hour treatment was assessed using gelatin zymography as previously described (3). Protein concentrations in the samples were determined using a Bradford protein assay (Bio-Rad protein assay kit II, Bio-Rad Laboratories, USA). 7.5 % acrylamide gels containing 1 mg/ml gelatin were loaded with equivalent volumes of protein, with samples from three or four independent experiments from each group run on the same gel. To assess the effects of IL-4 or IL-13 alone (see section 2.3.2.2), 10 μg or 20 μg protein was loaded for MMP9 and MMP2 expression, respectively. For assessment of the effects of IL-4 or IL-13 on M1 polarisation (see section 2.3.2.1), 5 μg or 10 μg protein was loaded for MMP9 and MMP2 expression, respectively. Gelatinolytic activity was indicated by clear bands and the densitometries assessed on the ChemiDoc MP system (BioRad Laboratories) using Image Lab Software (BioRad Laboratories). MMP densitometry was determined and expressed as the relative ratio of the values in the untreated control group (MΦ), which was expressed as 1.

2.9 Immunohistochemistry

2.9.1 Localisation of M2 macrophages, CCR8 and CCL8 in thoracic aortae from normotensive vs angiotensin II-treated hypertensive mice

Frozen mouse thoracic aortae were cut into 10 µm sections, three sections per slide, and mounted on Poly-L-Lysine coated glass slides. Sections were fixed in 4% paraformaldehyde (PFA; Sigma-Aldrich, USA) for 15 minutes and washed with PBS (137mM NaCl, 2.7mM KCl, 4.3 mM Na_2HPO_4, 1.47 mM KH_2PO_4; pH 7.4). Fixed sections were blocked with 2% bovine serum albumin (BSA; Sigma-Aldrich, USA) in PBS with 0.2% Triton X-100 (TX; Sigma Aldrich, USA) for 30 minutes and subsequently incubated with primary antibodies against mCCL8 (1:150 dilution; R and D systems, USA), mCCR8 (1:200 dilution; Abcam), M2 macrophage marker CD206 (1:500 dilution; Abcam) and endothelial cell marker Von Willebrand factor (vWF; 1:500 dilution; Abcam) at room temperature for 2 hours. Sections were then washed and incubated with secondary antibodies in the dark, at room temperature for 2 hours. Finally, slides were washed, and Vectashield mounting medium with diamidino-2-phenylindole (DAPI) added (Vector Laboratories, USA). Sections were imaged using a Nikon C1 upright confocal fluorescence microscope (x 40 objective lens; Monash Micro Imaging, Monash University, Clayton, Australia). CD206 and CCL8 positive cells were quantified using Image J (FIJI image analysis software, USA) in a blinded manner. Three sections were averaged per aorta and 6 aorta counted per group. Appropriate antibody controls were performed by staining sections in the absence of primary and/or secondary antibodies and imaged on the same day under identical settings to account for any autofluorescence of the tissue and non-specific binding of the antibodies.

2.9.2 Detection and localisation of F4/80 and IFIT1 in the aortic sinus and brachiocephalic arteries ApoE-/- mice

Frozen mouse hearts in OCT were cut into 10 µm sections through the aortic sinus and mounted on Poly-L-Lysine coated glass slides, 3 sections per slide. For brachiocephalic artery sections, frozen vessels in OCT were cut (10 µm sections) and mounted on Poly-L-Lysine coated glass slides, 4 sections per slide. Sections were fixed in 4% paraformaldehyde for 15 minutes and washed with PBS (3 x 10 minute washes). Fixed sections were blocked with 2% BSA in PBS with 0.2% Triton X-100 (TX; Sigma) and Mouse on Mouse (MOM) Ig blocking reagent (Vector Laboratories, USA) for 1 hour and subsequently incubated with primary antibodies against rabbit anti-IFIT1 (1:100, OriGene) and rat anti-F4/80 (cell surface macrophage marker, 1:100, Bio-Rad Laboratories) overnight at room temperature. Sections were then washed and incubated with the donkey anti-rabbit-488 (1:250, Life Technologies, USA) and goat anti-rat-564 (1:1000, Life Technologies, USA) secondary antibodies in the dark, at room temperature for 2 hours. Finally, slides were washed, Vectashield mounting medium with DAPI added (Vector Laboratories, USA) and slides cover slipped. Sections were imaged using a Nikon C1 upright confocal fluorescence microscope (x 20 and x 60 objective lenses; Monash Micro Imaging, Monash University, Clayton, Australia). Appropriate antibody controls were performed by staining sections in the absence of primary and/or secondary antibodies and imaged on the same day under identical settings to account for any autofluorescence of the tissue and non-specific binding of the antibodies.

2.10 Statistical Analysis

All data are expressed as mean ± SEM. Comparisons of multiple treatment groups were made using a 1-way ANOVA. Groups were compared using either a Sidak's, Dunnett's or Tukey's

post hoc test for selected comparisons, comparisons with control, and comparisons between all groups, respectively. Concentration response curves to IL-4 and IL-13 were fitted to a sigmoidal logistic equation and EC_{50} values determined based on fitted curves for the group data. Systolic BP data were analysed with a 2-way ANOVA followed by Bonferroni's post hoc test. When comparing two groups a student's unpaired t-test was used. $P<0.05$ was considered to be statistically significant and data were graphed and analysed using GraphPad Prism 7.02 software.

References

1. Cao ZH, Zheng QY, Li GQ, Hu XB, Feng SL, Xu GL, and Zhang KQ. STAT1-mediated down-regulation of Bcl-2 expression is involved in IFN-gamma/TNF-alpha-induced apoptosis in NIT-1 cells. *PLoS One* 10: e0120921, 2015.

2. Chiba Y, Todoroki M, and Misawa M. Interleukin-4 upregulates RhoA protein via an activation of STAT6 in cultured human bronchial smooth muscle cells. *Pharmacological research* 61: 188-192, 2010.

3. Chow BS, Chew EG, Zhao C, Bathgate RA, Hewitson TD, and Samuel CS. Relaxin signals through a RXFP1-pERK-nNOS-NO-cGMP-dependent pathway to up-regulate matrix metalloproteinases: the additional involvement of iNOS. *PLoS One* 7: e42714, 2012.

4. Jarnicki AG, Conroy H, Brereton C, Donnelly G, Toomey D, Walsh K, Sweeney C, Leavy O, Fletcher J, Lavelle EC, Dunne P, and Mills KH. Attenuating regulatory T cell induction by TLR agonists through inhibition of p38 MAPK signaling in dendritic cells enhances their efficacy as vaccine adjuvants and cancer immunotherapeutics. *J Immunol* 180: 3797-3806, 2008.

5. Krajisnik T, Bjorklund P, Marsel R, Ljunggren O, Akerstrom G, Jonsson KB, Westin G, and Larsson TE. Fibroblast growth factor-23 regulates parathyroid hormone and 1 alpha-hydroxylase expression in cultured bovine parathyroid cells. *Journal of Endocrinology* 195: 125-131, 2007.

6. Krege JH, Hodgin JB, Hagaman JR, and Smithies O. A noninvasive computerized tail-cuff system for measuring blood pressure in mice. *Hypertension* 25: 1111-1115, 1995.

7. Lin Z, Chiang NY, Chai N, Seshasayee D, Lee WP, Balazs M, Nakamura G, and Swem LR. In vivo antigen-driven plasmablast enrichment in combination with antigen-specific cell

sorting to facilitate the isolation of rare monoclonal antibodies from human B cells. *Nat Protoc* 9: 1563-1577, 2014.

8. Moore JP, Vinh A, Tuck KL, Sakkal S, Krishnan SM, Chan CT, Lieu M, Samuel CS, Diep H, Kemp-Harper BK, Tare M, Ricardo SD, Guzik TJ, Sobey CG, and Drummond GR. M2 macrophage accumulation in the aortic wall during angiotensin II infusion in mice is associated with fibrosis, elastin loss, and elevated blood pressure. *American journal of physiology Heart and circulatory physiology* 309: H906-917, 2015.

9. Schmittgen TD, and Livak KJ. Analyzing real-time PCR data by the comparative C-T method. *Nature Protocols* 3: 1101-1108, 2008.

10. Zhang Y, Ge C, Wang L, Liu X, Chen Y, Li M, and Zhang M. Induction of DKK1 by ox-LDL negatively regulates intracellular lipid accumulation in macrophages. *FEBS letters* 589: 52-58, 2015.

11. Ziegler-Heitbrock L, Ancuta P, Crowe S, Dalod M, Grau V, Hart DN, Leenen PJ, Liu YJ, MacPherson G, Randolph GJ, Scherberich J, Schmitz J, Shortman K, Sozzani S, Strobl H, Zembala M, Austyn JM, and Lutz MB. Nomenclature of monocytes and dendritic cells in blood. *Blood* 116: e74-80, 2010.

CHAPTER 3:

PROTEOMIC IDENTIFICATION OF INTERFERON-INDUCED PROTEINS WITH TETRATRICOPEPTIDE REPEATS (IFITs) AS MARKERS OF M1 MACROPHAGE POLARIZATION

Proteomic Identification of Interferon-induced Proteins with Tetratricopeptide Repeats (IFITs) as Markers of M1 Macrophage Polarization

Cheng Huang[†,⊥], Caitlin Lewis[‖,⊥] Natalie A. Borg[†], Meritxell Canals[‡], Henry Diep[‖], Grant Drummond[¶], Robert J. Goode[§], Ralf B. Schittenhelm[§], Antony Vinh[¶], Mingyu Zhu[‖], Barbara Kemp-Harper*[,‖], Oded Kleifeld*[,#] and Martin J. Stone*[,†]

One Sentence Summary: Proteomic studies of macrophage polarization to pro-inflammatory (M1) or tissue reparative (M2) phenotypes has identified interferon-induced proteins with tetratricopeptide repeats (IFIT1, IFIT2 and IFIT3) as potential biomarkers of inflammatory diseases such as atherosclerosis.

Affiliations:

[†] Infection and Immunity Program, Monash Biomedicine Discovery Institute & Department of Biochemistry and Molecular Biology, Monash University, VIC 3800, Australia

[‖] Cardiovascular Disease Program, Biomedicine Discovery Institute & Department of Pharmacology, Monash University, VIC 3800, Australia

[‡] Drug Discovery Biology, Monash Institute of Pharmaceutical Sciences, Monash University, Parkville, VIC 3052, Australia

[¶] Department of Physiology, Anatomy & Microbiology, School of Life Sciences, La Trobe University, VIC 3086, Australia

[§] Monash Biomedical Proteomics Facility, Monash Biomedicine Discovery Institute & Department of Biochemistry and Molecular Biology, Monash University, VIC 3800, Australia

[#] Faculty of Biology, Technion-Israel Institute of Technology, Technion City, Haifa 3200003, Israel

[⊥]Authors have contributed equally to this work

*To whom correspondence should be addressed: [redacted]

Abstract

Macrophages, which accumulate in tissues during inflammation, may be polarized towards pro-inflammatory (M1) or tissue reparative (M2) phenotypes. The balance between these phenotypes can have a substantial influence on the outcome of inflammatory diseases such as atherosclerosis. Improved biomarkers of M1 and M2 macrophages would be beneficial for research, diagnosis and monitoring the effects of trial therapeutics in such diseases. To identify novel biomarkers, we have characterized the global proteomes of THP-1 macrophages polarized to M1 and M2 states, in comparison with unpolarized (M0) macrophages. M1 polarization resulted in increased expression of numerous pro-inflammatory proteins, including the products of 31 genes under the transcriptional control of interferon regulatory factor 1 (IRF-1). In contrast, M2 polarization identified proteins regulated by components of the transcription factor AP-1. Among the most highly upregulated proteins under M1 conditions were the three interferon-induced proteins with tetratricopeptide repeats (IFIT1, IFIT2 and IFIT3), which function in antiviral defense. Moreover, IFIT1 was strongly upregulated in M1 polarized human primary macrophages and was also expressed in a subset of macrophages in aortic sinus and brachiocephalic artery sections from atherosclerotic ApoE$^{-/-}$ mice. Based on these results, we propose that IFIT proteins may serve as useful markers of atherosclerosis and potentially other inflammatory diseases.

Introduction

A common feature of inflammatory diseases is the accumulation of macrophages, derived from circulating monocytes, in the inflamed tissue. Rather than being a uniform cellular population, macrophages may be "polarized" in response to the local cytokine environment towards M1 or M2 phenotypes, which represent the two extremes of a spectrum of possible polarization states.[1] M1 macrophages, polarized by pro-inflammatory stimuli such as interferon-γ (IFN-γ) and tumor necrosis factor-α (TNF-α), generate pro-inflammatory cytokines (e.g. interleukin-1β (IL-1β), IL-6, IL-12, IL-18), are pro-oxidative and cause tissue damage. In contrast, M2 macrophages, polarized by anti-inflammatory cytokines such as IL-4 and IL-13, are generally considered to have anti-inflammatory, anti-oxidative and tissue reparative properties.[2] Thus, the balance between M1 and M2 macrophages plays a key role in determining whether the inflammation is exacerbated or readily resolved.

The balance between M1 and M2 macrophage populations is believed to have a significant influence on the outcome of vascular inflammation and the progression of atherosclerosis. M1 macrophages are most prevalent in the rupture prone "shoulder" regions of atherosclerotic plaques and are key contributors to plaque instability, whereas the fibrous caps of atherosclerotic plaques have a more even balance of M1 and M2 macrophages, consistent with the tissue reparative properties of M2 macrophages.[3] Thus, to reduce inflammation and to stabilise atherosclerotic plaques, it would be advantageous to maintain and/or enhance M2 macrophages while limiting M1 macrophages.

In order to understand the physiological and pathological roles of macrophages and to monitor the disease progression and the effects of trial therapeutics, it is important to identify the phenotypes of macrophages present in specific inflamed tissues. Traditionally, M1 macrophages have been identified via the expression of pro-inflammatory cytokines (e.g. IL-1β, TNF-α and IL-6), chemokines (e.g. CXCL9, CXCL10 and CXCL11) and their receptors (e.g. CCR7) together with inducible nitric oxide synthase (iNOS) and the co-stimulatory molecules CD80 and CD86.[4] Conversely, M2 macrophages are identified via the expression of pro-fibrotic (e.g. transforming growth factor-β (TGF-β) and insulin-like growth factor-1 (IGF-1))[5] and anti-inflammatory (IL-10) cytokines and scavenger receptors (mannose receptor C-type 1 (MRC-1), CD36)[6] and the anti-

inflammatory cell surface marker, CD163.[4] Whilst such biomarkers are useful, current limitations include differences between the expression profiles of murine and human M1 and M2 macrophages[7,8] and differences between *in vitro* and *in vivo* macrophages.[9,10] As such, investigations would greatly benefit from an improved set of biomarkers for M1 and M2 macrophages.

Several previous studies have explored the proteomes of polarized macrophages. An early study of primary human macrophages[11] identified a number of proteins that are specifically up- or down-regulated in macrophages treated with lipopolysaccharide (LPS) or IFN-γ compared to untreated controls, but did not investigate the more typical dual LPS/IFN-γ treatment or M2 polarized cells. Another study[12] focused on membrane associated proteins, identifying several that distinguish M1 or M2 polarized from non-polarized primary mouse macrophages. More recently, two studies[13,14] have used comparative proteomic methods (2D electrophoresis or SILAC) and the well-established THP-1 cell line to identify proteins expressed differentially between M1 and M2 macrophages, although neither of these studies included comparisons to non-polarized cells.

In light of recent advances in label-free proteomics methodologies, we have now performed a systematic global proteomics comparison of M1 polarized, M2 polarized and non-polarized THP-1 macrophages. From these data we have identified proteins that are either up- or down-regulated in the M1 or the M2 phenotypes and we have further validated these proteins using targeted proteomics and, for a subset of proteins, Western blot analysis. Importantly, these observations were confirmed in human primary macrophages and *in vivo*, utilizing a murine model of atherosclerosis. The study provides an expanded set of macrophage polarization markers that will serve as a valuable benchmark for future studies of inflammatory diseases and treatments.

Materials and Methods

Materials

RPMI-1640 media and heat-inactivated fetal bovine serum (FBS) were purchased from Life Technologies. Phorbol 12,13-dibutyrate, was purchased from Calbiochem. Human pan monocyte isolation kit and M-CSF were purchased from Miltenyi Biotec and Ficoll-Paque PLUS gradient from GE Healthcare. Formic acid, sodium deoxycholate (SDC), HEPES, β-casein from bovine milk, ethyl acetate, chloroacetamide (CAA), LPS, IFN- γ, IL-4, phosphate buffered saline (PBS) and Tris (2-carboxyethyl)phosphine hydrochloride solution (TCEP) were purchased from Sigma Aldrich. Sequencing grade modified trypsin was purchased from Promega. The RNeasy Mini kit and RNase-free DNase were purchased from Qiagen. The following antibodies were used: rabbit anti-SOD2 (Merck Millipore); mouse anti-p47-phox (neutrophil cytosolic factor 1, NCF1) (Santa Cruz Biotech); mouse anti-NFkB p100/p52 (Abcam); mouse anti-STAT1 (BD Biosciences); rabbit anti-IFIT1 (OriGene); mouse anti-iNOS (Abcam); anti-F4/80 (BioRad), rabbit anti-GADPH (Cell Signaling Technology); goat anti-mouse IgG (Sigma Aldrich) and goat anti-rabbit IgG (Cell Signaling Technology), goat anti-rat Alexa Fluor 594 IgG and chicken anti-rabbit Alexa Fluor 647 IgG (Life Technologies) as the secondary antibodies. The Mouse on Mouse Immunodetection kit and Vectashield mounting medium with diamidino-2-phenylindole (DAPI) were purchased from Vector Laboratories. The High Capacity cDNA Reverse Transcription kit and PCR primers for IFIT1, IFIT3, ICAM1, CXCL11, CCR7, IL-1β, MRC-1, β-actin and 18s were all purchased from Applied Biosystems.

Isolation of Primary Human Monocytes

Primary human monocytes were isolated from healthy blood donor buffy coats (Australian Red Cross Blood Service, Melbourne, Australia). Buffy coats were mixed with PBS supplemented with 0.5% FBS and 2 mM ethylenediaminetetraacetic acid (EDTA; Sigma-Aldrich) and layered onto Ficoll-Paque PLUS for density gradient centrifugation (400*g*, 40 min, acceleration=1, deceleration=0). The peripheral blood mononuclear cell (PBMCs) layer was collected and monocytes isolated using the human pan monocyte isolation kit according to the manufacturer's instructions. The purity of the

monocyte population was confirmed to be at least 85% as determined by Flow cytometry using $CD14^+$ /$CD16^+$ expression.

Cell Treatment Conditions

Human monocytic cells (THP-1) were cultured in high glucose RPMI 1640 medium, supplemented with 10% heat-inactivated FBS. Monocytes were grown in T75 tissue culture flasks in a humidified incubator (Sanyo MCO-18AIC CO_2 incubator, 5% CO_2, 37°C) and passaged every 3-4 days. For cell treatment, monocytes were seeded into 6 well plates at a density of $1x10^6$ cells/well and differentiated to macrophages with phorbol 12,13-dibutyrate (PDBu; 10 nM) for 24 hours. The successfully differentiated macrophages were subsequently treated with IFN-γ (5 ng/ml) and LPS (10 ng/ml) for M1 phenotype, IL-4 (25 ng/ml) for M2 phenotype, or left untreated (M0) as control for 48 hours (37 °C, 5% CO_2). After the treatment: for real time-PCR analysis and Western blotting, the cells were lysed directly on the plate; for secretome analysis, the media were collected; and for analysis of the global cellular proteome, the cells were trypsinized, washed with ice-cold PBS and stored at -80 °C for later use. Isolated donor blood-derived primary monocytes (1 x 10^6cells/ml) were differentiated into macrophages by culturing for 7 days in RPMI 1640 Glutamax medium, supplemented with 10% FBS, 1x antibiotic/antimyotic (Gibco Life Technologies, USA), 1 mM sodium pyruvate (Sigma-Aldrich), 1 x non-essential amino acids (NEAA; Gibco Life Technologies) and 50 ng/ml M-CSF. Following differentiation, the primary human macrophages were either left untreated (M0), treated with 100 ng/ml LPS and 20 ng/ml IFN-γ (M1), or treated with 25ng/ml IL-4 (M2). Cells were polarized for either 6 hours for real-time PCR or 24 hours for Western blotting. All the experiments were performed at least 3 times independently.

RNA Extraction and Real Time-PCR

Total RNA was extracted from macrophages using the RNeasy Mini Kit according to the manufacturer's instructions. RNase-free DNase was used to remove any contaminating DNA. The amount of RNA in each sample was quantified using a Nanodrop 1000D spectrophotometer (ThermoScientific), which measures absorbance at 260 nm and 280 nm. An A_{260}:A_{280} ratio of 2 or

more was considered sufficiently pure. 1 µg of RNA from each sample was reverse transcribed into cDNA using the High Capacity cDNA Reverse Transcription Kit with the reaction run in a thermal cycler (BioRad MyCycler, BioRad Laboratories). The resultant cDNA was used as a template for real time PCR with Taqman® primers and probes for IFIT1, IFIT3, ICAM1, CXCL11, CCR7, IL-1β, and MRC-1. β-actin and 18S were used as housekeeping genes. Real-time PCR was run in triplicate on the CFX96 Touch™ Real-Time PCR Detection Machine (BioRad Laboratories). Gene expression was quantified relative to the average M0 value using the comparative cycle threshold (Ct) method with the formula: Fold change= $2^{-\Delta\Delta Ct}$.[15]

Sample Preparation for Mass Spectrometric Analyses

To prepare samples for analysis of global proteomes, THP-1 cells were thawed and then lysed in 100 mM HEPES, 1% sodium deoxycholate, pH 8.2. The sample was sonicated and the protein concentration was determined with a BCA kit (Thermo Fisher Scientific). Two hundred µg of proteins from the cell lysate were reduced with 10 mM TCEP, alkylated with 40 mM CAA and then digested overnight with sequencing grade trypsin (Promega) with the ratio of 1:100 (trypsin to total protein, w/w) at 37°C, overnight. Phase transfer was used to remove sodium deoxycholate.[16] For better coverage of the proteome, off-line basic pH reverse-phase fractionation was performed using an Agilent Zorbax 300 Extend-C18 5 µM column (4.6*250 mm) on a HPLC 1100 (Agilent Technologies). The gradient was run as follows: 100% buffer A (10mM ammonium hydroxide) for 10min, 2.5% buffer B (10mM ammonium hydroxide, 80% acetonitrile) for 4min, 2.5% buffer B to 40% buffer B for 60min, 55% buffer B for 8 min, 100% buffer B for 8min, 0% buffer B for 10 min. The fractions were collected from 10 to 82 min. Seventy-two fractions were collected and pooled in a non-contiguous manner as previously described to obtain a total of 6 fractions.[17] Fractions were then dried completely in a lyophiliser (Labconco) and dissolved in buffer A (0.1% formic acid, 2% acetonitrile).

To prepare samples for protein quantification by parallel reaction monitoring (PRM), the cells were identically processed, but the fractionation step was omitted. Instead, the tryptic peptides were directly desalted with C18 StageTips[18], dried in a Speed Vac and dissolved in buffer A (0.1% formic acid, 2% acetonitrile).

To prepare samples for the analysis of secreted proteins, 8 mL of media from the THP-1 cell cultures were concentrated with 3 kDa-cutoff Amicon Ultra-4 Centrifugal Filter Devices (Millipore) and the buffer was exchanged to 50 mM Tris, 150 mM NaCl, pH 8.0 by centrifuging multiple times for 30-40 min, 4000*g*, 4°C. The protein concentration was determined using a Bradford assay (Expedeon). Two milligrams of protein were reduced with 10 mM TCEP at 50°C for 20 min and alkylated by incubation with 20 mM CAA for 20 min in the dark. The protein mixture was loaded into a 50 kDa-cutoff Amicon Ultra-0.5 Centrifugal Filter Device (Millipore) and centrifuged at 14,000*g* for 15 min. The concentration of the filtrate was determined using a NanoDrop spectrophotometer. Trypsin was added at a ratio of 1:100 (w/w) and the sample incubated overnight at 37 °C. The sample was acidified with formic acid and desalted using C18 Omix tips (Agilent). The eluted peptides were dried in a Speed Vac (Labconco) and dissolved in buffer A.

LC-MS/MS for Proteome Analysis

For analysis of global cellular proteomes and secretomes, the peptide samples were analyzed by LC-MS/MS using a Q Exactive and Q Exactive Plus mass spectrometer (Thermo Fisher Scientific) respectively, coupled online to a RSLC nano HPLC (Ultimate 3000, UHPLC Thermo Fisher Scientific). Samples were loaded onto a 100 µm, 2 cm nanoviper Pepmap100 trap column and the peptides were separated on a RSLC nanocolumn 75 µm x 50 cm, Pepmap100 C18 analytical column (Thermo Fisher Scientific) using the following gradient of buffer A (0.1% formic acid, 2% acetonitrile) and buffer B (0.1% formic acid in 80% acetonitrile): 2.5% buffer B for 5 min; 2.5% to 12.5% buffer B over 1 min; 12.5% to 32.5% buffer B over 108 min; 32.5% to 42.5% buffer B over 6 min; 42.5% to 99% buffer B over 5 min; 99% buffer B for 7 min; 99% to 2.5% buffer B over 1 min; re-equilibration at 2.5% buffer B for 20 min. The eluent was nebulized and ionized using a Thermo nano Flex electrospray source with a distal coated fused silica emitter (New Objective). The capillary voltage was set at 1.7 kV. The Q Exactive instrument was operated in the data dependent acquisition mode to automatically switch between full scan MS and MS/MS acquisition. Each survey full scan (m/z 375–1800) was acquired in the Orbitrap with 70,000 resolution (at m/z 200) after accumulation of ions to a 3 x 10^6 target value with maximum injection time of 30 ms. Dynamic exclusion was set to 20 seconds. The 10 most intense multiply charged ions ($z \geq 2$) were sequentially isolated and fragmented in the collision cell by higher-energy collisional

dissociation (HCD) with a fixed injection time of 60 ms, 17,500 resolution and automatic gain control (AGC) target of 5×10^4.

For analysis of targeted proteomics by PRM, peptide samples were subjected to LC-MS/MS using the same LC gradient as used for the analysis of global cellular proteomes and secretomes (above). The 224 precursor ions with scheduled retention times were set to target the MS2 scans. The inclusion list can be found in Table S1. A survey full scan and data-independent acquisition (DIA) mode were applied to generate targeted data. The survey full scan MS spectra (m/z 375-1800) were acquired in the Orbitrap with 70,000 resolution (at 200m/z), after accumulation of ions to a 1×10^6 target value with maximum injection time of 50 ms. The DIA scan was acquired with 17,500 resolution, AGC target 2×10^5, loop counts of 20 and an isolation window of 2 m/z.

Raw DDA data files have been deposited at PRIDE[19] with the dataset identifier PXD008204 (password: 3fFbrLyP).

Global Proteomics Data Analysis and Statistics

For identification of the global cellular proteome, all generated files were submitted to MaxQuant (version 1.5.2.8), coupled with the Andromeda search engine[20], to generate a list of proteins with label-free quantitation (LFQ) intensities. Database searching was performed with the following parameters: cysteine carbamidomethylation as a fixed modification; methionine oxidation and N-terminal acetylation as variable modifications; up to 2 missed cleavages permitted; mass tolerance of 20 ppm; 1% protein false discovery rate (FDR) for protein and peptide identification; and minimum 2 peptides for pair-wise comparison in each protein. The human protein sequence database was downloaded from Uniprot in July 2014.

The lists of proteins with LFQ values were processed with Perseus (Version 1.5.0.31), a module from the MaxQuant suite. After removing the reversed and known contaminating proteins, the LFQ values were $\log_2$ transformed and the reproducibility across the biological replicates was evaluated by Pearson's correlation analysis. The replicates were grouped into M0, M1 and M2 with categorical annotation rows. At least 2 valid

values out of the 3 repeats in at least one treatment condition was set to filter out the proteins without LFQ intensity. Missing values after filtering were replaced by imputation. Multiple-samples Test based on ANOVA (FDR = 5%) was performed to obtain identify the proteins with significantly changed expression levels. Only the proteins with ANOVA significant were used for the subsequent analyses.

For identification of the secretome under each treatment condition, LFQ values were generated in the same manner as for the global cellular proteome, except we used updated versions of MaxQuant (1.5.3.30), Perseus (1.5.4.0) and the protein sequence database (May 2016). The proteins were submitted to ProteinSide (http://www.proteinside.org/) for signal peptide prediction. The secreted proteins were imported back into Perseus for statistical analysis. The statistical analysis was the same as that used for the global cellular proteome.

Targeted Proteomics Data Analysis

A spectral library was built in Skyline 3.1[21], based on the global proteomics MS/MS data from MaxQuant generated from global proteome identification. All precursors from 18 selected proteins were refined in Skyline, making sure that at least three proteotypic peptides were used for quantification of each protein. In total, a transition list of 224 precursor ions with scheduled retention times was generated in and exported from Skyline. All PRM data analysis and data integration was performed in Skyline. The mass spectrometric raw files were imported into Skyline under the targeted acquisition mode and each peak was manually examined to ensure accurate quantification. A dot product cut-off of 0.9 was chosen (1 indicates a perfect match to the spectral library) and the sum of the peak area for each protein was exported to Excel and normalized to the corresponding peak area in untreated cells (M0). Statistical analysis was based on a one way ANOVA, Dunnett's post hoc test in GraphPad Prism 6.0.

Western Blot

Equal amounts of protein from M0, M1 or M2 treated THP-1 or primary macrophages were separated with a NuPAGE 4-12% SDS-PAGE (Invitrogen) and electro-transferred to a polyvinylidene difluoride (PVDF) membrane. The PVDF membrane was blocked with 5% skim milk in Tris-Buffered Saline (TBS, 200mM Tris, 150mM NaCl, pH 7.5) with 0.1 % tween-20 for 1 hour and subsequently probed with primary antibodies

overnight at 4 °C. Secondary antibodies bound with horseradish peroxidase were incubated at room temperature for 1 hour, detected by enhanced chemiluminescence (Western Lightning Plus ECL, PerkinElmer), documented and quantitated with the ChemiDoc MP Imager and ImageLab software (Bio-Rad). All the band intensities generated from ImageLab software were first normalized to the housekeeping gene GADPH and then expressed relative to the untreated (M0) conditions. Statistical significance was based on one way ANOVA, Dunnett's post hoc test in GraphPad 6.0.

Functional Annotation

Data for proteins showing significant differences between treatment conditions in the global cellular proteome and secretome were combined and submitted to Perseus for Z-score normalization, with matrix access by rows. Hierarchical clustering was used to assess the similarity between each replicate and treatment condition using the Euclidean for distance calculation and average for linkage in row and column trees with a maximum of 300 clusters.[22] Subsequently, TM4:MeV[23] was used to group the proteins into different clusters based on k-Means/Medians Clustering[24] with the setting of 6 clusters. The proteins from different clusters were submitted into FunRich 3.0[25] for biological pathway and transcription factor enrichment analysis.

Experimental Animals

All procedures were approved by the Monash Animal Research Platform (MARP) Animal Ethics Committee and conducted in compliance with the National Health and Medical Research Council of Australia's (NHMRC) Guidelines for the Ethical and Humane Use of Animals in research. ApoE$^{-/-}$ mice were obtained from the Animal Resources Centre (Canning Vale, WA, Australia). Mice were bred on the C57BL6/J background and only male mice were used in this study.

ApoE$^{-/-}$ mice were weaned at 3 weeks of ages, housed in groups of up to 4 littermates and given access to normal chow and water *ad libitum*. At 5 weeks of age they were placed on a high fat diet (HFD; 22% fat, 0.15% cholesterol; SFOO-219, Specialty Feeds, WA, Australia) and maintained on this diet for a further 14 weeks. At this time point mice were killed by an overdose of isoflurane inhalation (Baxter Healthcare,

Australia) and hearts and brachiocephalic arteries were frozen in Optimal Cutting Temperature compound (OCT; Sakura Finetek, USA) for immunohistochemistry.

Immunohistochemistry

Frozen mouse hearts in OCT were cut into 10 µm sections through the aortic sinus and mounted on Poly-L-Lysine coated glass slides. Brachiocephalic arteries in OCT were also cut into 10 µm sections and mounted on Poly-L-Lysine coated glass slides. Sections were fixed in 4% paraformaldehyde (PFA; Sigma-Aldrich, USA) for 15 min and washed with PBS. Fixed sections were blocked with 2% bovine serum albumin (BSA; Sigma) in PBS with 0.2% Triton X-100 (TX; Sigma) and Mouse on Mouse (MOM) Ig blocking reagent (Vector Laboratories, USA) for 1 hour and subsequently incubated with primary antibodies against rabbit anti-IFIT1 (1:100, OriGene) and rat anti-F4/80 (cell surface macrophage marker, 1:100, Bio-Rad Laboratories) overnight at room temperature. Sections were then washed and incubated with the donkey anti-rabbit-488 (1:250, Life Technologies, USA) and goat anti-rat-564 (1:1000, Life Technologies, USA) secondary antibodies in the dark, at room temperature for 2 hours. Finally, slides were washed, Vectashield mounting medium with diamidino-2-phenylindole (DAPI) added (Vector Laboratories, USA) and slides cover slipped. Appropriate antibody controls were performed by staining sections in the absence of primary or secondary antibodies and imaged on the same day under identical settings. Sections were imaged using a Nikon C1 upright confocal fluorescence microscope equipped with x 20 or x 60 objectives and run on NIS Elements Software (Nikon, Tokyo, Japan). Representative images were chosen from n=6 (brachiocephalic arteries) or n=8 (aortic Sinus) $ApoE^{-/-}$ mice, 3 sections per animal.

Results

M1 and M2 Polarization of THP-1 Macrophages

THP-1 cells are an immortalized human monocytic cell line commonly used as a model for monocytes and macrophages. In this study THP-1 cells were differentiated to a macrophage state by treatment with PDBu, then polarized towards either an M1 or M2 phenotype by treatment with IFN-γ and LPS or with IL-4, respectively; untreated control cells (differentiated but not polarized) are labeled M0. To validate these polarization conditions we used qRT-PCR to determine the mRNA levels for several recognized polarization markers (Fig 1). Treatment with IFN-γ/LPS lead to a significant increase in the M1 markers IL-1β (8-fold), CCR7 (500-fold) and CXCL11 (50-fold). Whilst IL-4 treatment had no effect on M1 marker expression, the M2 marker MRC-1 was increased 5-fold. In addition, M1 polarization was associated with an ~80% reduction in MRC-1 mRNA expression. Taken together, these results confirm polarization to M1 and M2 macrophage phenotypes by IFN-γ/LPS and IL-4 treatments, respectively.

Global Proteomics of Differentially Polarized THP-1 Macrophages

We used global label-free quantification (LFQ) proteomics[26] to compare cellular protein expression levels in unpolarized (M0), M1-polarized and M2-polarized THP-1 macrophages. Using a FDR cutoff of 0.01, we identified 6,656 proteins and we were able to quantify 6,131 proteins in at least 2 out of 3 independent repeats of each treatment (Table S2). The excellent reproducibility of the LFQ methods is illustrated by the coefficient of variation (CV) curves (Fig S1); the median CV values were 14.7% for M0, 15.1% for M1 and 16.3% for M2 conditions, respectively.

Statistical analysis (ANOVA, permutation-based FDR<0.05) identified 280 proteins (Table S3) that show significantly different expression levels between any two of the three treatment conditions. Hierarchical clustering, based on the expression levels of these proteins, indicated that the three repeats from each treatment are clustered together and that the expression profiles for the M0 and M2 conditions are more similar to each other than to the profile for M1 conditions (Fig 2A). This is confirmed by a principal component analysis (Fig S2) and is also consistent with previous reports that IL-4 treated macrophages showed less

substantial changes in transcriptional and protein expression levels in comparison to LPS and IFN-γ treated cells.[8,13]

Cluster Analysis of Significantly Regulated Proteins

The 280 differentially expressed proteins were subjected to cluster analysis, yielding the six clusters shown in Fig 2B and C and summarized in Table 1. Among the 280 differentially expressed proteins, 97 were classified as upregulated in M1 conditions (cluster $M1^{Hi}$), 44 as upregulated in M2 conditions (cluster $M2^{Hi}$) and 29 additional proteins as upregulated in both M1 and M2 conditions (cluster $M1^{Hi}/M2^{Hi}$). In addition, 44 and 24 proteins were downregulated under M1 and M2 conditions, respectively, and 42 additional proteins were downregulated in both polarization conditions; these three clusters are labeled $M1^{Lo}$, $M2^{Lo}$ and $M1^{Lo}/M2^{Lo}$, respectively. Interestingly, none of the clusters involved predominant upregulation of proteins under one polarization condition and downregulation of the same proteins under the alternative polarization condition and a figure of merit analysis (Fig S3) indicated that extension to a larger number of clusters was not justified.

The proteins in each cluster were analyzed to identify significantly enriched biological processes and transcription factors whose target gene products were significantly enriched in each cluster (Table 1). Cluster $M1^{Hi}$ was significantly enriched ($p<0.01$; at least 4 proteins per process) for 24 biological processes, many of which are related to interferon or cytokine signaling, as expected from the M1 treatment conditions. Consistent with this finding, transcription factor enrichment analysis strongly indicated enhanced activity of interferon regulatory factor 1 (IRF1) in the $M1^{Hi}$ group; the mechanistic significance of this finding is discussed below. Smaller numbers of significantly enriched processes were found for other clusters. In particular, cluster $M2^{Hi}$ was enriched in processes related to signal transduction, platelet degranulation and aggregation, oxidation-reduction, cell-cell adhesion and the innate immune response. Among the 12 transcription factors whose gene products were significantly enriched in the $M2^{Hi}$ cluster, the top five (FOS, FOSB, JUN, JUNB and JUND) are all components of the activator protein 1 (AP-1) transcription factor, which is responsible for a various of cellular functions, including cell proliferation, differentiation and apoptosis.[27]

Identification of Secreted Proteins from Differentially Polarized THP-1 Macrophages

Previous studies indicate that M1 and M2 macrophages differ substantially in the cytokines that they secrete. Therefore, to complement the cellular proteomics data, we analyzed the secreted proteins (secretome) from M1 and M2 polarized in comparison to unpolarized THP-1 macrophages. Although the use of serum-free media may have allowed detection of a larger number of secreted proteins, we chose to retain the same growth conditions as in the above analysis of cellular proteins because growth in serum-free media could also have altered the secretome. To reduce interference from serum proteins, we focused our analysis on proteins with molecular masses below ~30 kDa, which were separated by dialysis from higher molecular weight proteins, including the major serum proteins albumin and immunoglobulins.

Using the same global LFQ workflow as for the cellular proteins above, we identified 168 secreted proteins from the media (Table S4), of which forty were derived from precursor proteins containing signal peptides, as determined using Proteinside (http://www.proteinside.org/), and an additional 76 were determined to be potentially secreted proteins without signal peptides (Table S5). Six of these proteins (Table S6) were observed in one treatment condition and, strikingly, these included four members of the chemokine family (CCL3, CCL4, CCL5 and CXCL10), all of which were detected in media from M1 polarized cells but not in either unpolarized or M2 polarized cells. Consistent with our observations, Cassol et al. have reported previously that M1 polarization of human monocyte-derived macrophages can significantly increase the expression of these chemokines.[28]

Validation of Significantly Regulated Proteins

To verify the changes in the protein expression observed above, eighteen of the cellular proteins that showed differential expression in the global proteomics data set were arbitrarily selected for analysis by parallel reaction monitoring (PRM), a targeted, quantitative MS-MS method.[29] These included eleven proteins from the $M1^{Hi}$ cluster, six proteins from $M2^{Hi}$ cluster and one protein from the $M1^{Hi}/M2^{Hi}$ cluster. The changes in protein levels for the eighteen selected proteins under M1 and M2 polarization conditions are listed in Table 2 for the PRM data set in comparison with the global proteomics data set. Among the eleven proteins from the $M1^{Hi}$ cluster, all showed significant increases under M1 conditions and none showed significant changes under M2 conditions in the PRM data set. Similarly, among the six proteins from the $M2^{Hi}$ cluster, all showed

significant increases under M2 conditions and none showed significant changes under M1 conditions in the PRM data set. Finally, the protein from the $M1^{Hi}/M2^{Hi}$ cluster displayed significant increases under both M1 and M2 conditions in the PRM data set. Thus, the PRM data set was in excellent agreement with the global LFQ proteomics data set.

Considering that the major changes in protein expression levels observed were induced by M1 polarization, we used Western blots to further evaluate changes for four of the proteins found to be significantly increased under M1 conditions in the global proteomics and PRM data sets (NCF1, NF□B2, SOD2, STAT1); these proteins have previously been reported to be overexpressed in M1 macrophages. [30-32] As shown in Fig 3 and Table 2, all four proteins showed significant increases by Western blot under M1 conditions but not under M2 conditions, confirming the changes observed by proteomics methods.

Enhanced Expression of Interferon-induced Protein with Tetratricopeptide Repeats 1 (IFIT1) in Primary Human Macrophages

The THP-1 macrophage proteomics data revealed large and significant increases, under M1 conditions, in the expression levels of three closely related proteins known as interferon-induced proteins with tetratricopeptide repeats 1, 2 and 3 (IFIT1, IFIT2 and IFIT3)[33-35]; levels of these proteins were increased by factors of 236 ± 101, 25 ± 17 and 26 ± 4, respectively, in M1-polarized THP-1 macrophages relative to vehicle-treated controls. Since THP-1 cells are an immortalized cell line, it is important to determine whether the expression changes we observed in THP-1 macrophages are relevant to macrophages derived from primary monocytes. To this end, we initially used macrophages differentiated *in vitro* (using macrophage-colony stimulating factor (M-CSF)) from primary human monocytes, isolated from the buffy coat of donor blood, to determine the mRNA levels for IFIT1 and IFIT3 as well as the established M1 polarization marker intercellular adhesion molecule 1 (ICAM-1). M1 polarization was associated with an increase in mRNA expression of IFIT1, IFIT3 and ICAM-1 by 250-, 80- and 20-fold, respectively (Fig 4A). Moreover, Western blotting confirmed a robust increase in IFIT1 protein expression in M1 polarized human primary macrophages (Fig 4B and C).

Expression of IFIT1 in Atherosclerotic Plaque Macrophages of $ApoE^{-/-}$ mice

Considering that macrophages are abundant in atherosclerotic plaques and M1 macrophages are particularly implicated in atherosclerosis[36], we used the $ApoE^{-/-}$ mouse model of atherosclerosis to assess the potential

of IFIT1 as a M1 macrophage marker *in vivo*. The expression of IFIT1 in aortic sinus and brachiocephalic artery sections from atherosclerotic ApoE$^{-/-}$ mice was assessed by immunohistochemistry. Immunofluorescent staining revealed a subpopulation of atherosclerotic plaque macrophages (F4/80 positive cells) expressing IFIT1 in both the aortic sinus and brachiocephalic arteries (Figure 5 and 6). IFIT1 expression was also evident in non-macrophage cells within the plaque and in the media and adventitia of the vessels. Despite this diffuse expression of IFIT1 there was a substantial population of F4/80 positive cells that did not appear to express IFIT1, likely to represent macrophage phenotypes other than the pro-inflammatory M1 subset, suggesting that IFIT1 could potentially be used as a marker to distinguish between macrophage subsets.

Discussion

The balance between pro-inflammatory (M1-like) and anti-inflammatory (M2-like) polarized macrophages is thought to be critical in controlling the exacerbation versus resolution of macrophage-mediated inflammatory diseases such as atherosclerosis. To understand the biochemical factors contributing to the functions of polarized macrophages and to identify macrophages with distinct phenotypes, it is important to identify proteins with differential expression in differently polarized (and non-polarized) macrophages. In this study, we applied quantitative proteomics to identify differences in protein expression between THP-1 macrophages polarized to M1 and M2 states, in comparison with non-polarized THP-1 macrophages. We found numerous significant differences between the differently treated cells and identified a number of proteins whose expression is significantly enhanced under either M1 or M2 conditions as well as a small number exhibiting significantly reduced expression levels (Fig 2). Here we focus on the proteins with expression enhancements of ≥4-fold (Table 3), most of which were observed under M1 conditions.

Among the most upregulated proteins in M1 conditions, there are some that have previously been identified as M1 markers, including: the adhesion molecule ICAM1; two components of the non-canonical NFκB pathway (NFκB2 and RELB); and NCF1 (Fig 3, Table 2), a subunit of NADPH oxidase, which promotes formation of reactive oxygen species (ROS), a characteristic feature of M1 macrophages (Fig 3 and 4 and Table 2).[37] Some other M1 markers, such as CD38[38], NFκB1[1] and CD14[39] were also significantly upregulated in M1 conditions, albeit more weakly. Similarly, under M2 polarization conditions, we observed strong induction of CD209 (Table 2), a C-type lectin receptor expressed on macrophages, which is induced by IL-4[40] and has been used previously as a M2 polarization marker.[41] In addition, TGM2, a potential M2 marker[42,43], was also strongly upregulated under M2 conditions. The observation of these proteins in the current study is reassuring and helps to validate THP-1 cells as an appropriate model for macrophage polarization. Furthermore, several of the upregulated proteins identified in this study have also been observed in previous proteomics studies of polarized THP-1 or primary macrophages, including ICAM1[12], ACSL1[12], C3[13] and SOD2[13]. Nevertheless, as discussed below, the current study also identified a number of proteins that have not been found previously to be polarization markers, including IFIT1, IFIT2, IFIT3, OASL, OAS2, MX1 and MX2.

Perhaps our most striking observation was that the three related proteins IFIT1, IFIT2 and IFIT3 were all enhanced by at least 25-fold under M1 treatment conditions (Table 3). The enhanced expression in M1 macrophages was validated at the mRNA level for IFIT1 and IFIT3 in macrophages obtained by differentiation and subsequent polarization of primary human monocytes *in vitro.* IFIT1 protein upregulation was also confirmed in these cells. Furthermore, IFIT1 staining was clearly evident in the atherosclerotic plaques of $ApoE^{-/-}$ mice. For a population of cells, this staining co-localized with the macrophage marker F4/80; the identities of other IFIT1-positive cells remain to be determined. As not all F4/80 positive cells were IFIT1 positive, the double positive cells are likely to represent the M1 macrophage population in plaques. IFIT proteins are antiviral proteins whose expression is strongly induced by type I interferons (IFN-α and IFN-β).[34] Although they are structurally related, each being composed of several tetratricopeptide repeat (TPR) domains, they have different mechanisms of antiviral action.[33-35] IFIT1 and IFIT2 inhibit translation of viral mRNAs by binding to structural features present in viral mRNA, but not cellular mRNA, and also by binding elongation initiation factor 3 (eIF3).[34,35] IFIT1 has also been reported to inhibit viral replication by binding to the E1 helicase of human papilloma virus.[44] By contrast, IFIT3 acts as an adaptor protein, bridging the mitochondrial antiviral signaling (MAVS) complex to TANK-binding kinase (TBK1) and thereby causing derepression of the transcription factor nuclear factor kappa B (NFκB) in response to viral infection.[33,45] Considering previous reports that IFIT gene expression is only weakly induced by IFN-γ[46], our observation of robust induction in THP-1 macrophages polarized by treatment with IFN-γ and LPS is novel and suggests that IFIT proteins may be useful markers for M1 polarization. To our knowledge, these proteins have not previously been identified as M1 polarization markers, although Jablonski et al reported 3.5- and 2-fold induction of IFIT-1 and IFIT-2 mRNA, respectively, in M1-polarized murine macrophages.[38] Interestingly, two studies have shown reductions in IFIT mRNA in mouse macrophages or THP-1 monocytes treated with reputedly anti-inflammatory food extracts (from pistachio nuts and cranberries, respectively), prompting the authors of one study to suggest that IFIT-2 may be a biomarker for inflammatory cardiovascular disease.[47,48] The validation of IFIT proteins as cardiovascular disease markers will require future comparisons of tissue samples from patients and healthy controls.

Consistent with the elevation of IFIT proteins under M1 polarization conditions, we also observed significantly higher levels of several other proteins, or groups of proteins, involved in virus detection and MAVS-mediated antiviral signaling. In particular, we observed 7- and 8-fold enhancements of the two retinoic acid-inducible gene 1 (RIG-I)-like helicases, RIG-I and melanoma differentiation associated protein 5 (MDA5), which sense viral RNA and, upon activation, associate with MAVS on the surface of mitochondria. In addition, we found 8- and 7-fold enhancements, respectively, of interferon-stimulated gene 15 (ISG15), which is an antiviral ubiquitin-like protein, and Ubch8, the ubiquitin-conjugating (E2) enzyme that catalyzes conjugation of ISG15 to target proteins, including both RIG-I and IFIT1.[49,50] Under M1 conditions, there was also a large (18-fold) increase in the level of the 2´-5´-oligoadenylate synthetase (OAS)-like protein (OASL), which can bind to viral double-stranded RNA (dsRNA) and mediate RIG-I activation and consequent MAVS formation and signaling.[51,52] In addition, the related OAS1, OAS2 and OAS3 were all increased 7- to 10-fold under M1 conditions. Although these proteins are not known to regulate the RIG-I/MAVS pathway, they inhibit viral translation by sensing viral dsRNA and, in response, synthesizing oligoadenylate dimers, which activate RNase L, leading to degradation of viral RNA.[53] Finally, under M1 polarization conditions we also observed substantial (13- to 15-fold) increases in the levels of the two myxovirus resistance proteins MX1 and MX2, which bind to components of viral capsids, thereby sequestering them or preventing their translocation into the nucleus [53]. Notably, MX1 is also a target of ISG15 conjugation.

All of the viral defense proteins discussed above have previously been identified as products of interferon stimulated genes (ISGs).[54] ISGs are a large family (hundreds) of proteins, mostly involved in priming cells for defense against viruses and bacteria, whose expression is upregulated by either type I interferons (including IFN-α and -β), type II interferons (IFN-γ) or type III interferons (IFN-λ1 to IFN-λ4).[53] Considering that M1 polarization was induced in the current study by treatment of the cells with IFN-γ and LPS, it is possible to rationalize the upregulation of these ISG proteins in terms of known aspects of interferon and LPS signaling. In one likely mechanism, presented in Fig 7, LPS signals via toll-like receptor 4 (TLR4), leading to activation of the transcription factor nuclear factor kappa B (NFκB) and consequent upregulation of numerous inflammatory genes (IGs). In parallel, IFN-γ signals via the IFN-γ receptor, thereby activating the *Janus kinase*

and *signal* transducer and activator of transcription (JAK-*STAT*) pathway, driving the expression of hundreds of IFN-γ responsive genes, including transcription factors of the interferon regulatory factor 1 (IRF-1) family.[55] Importantly, transcription of IRF-1 can be upregulated synergistically in response to STAT-1 and NFκB [56] and this mechanism has been proposed to induce expression of IFN-β[55] In turn, IFN-β is expected to be secreted and to act in an autocrine manner to further stimulate the JAK-*STAT pathway* via the type I IFN receptor[53], thereby upregulating expression of additional ISGs. In support of this proposed mechanism, transcription factor enrichment analysis of the 97 proteins in the $M1^{Hi}$ cluster indicated that this cluster is highly enriched with the products of genes previously determined to be regulated by IRF-1 (31 genes; $p = 4 \times 10^{-17}$, Bonferroni correction), including IFIT1-3, RIG-I (gene DDX58), ISG15, Ubch8 (gene UBE2L6), OAS1, OAS3, and MX1. Moreover, expression of CCL5, one of four chemokines whose secretion levels were upregulated in M1 polarization conditions, has also been reported to be mediated by IRF-1.[57] In summary, the proposed mechanism accounts for many of our observations of enhanced protein expression under M1 conditions.

While the relatively simple scheme in Fig 7 may account for many of the protein enhancements observed under M1 polarization conditions, we also observed enhancements of several proteins that suggest the existence of feedback mechanisms that could further amplify the proposed pathways. These include: STAT1 (a known IRF-1-regulated gene); STAT2; the canonical NFκB transcription factor NFκB1; two components of the non-canonical NFκB pathway, NFκB2 and RelB; and CD14, an LPS pattern-recognition co-receptor.[58] Although the mechanisms leading to induction of these factors remain to be determined, they are likely to amplify the initial responses to IFN-γ and LPS as well as the induced response to IFN-β.

The addition of IL-4 (M2 stimulus) to macrophages resulted in less pronounced protein changes than the addition of M1 stimuli. Nonetheless, the upregulation of several known M2 markers was observed with increases in the cell surface marker CD209[8], the transglutaminase TGM2[59], and proteins consistent with the pro-fibrotic functions of M2 macrophages such as TGF-β1 and COL6A1.[60] However, subsequent pathway analyses did not produce conclusive outcomes to explain the M2 induced effects from a mechanistic point of view. AP-1 transcription factor, the major enriched transcription factor in M2 macrophages, has been mainly implicated in regulating M1 polarized macrophages.[61] However, Fontana *et al*.[62,63] found that JUNB, a

member of the AP-1 family, was involved in regulating both M1 and M2 polarized macrophages and further investigation performed by Yang *et al.*[64] identified that JUN transcription factor was significantly over-expressed in mouse M2 polarized macrophages. This observation is consistent with our findings, but it also highlights the need for additional studies to unravel the mechanisms underlying M2 polarization.

Conclusion

In conclusion, proteomic analysis has shown that M1 polarized macrophages express high levels of numerous antiviral proteins, predominantly under the control of the transcription factor IRF-1, whereas M2 polarization results in more modest changes in expression of proteins related to pro-fibrotic functions. This study has identified IFIT proteins as highly upregulated by M1 polarization. Moreover, the high expression level of IFIT1 in a subset of macrophages within atherosclerotic plaques suggests that the IFIT proteins may serve as useful markers (in combination with other proteins) of M1 macrophages in experimental animals or in human pathology applications. Future studies will be needed to determine whether the IFITs and other proteins overexpressed under M1 conditions also contribute to the pathology of atherosclerosis or other macrophage-associated diseases.

References

(1) Wang, N.; Liang, H.; Zen, K., Molecular mechanisms that influence the macrophage m1-m2 polarization balance. *Front. Immunol.* 2014, 5, 614.

(2) Mantovani, A.; Garlanda, C.; Locati, M., Macrophage diversity and polarization in atherosclerosis: a question of balance. *Arterioscler. Thromb. Vasc. Biol.* 2009, 29, 1419-1423.

(3) Stoger, J. L.; Gijbels, M. J.; van der Velden, S.; Manca, M.; van der Loos, C. M.; Biessen, E. A.; Daemen, M. J.; Lutgens, E.; de Winther, M. P., Distribution of macrophage polarization markers in human atherosclerosis. *Atherosclerosis* 2012, 225, 461-468.

(4) Colin, S.; Chinetti-Gbaguidi, G.; Staels, B., Macrophage phenotypes in atherosclerosis. *Immunol. Rev.* 2014, 262, 153-166.

(5) Gordon, S.; Martinez, F. O., Alternative Activation of Macrophages: Mechanism and Functions. *Immunity* 2010, 32, 593-604.

(6) Stein, M.; Keshav, S.; Harris, N.; Gordon, S., Interleukin 4 potently enhances murine macrophage mannose receptor activity: a marker of alternative immunologic macrophage activation. *J. Exp. Med.* 1992, 176, 287-292.

(7) Raes, G.; Van den Bergh, R.; De Baetselier, P.; Ghassabeh, G. H.; Scotton, C.; Locati, M.; Mantovani, A.; Sozzani, S., Arginase-1 and Ym1 are markers for murine, but not human, alternatively activated myeloid cells. *J. Immunol.* 2005, 174, 6561.

(8) Martinez, F. O.; Gordon, S.; Locati, M.; Mantovani, A., Transcriptional profiling of the human monocyte-to-macrophage differentiation and polarization: new molecules and patterns of gene expression. *J. Immunol.* 2006, 177, 7303-7311.

(9) Sica, A.; Mantovani, A., Macrophage plasticity and polarization: in vivo veritas. *J. Clin. Invest.* 2012, 122, 787-795.

(10) Murray, P. J.; Allen, J. E.; Biswas, S. K.; Fisher, E. A.; Gilroy, D. W.; Goerdt, S.; Gordon, S.; Hamilton, J. A.; Ivashkiv, L. B.; Lawrence, T.; Locati, M.; Mantovani, A.; Martinez, F. O.; Mege, J. L.; Mosser, D. M.; Natoli, G.; Saeij, J. P.; Schultze, J. L.; Shirey, K. A.; Sica, A.; Suttles, J.; Udalova, I.; van Ginderachter, J. A.; Vogel, S. N.;

Wynn, T. A., Macrophage activation and polarization: nomenclature and experimental guidelines. *Immunity* 2014, 41, 14-20.

(11) Brown, J.; Wallet, M. A.; Krastins, B.; Sarracino, D.; Goodenow, M. M., Proteome bioprofiles distinguish between M1 priming and activation states in human macrophages. *J. Leukoc. Biol.* 2010, 87, 655-662.

(12) Becker, L.; Liu, N. C.; Averill, M. M.; Yuan, W.; Pamir, N.; Peng, Y.; Irwin, A. D.; Fu, X.; Bornfeldt, K. E.; Heinecke, J. W., Unique proteomic signatures distinguish macrophages and dendritic cells. *PLoS One* 2012, 7, e33297.

(13) Meijer, K.; Weening, D.; de Vries, M. P.; Priebe, M. G.; Vonk, R. J.; Roelofsen, H., Quantitative proteomics analyses of activation states of human THP-1 macrophages. *J. Proteomics* 2015, 128, 164-172.

(14) Zhang, F.; Liu, H.; Jiang, G.; Wang, H.; Wang, X.; Wang, H.; Fang, R.; Cai, S.; Du, J., Changes in the proteomic profile during the differential polarization status of the human monocyte-derived macrophage THP-1 cell line. *Proteomics* 2015, 15, 773-786.

(15) Schmittgen, T. D.; Livak, K. J., Analyzing real-time PCR data by the comparative C(T) method. *Nat. Protoc.* 2008, 3, 1101-1108.

(16) Masuda, T.; Tomita, M.; Ishihama, Y., Phase transfer surfactant-aided trypsin digestion for membrane proteome analysis. *J. Proteome Res.* 2008, 7, 731-740.

(17) Batth, T. S.; Francavilla, C.; Olsen, J. V., Off-line high-pH reversed-phase fractionation for in-depth phosphoproteomics. *J. Proteome Res.* 2014, 13, 6176-6186.

(18) Rappsilber, J.; Mann, M.; Ishihama, Y., Protocol for micro-purification, enrichment, pre-fractionation and storage of peptides for proteomics using StageTips. *Nat. Protoc.* 2007, 2, 1896-1906.

(19) Vizcaino, J. A.; Csordas, A.; del-Toro, N.; Dianes, J. A.; Griss, J.; Lavidas, I.; Mayer, G.; Perez-Riverol, Y.; Reisinger, F.; Ternent, T.; Xu, Q. W.; Wang, R.; Hermjakob, H., 2016 update of the PRIDE database and its related tools. *Nucleic Acids Res.* 2016, 44, D447-456.

(20) Cox, J.; Mann, M., MaxQuant enables high peptide identification rates, individualized p.p.b.-range mass accuracies and proteome-wide protein quantification. *Nat. Biotechnol.* 2008, 26, 1367-1372.

(21) MacLean, B.; Tomazela, D. M.; Shulman, N.; Chambers, M.; Finney, G. L.; Frewen, B.; Kern, R.; Tabb, D. L.; Liebler, D. C.; MacCoss, M. J., Skyline: an open source document editor for creating and analyzing targeted proteomics experiments. *Bioinformatics* 2010, 26, 966-968.

(22) Devaux, S.; Cizkova, D.; Quanico, J.; Franck, J.; Nataf, S.; Pays, L.; Hauberg-Lotte, L.; Maass, P.; Kobarg, J. H.; Kobeissy, F.; Meriaux, C.; Wisztorski, M.; Slovinska, L.; Blasko, J.; Cigankova, V.; Fournier, I.; Salzet, M., Proteomic Analysis of the Spatio-temporal Based Molecular Kinetics of Acute Spinal Cord Injury Identifies a Time- and Segment-specific Window for Effective Tissue Repair. *Mol. Cell. Proteomics* 2016, 15, 2641-2670.

(23) Howe, E. A.; Sinha, R.; Schlauch, D.; Quackenbush, J., RNA-Seq analysis in MeV. *Bioinformatics* 2011, 27, 3209-3210.

(24) Soukas, A.; Cohen, P.; Socci, N. D.; Friedman, J. M., Leptin-specific patterns of gene expression in white adipose tissue. *Genes Dev.* 2000, 14, 963-980.

(25) Pathan, M.; Keerthikumar, S.; Ang, C. S.; Gangoda, L.; Quek, C. Y.; Williamson, N. A.; Mouradov, D.; Sieber, O. M.; Simpson, R. J.; Salim, A.; Bacic, A.; Hill, A. F.; Stroud, D. A.; Ryan, M. T.; Agbinya, J. I.; Mariadason, J. M.; Burgess, A. W.; Mathivanan, S., FunRich: An open access standalone functional enrichment and interaction network analysis tool. *Proteomics* 2015, 15, 2597-2601.

(26) Cox, J.; Hein, M. Y.; Luber, C. A.; Paron, I.; Nagaraj, N.; Mann, M., Accurate proteome-wide label-free quantification by delayed normalization and maximal peptide ratio extraction, termed MaxLFQ. *Mol. Cell. Proteomics* 2014, 13, 2513-2526.

(27) Karin, M.; Liu, Z.; Zandi, E., AP-1 function and regulation. *Curr. Opin. Cell Biol.* 1997, 9, 240-246.

(28) Cassol, E.; Cassetta, L.; Rizzi, C.; Alfano, M.; Poli, G., M1 and M2a polarization of human monocyte-derived macrophages inhibits HIV-1 replication by distinct mechanisms. *J. Immunol.* 2009, 182, 6237-6246.

(29) Peterson, A. C.; Russell, J. D.; Bailey, D. J.; Westphall, M. S.; Coon, J. J., Parallel reaction monitoring for high resolution and high mass accuracy quantitative, targeted proteomics. *Mol. Cell. Proteomics* 2012, 11, 1475-1488.

(30) Biswas, S. K.; Mantovani, A., Macrophage plasticity and interaction with lymphocyte subsets: cancer as a paradigm. *Nat. Immunol.* 2010, 11, 889-896.

(31) Padgett, L. E.; Burg, A. R.; Lei, W.; Tse, H. M., Loss of NADPH oxidase-derived superoxide skews macrophage phenotypes to delay type 1 diabetes. *Diabetes* 2015, 64, 937-946.

(32) Leopold Wager, C. M.; Hole, C. R.; Wozniak, K. L.; Olszewski, M. A.; Mueller, M.; Wormley, F. L., Jr., STAT1 signaling within macrophages is required for antifungal activity against Cryptococcus neoformans. *Infect. Immun.* 2015, 83, 4513-4527.

(33) Zhou, X.; Michal, J. J.; Zhang, L.; Ding, B.; Lunney, J. K.; Liu, B.; Jiang, Z., Interferon induced IFIT family genes in host antiviral defense. *Int. J. Biol. Sci.* 2013, 9, 200-208.

(34) Fensterl, V.; Sen, G. C., Interferon-induced Ifit proteins: their role in viral pathogenesis. *J. Virol.* 2015, 89, 2462-2468.

(35) Vladimer, G. I.; Gorna, M. W.; Superti-Furga, G., IFITs: Emerging Roles as Key Anti-Viral Proteins. *Front. Immunol.* 2014, 5, 94.

(36) Chinetti-Gbaguidi, G.; Colin, S.; Staels, B., Macrophage subsets in atherosclerosis. *Nature reviews. Cardiology* 2015, 12, 10-17.

(37) Tan, H.-Y.; Wang, N.; Li, S.; Hong, M.; Wang, X.; Feng, Y., The Reactive Oxygen Species in Macrophage Polarization: Reflecting Its Dual Role in Progression and Treatment of Human Diseases. *Oxid. Med. Cell. Longev.* 2016, 2016, 16.

(38) Jablonski, K. A.; Amici, S. A.; Webb, L. M.; Ruiz-Rosado Jde, D.; Popovich, P. G.; Partida-Sanchez, S.; Guerau-de-Arellano, M., Novel Markers to Delineate Murine M1 and M2 Macrophages. *PLoS One* 2015, 10, e0145342.

(39) Italiani, P.; Boraschi, D., From Monocytes to M1/M2 Macrophages: Phenotypical vs. Functional Differentiation. *Front. Immunol.* 2014, 5, 514.

(40) Relloso, M.; Puig-Kroger, A.; Pello, O. M.; Rodriguez-Fernandez, J. L.; de la Rosa, G.; Longo, N.; Navarro, J.; Munoz-Fernandez, M. A.; Sanchez-Mateos, P.; Corbi, A. L., DC-SIGN (CD209) expression is IL-4 dependent and is negatively regulated by IFN, TGF-beta, and anti-inflammatory agents. *J. Immunol.* 2002, 168, 2634-2643.

(41) Fujisaka, S.; Usui, I.; Bukhari, A.; Ikutani, M.; Oya, T.; Kanatani, Y.; Tsuneyama, K.; Nagai, Y.; Takatsu, K.; Urakaze, M.; Kobayashi, M.; Tobe, K., Regulatory Mechanisms for Adipose Tissue M1 and M2 Macrophages in Diet-Induced Obese Mice. *Diabetes* 2009, 58, 2574-2582.

(42) Martinez, F. O.; Helming, L.; Milde, R.; Varin, A.; Melgert, B. N.; Draijer, C.; Thomas, B.; Fabbri, M.; Crawshaw, A.; Ho, L. P.; Ten Hacken, N. H.; Cobos Jimenez, V.; Kootstra, N. A.; Hamann, J.; Greaves, D. R.; Locati, M.; Mantovani, A.; Gordon, S., Genetic programs expressed in resting and IL-4 alternatively activated mouse and human macrophages: similarities and differences. *Blood* 2013, 121, e57-69.

(43) Arnold, C. E.; Gordon, P.; Barker, R. N.; Wilson, H. M., The activation status of human macrophages presenting antigen determines the efficiency of Th17 responses. *Immunobiology* 2015, 220, 10-19.

(44) Terenzi, F.; Saikia, P.; Sen, G. C., Interferon-inducible protein, P56, inhibits HPV DNA replication by binding to the viral protein E1. *EMBO J.* 2008, 27, 3311-3321.

(45) Liu, X. Y.; Chen, W.; Wei, B.; Shan, Y. F.; Wang, C., IFN-induced TPR protein IFIT3 potentiates antiviral signaling by bridging MAVS and TBK1. *J. Immunol.* 2011, 187, 2559-2568.

(46) Der, S. D.; Zhou, A.; Williams, B. R.; Silverman, R. H., Identification of genes differentially regulated by interferon alpha, beta, or gamma using oligonucleotide arrays. *Proc. Natl. Acad. Sci. U. S. A.* 1998, 95, 15623-15628.

(47) Hannon, D. B.; Thompson, J. T.; Khoo, C.; Juturu, V.; Vanden Heuvel, J. P., Effects of cranberry extracts on gene expression in THP-1 cells. *Food Sci. Nutr.* 2017, 5, 148-159.

(48) Zhang, J.; Kris-Etherton, P. M.; Thompson, J. T.; Vanden Heuvel, J. P., Effect of pistachio oil on gene expression of IFN-induced protein with tetratricopeptide repeats 2: a biomarker of inflammatory response. *Mol. Nutr. Food Res.* 2010, 54 Suppl 1, S83-92.

(49) Morales, D. J.; Lenschow, D. J., The antiviral activities of ISG15. *J. Mol. Biol.* 2013, 425, 4995-5008.

(50) Zhang, D.; Zhang, D. E., Interferon-stimulated gene 15 and the protein ISGylation system. *J. Interferon Cytokine Res.* 2011, 31, 119-130.

(51) Ibsen, M. S.; Gad, H. H.; Andersen, L. L.; Hornung, V.; Julkunen, I.; Sarkar, S. N.; Hartmann, R., Structural and functional analysis reveals that human OASL binds dsRNA to enhance RIG-I signaling. *Nucleic Acids Res.* 2015, 43, 5236-5248.

(52) Zhu, J.; Zhang, Y.; Ghosh, A.; Cuevas, R. A.; Forero, A.; Dhar, J.; Ibsen, M. S.; Schmid-Burgk, J. L.; Schmidt, T.; Ganapathiraju, M. K.; Fujita, T.; Hartmann, R.; Barik, S.; Hornung, V.; Coyne, C. B.; Sarkar, S. N., Antiviral activity of human OASL protein is mediated by enhancing signaling of the RIG-I RNA sensor. *Immunity* 2014, 40, 936-948.

(53) Schneider, W. M.; Chevillotte, M. D.; Rice, C. M., Interferon-stimulated genes: a complex web of host defenses. *Annu. Rev. Immunol.* 2014, 32, 513-545.

(54) Rusinova, I.; Forster, S.; Yu, S.; Kannan, A.; Masse, M.; Cumming, H.; Chapman, R.; Hertzog, P. J., Interferome v2.0: an updated database of annotated interferon-regulated genes. *Nucleic Acids Res.* 2013, 41, 1040-1046.

(55) Boehm, U.; Klamp, T.; Groot, M.; Howard, J. C., Cellular responses to interferon-gamma. *Annu. Rev. Immunol.* 1997, 15, 749-795.

(56) Pine, R., Convergence of TNFalpha and IFNgamma signalling pathways through synergistic induction of IRF-1/ISGF-2 is mediated by a composite GAS/kappaB promoter element. *Nucleic Acids Res.* 1997, 25, 4346-4354.

(57) Liu, H.; Ning, H.; Men, H.; Hou, R.; Fu, M.; Zhang, H.; Liu, J., Regulation of CCL5 expression in smooth muscle cells following arterial injury. *Plos One* 2012, 7, e30873.

(58) Kitchens, R. L., Role of CD14 in cellular recognition of bacterial lipopolysaccharides. *Chem. Immunol.* 2000, 74, 61-82.

(59) Beljaars, L.; Schippers, M.; Reker-Smit, C.; Martinez, F. O.; Helming, L.; Poelstra, K.; Melgert, B. N., Hepatic Localization of Macrophage Phenotypes during Fibrogenesis and Resolution of Fibrosis in Mice and Humans. *Front. Immunol.* 2014, 5, 430.

(60) Wynn, T. A.; Vannella, K. M., Macrophages in Tissue Repair, Regeneration, and Fibrosis. *Immunity* 2016, 44, 450-462.

(61) Juhas, U.; Ryba-Stanislawowska, M.; Szargiej, P.; Mysliwska, J., Different pathways of macrophage activation and polarization. *Postepy Hig Med Dosw (Online)* 2015, 69, 496-502.

(62) Fontana, M. F.; Baccarella, A.; Kellar, D.; Oniskey, T. K.; Terinate, P.; Rosenberg, S. D.; Huang, E. J.; Herbert, D. R.; Kim, C. C., Myeloid expression of the AP-1 transcription factor JUNB modulates outcomes of type 1 and type 2 parasitic infections. *Parasite Immunol.* 2015, 37, 470-478.

(63) Fontana, M. F.; Baccarella, A.; Pancholi, N.; Pufall, M. A.; Herbert, D. R.; Kim, C. C., JUNB is a key transcriptional modulator of macrophage activation. *J. Immunol.* 2015, 194, 177-186.

(64) Yang, Y.; Qin, J.; Lan, L.; Li, N.; Wang, C.; He, P.; Liu, F.; Ni, H.; Wang, Y., M-CSF cooperating with NFkappaB induces macrophage transformation from M1 to M2 by upregulating c-Jun. *Cancer Biol. Ther.* 2014, 15, 99-107.

Figures and tables

Table 1. Summary of protein clusters identified

Cluster	Number of Proteins	Biological Pathways	Transcription Factors
$M1^{Hi}$	97	type I IFN-mediated signaling; defense response to virus; response to virus; negative regulation of viral genome replication; IFN-γ-mediated signaling; innate immune response; negative regulation of type I IFN production; inflammatory response; positive regulation of NF-κB activity; apoptotic process; response to cytokine stimulus; I-κB kinase/NF-κB cascade; leukocyte migration; positive regulation of protein phosphorylation; negative regulation of apoptotic process; cellular response to LPS; positive regulation of angiogenesis; positive regulation of transcription from RNA polymerase II promoter; cell adhesion; angiogenesis; negative regulation of neuron apoptotic process; T cell receptor signaling; aging; protein homooligomerization	IRF-1
$M2^{Hi}$	44	platelet aggregation; platelet degranulation; cell-cell adhesion; signal transduction; oxidation-reduction process; innate immune response	FOS; FOSB; JUN; JUNB; JUND; SRF; PPARA; BACH2; BACH1; SP1; RUNX2; STRA13
$M1^{Hi}/M2^{Hi}$	29	tRNA aminoacylation for protein translation	
$M1^{Lo}$	44	positive regulation of GTPase activity	ZEB1; SP1; ELF2; TGIF1; TEAD1; SP4; MEIS2; FOXD1; HOXB3; EGR1; NFYA; IRF1; ELF1
$M2^{Lo}$	24	mitosis	MYC; ESRRA
$M1^{Lo}/M2^{Lo}$	42	-	FOXK1; FOXJ2

Table 2. Comparison of changes in protein levels determined by global proteomics, targeted proteomics and Western blot.

	Fold Change Global Proteomics (DDA)		Fold Change Targeted Proteomics (PRM)		Fold Change Western Blot	
Gene name	M1	M2	M1	M2	M1	M2
DTX3L	2.7 ± 0.4 ***	0.9 ± 0.1	5.4 ± 0.8 **	1.3 ± 0.1		
IFIT3	25.8 ± 3.6 ****	0.5 ± 0.1	39.1 ± 4.2 ***	0.9 ± 0.1		
NCF1	6.3 ± 0.3 ****	1.4 ± 0.2	6.0 ± 1.0 **	1.7 ± 0.4	5.5 ± 0.4 ***	1.7 ± 0.4
NFKB2	6.9 ± 0.7 ****	1.0 ± 0.1	10.5 ± 0.7 **	1.2 ± 0.2	2.2 ± 0.4 *	0.9 ± 0.1
OAS3	10.4 ± 2.3 ****	0.6 ± 0.2	15.7 ± 2.4 ****	1.0 ± 0.1		
OASL	17.4 ± 3.3 ****	0.9 ± 0.2	12.1 ± 1.0 ***	1.6 ± 0.6		
PARP9	11.5 ± 5.4 **	1.0 ± 0.5	15.1 ± 2.5 ****	1.2 ± 0.1		
RELB	4.7 ± 0.8 ***	0.9 ± 0.1	13.6 ± 3.1 **	2.5 ± 0.1		
SOD2	7.5 ± 0.8 ****	1.1 ± 0.1	6.9 ± 0.9 ***	1.3 ± 0.2	2.2 ± 0.2 **	1.0 ± 0.2
STAT1	3.2 ± 0.1 ****	0.8 ± 0.1	4.5 ± 0.7 ***	1.1 ± 0.1	1.8 ± 0.1 **	0.9 ± 0.1
EIF2AK2	2.8 ± 0.4 ****	1.0 ± 0.1	3.0 ± 0.5 **	1.1 ± 0.1		
TGM2	0.3 ± 0.1	149 ± 68 ***	0.8 ± 0.2	32 ± 15 **		
CD209	0.8 ± 0.1	8. 1± 1.2 ***	1.3 ± 0.2	5.7 ± 0.1 ****		
F13A1	0.1 ± 0.1	65 ± 22 ****	2.6 ± 1.1	666 ± 65 ****		
DOK2	0.9 ± 0.1	1.7 ± 0.2 **	0.9 ± 0.2	1.5 ± 0.1 *		
LSP1	0.4 ± 0.1	3.4 ± 0.4 ****	0.6 ± 0.1	2.1 ± 0.2 ***		
SORT1	0.9 ± 0.1	12.5 ± 2.1 ****	0.7 ± 0.1	17.0 ± 0.7****		
TGFBI	1.5 ± 0.1 *	1.8 ± 0.2 **	1.8 ± 0.3 *	1.8 ± 0.1 *		

* $p < 0.05$; ** $p < 0.01$; *** $p < 0.001$; **** $p < 0.0001$

Table 3. Proteins whose expression was enhanced by ≥4-fold under polarization conditions.

Gene Name	M1/M0	M2/M0	Cluster
IFIT1	236 ± 101	1.3 ± 0.7	$M1^{Hi}$
ICAM1	57 ± 6	7.4 ± 0.6	$M1^{Hi}$
AMPD3	49 ± 18	1.7 ± 0.7	$M1^{Hi}$
IL4I1	434± 14	0.8 ± 0.2	$M1^{Hi}$
IFIT3	25.8 ± 3.6	0.5 ± 0.1	$M1^{Hi}$
IFIT2	25 ± 17	1.0 ± 0.7	$M1^{Hi}$
OASL	17.6 ± 3.3	0.9 ± 0.2	$M1^{Hi}$
MX1	15.5 ± 6.8	1.1 ± 0.3	$M1^{Hi}$
SIGLEC1	13.4 ± 5.3	0.8 ± 0.2	$M1^{Hi}$
C3	13.4 ± 1.7	1.4 ± 0.4	$M1^{Hi}$
MX2	12.6 ± 2.5	0.4 ± 0.1	$M1^{Hi}$
PARP9	11.5 ± 5.4	1.0 ± 0.5	$M1^{Hi}$
OAS3	10.4 ± 2.3	0.6 ± 0.2	$M1^{Hi}$
MARCKS	10.3 ± 3.1	1.6 ± 0.3	$M1^{Hi}$
HELZ2	9.6 ± 2.3	0.8 ± 0.2	$M1^{Hi}$
CD14	8.7 ± 0.6	0.62 ± 0.02	$M1^{Hi}$
OAS2	8.2 ± 2.3	0.7 ± 0.2	$M1^{Hi}$
MMP9	8.1 ± 2.2	1.1 ± 0.3	$M1^{Hi}$
DDX58	8.0 ± 2.2	0.6 ± 0.1	$M1^{Hi}$
ISG15	7.7 ± 2.3	0.7 ± 0.2	$M1^{Hi}$
EPB41L3	7.5 ± 0.8	2.0 ± 0.2	$M1^{Hi}$
SOD2	7.5 ± 0.8	1.1 ± 0.1	$M1^{Hi}$
OAS1	7.5 ± 2.7	1.1 ± 0.2	$M1^{Hi}$
UBE2L6	7.3 ± 1.4	1.4 ± 0.3	$M1^{Hi}$
IFIH1	7.3 ± 2.6	0.5 ± 0.3	$M1^{Hi}$
NFKB2	6.9 ± 0.7	1.0 ± 0.1	$M1^{Hi}$
HMOX1	6.3 ± 1.0	2.5 ± 0.3	$M1^{Hi}$
NCF1	6.3 ± 0.3	1.4 ± 0.2	$M1^{Hi}$
GBP1	5.8 ± 1.6	1.7 ± 0.5	$M1^{Hi}$

MGLL	5.1 ± 0.9	1.4 ± 0.1	$M1^{Hi}$
RELB	4.7 ± 0.8	0.9 ± 0.1	$M1^{Hi}$
CYP27A1	4.6 ± 0.7	1.7 ± 0.2	$M1^{Hi}$
APOE	4.2 ± 0.8	0.9 ± 0.2	$M1^{Hi}$
SAMD9L	4.1 ± 0.8	0.7 ± 0.2	$M1^{Hi}$
PLXND1	4.1 ± 1.1	0.7 ± 0.1	$M1^{Hi}$
ADA	4.0 ± 0.5	1.0 ± 0.2	$M1^{Hi}$
GBP4	4.0 ± 0.9	0.8 ± 0.2	$M1^{Hi}$
TGM2	0.3 ± 0.1	149 ± 68	$M2^{Hi}$
F13A1	0.1 ± 0.1	64.9 ± 22	$M2^{Hi}$
SORT1	0.9 ± 0.1	12.5 ± 2.1	$M2^{Hi}$
FCER2	1.0 ± 0.1	8.5 ± 2.5	$M2^{Hi}$
CD209	0.8 ± 0.1	8.1 ± 1.2	$M2^{Hi}$
GAS6	0.8 ± 0.1	5.8 ± 0.4	$M2^{Hi}$
HLA-DRB1	1.2 ± 0.2	4.0 ± 0.8	$M2^{Hi}$
FABP4	5.0 ± 1.7	3.6 ± 1.2	$M1^{Hi}/M2^{Hi}$
TLR8	4.9 ± 0.9	2.5 ± 0.4	$M1^{Hi}/M2^{Hi}$
COL6A1	2.6 ± 0.3	4.1 ± 0.2	$M1^{Hi}/M2^{Hi}$

Figure Legends

Figure 1. M1 and M2 marker mRNA expression in THP-1 macrophages. PDBu-differentiated THP-1 macrophages were left untreated (M0) or treated with IFN-γ/LPS (5 ng/ml IFN-γ + 10 ng/ml LPS; M1 conditions) or IL-4 (25 ng/ml; M2 conditions) for 48 hours. mRNA expression of (A-C) M1 markers (A) IL-1β, (B) CCR7 and (C) CXCL11 and (D) M2 marker MRC-1 were determined by qRT-PCR and expressed relative to untreated macrophages (M0). All data are presented as mean ± SEM, n=8. **P<0.01 vs M0 (1-way ANOVA followed by Dunnett's post hoc test).

Figure 2. **Cluster analysis of proteomics data.** (A) Hierarchical clustering of the protein intensities determined for 3 repeats under each of 3 conditions; labels indicate the condition followed by the repeat number (e.g. M1-2 is the second repeat under M1 conditions). The significantly up- or down-regulated proteins were clustered in Perseus. The colour bar indicates the Z-score of intensities. (B) Z-score graphs for each of the 6 clusters. Each graph shows a set of thin gray lines, each connecting the Z-scores for one protein in the cluster, and a thick red line connecting the average Z-score for proteins in the cluster. Z-scores are presented for 3 repeats under each of 3 conditions, labelled as in (A). (C) Scatter plot showing the changes in protein intensities under M1 and M2 conditions, expressed relative to the basal (M0) conditions, for the clusters $M1^{Hi}$ (filled red circles), $M1^{Lo}$ (open red circles), $M2^{Hi}$ (filled blue squares), $M2^{Lo}$ (open blue squares), $M1^{Hi}/M2^{Hi}$ (filled green triangles) and $M1^{Lo}/M2^{Lo}$ (open green triangles). The black boxes indicate 4-fold and 8-fold changes.

Figure 3. Validation of selected M1 markers by targeted proteomics and Western blot in THP-1 macrophages. (A) PDBu-differentiated THP-1 macrophages were left untreated (M0, black) or treated for 48 hours with IFN-γ/LPS (5 ng/ml IFN-γ + 10 ng/ml LPS; M1, red) or IL-4 (25 ng/ml; M2, blue). The four proteins listed (left side) were independently quantified by DDA (left panels), PRM (centre panels) and Western blot (right panels); quantities are shown relative to basal (M0) control. Data are presented as mean ± SEM, n=3. *P<0.05, **P<0.01, ***P<0.001, **** P<0.0001 vs M0 (1-way ANOVA followed by Dunnett's post hoc test). (B) The Western blot from a single representative experiment; glyceraldehyde 3-phosphate dehydrogenase (GAPDH) was used as a loading control.

Figure 4. Validation of IFIT1, IFIT3 and ICAM1 expression in human primary macrophages. Monocytes from donor buffy coats were differentiated to macrophages and subsequently left untreated (M0, black), treated with IFN-γ/LPS (20 ng/ml IFN-γ + 100 ng/ml LPS; M1, red) or treated with IL-4 (25 ng/ml; M2, blue). (A)

Following 6 hours of polarization, mRNA expression of IFIT1, IFIT3 and ICAM1 was determined by qRT-PCR and expressed relative to untreated macrophages (M0). (B) Protein levels of IFIT1 in THP-1 and primary macrophages were assessed, via Western blotting, following 48 and 24 hours of polarization, respectively and expressed relative to untreated macrophages (M0). All data are presented as mean ± SEM, n=5-7. *P<0.05, **P<0.01, ***P<0.001, ****P<0.0001 vs M0 (1-way ANOVA followed by Dunnett's post hoc test).

Figure 5. Expression and co-localisation of IFIT1 with macrophage marker F4/80 in the aortic sinus of ApoE$^{-/-}$ mice. Immunohistochemical staining for IFIT1 (green), F4/80 (macrophage marker, red), and DAPI (nucleated cells, blue) in the aortic sinus of ApoE$^{-/-}$ mice fed a high fat diet for 14 weeks. 'L' indicates vessel lumen and 'M' indicates media layer, arrows indicated cells in which co-localisation was observed. Images were taken at a magnification of x20 (top panel) and x60 (bottom panel, field of view indicated with white box on x20 image). Scale bar=50 µm. Representative images from n=8 are shown.

Figure 6. Expression and co-localisation of IFIT1 with macrophage marker F4/80 in the brachiocephalic arteries of ApoE$^{-/-}$ mice. Immunohistochemical staining for IFIT1 (green), F4/80 (macrophage marker, red), and DAPI (nucleated cells, blue) in brachiocephalic arteries of ApoE$^{-/-}$ mice fed a high fat diet for 14 weeks. 'L' indicates vessel lumen and 'M' indicates media layer, arrows indicated cells in which co-localisation was observed. Images were taken at a magnification of x20 (top panel) and x60 (bottom panel, field of view indicated with white box on x20 image). Scale bar=50 µm. Representative images from n=6 are shown.

Figure 7. Proposed mechanism for induction of interferon-stimulated genes (ISGs) under M1 polarization conditions. LPS activates TLR4, stimulating expression of NF□B-regulated inflammatory genes (IGs). IFN-γ activates the JAK-STAT pathway, thereby inducing expression of ISGs as well as synergizing with NF□B to upregulate IRF-1. IRF-1 induces expression of numerous ISGs, including IFN-β, which, in turn, activates additional ISG expression via the JAK-STAT pathway and interferon regulatory factor 9 (IRF-9). Signal transduction and transport pathways are indicated by black arrows, whereas transcription and translation are indicated by red arrows.

Figure 1

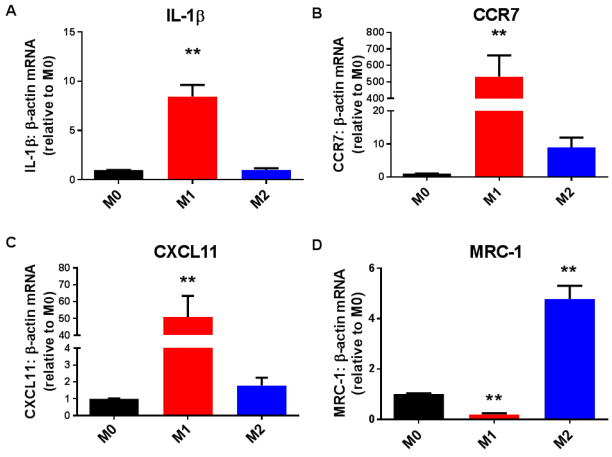
A
IL-1β
IL-1β: β-actin mRNA (relative to M0)
**
M0
M1
M2
B
CCR7
CCR7: β-actin mRNA (relative to M0)
**
C
CXCL11
CXCL11: β-actin mRNA (relative to M0)
**
D
MRC-1
MRC-1: β-actin mRNA (relative to M0)
**
**

Figure 2

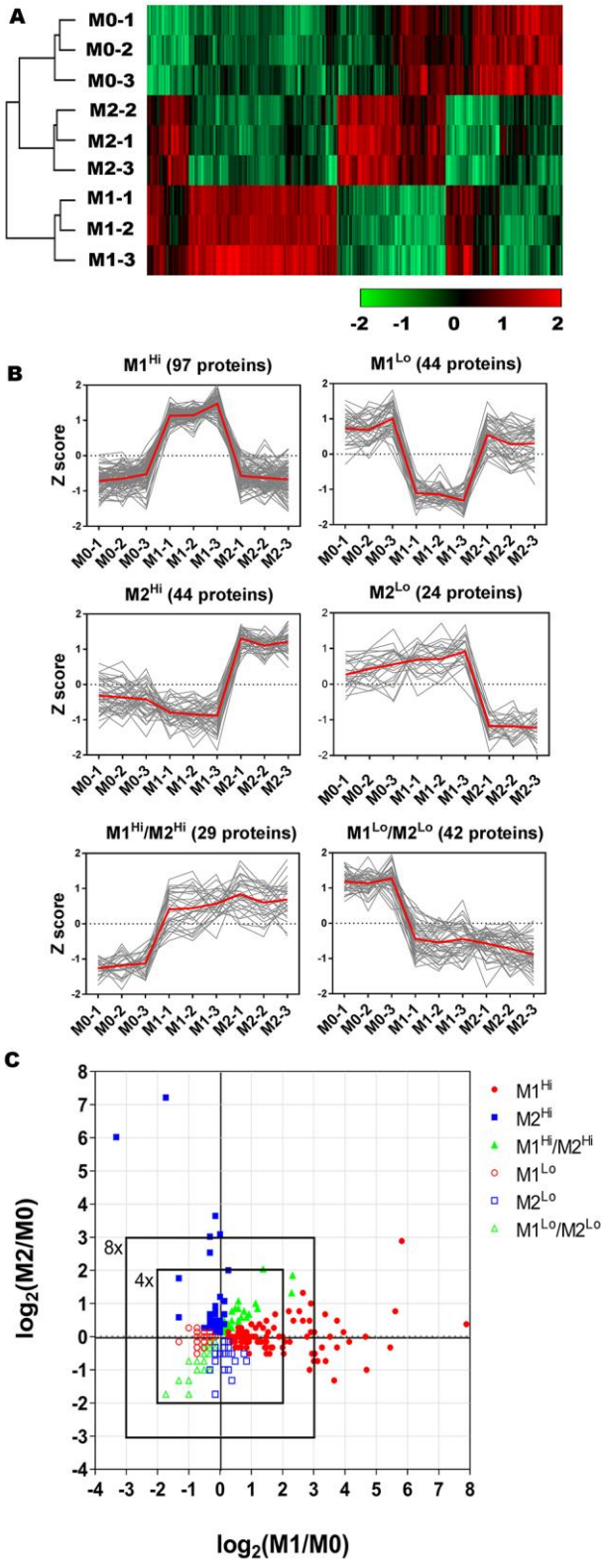
A
M0-1
M0-2
M0-3
M2-2
M2-1
M2-3
M1-1
M1-2
M1-3
-2 -1 0 1 2
B
M1Hi (97 proteins)
M1Lo (44 proteins)
M2Hi (44 proteins)
M2Lo (24 proteins)
M1Hi/M2Hi (29 proteins)
M1Lo/M2Lo (42 proteins)
Z score
C
log2(M2/M0)
log2(M1/M0)
8x
4x
M1Hi
M2Hi
M1Hi/M2Hi
M1Lo
M2Lo
M1Lo/M2Lo

Figure 3

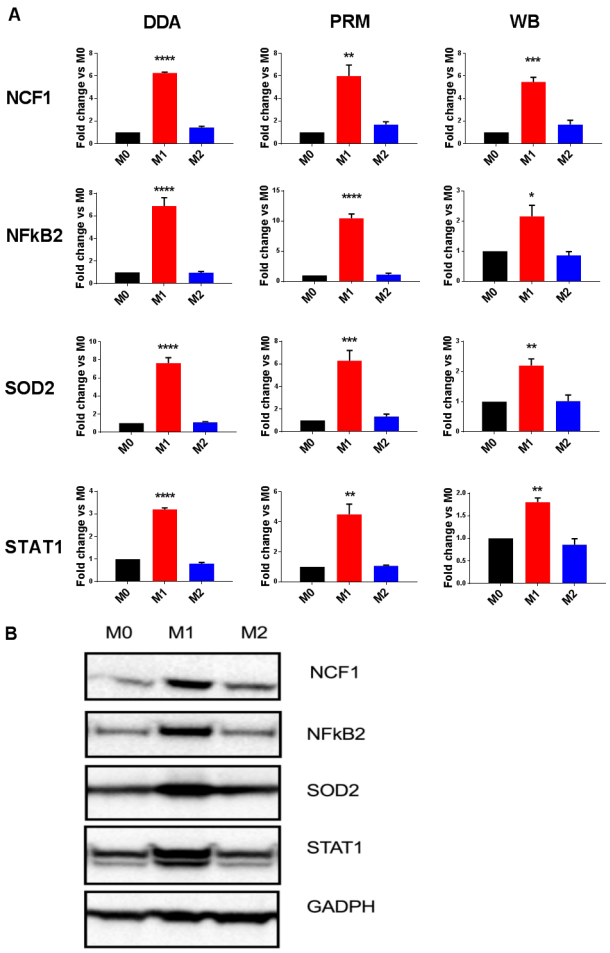
A
DDA
PRM
WB
NCF1
NFkB2
SOD2
STAT1
Fold change vs M0
M0
M1
M2
B
M0
M1
M2
NCF1
NFkB2
SOD2
STAT1
GADPH

Figure 4

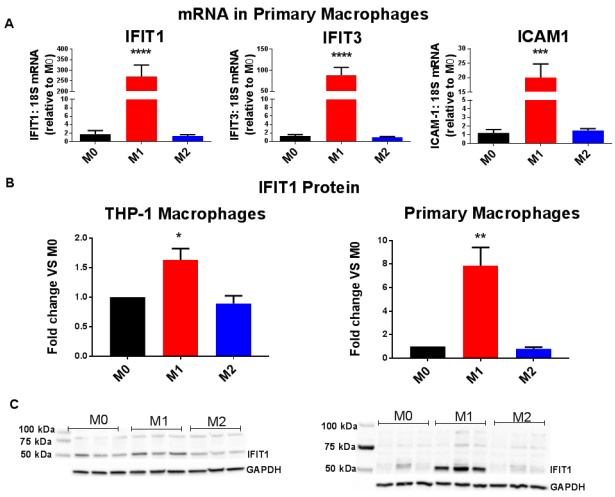
A
mRNA in Primary Macrophages
IFIT1
IFIT3
ICAM1
IFIT1: 18S mRNA (relative to M0)
IFIT3: 18S mRNA (relative to M0)
ICAM-1: 18S mRNA (relative to M0)
M0
M1
M2
B
IFIT1 Protein
THP-1 Macrophages
Primary Macrophages
Fold change VS M0
C
100 kDa
75 kDa
50 kDa
IFIT1
GAPDH

Figure 5

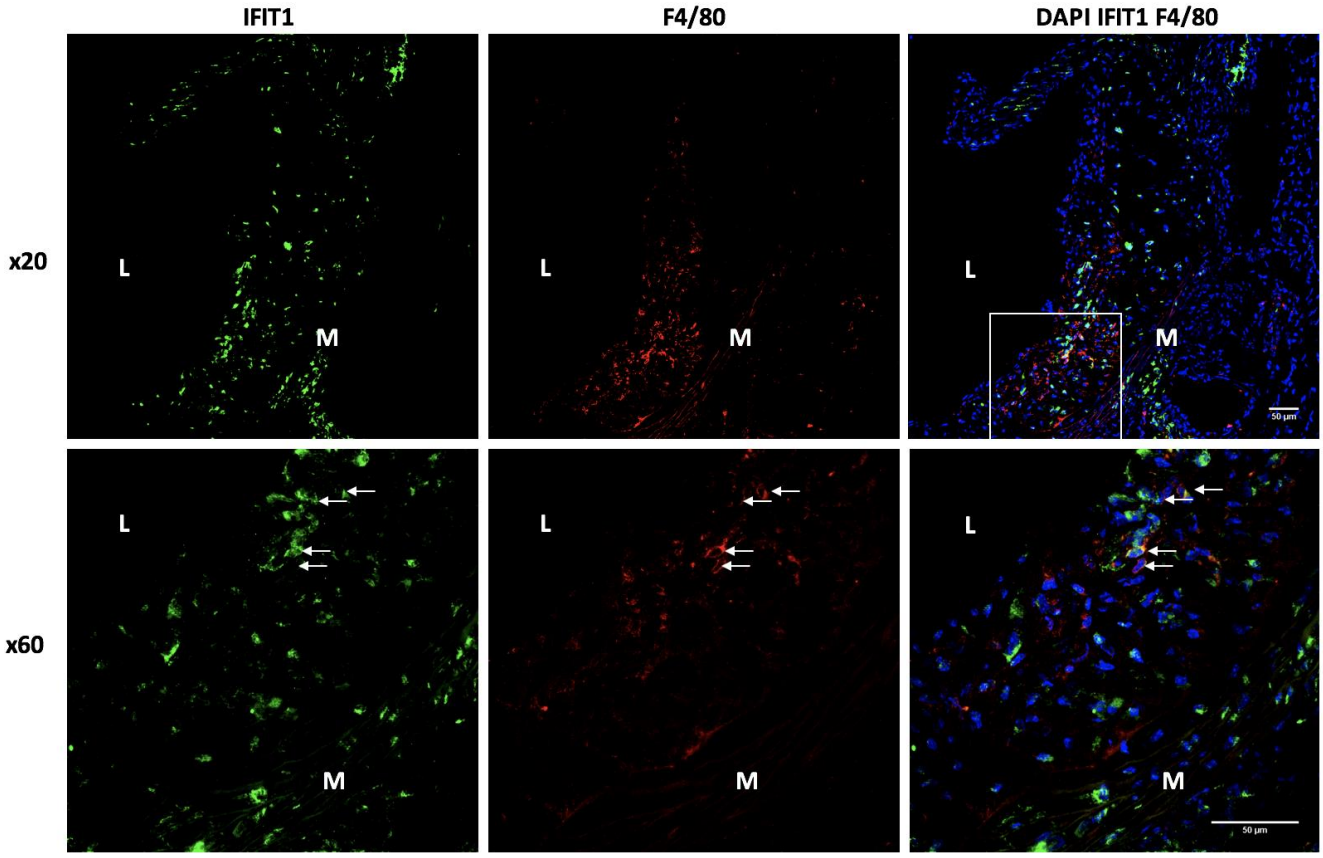

Figure 6

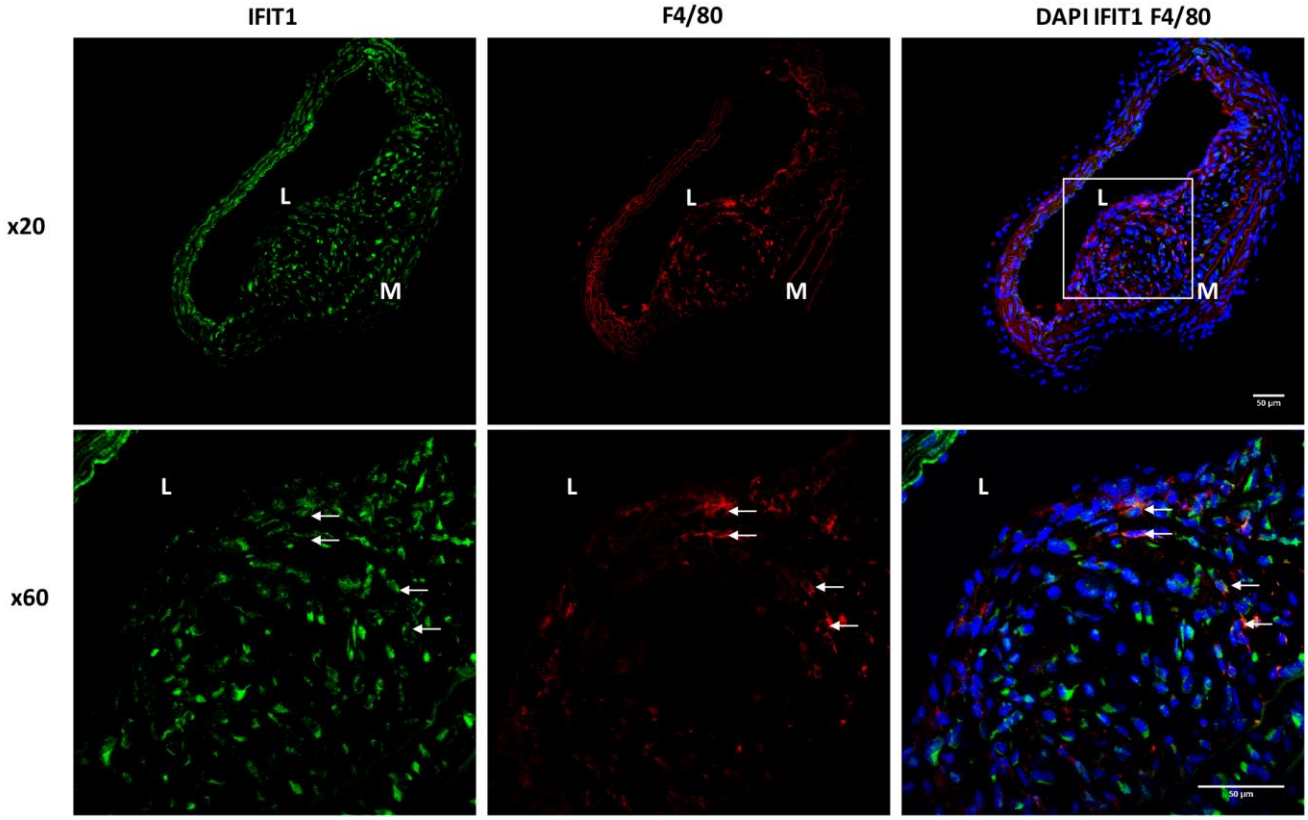

Figure 7

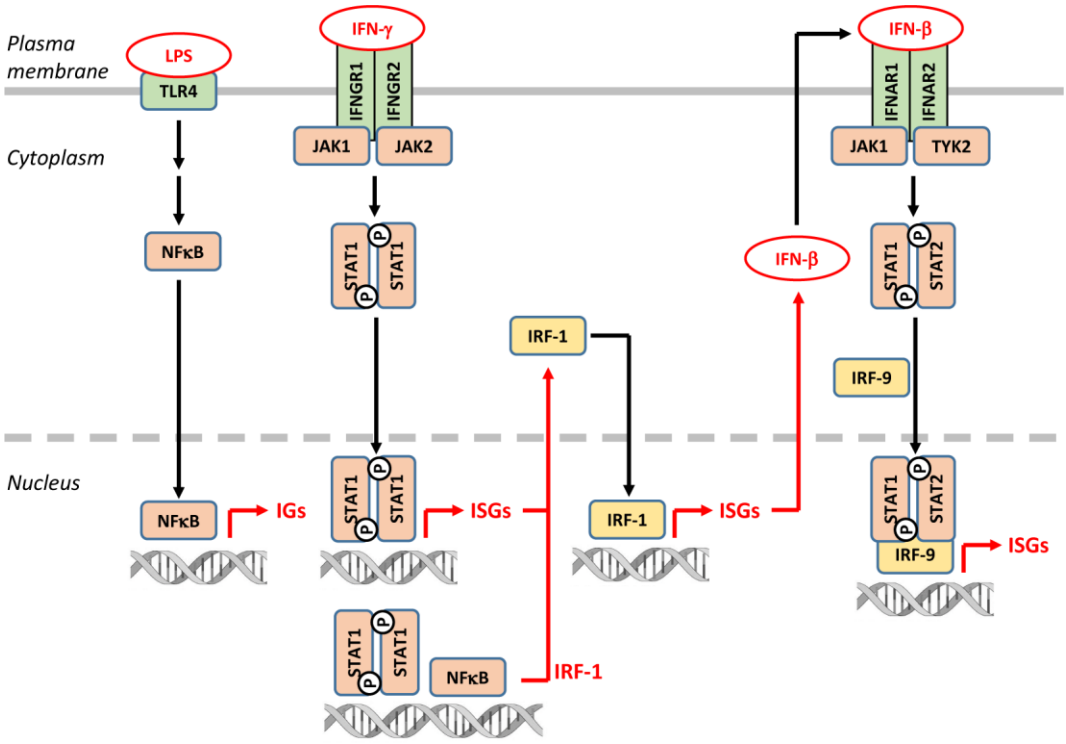
Plasma membrane
Cytoplasm
Nucleus
LPS
TLR4
NFκB
IGs
IFN-γ
IFNGR1
IFNGR2
JAK1
JAK2
STAT1
STAT1
ISGs
IRF-1
IRF-1
ISGs
IFN-β
IFN-β
IFNAR1
IFNAR2
JAK1
TYK2
STAT1
STAT2
IRF-9
IRF-9
ISGs
STAT1
STAT1
NFκB
IRF-1

Supplementary Information

As controls for the immunohistochemistry experiments, additional brachiocephalic artery and aortic sinus sections were stained and imaged in the absence of primary antibody, to account for any autofluorescence of the tissue and non-specific binding of the secondary antibody. These sections were fixed, blocked and stained as described in the methods section with the exception of the primary antibody incubation step in which control slides were again incubated with blocking buffer in the absence of primary antibody. Slides were imaged on the same day and under identical settings as those presented in Figures 5 and 6, with one control slide analysed for each. Representative images are shown from aortic sinus (Supplementary Figure 1) and brachiocephalic artery (Supplementary Figure 2) sections from ApoE$^{-/-}$ mice, 3 sections per slide. Although some non-specific fluorescent staining was observed in each tissue, no clear co-localisation with the cell nuclei marker, DAPI, was observed (Supplementary Figures 1 and 2) and the staining presented in Figures 5 and 6 was specific for the primary antibodies used.

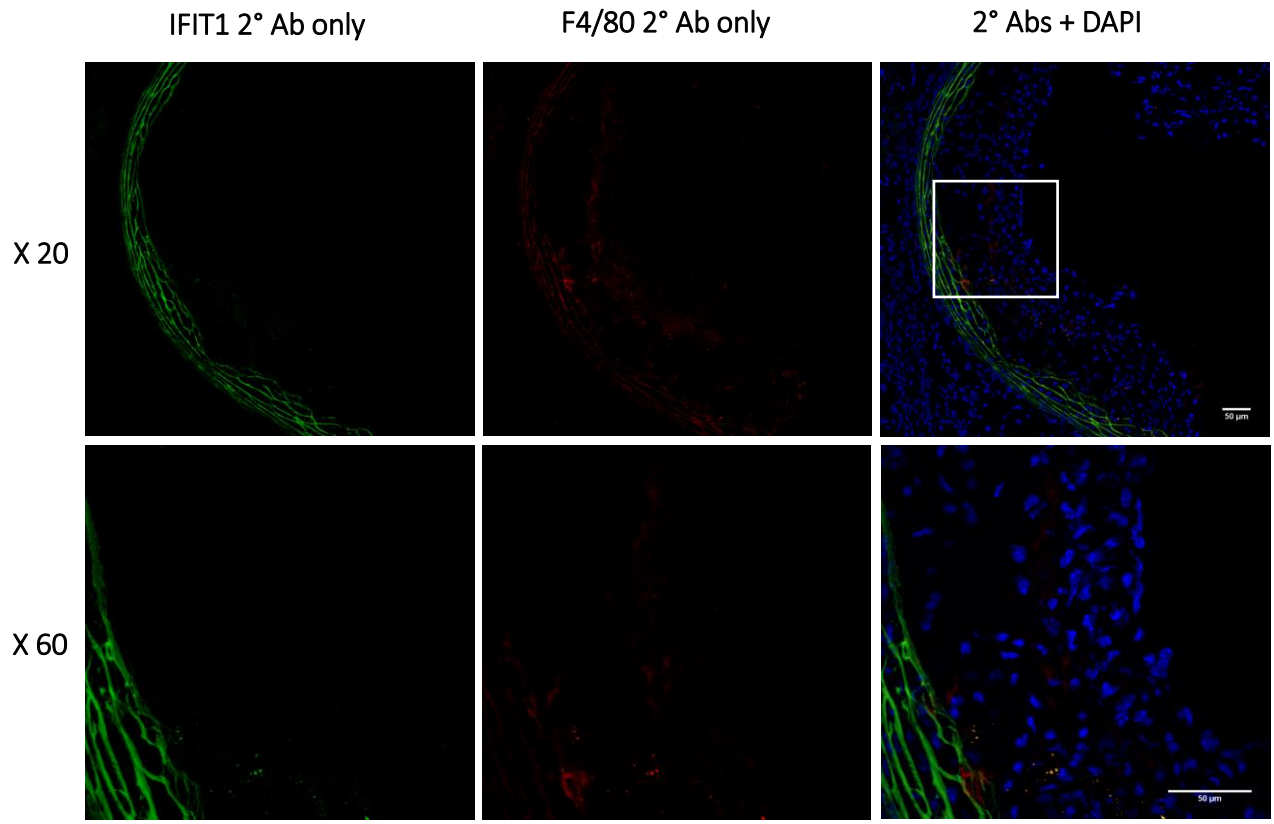

Supplementary Figure 1. Secondary antibody controls in the aortic sinus of ApoE$^{-/-}$ mice. Immunohistochemical staining with the secondary antibodies used for IFIT1 (green) and F4/80 (red) with DAPI (nucleated cells, blue) in the aortic sinus of ApoE$^{-/-}$ mice fed a high fat diet for 14 weeks. Images were taken at a magnification of x20 (top panel) and x60 (bottom panel, field of view indicated with white box on x20 image). Scale bar = 50 µm. Representative images selected from three sections stained and imaged on the same day as Figure 5.

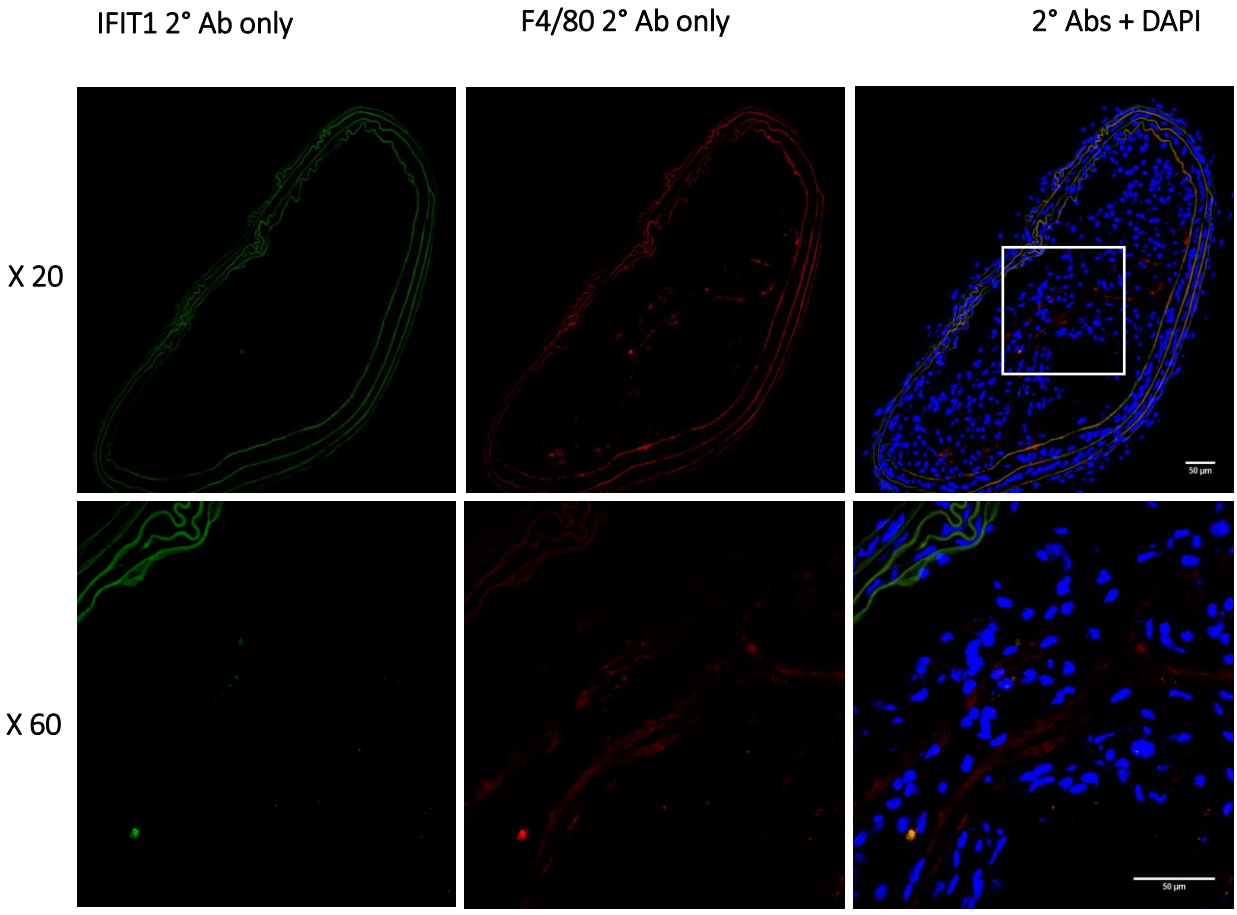

Supplementary Figure 2. Secondary antibody controls in the brachiocephalic arteries of ApoE$^{-/-}$ mice. Immunohistochemical staining with the secondary antibodies used for IFIT1 (green) and F4/80 (red) with DAPI (nucleated cells, blue) in brachiocephalic arteries of ApoE$^{-/-}$ mice fed a high fat diet for 14 weeks. Images were taken at a magnification of x20 (top panel) and x60 (bottom panel, field of view indicated with white box on x20 image). Scale bar = 50 µm. Representative images selected from three sections stained and imaged on the same day as Figure 6.

CHAPTER 4:

M1 AND M2 MACROPHAGE PHENOTYPES ARE ASSOCIATED WITH DISTINCT REDOX SIGNALLING: IMPACTS ON FIBROSIS

M1 and M2 macrophage phenotypes are associated with distinct redox signalling: impacts on fibrosis

Caitlin Lewis[‖], Antony Vinh[¶], Grant Drummond[¶], Barbara Kemp-Harper[‖]

Affiliations

[‖] Cardiovascular Disease Program, Biomedicine Discovery Institute & Department of Pharmacology, Monash University, VIC 3800, Australia

[¶] Department of Physiology, Anatomy & Microbiology, School of Life Sciences, La Trobe University, VIC 3086, Australia

Abstract

Macrophages exist as a heterogenous population with M1 (inflammatory) and M2 (tissue reparative) macrophages at opposing ends of a spectrum of phenotypes. Whilst reactive oxygen species (ROS) generation is a recognised function of M1 macrophages, potential roles for ROS in M2 macrophage function have emerged. We hypothesised that the ultimate ROS generated from M1 and M2 macrophages may differ and that M2 macrophage-derived ROS may be pro-fibrotic. To this end, we compared the expression of ROS-producing enzymes (NADPH oxidases), the ROS-generating capacities, and the pro-fibrotic effects of unpolarised (MΦ), M1 and M2 macrophages *in vitro*. Human macrophages were polarised toward M1 (IFN-γ + LPS) or M2 (IL-4) phenotypes and M1 (CXCL11, CCR7, IL-1β) and M2 (MRC-1, CCL18, CCL22) marker and NOX expression assessed by RT-PCR and western blotting. Superoxide and hydrogen peroxide generation was assessed by L-012(100 μM)-enhanced chemiluminescence and Amplex Red/DCF fluorescence, respectively. Compared to MΦ, superoxide generation was enhanced in M1 (~219%) and M2 (~115%) macrophages and increased hydrogen peroxide was observed following M2 polarisation (~150%). Corresponding increases in expression of the p47phox (up to 20-fold) and p67phox (up to 6-fold) subunits of the NOX2 oxidase complex were evident in M1 and M2 macrophages, respectively. Co-culture with human aortic adventitial fibroblasts revealed that both M1 (~1.5-fold) and M2 macrophages (~2-fold) could promote fibroblast collagen I protein expression, and macrophage pre-treatment with the hydrogen peroxide scavenger, PEG-catalase attenuated this effect. Thus we demonstrate clearly an enhanced capacity for M2 macrophages to generate ROS, and reveal a potential role for M2 macrophage-derived hydrogen peroxide in promoting aortic fibrosis through stimulation aortic fibroblast collagen synthesis.

Introduction

Macrophages are key cells of the innate immune system and crucial to effective host defense, whilst also playing homeostatic roles in wound healing and metabolic function (17). Macrophages exist as a heterogeneous population, dependent on the local microenvironment (38), with the 'classically activated' pro-inflammatory M1 macrophage and the 'alternatively activated' M2 macrophage, representing either ends of the diverse spectrum. Traditionally, M1 and M2 macrophages are considered to play predominant roles in inflammation and tissue repair, respectively.

The initial infiltration of macrophages to a site of injury leads to the generation of pro-inflammatory cytokines and reactive oxygen species (ROS). Whilst this defense mechanism contributes to microbial killing, it also exacerbates inflammatory disease. M1 macrophages play a predominant role in this setting and a contribution of ROS to these processes is evident (7). Thus M1 macrophage-derived superoxide, together with inducible NOS-derived nitric oxide (NO), can lead to the generation of the powerful oxidant, peroxynitrite. Whilst peroxynitrite is central to pathogen killing it can also cause oxidation and nitration of proteins and lipids. Importantly, the ROS generating capacity of M1 macrophages is reliant predominantly on the activity of the NOX2 isoform of the NADPH oxidase (NOX) family of enzymes which is highly expressed in macrophages. Inflammatory stimuli and LPS increase the expression and activity of NOX2 oxidase as an important mechanism of microbial killing (19, 46, 47). Given their well-recognized ROS-generating capacity (56, 61), M1 macrophages have been shown to contribute to inflammation-associated organ damage (27), observed in diseases such as hypertension, diabetes and kidney disease (9, 32, 33).

In the later phases of the disease process, macrophages release anti-inflammatory molecules and growth factors and promote healing and regeneration. Whilst initially beneficial, the healing process becomes pathological when it is continuous, leading to remodeling of the extracellular matrix. M2 macrophages have been associated with these remodelling processes. Thus, with an ability to generate TGF-β and platelet derived growth factor (PDGF) (17, 44), M2 macrophages promote differentiation of fibroblasts to collagen generating myofibroblasts (16, 18). Of note, M2 macrophages also express NOX2 oxidase and have the capacity to generate ROS (28). As such, it is possible that their generation of ROS, particularly hydrogen peroxide, may also contribute to this pro-fibrotic response. Evidence in support of this concept comes from the observation that NOX-derived superoxide can be rapidly converted to hydrogen peroxide, which has been shown to directly stimulate collagen production and myofibroblast differentiation of fibroblasts *in vitro* (62). Furthermore, the pro-fibrotic effect of co-culturing pulmonary fibroblasts with macrophages was shown to be reduced in the presence of the NOX inhibitor apocynin (10). Thus ROS may represent a novel mediator of the detrimental actions of M2 macrophages in fibrotic diseases (45, 59) and hypertension (43).

To date, it has been generally assumed that M1 macrophages have an enhanced oxidative capacity (38, 56, 61), contributing to their pro-inflammatory properties and tissue damaging effects. Hence ROS generation is considered an 'M1' function. However, no studies have directly compared the oxidative capacity, NOX2 activity and the nature of the ROS generated by M1 and M2 macrophages. Whether the amount and type of ROS generated impacts on their functions in disease, particularly with regard to fibrosis, remains to be determined. This study aims to elucidate whether M1 and M2 polarised macrophages exhibit a differential

capacity to generate ROS, determine the nature of the ROS generated and whether this may in turn, influence their pro-fibrotic capacity.

Materials and Methods

Primary human monocyte isolation

Primary human monocytes were isolated from healthy blood donor buffy coats (Australian Red Cross Blood Service, Melbourne, Australia). Buffy coats were mixed with Phosphate Buffered Saline (PBS; without Ca^{2+}or Mg^{2+}; Sigma-Aldrich) supplemented with 0.5% fetal bovine serum (FBS; Sigma-Aldrich) and 2 mM ethylenediaminetetraacetic acid (EDTA; Sigma-Aldrich) and layered onto Ficoll-Paque PLUS (GE Healthcare no. 17-144) for density gradient centrifugation (400 g, 40 minutes, acceleration=1, deceleration=0). The peripheral blood mononuclear cell (PBMCs) layer was collected and monocytes isolated using a human pan monocyte isolation kit (Miltenyi Biotec no. 130-096-537), according to the manufacturer's instructions. The purity of the monocyte population was confirmed to be at least 85% as determined by flow cytometry using $CD14^+$ /$CD16^+$ expression.

Monocyte to macrophage differentiation and macrophage polarisation

The THP-1 human monocytic cell line was supplied by Dr Meritxell Canals (Monash Institute of Pharmaceutical Sciences, Parkville, Australia). THP-1 cells were cultured in high glucose RPMI 1640 medium (Gibco Life Technologies), supplemented with 10% heat-inactivated FBS and grown in T75 tissue culture flasks in a humidified incubator maintained at 37˚C with 5% CO_2 (Sanyo MCO-18AIC CO_2 incubator, Quantum Scientific). THP-1 monocytes were passaged every 3-4 days and seeded on 6-well plates ($1x10^6$ cells/well) for RNA and protein extraction, or 96 well plates ($5x10^4$ cells/well) for superoxide and hydrogen peroxide detection. THP-1 monocytes were differentiated to macrophages (MΦ) via the addition of 100 nM phorbol-12,13-dibutyrate (PDBu, Calbiochem) for 24 hours. THP-1 macrophages were subsequently left untreated (MΦ) or treated with either a combination of 5 ng/ml interferon-γ (IFN-γ;

Sigma-Aldrich no. I3265) and 10 ng/ml lipopolysaccharide (LPS; Sigma-Aldrich no. L2630, E.coli 0111:B4 strain) for M1 polarisation, or with 25 ng/ml interleukin-4 (IL-4; Sigma-Aldrich no. I4269) for M2 polarisation, for 24, 48 or 72 hours for PCR, western blotting and ROS detection. A subset of macrophages were polarised in the presence of 100 nM NOX2 siRNA (Santa-Cruz no. sc-35503) or missense siRNA (control siRNA-A; Santa-Cruz no. sc-37007). These cells were transfected using Lipofectamine RNAiMAX (Gibco Life Technologies) in opti-minimum essential medium (Opti-MEM, Gibco Life Technologies) for 6 hours prior to polarisation in complete RPMI 1640 culture medium.

Isolated donor blood-derived primary monocytes (1 x 10^6cells/ml) were differentiated into macrophages by culturing for 7 days in RPMI 1640 Glutamax medium (Gibco Life Technologies), supplemented with 10% FBS, 1x antibiotic/antimyotic (Gibco Life Technologies, USA), 1 mM sodium pyruvate (Sigma-Aldrich), 1 x non-essential amino acids (NEAA; Gibco Life Technologies) and 50 ng/ml macrophage colony stimulating factor (M-CSF; Miltenyi Biotec no. 130-096-491). Following 7 day macrophage differentiation, primary human macrophages were either left untreated (MΦ), treated with 100 ng/ml LPS and 20 ng/ml IFN-γ (M1), or treated with 25 ng/ml IL-4 (M2) in the absence of M-CSF. Cells were polarised for either 3, 6 or 24 hours for real-time PCR or for 24 hours for western blotting and L-012-enhanced chemiluminescence.

Aortic fibroblast treatment and co-culture with macrophages

Primary human aortic adventitial fibroblasts (AoAF; Lonza no. CC-7014; Lonza) were grown in Stromal Cell Growth Medium (SCGM; Lonza no. CC-3205), containing 5% FBS and used from passages 2 to 8. Fibroblasts were maintained in T-75 flasks in a humidified incubator at 37°C with 5% CO_2. Once confluent, AoAFs were passaged in SCGM using Trypsin-EDTA solution

(Lonza no. CC-5012) for cell detachment. Cells were seeded in 6-well plates ($2x10^5$ cells per well) for 24 hours prior to being left untreated, treated with hydrogen peroxide (1-10 µM, Invitrogen) for 24 hours in serum free medium. For co-culture experiments, THP-1 macrophages were first polarised for 72 hours in complete RPMI 1640 medium in 24-well cell culture inserts (0.4 µm pore, <0.85 x 10^8 pores/cm^2; 5 x 10^4 cells/insert; ThermoFisher Scientific). The THP-1 medium was replaced with serum free RPMI 1640 medium and the inserts were transferred to wells with AoAF (5 x 10^4 cells/well) in serum free SCGM. THP-1 macrophages were stimulated with 10 µM PDBu in the presence or absence of 1000 U/ml PEG-catalase (Sigma-Aldrich no. C4963) and the cultures incubated for a further 24 hours before lysates were harvested for western blotting.

RNA extraction and real time-PCR

Total RNA was extracted from macrophages using the RNeasy Mini Kit (Qiagen) according to the manufacturer's instructions. RNase-free DNase (Qiagen) was used to remove any contaminating DNA. The amount of RNA in each sample was quantified using the Nanodrop 1000D spectrophotometer (ThermoScientific), which measures absorbance at 260 nm and 280 nm. An A_{260}:A_{280} ratio of 2 or more was considered sufficiently pure. 1 µg of RNA from each sample was reverse transcribed into cDNA using the High Capacity cDNA Reverse Transcription Kit (Applied Biosystems) with the reaction run in a thermal cycler (BioRad MyCycler, BioRad Laboratories). The resultant cDNA was used as a template for real time PCR with Taqman® primers and probes for IL-1β, IL-6, IL-10, CXCL11, CCR7, MRC-1, CCL22, CCL18, CYBA (p22phox), CYBB (NOX2), NCF1 (p47phox), NCF2 (p67phox), NCF4 (p40phox), NOX1, NOX4, NOX5, SOD1, SOD2, SOD3, TGF-β1 and TNFα (Applied Biosystems). β-actin and 18S were used as housekeeping genes. Real-time PCR was run in triplicate on the CFX96 Touch™

Real-Time PCR Detection Machine (BioRad Laboratories). Gene expression was normalised to β-actin or 18S and quantified relative to the average MΦ value using the comparative cycle threshold (Ct) method with the formula: Fold change= $2^{-\Delta\Delta Ct}$ (54).

Protein extraction and Western blotting

Total protein from macrophage and fibroblast cell lysates was collected in 1.5 x Laemmli buffer (7.5% glycerol; 3.75% β-mercaptoethanol; 2.25% SDS; 75 mM Tris-HCl pH 6.8; 0.004% bromophenol blue) and 1x RIPA Lysis and extraction buffer (Cell Signalling Technology, USA), respectively. Cell debris was cleared by centrifugation (13,000 rpm, 10 min, 4°C) and supernatants collected. Protein concentrations were determined using either a modified Lowry protocol (RCDC colorimetric protein assay kit; BioRad Laboratories) or Bicinchonic acid (BCA) based colorimetric quantification (Pierce™ BCA Protein Assay, ThermoScientific). Equivalent volumes of protein in 1.5 x Laemmli buffer were loaded into 7.5%, 10% or 4-15% polyacrylamide gels. Proteins were separated by SDS-PAGE and transferred onto low fluorescence polyvinylidene fluoride (LF PVDF) membranes using the Bio-Rad Trans Blot Turbo transfer system (Bio-Rad Laboratories). Membranes were blocked with 5% skim milk in Tris-Buffered Saline (TBS; 200 mM Tris, 150 mM NaCl, pH 7.5) with 0.1 % tween-20 for 1 hour and subsequently probed with primary antibodies against NOX2 (1:500; Santa-Cruz no. sc-130549 (CL5)), p47phox (1: 1000; BD Transduction Laboratories no. 610354), p67phox (1:2000; EMD Millipore no. 07-002), SOD2 (1:1000; EMD Millipore no. 06-984), SOD3 (1:1000; EMD Millipore no. 07-704), α-SMA (1:2500; Abcam no. ab5694) or collagen 1 (1:1000; Abcam no. ab34710), and the house-keeping protein GAPDH (1: 20000; Abcam no. ab8245) overnight at 4 °C. 1 hour incubation with horseradish peroxidase(HRP)-conjugated anti-rabbit (1:10000; Dako) or anti-mouse (1:10000; Jackson ImmunoResearch Laboratories) secondary antibodies was then

performed and protein bands visualised using Clarity ECL substrate (BioRad Laboratories) and the ChemiDoc MP system (BioRad Laboratories). Densitometries of protein bands were quantified using Image Lab Software (BioRad Laboratories) and normalised to the housekeeping protein, GAPDH.

Superoxide detection via L-012-enhanced chemiluminescence

THP-1 or primary macrophages were seeded and polarised on white 96-well tissue culture plates (Perkin Elmer) at 5 x 10^4 and 2 x 10^5 cells/well, respectively. Groups were set up in quintuplicate with a cell free control group, comprising media alone, included to provide a background reference. On the day of experimentation, culture medium was removed and cells were washed and incubated in warmed Krebs-HEPES buffer (118 mM NaCl, 4.7 mM KCl 1.2 mM KH_2PO_4, 1.2 mM $MgSO_4 \cdot 7H_2O$, 2.5 mM $CaCl_2$, 25 mM $NaHCO_3$, 11.7 mM glucose, 20 mM HEPES; pH 7.4) and background chemiluminescence measured for 30 minutes. Chemiluminescence was measured using a Chameleon Luminescence Plate Reader (Hidex Ltd, Turku, Finland) and data acquired using the MicroWin (Mikrotek, Overath, Germany) data acquisition system. 100 µM L-012 (Wako Pure Chemical Industries) was then added to each well and basal superoxide levels were monitored for 30 minutes. Finally, the protein kinase C (PKC) activator PDBu (10 µM) was added to each well and superoxide production was then measured for a further 30 minutes. Peak PDBu-stimulated superoxide production was quantified as the average of 5 minutes at the peak of the signal for each group with the basal signal (average of the final 5 basal readings) subtracted. In a subset of experiments, cells were treated with superoxide dismutase (SOD; 1000 U/ml; human recombinant, expressed in *E. coli;* Sigma-Aldrich S9076) just prior to the beginning of the assay, to confirm signal specificity for superoxide.

Hydrogen peroxide detection via Amplex Red

THP-1 macrophages were seeded and polarised on black 96-well tissue culture plates (Perkin Elmer) at 5 x 10^4 cells/well in quintuplicate. On the day of experimentation, the media was removed, cells rinsed with Krebs-HEPES solution and Krebs-HEPES added to each well in the absence or presence of 1000 U/ml SOD or PEG-Catalase. Working amplex red solution (Invitrogen), comprising of amplex red (5 µM) and HRP (0.2 U/µl), was then added to sample wells and fluorescence detected over 90 minutes using a Hidex Chameleon Plate Reader at 37°C (520 nm excitation filter, 590 nm emission filter). Cells were either left unstimulated or stimulated with 10 µM PDBu stimulation immediately prior to reading. The final fluorescence measurement from each group was fitted to a hydrogen peroxide standard curve (0-5 µM). Fold changes in hydrogen peroxide concentration were calculated relative to the MΦ value recorded on the same day.

Intracellular ROS detection via DCF

THP-1 macrophages were polarised for 72 hours in complete RPMI 1640 medium on 6-well plates at 1 x 10^6 cells/well. Adherent cells were washed with warmed PBS prior to incubation with a cell permeable ROS-sensitive dye, 5-(and-6)-chloromethyl-2',7'-dichlorodihydrofluorescein diacetate, acetyl ester (CM-H_2DCFDA; 1 µM, Sigma-Aldrich no. D6883) for 30 minutes at 37°C. Cells were then left unstimulated, or stimulated with 10 µM PDBu for a further 30 minutes. In a subset of experiments macrophages were incubated with 1000 U/ml PEG-Catalase for 15 minutes prior to PDBu stimulation. Following stimulation, cells were detached with Accutase® solution (Sigma-Aldrich), centrifuged at 1500 RPM for 5 mins and resuspended in PBS. Cells were then analysed on a LSR II flow cytometer (BD Biosciences).

Fold changes in DCF fluorescence were calculated relative to the MΦ value recorded on the same day.

Statistical analysis

All data are expressed as mean ± SEM. Comparisons of multiple treatment groups were made using an ordinary or repeated measures one-way analysis of variance (ANOVA) with a Dunnett's or Sidak's post hoc test, respectively. When comparing two groups, a student's unpaired t-test was used. $P<0.05$ was considered to be statistically significant and data were graphed and analysed using GraphPad Prism 7.02 software.

Results

Characterisation of M1 and M2 macrophages and their capacity to generate superoxide

Treatment of both PDBu-differentiated THP-1 macrophages and M-CSF-differentiated human primary monocyte-derived macrophages, with the combination of IFN-γ and LPS, lead to marked increases in the expression of M1 genes (CXCL11, CCR7 and IL-1β). In THP-1 cells, CXCL11 and CCR7 increased by up to 1000-fold, with the greatest change observed following 24 hours of treatment. IL-1β expression increased between 5- and 10-fold throughout the 72 hour treatment period (Figure 1A). The magnitude of increase in M1 genes was larger in primary macrophages, with increases of ~5000-fold for CXCL11, ~2000-fold for CCR7, and ~200-fold for IL-1β apparent at 6 hours (Figure 1A). Treatment with the M2-stimulus IL-4, resulted in an increase in the M2 marker MRC-1 (CD206) by approximately 5-fold throughout the treatment period in both THP-1 and primary macrophages (Figure 1B). A time-dependent increase in the M2 markers CCL18 and CCL22 was observed with CCL18 elevated 15- and 800-fold and CCL22 20- and 5-fold, in THP-1 and primary macrophages respectively (Figure 1B). The expression of additional pro- (IL-6, TNFα) and anti- (IL-10, TGF-β) inflammatory cytokine mRNA was also assessed (Supplementary Figure 1). Variable effects of M1 and M2 polarisation on IL-10 and TGF-β1 expression were observed and both treatment conditions increased IL-6 expression in all macrophage types. As expected M1 polarisation also resulted in increased TNFα expression (Supplementary Figure 1).

Having established unpolarised (MΦ), M1 (IFN-γ + LPS) and M2 (IL-4) phenotypes, we then assessed their basal and PDBu-stimulated superoxide generation at the final time point of treatment. In THP-1 cells, whilst basal superoxide levels did not differ significantly between macrophage phenotypes, PDBu-stimulated superoxide generation was increased by ~219%

and ~115% in M1 and M2 macrophages, respectively, as compared to unpolarised macrophages (Figure 2A). Of note, both the basal and PDBu-stimulated superoxide signal was much larger in primary macrophages as compared to THP-1. Peak superoxide generation in response to PDBu in unpolarised primary macrophages (30,560 ± 7162) was ~30-fold greater than that in unpolarised THP-1 macrophages (797 ± 112). Nonetheless, PDBu-stimulated superoxide generation was similar in primary M1 and M2 macrophages and up to 91% greater than that observed in MΦ (Figure 2B). The L-012 chemiluminescence signal was confirmed to be specific for superoxide via treatment with superoxide dismutase (Supplementary Figure 2A).

Differential regulation of NOX2 oxidase subunit expression in M1 and M2 macrophages to generate increased NOX2-derived superoxide

To examine the mechanisms contributing to increased superoxide generation in both M1 and M2 macrophages, NOX isoform and subunit expression were assessed. In THP-1 macrophages, NOX2 mRNA was increased approximately 2-fold, at all time points studied, following M1 polarisation, yet remained unchanged in the M2 phenotype (Figure 3A). Interestingly, mRNA expression of the p47phox subunit was upregulated in M1 macrophages (20-fold at 24 hours; 6-fold at 48 and 72 hours), while the p67phox subunit was upregulated in M2 macrophages (up to 6-fold at 48 and 72 hours, Figure 3A) and the p22phox and p40phox subunits were unchanged (Supplementary Figure 4). At the level of the protein, assayed at 72 hours, NOX2 expression didn't appear to differ between macrophage phenotypes, however the observed changes in p47phox and p67phox mRNA were found to translate to increases in protein expression (Figure 3B). p47phox protein was increased approximately 2.5-fold in M1 macrophages whilst p67phox protein was increased approximately 2-fold in M2 macrophages

(Figure 3B). In contrast to THP-1 macrophages, M1 polarisation in human primary macrophages was not associated with a change in NOX2 subunit mRNA expression. Although a decrease in NOX2 mRNA was observed in M2 macrophages at 24 hours, NOX2 was unchanged at the level of the protein (Supplementary Figure 3). Whilst a time-dependent increase in p47phox mRNA (6 hours) and p67phox mRNA (24 hours) was also associated with M1 and M2 polarisation, respectively, in human primary macrophages, such changes were not observed at the level of the protein (Supplementary Figure 3). Furthermore no significant differences were observed for p22phox mRNA expression and the p40phox subunit was decreased at the mRNA level in primary M1 macrophages (Supplementary Figure 4) yet whether this translated to a reduction in p40phox protein was not confirmed. NOX1 and NOX4 mRNA could not be detected in either THP-1 or primary macrophages, in any of the polarisation states (Ct values > 40). NOX5 mRNA expression however was observed in both cell lines and was increased in THP-1 M2 macrophages (Supplementary Figure 4).

To confirm that the superoxide signal in THP-1 macrophages was indeed NOX2 oxidase-derived, NOX2 siRNA was utilised to knock down its expression in all macrophages phenotypes. In M1 and M2 macrophages, NOX2 mRNA expression was reduced by 74% (Figure 4A) and 79% (Figure 4B), respectively, following NOX2 siRNA treatment as compared to macrophages treated with missense siRNA. In both M1 and M2 macrophages, there was a trend for missense siRNA to increase the PDBu-stimulated superoxide signal to levels above the vehicle-treated cells (Figure 4C and F). Nonetheless, the marked reduction in NOX2 expression in M1 and M2 macrophages attenuated the superoxide signal to levels similar to those observed in unpolarised macrophages (Figure 4). Specifically, treatment with NOX2

siRNA reduced the peak PDBu-stimulated superoxide signal in M1 and M2 macrophages by 71% (Figure 4C) and 78% (Figure 4F), respectively.

Increased hydrogen peroxide generation from M2 macrophages

In addition to superoxide, hydrogen peroxide generation was assessed in polarised THP-1 macrophages using two methods, amplex red for extracellular, and H_2DCFDA for intracellular detection. Of note a robust basal hydrogen peroxide signal was detected in all macrophage phenotypes and was not further modulated by PDBu stimulation (Supplementary Figure 5). Nevertheless, subsequent experiments comparing hydrogen peroxide generation between macrophage phenotypes incorporated PDBu. Amplex red fluorescence following PDBu stimulation for 90 minutes showed a mean hydrogen peroxide concentration of approximately 2 μM for M2 macrophages, compared to 1 μM in both M1 and MΦ (Figure 5B). When calculated relative to the MΦ signal, there was a 1.5-fold increase in hydrogen peroxide generation following M2 polarisation with no change in M1 macrophages (Figure 5C). The hydrogen peroxide signal was abolished in the presence of PEG-catalase and amplified with superoxide dismutase, demonstrating that the assay was specific for hydrogen peroxide (Supplementary Figure 2B). To further demonstrate increased hydrogen peroxide production in M2 macrophages, the intracellular ROS indicator H_2DCFDA was used and fluorescence detected via flow cytometry (Figure 5D). As with the amplex red assay, hydrogen peroxide levels were significantly greater in M2, as compared to M1, macrophages, (Figure 5E). As shown in the representative histogram, PEG-catalase reduced the signal in M2 macrophages, suggesting that it was primarily hydrogen peroxide being detected.

To elucidate the potential mechanisms underlying the increased hydrogen peroxide generation in M2 macrophages we assessed the mRNA expression of different superoxide

dismutase isoforms. While SOD1 (cytoplasmic) expression was not altered, SOD2 (mitochondrial) mRNA expression was increased in M1 macrophages by 25-fold at 24 hours and 10-fold at 48 and 72 hours (Figure 5G). These changes were reflected at the protein level with a 3-fold increase in SOD2 expression in M1 macrophages at 72 hours (Figure 5I). SOD3 (extracellular) mRNA expression was unchanged in response to M1 polarisation but increased by 4-fold in M2 macrophages at 72 hours (Figure 5H). However, no change in SOD3 protein expression was observed (Figure 5J).

Hydrogen peroxide generation contributes to the pro-fibrotic activity of M2 macrophages

To investigate whether M2-derived hydrogen peroxide may contribute to the pro-fibrotic actions of M2 macrophages in the vessel wall, macrophages were co-cultured with human aortic adventitial fibroblasts and markers of fibrosis (collagen I, α-SMA) measured. Treatment of aortic fibroblasts alone with exogenous hydrogen peroxide resulted in an apparent 1.5- to 2-fold increase in pro-collagen I protein expression which appeared to peak at 3 μM hydrogen peroxide. By contrast, no effect of hydrogen peroxide on α-SMA expression was observed (Figure 6B). Culture of aortic fibroblasts with either M1 or M2 macrophages tended to increase fibroblast pro-collagen I expression, as compared to unpolarised macrophages. This effect was the greatest for M2 macrophages, with an approximate doubling of aortic fibroblast pro-collagen I expression (Figure 6D). PEG-catalase treatment appeared to attenuate aortic fibroblast pro-collagen I expression following culture with MΦ, M1 or M2 macrophages (Figure 6D). As with exogenous hydrogen peroxide treatment, no effect on aortic fibroblast α-SMA expression was observed (Figure 6E), suggesting a lack of effect of macrophage-derived hydrogen peroxide on myofibroblast differentiation.

Figures

Figure 1. Time course of M1 and M2 marker mRNA expression in human macrophages. PDBu-differentiated THP-1 macrophages or M-CSF-differentiated human primary macrophages were left untreated (MΦ) or treated with IFN-γ/LPS (5 or 20 ng/ml IFN-γ + 10 or 100 ng/ml LPS) or IL-4 (25 ng/ml) for 3-72 hours. mRNA expression of A) M1 (CXCL11, CCR7, IL-1β) and B) M2 (MRC-1, CCL18, CCL22) markers were determined by RT-PCR and expressed relative to untreated macrophages (MΦ). Results presented as mean ± SEM, n=4-8. *P<0.05, **P<0.01 vs MΦ (1-way ANOVA followed by Dunnett's post hoc test).

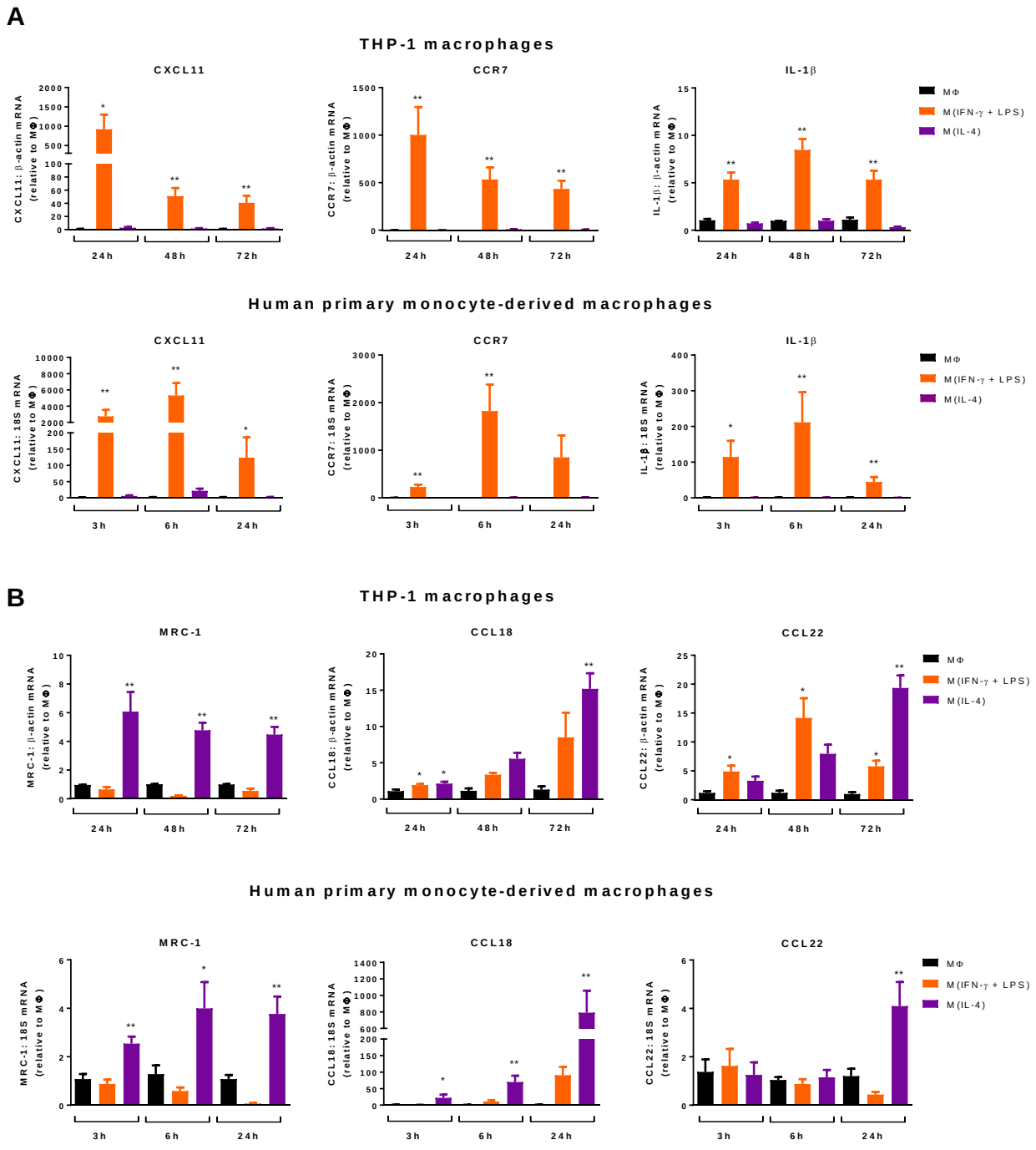
A
THP-1 macrophages
CXCL11
CCR7
IL-1β
CXCL11: β-actin mRNA (relative to MΦ)
CCR7: β-actin mRNA (relative to MΦ)
IL-1β: β-actin mRNA (relative to MΦ)
24h
48h
72h
MΦ
M(IFN-γ + LPS)
M(IL-4)
Human primary monocyte-derived macrophages
CXCL11: 18S mRNA (relative to MΦ)
CCR7: 18S mRNA (relative to MΦ)
IL-1β: 18S mRNA (relative to MΦ)
3h
6h
24h
B
THP-1 macrophages
MRC-1
CCL18
CCL22
MRC-1: β-actin mRNA (relative to MΦ)
CCL18: β-actin mRNA (relative to MΦ)
CCL22: β-actin mRNA (relative to MΦ)
Human primary monocyte-derived macrophages
MRC-1: 18S mRNA (relative to MΦ)
CCL18: 18S mRNA (relative to MΦ)
CCL22: 18S mRNA (relative to MΦ)

Figure 2. PDBu-stimulated superoxide generation in polarised human macrophages. PDBu-differentiated THP-1 macrophages (A and B) or M-CSF-differentiated human primary macrophages (C and D) were left untreated (MΦ) or treated with IFN-γ/LPS (M1) or IL-4 (M2) for 72 hours (THP-1) or 24 hours (primary macrophages) and superoxide generation was detected via L-012-enhanced chemiluminescence. Left hand side (LHS): Average recordings demonstrating initial background readings (1-30 mins), basal superoxide as detected following L-012 (100 μM) addition (31-60mins) and PDBu (10 μM)-stimulated superoxide generation (61-90 mins) measured in relative light units (RLU, counts/sec) in THP-1 (A) and primary (C) macrophages. Right hand side (RHS): Peak PDBu-stimulated (basal signal subtracted) superoxide generation in THP-1 (B) and primary (D) macrophages. All results presented as mean ± SEM, n=7. *P<0.05, **P<0.01 vs MΦ (1-way repeated measures ANOVA followed by Dunnett's post hoc test).

THP-1 macrophages

A

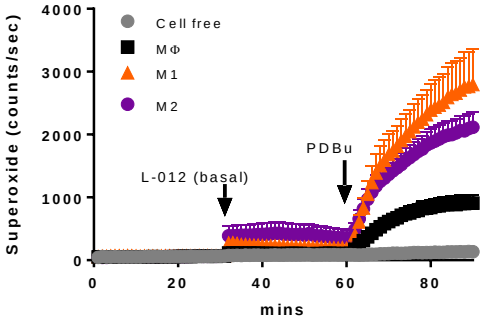

B

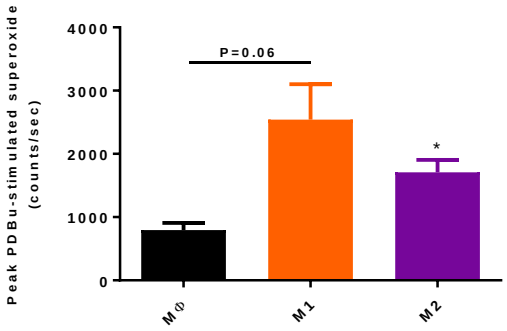

Human primary monocyte-derived macrophages

C

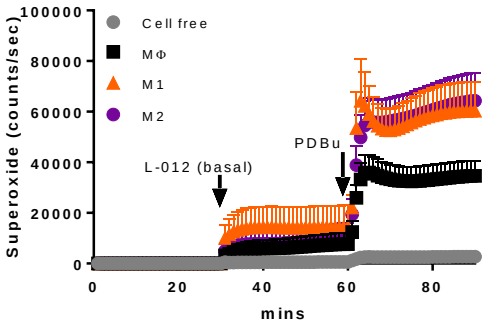

D

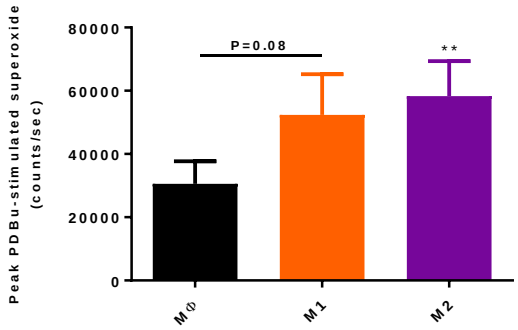

Figure 3. NOX2 oxidase subunit expression in polarised human macrophages. PDBu-differentiated THP-1 macrophages were left untreated (MΦ) or treated with IFN-γ/LPS (M1) or IL-4 (M2) for 24, 48 or 72 hours. A) Time course of NOX2, p47phox and p67phox mRNA expression determined by RT-PCR and expressed relative to the average MΦ (untreated) value. B) Protein expression of NOX2, p47phox and p67phox after 72 hours, determined via western blotting. Representative blots, depicting n=3, are shown below each graph with GAPDH used as a loading control. All results presented as mean ± SEM, n=5-8. *P<0.05, **P<0.01, ***P<0.001 vs MΦ, (1-way ANOVA followed by Dunnett's post hoc test).

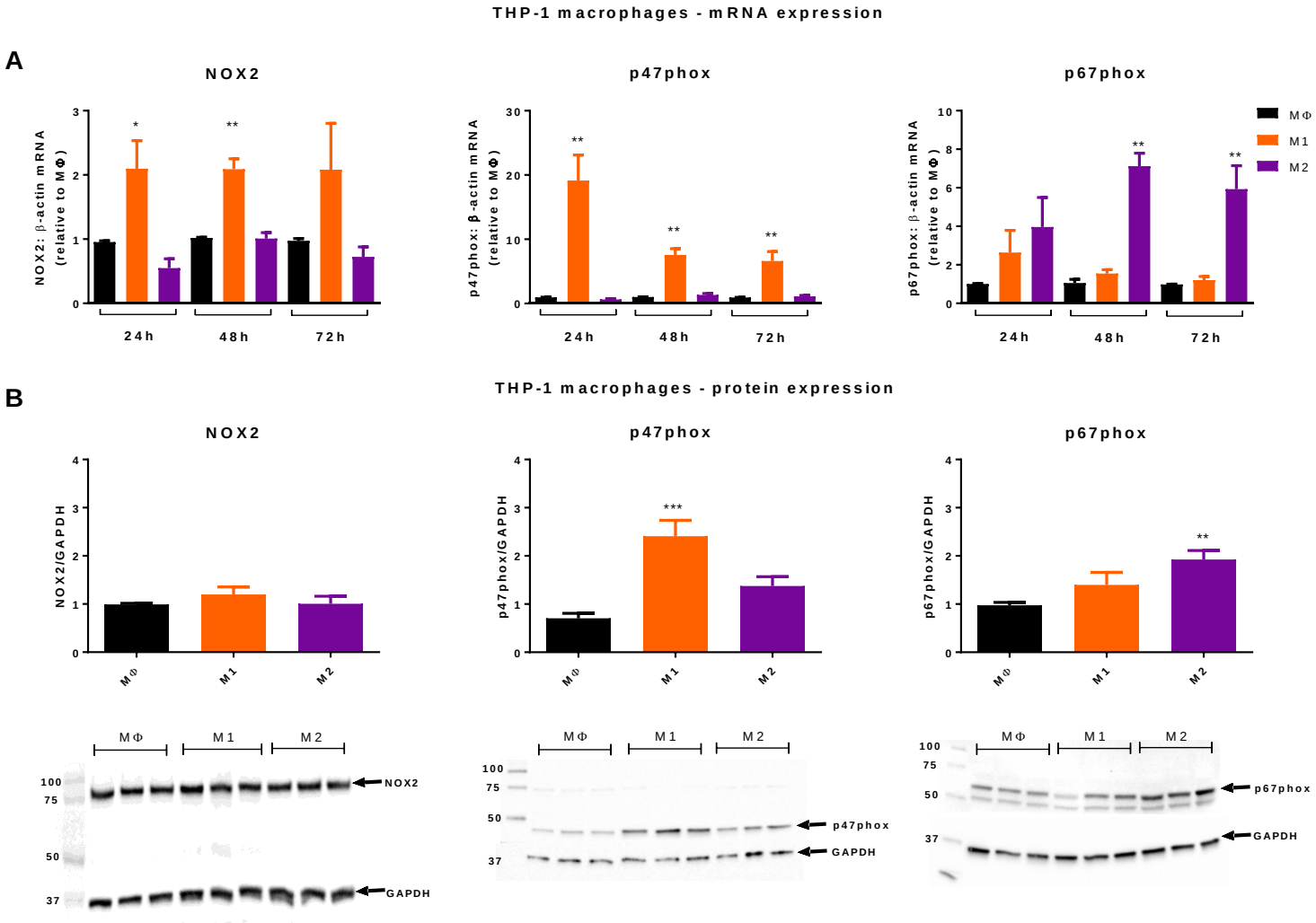
THP-1 macrophages - mRNA expression
A
NOX2
p47phox
p67phox
NOX2: β-actin mRNA (relative to MΦ)
p47phox: β-actin mRNA (relative to MΦ)
p67phox: β-actin mRNA (relative to MΦ)
MΦ
M1
M2
24h
48h
72h
B
THP-1 macrophages - protein expression
NOX2
p47phox
p67phox
NOX2/GAPDH
p47phox/GAPDH
p67phox/GAPDH
MΦ
M1
M2
100
75
50
37
NOX2
GAPDH
p47phox
GAPDH
p67phox
GAPDH

Figure 4. Effect of NOX2 siRNA on M1 and M2 macrophage-derived superoxide. Knockdown of NOX2 mRNA expression in THP-1 macrophages using NOX2 siRNA was confirmed in both M1 (A) and M2 (D) macrophages after 72 hours of polarisation via RT-PCR and expressed relative to the average MΦ (untreated) value. Effect of NOX2 siRNA and missense siRNA on the PDBu-stimulated superoxide signal in M1 and M2 macrophages detected via L-012-enhanced chemiluminescence. LHS: Average recordings demonstrating initial background readings (1-30 mins), basal superoxide as detected following L012 (100 µM) addition (31-60 mins) and PDBu (10 µM)-stimulated superoxide generation (61-120 mins) measured in relative light units (RLU, counts/sec) in M1 (B) and M2 (E) macrophages. RHS: Peak PDBu-stimulated (vassal signal subtracted) superoxide generation in M1 (C) and M2 (F) macrophages. All results presented as mean ± SEM, n=5-6. *P<0.05, **P<0.01 vs MΦ (1-way repeated measures ANOVA followed by Dunnett's post hoc test).

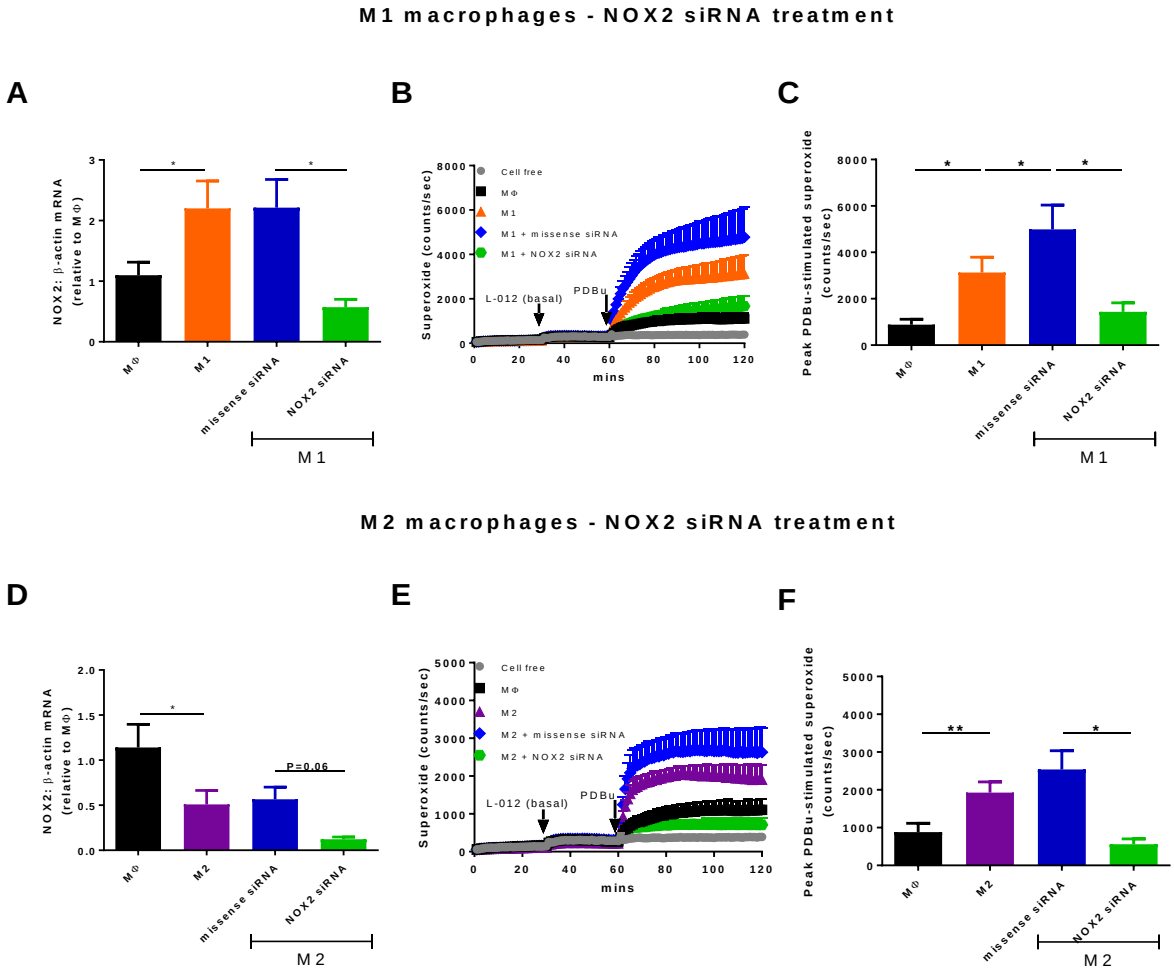
M1 macrophages - NOX2 siRNA treatment
A
B
C
NOX2: β-actin mRNA (relative to MΦ)
MΦ
M1
missense siRNA
NOX2 siRNA
M1
Superoxide (counts/sec)
Cell free
MΦ
M1
M1 + missense siRNA
M1 + NOX2 siRNA
L-012 (basal)
PDBu
mins
Peak PDBu-stimulated superoxide (counts/sec)
M2 macrophages - NOX2 siRNA treatment
D
E
F
NOX2: β-actin mRNA (relative to MΦ)
P=0.06
M2
M2 + missense siRNA
M2 + NOX2 siRNA

Figure 5. PDBu-stimulated hydrogen peroxide generation in polarised human macrophages. PDBu-differentiated THP-1 macrophages were left untreated (MΦ) or polarised to M1 or M2 phenotypes for 72 hours. A) Average trace depicting the accumulation of PDBu (10 µM)-stimulated hydrogen peroxide in the culture media over 90 mins detected via Amplex Red fluorescence. B) Hydrogen peroxide concentration was calculated at 90 minutes, results expressed as mean concentration ± SEM. C) M1 and M2 hydrogen peroxide expressed relative to untreated macrophage (MΦ) control on the day of assay, n=8. D) Representative histogram and gating strategy for DCF+ macrophages, depicting M1 versus M2 polarisation and the effect of catalase-polyethylene glycol (PEG-Cat; 1000 U/ml) on the M2 signal. E) Mean DCF+ macrophages, normalised to the response in untreated macrophages (MΦ), n=3-7. F) SOD1, G) SOD2, and H) SOD3 mRNA expression in polarised THP-1 macrophages at 24, 48 and 72 hours, determined by RT-PCR and expressed relative to the average MΦ (untreated) value, n=5-8. I) SOD2, and J) SOD3 protein expression in polarised THP-1 macrophages at 72 hours, determined by western blotting, n=6. Representative blots, depicting for n=3, shown on RHS, with GAPDH used as a loading control. All results expressed as mean ± SEM, *P<0.05, **P<0.01, ***P<0.001 (1-way ANOVA followed by Dunnett's (G, H, I) or Sidak's (E) post hoc test or student's unpaired t-test- C).

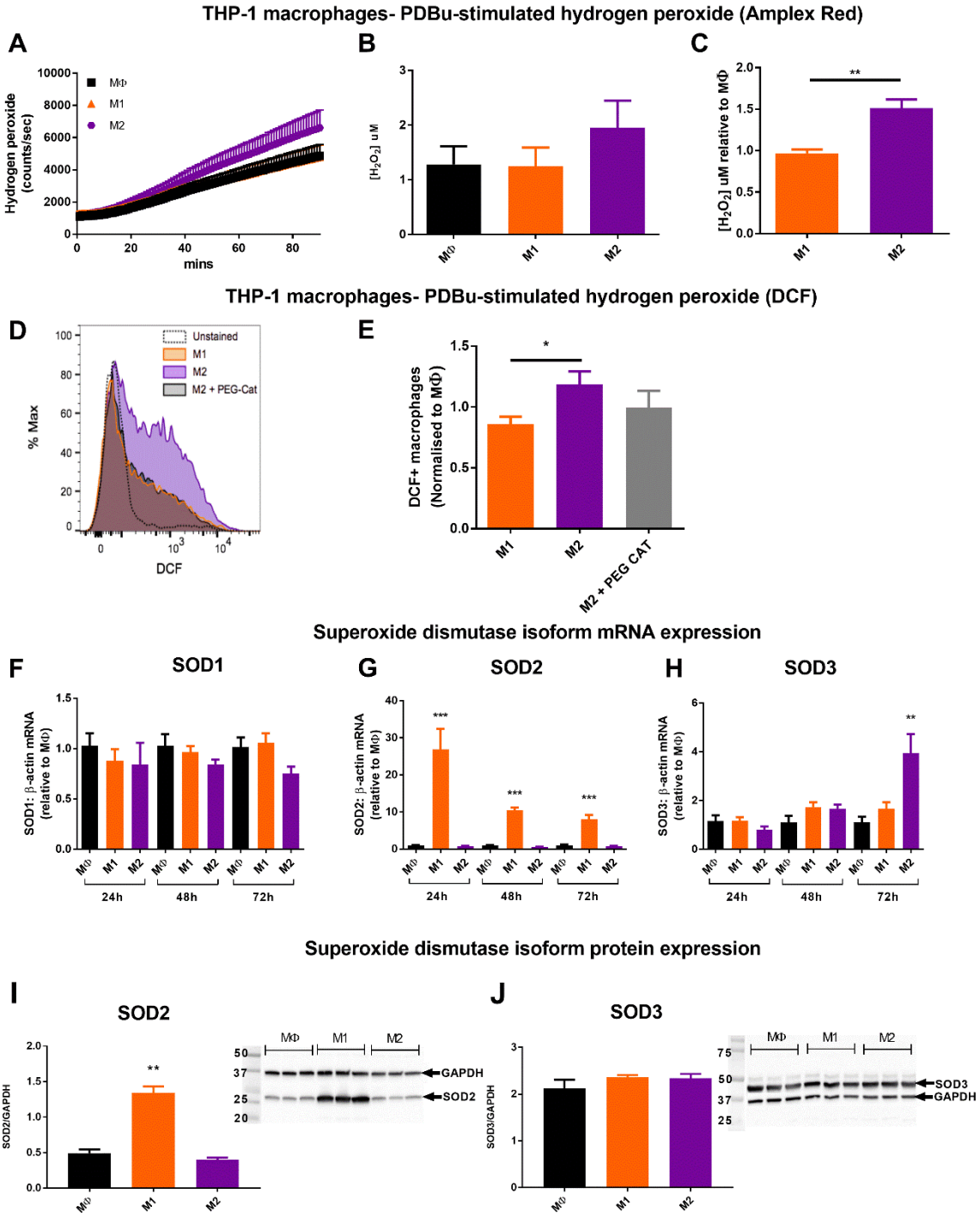
THP-1 macrophages- PDBu-stimulated hydrogen peroxide (Amplex Red)
A
B
C
Hydrogen peroxide (counts/sec)
MΦ
M1
M2
mins
[H2O2] uM
[H2O2] uM relative to MΦ
**
THP-1 macrophages- PDBu-stimulated hydrogen peroxide (DCF)
D
E
% Max
Unstained
M1
M2
M2 + PEG-Cat
DCF
DCF+ macrophages (Normalised to MΦ)
*
M2 + PEG CAT
Superoxide dismutase isoform mRNA expression
F
SOD1
G
SOD2
H
SOD3
SOD1: β-actin mRNA (relative to MΦ)
SOD2: β-actin mRNA (relative to MΦ)
SOD3: β-actin mRNA (relative to MΦ)
***
24h
48h
72h
Superoxide dismutase isoform protein expression
I
SOD2
J
SOD3
SOD2/GAPDH
SOD3/GAPDH
GAPDH
SOD2
SOD3

Figure 6. Effect of hydrogen peroxide and macrophage co-culture on collagen and alpha-smooth muscle actin expression in human aortic adventitial fibroblasts. A-C) Aortic adventitial fibroblasts (AoAF) were either left untreated (control) or treated with 1, 3 or 10 μM hydrogen peroxide for 24 hours and protein expression of pro-collagen I (A) and α-SMA (B) measured via western blotting, n=6. C) Representative blot, depicting n=3, is shown with GAPDH used as a loading control. D-F) PDBu-differentiated THP-1 macrophages were left untreated (MΦ) or polarised to M1 or M2 phenotypes for 72 hours in cell culture inserts. THP-1 macrophages were subsequently stimulated with 10 μM PDBu in the absence or presence of 1000 U/ml PEG-catalase, and transferred to wells containing AoAF and incubated for 24 hours. Pro-collagen 1 (D) and α-SMA (B) protein was measured, n=4. F) Representative blot, depicting n=1, is shown with GAPDH used as a loading control. Results presented as mean ± SEM. Hydrogen peroxide results expressed relative to the control (untreated) sample. P=0.07, M2 vs M2 + PEG-catalase, (1-way ANOVA followed by Sidak's post hoc test).

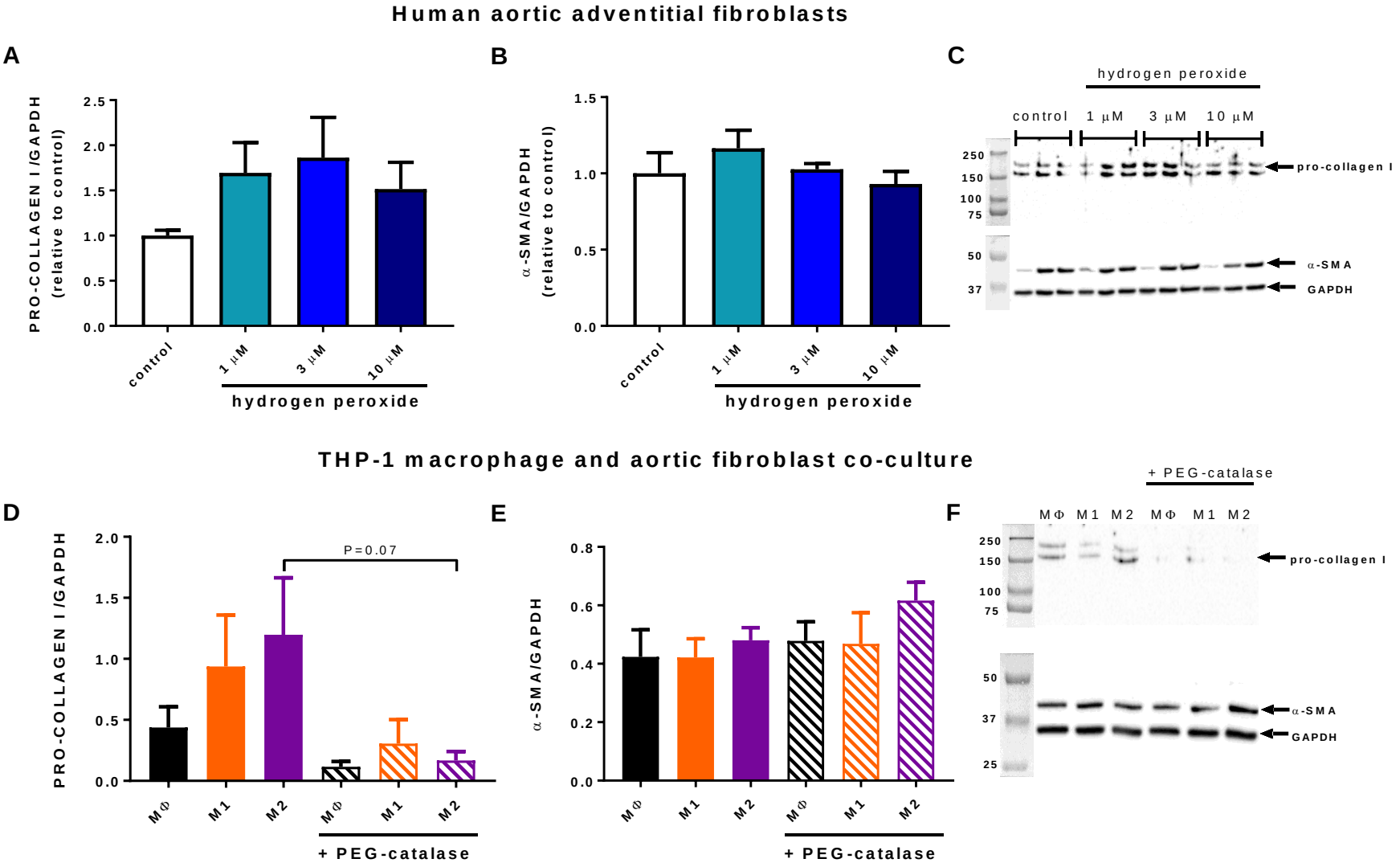
Human aortic adventitial fibroblasts
A
PRO-COLLAGEN I /GAPDH
(relative to control)
2.5
2.0
1.5
1.0
0.5
0.0
control
1 μM
3 μM
10 μM
hydrogen peroxide
B
α-SMA/GAPDH
(relative to control)
1.5
1.0
0.5
0.0
control
1 μM
3 μM
10 μM
hydrogen peroxide
C
hydrogen peroxide
control
1 μM
3 μM
10 μM
250
150
100
75
pro-collagen I
50
37
α-SMA
GAPDH
THP-1 macrophage and aortic fibroblast co-culture
D
PRO-COLLAGEN I /GAPDH
P=0.07
2.0
1.5
1.0
0.5
0.0
MΦ
M1
M2
MΦ
M1
M2
+ PEG-catalase
E
α-SMA/GAPDH
0.8
0.6
0.4
0.2
0.0
MΦ
M1
M2
MΦ
M1
M2
+ PEG-catalase
F
+ PEG-catalase
MΦ
M1
M2
MΦ
M1
M2
250
150
100
75
pro-collagen I
50
37
25
α-SMA
GAPDH

Supplementary Figure 1. Expression of additional cytokines in polarised THP-1 and human primary macrophages. PDBu-differentiated THP-1 macrophages (A) or M-CSF-differentiated human primary macrophages (B) were left untreated (MΦ) or treated with IFN-γ/LPS (5 or 20 ng/ml IFN-γ + 10 or 100 ng/ml LPS) or IL-4 (25 ng/ml) for 3-72 hours. mRNA expression IL-10 TGF-β1, IL-6 and TNFα were determined by RT-PCR and expressed relative to the average MΦ (untreated) value. Results presented as mean ± SEM, n=4-8. *P<0.05, **P<0.01, ***P<0.001 vs MΦ (1-way ANOVA followed by Dunnett's post hoc test).

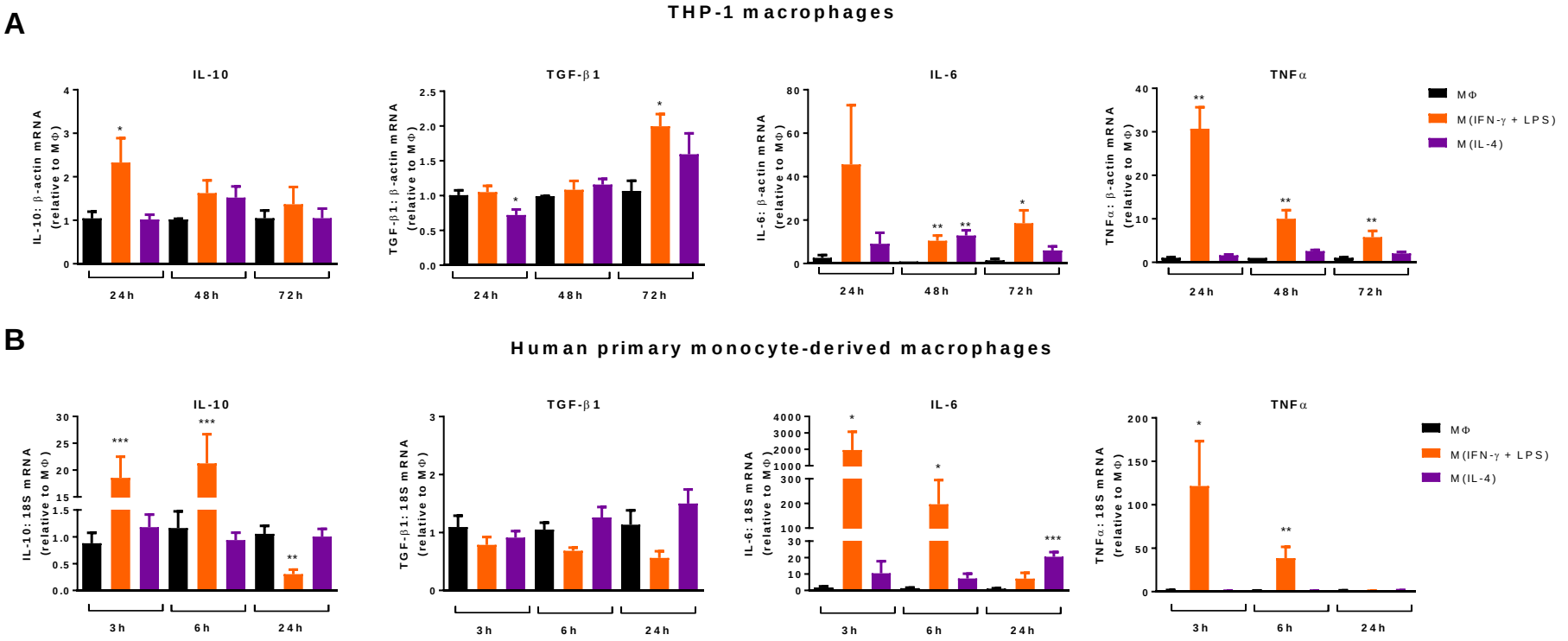
A
THP-1 macrophages
IL-10
IL-10: β-actin mRNA (relative to MΦ)
TGF-β1
TGF-β1: β-actin mRNA (relative to MΦ)
IL-6
IL-6: β-actin mRNA (relative to MΦ)
TNFα
TNFα: β-actin mRNA (relative to MΦ)
24h
48h
72h
MΦ
M(IFN-γ + LPS)
M(IL-4)
B
Human primary monocyte-derived macrophages
IL-10
IL-10: 18S mRNA (relative to MΦ)
TGF-β1
TGF-β1: 18S mRNA (relative to MΦ)
IL-6
IL-6: 18S mRNA (relative to MΦ)
TNFα
TNFα: 18S mRNA (relative to MΦ)
3h
6h
24h
MΦ
M(IFN-γ + LPS)
M(IL-4)

Supplementary Figure 2. Confirmation of superoxide and hydrogen peroxide detection in L-012-enhanced chemilumiscence and Amplex Red assays. A) LHS: Average recording demonstrating initial background readings (1-30 minutes), basal superoxide as detected following L-012 (100µM) addition (31-60 minutes) and PDBu (10 µM)-stimulated superoxide generation (61-120 minutes) measured in relative light units (RLU, counts/sec) showing, from left to right, the effect of superoxide dismutase (SOD; 1000 U/ml) on the signal in response to PDBu in unpolarised (MΦ), M1 and M2 macrophages. As quantified on the RHS, SOD diminishes each peak PDBu-stimulated (basal signal subtracted) superoxide signal, confirming superoxide detection in this assay. B. LHS: Average trace depicting the accumulation of PDBu (10 µM)-stimulated hydrogen peroxide in the culture media over 90 mins detected via amplex red fluorescence in unpolarised macrophages (MΦ) in the presence of 1000 U/ml SOD or PEG-catalase. RHS: Hydrogen peroxide concentration was calculated at 90 minutes and expressed relative to the untreated macrophages (MΦ) control on the day of assay, mean ± SEM. SOD enhances, whilst PEG-catalase diminishes, the signal, confirming hydrogen peroxide detection in this assay. All results presented as mean ± SEM, n=4. *P<0.05, **P<0.01 vs MΦ (1-way repeated measures ANOVA followed by Sidak's post hoc test).

A

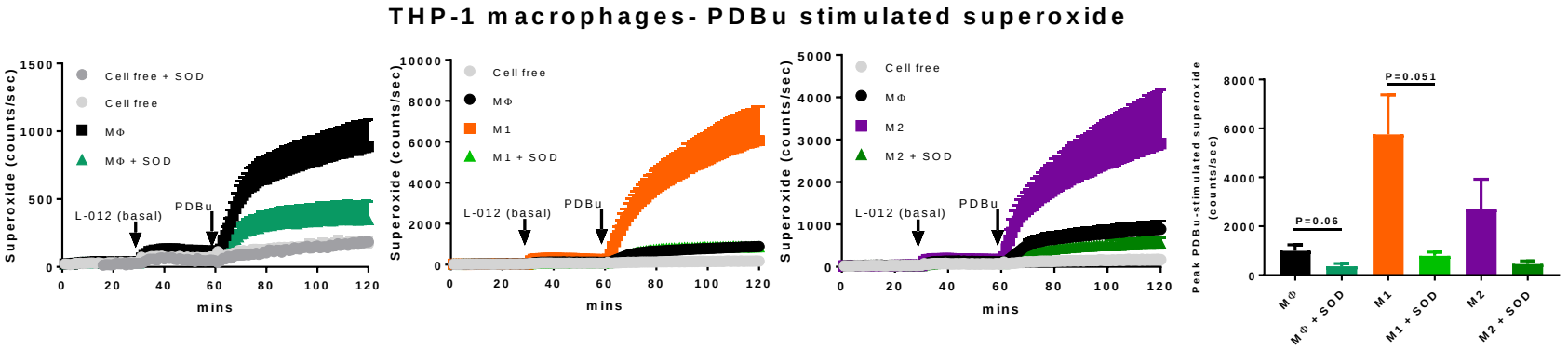
THP-1 macrophages- PDBu stimulated superoxide
Superoxide (counts/sec)
Cell free + SOD
Cell free
MΦ
MΦ + SOD
L-012 (basal)
PDBu
mins
Cell free
MΦ
M1
M1 + SOD
M2
M2 + SOD
Peak PDBu-stimulated superoxide (counts/sec)
P=0.06
P=0.051

B

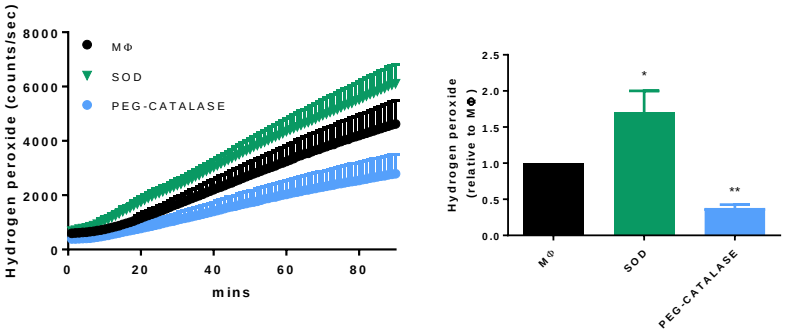
THP-1 macrophages- PDBu stimulated hydrogen peroxide
Hydrogen peroxide (counts/sec)
MΦ
SOD
PEG-CATALASE
mins
Hydrogen peroxide (relative to MΦ)

Supplementary Figure 3. NOX2 oxidase subunit expression in polarised human primary macrophages. M-CSF-differentiated primary macrophages were left untreated (MΦ) or treated with IFN-γ/LPS (M1) or IL-4 (M2) for 3, 6 or 24 hours. A) Time course of NOX2, p47phox and p67phox mRNA expression determined by RT-PCR and expressed relative to the average MΦ (untreated) value. B) Protein expression of NOX2, p47phox and p67phox after 24 hours, determined via western blotting. Representative blots, depicting n=3, are shown below each graph with GAPDH used as a loading control. All results presented as mean ± SEM, n=6-9. *P<0.05, **P<0.01 vs MΦ (1-way ANOVA followed by Dunnett's post hoc test).

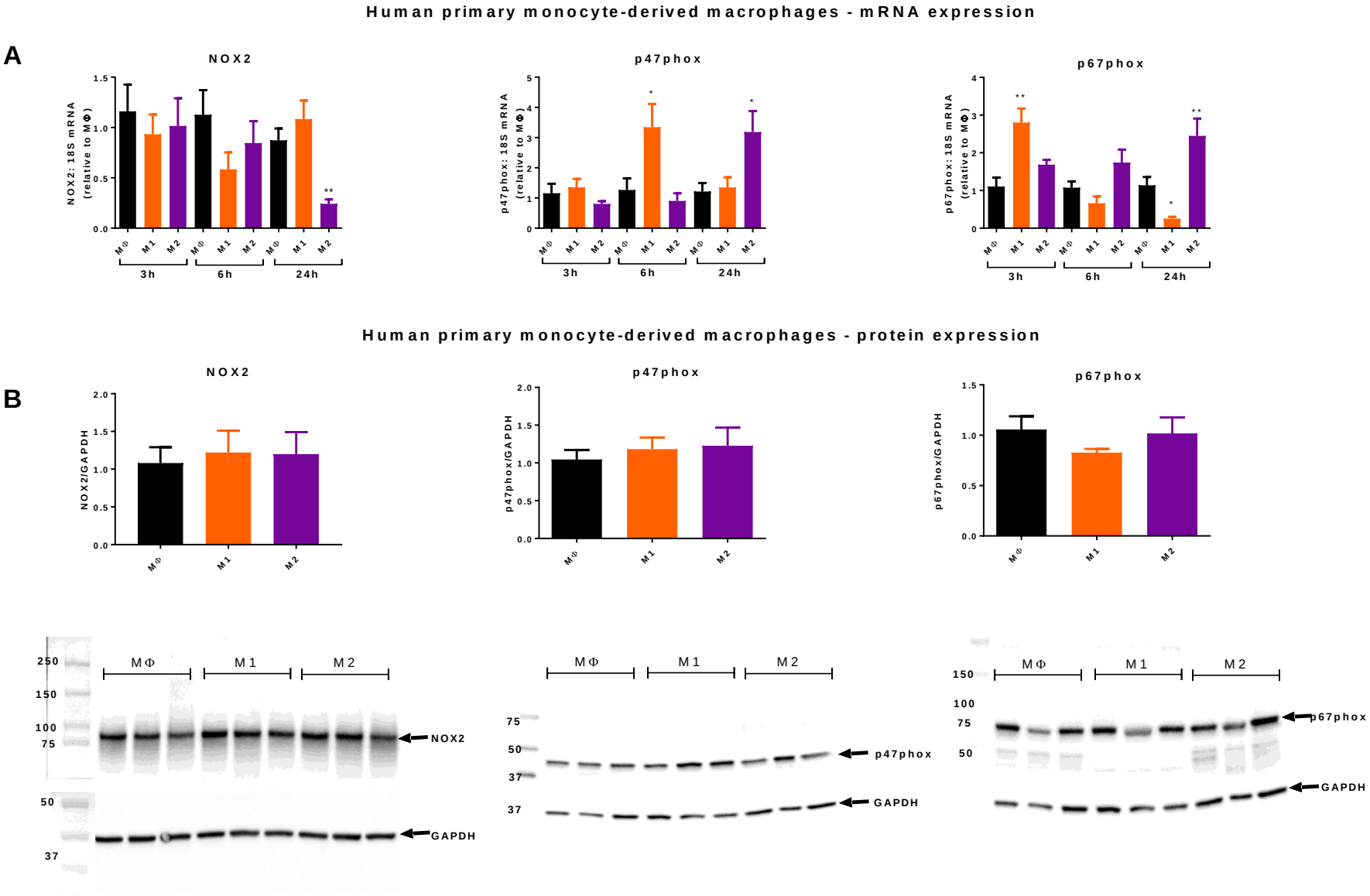
Human primary monocyte-derived macrophages - mRNA expression
A
NOX2
NOX2: 18S mRNA (relative to MΦ)
p47phox
p47phox: 18S mRNA (relative to MΦ)
p67phox
p67phox: 18S mRNA (relative to MΦ)
MΦ M1 M2
3h 6h 24h
Human primary monocyte-derived macrophages - protein expression
B
NOX2
NOX2/GAPDH
p47phox
p47phox/GAPDH
p67phox
p67phox/GAPDH
MΦ M1 M2
250 150 100 75 50 37
NOX2
GAPDH
75 50 37 37
p47phox
GAPDH
150 100 75 50
p67phox
GAPDH

Supplementary Figure 4. Expression of additional NOX2 oxidase subunits and NOX5 in polarised THP-1 and human primary macrophages. PDBu-differentiated THP-1 macrophages (A) or M-CSF-differentiated human primary macrophages (B) were left untreated (MΦ) or treated with IFN-γ/LPS (5 or 20 ng/ml IFN-γ + 10 or 100 ng/ml LPS) or IL-4 (25 ng/ml) for 3-72 hours. mRNA expression of p22phox, p40phox and NOX5 were determined by RT-PCR and expressed relative to the average MΦ (untreated) value. NOX1 and NOX4 isoforms were not detected in any treatment group in either cell line (Ct > 40). Results presented as mean ± SEM, n=4-8. *P<0.05, **P<0.01 vs MΦ (1-way ANOVA followed by Dunnett's post hoc test). N.D = not determined.

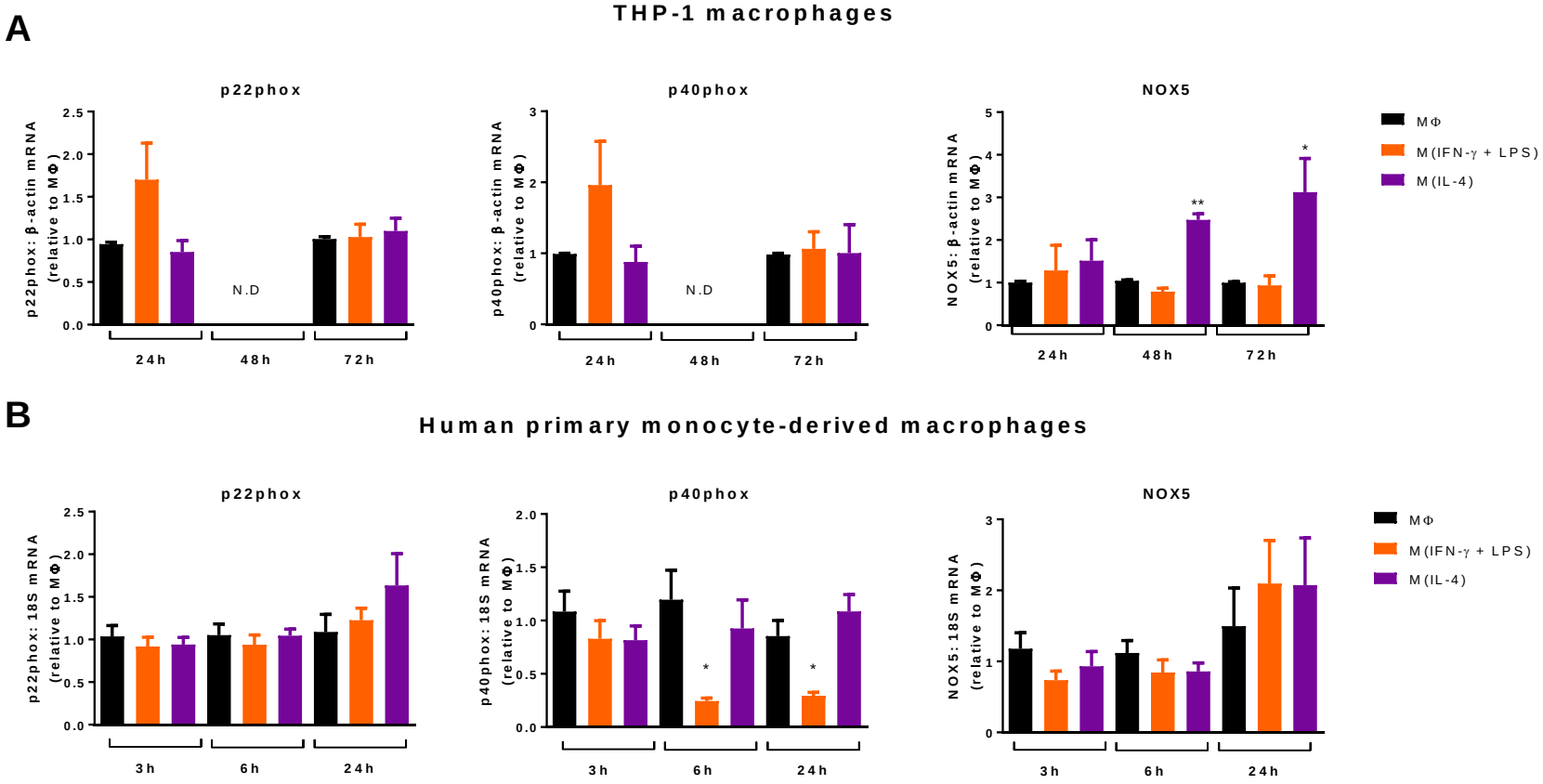
A
THP-1 macrophages
p22phox
p40phox
NOX5
p22phox: β-actin mRNA (relative to MΦ)
p40phox: β-actin mRNA (relative to MΦ)
NOX5: β-actin mRNA (relative to MΦ)
N.D
N.D
24h
48h
72h
MΦ
M(IFN-γ + LPS)
M(IL-4)
B
Human primary monocyte-derived macrophages
p22phox
p40phox
NOX5
p22phox: 18S mRNA (relative to MΦ)
p40phox: 18S mRNA (relative to MΦ)
NOX5: 18S mRNA (relative to MΦ)
3h
6h
24h
MΦ
M(IFN-γ + LPS)
M(IL-4)

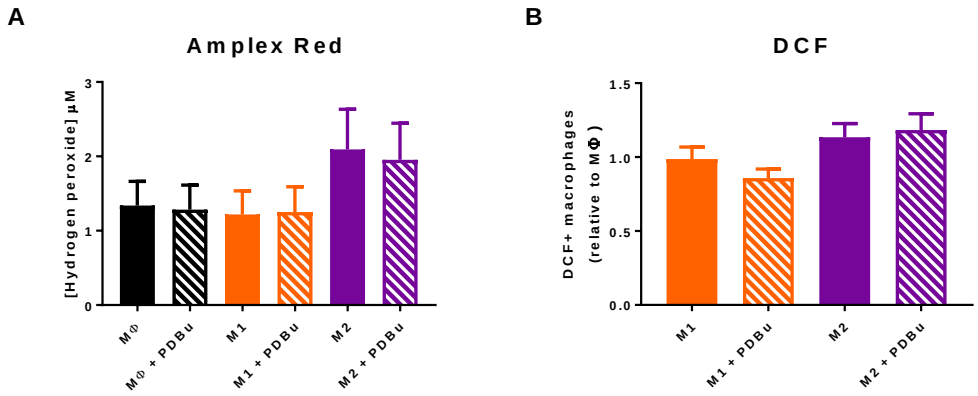

Supplementary Figure 5. Effect of PDBu on the hydrogen peroxide signal in polarised THP-1 macrophages detected with Amplex Red or DCF. PDBu-differentiated THP-1 macrophages were left untreated (MΦ) or polarised to M1 or M2 phenotypes for 72 hours. Immediately prior to the assay, cells from each macrophage phenotype were either left untreated or stimulated with 10 µM PDBu. A) Hydrogen peroxide concentration detected via amplex red fluorescence was calculated after 90 minutes, results expressed as mean concentration ± SEM, n=7-8. B) Mean number of DCF+ macrophages, normalised to the number of DCF+ macrophages in the untreated (MΦ) group, mean ± SEM, n=7-8.

Discussion

M1 macrophage infiltration into tissues is a hallmark of inflammatory diseases and NOX2 oxidase activity has long been associated with M1 function (38). In this study we challenge the idea that ROS generation is solely a function of M1 macrophages, demonstrating that M2 polarisation with IL-4 enhances superoxide generation to an equivalent degree as M1 polarisation and increases hydrogen peroxide generation above the levels observed in M1 or unpolarised macrophages. Of particular relevance to aortic stiffening, an important process involved in the development, and clinical consequences, of hypertension (25, 41), we reveal a potential role for M2 macrophage-derived hydrogen peroxide in promoting pro-fibrotic responses in aortic adventitial fibroblasts.

Upregulation of NOX2 oxidase activity is observed in M1 macrophages as part of the response to microbial infection (46, 47). This has been generally assumed to be a specific M1 function (44). Although IL-4 has been shown to inhibit LPS-stimulated, but enhance IFN-γ-stimulated, ROS production in macrophages (4), we are the first to demonstrate that it can drive an increase in macrophage superoxide production alone. Importantly, the superoxide signal in both M1 and M2 macrophages was at least 2-fold higher than in unpolarised THP-1 and human primary macrophages and was confirmed to be NOX2-derived using NOX2 siRNA. Our findings that M2 polarisation results in increased NOX2-derived ROS further support a contribution of NOX2 to the polarisation of M2 macrophages, as suggested in previous studies (65, 66). It should be noted that our findings are at odds with a study by Kraaij *et al*. (2013), who reported a reduction in ROS when macrophage differentiation occurred in the presence of IL-4. However, distinct methodological approaches may account for these apparent differences. Thus Kraaij *et al.,* (2013) treated monocytes with IL-4 during the 7 day M-CSF differentiation period (28), rather than post-differentiation, as is the more commonly

accepted method of M2 polarisation (39, 58, 60). As such, this previous study may be indicative of the effects of IL-4 on monocyte to macrophage differentiation rather than on macrophage ROS generation *per se*.

Our observation that M2 macrophage function may involve ROS is perhaps not unexpected. M2 macrophages upregulate several scavenger receptors (17), to phagocytose cell debris as part of their tissue repair function (64), and roles for ROS in phagocytosis are well documented (52). Indeed, ROS have been shown to play a critical signalling role in the polarisation of macrophages towards the M2 phenotype in both humans and mice (65, 66). Furthermore, M2 macrophage accumulation and wound healing responses are impaired in NOX1 and NOX2 double knockout mice (65). Whilst these findings suggested an important role for NOX2 in promoting an M2 phenotype, the authors did not determine whether this delayed wound healing response was a direct result of reduced M2 macrophage accumulation *per se* or whether NOX activity was involved in the wound healing response itself. In addition to potential roles in wound healing, a contribution of NOX2-derived ROS to the resolution of inflammation has also emerged (22, 23) and M2c (IL-10-stimulated) macrophage-derived ROS have been shown to induce the activation of T-regulatory cells (29). Collectively, these previous studies support our findings for the involvement of NOX2 oxidase, in not only M1, but also M2 function and signalling, suggesting roles for NOX2 in immunoregulatory and pro-fibrotic responses in addition to well-known roles in inflammation and microbial killing.

To further investigate the role of NOX2 oxidase in M2 macrophage ROS generation we examined the expression of individual NOX2 oxidase subunits. Our findings with regard to NOX2 subunit expression suggest that the mechanism by which each macrophage phenotype increases superoxide differs. Upregulation of the p47phox and, to a lesser extent, the NOX2

catalytic subunit appeared to drive the increase in M1 macrophage superoxide generation. Given NOX2 and p47phox expression are downstream of pro-inflammatory signalling pathways involving the M1 transcription factors NFκB (1), STAT1 (30) and IRF-1 (30, 48) such an observation was expected. By contrast, M2 macrophage polarisation was associated with upregulation of the p67phox subunit alone. Moreover, STAT3 may mediate this response as STAT3 has previously been reported to be involved in IL-4 signalling in macrophages (5) and p67phox can be induced by STAT3 activation in smooth muscle cells (37). Additionally, p38 MAPK pathways are induced by IL-4 (24) and can enhance NOX activity and expression (14, 53). Thus IL-4 signalling through STAT3 and/or p38 MAPK, may enhance NOX2 oxidase activity in M2 macrophages; a concept which remains to be investigated in future studies. In support of a role for these three subunits in enhancing macrophage NOX2 oxidase activity, the M1 macrophage-derived cytokine TNFα has been shown to augment macrophage superoxide generation via increased p47phox, p67phox and NOX2 expression (15). Similar to the magnitude of increases we observed, the rank order of expression was p47phox (up to 20-fold) > p67phox (up to 5-fold) > NOX2 (up to 2.5-fold) (15). In addition, an important role for both p47phox and p67phox in driving NOX2 oxidase activity has also been demonstrated in THP-1 monocytes (57).

Collectively our data support a predominant role of NOX2 oxidase activity in M1 and M2 superoxide generation. However, in agreement with recent reports (36, 40), we also observed NOX5 expression, at least at the mRNA level, in all macrophage phenotypes. Moreover, NOX5 mRNA expression was upregulated by IL-4 in THP-1 cells. Although NOX2 siRNA treatment revealed that the superoxide signal was predominantly NOX2-derived, a contribution of NOX5 to the signal cannot be excluded, particularly considering that it too can be activated via PKC (induced by PDBu stimulation) (11, 55). It should be acknowledged that a limitation of the

current study was that our findings of enhanced p47phox and p67phox expression in M1 and M2 macrophages were not observed at the protein level in human primary macrophages. This may be due to the heterogeneity of donor blood monocytes as compared to the immortalised THP-1 line, but does question the relevance of these findings and highlights the importance of confirming observations in primary cells. Nonetheless, we show for the first time that the superoxide generating capacity of M1 and M2 macrophages is equivalent and driven predominantly via NOX2 oxidase.

Following generation, superoxide can interact with nitric oxide to form the powerful oxidant, peroxynitrite, or be dismutated to form hydrogen peroxide. Considering the pro-inflammatory and reparative properties of M1 and M2 macrophages, respectively, we suggest that whilst both phenotypes generate similar levels of superoxide the final oxidative end product may differ. Indeed, a role for peroxynitrite in M1 macrophage function is observed whereby increased iNOS expression, in response to pro-inflammatory stimuli, will lead to increased nitric oxide production, in turn reacting with superoxide to form peroxynitite (50). Given that nitric oxide is highly reactive with superoxide (13) and M1 stimuli drive superoxide generation, peroxynitrite will form inside the phagosome for microbial killing, but can also be released from M1 macrophages and result in tissue damage. Indeed M1 macrophage-derived peroxynitrite has been shown to contribute to endothelial cell injury (63). Whilst we attempted to investigate differences in peroxynitrite generation between macrophage phenotypes using 3-nitrotyrosine staining, these experiments were unsuccessful due to difficulties with signal detection and antibody specificity (data not shown). Interestingly, potential for increased mitochondrial hydrogen peroxide generation in M1 macrophages was observed in our study with robust upregulation of the mitochondrial SOD isoform, SOD2, following M1 polarisation. This is in agreement with findings following TLR receptor activation

and LPS stimulation of macrophages (49, 51). Although this was not associated with increased hydrogen peroxide generation in M1 macrophages in our study, we did not specifically investigate mitochondrial ROS, which would not be released from the cell. It remains likely that SOD2 upregulation may be a mechanism by which M1 macrophages are protected against oxidative stress during infection and could be linked with mitochondrial dysfunction, as M1 activation shifts cells from oxidative to glycolytic metabolism (12). Hence macrophage phenotype may influence mitochondrial ROS production and mitochondrial dysfunction could contribute to the overall oxidative capacity of M1 macrophages. This remains to be investigated in future studies.

Importantly, we demonstrated increases in both extracellular and intracellular hydrogen peroxide following polarisation to the M2 phenotype with IL-4, an effect which was not evident with M1 polarisation. Whilst we acknowledge that the probe we have used for intracellular hydrogen peroxide (H_2DCF) can detect other forms of ROS, the increase in the M2 macrophage H_2DCF signal was no longer evident with the addition of PEG-catalase. Hence we suggest that the enhanced M2 macrophage H_2DCF signal is hydrogen peroxide. Furthermore, a more specific probe for hydrogen peroxide, amplex red, revealed similar results for extracellular hydrogen peroxide and was also validated using SOD and catalase treatment. Similarly, a previous study reported that augmented macrophage-derived hydrogen peroxide and Cu,Zn-SOD (SOD1) expression were associated with M2 polarisation in the setting of pulmonary fibrosis (21). Although we did not detect a change in SOD1 mRNA, a modest increase in extracellular SOD (SOD3) mRNA was observed following M2 polarisation. However, this did not translate to enhanced SOD3 protein in the macrophage lysates. Additional potential levels of regulation of the hydrogen peroxide signal are via catalase, or antioxidant enzymes such as glutathionine peroxidase (GPx) and thioredoxin reductase

(TrxR). Future studies could also investigate whether the expression of theses enzymes and the glutathione: glutathione disulfide ratio are influenced by macrophage phenotype. Nonetheless, our findings that SOD protein levels are unchanged in M2 macrophages suggest that dismutation of NOX2-derived superoxide may not necessarily be the major source of the hydrogen peroxide signal observed. This is further supported by a lack of effect of PDBu stimulation *per se* on hydrogen peroxide generation, implying a constitutively active hydrogen peroxide-producing enzyme, such as NOX4, could be involved. Although we did not detect NOX4 mRNA in any of our macrophage samples, NOX4 mRNA and protein expression has been observed in two recent studies of human primary macrophages (31, 42). Interestingly, NOX4 expression was induced via MEK/ERK pathways in human macrophages (31), and IL-4 signalling appears to involve these pathways (26, 34), suggesting that it could enhance NOX4 expression. Further investigation of NOX4 protein expression and the use of NOX2 and NOX4 siRNA, in future studies, will aid in the identification of the source of M2 macrophage-derived hydrogen peroxide.

Regardless of the source, enhanced hydrogen peroxide generation appears to be a function of M2 macrophages and may be implicated in fibrotic diseases. ROS have been shown to contribute to a multitude of pro-fibrotic and remodelling actions in the vessel wall (3, 6, 20, 35). Given its stability in comparison with superoxide, hydrogen peroxide has strong potential as a paracrine signalling molecule (2). Thus hydrogen peroxide has been shown to further enhance ROS production in vascular and cardiac cells *in vitro* (8, 62) and promote remodelling in the intact vasculature (3). We show that stimulation of aortic adventitial fibroblasts with exogenous hydrogen peroxide can modestly increase pro-collagen expression. Although in this set of experiments we were unable to detect mature (cleaved) collagen I bands, due to low protein yields and limitations with the antibody used, this is the first investigation of such

an effect in this cell line and concurs with findings with respect to hydrogen peroxide stimulation of collagen production in cardiac fibroblasts (62). We next sought to determine if M2 macrophage-derived hydrogen peroxide can promote vascular fibrosis. Indeed, co-culture of M2 polarised macrophages with aortic fibroblasts lead to increased collagen I expression, an effect which was negated by the hydrogen peroxide scavenger, PEG-catalase. These observations are supported by a study of pulmonary fibroblasts co-cultured with alveolar macrophages, in which enhanced myofibroblast differentiation during co-culture was attenuated when macrophages were treated with the NOX inhibitor apocynin (10). Thus hydrogen peroxide, generated by M2 macrophages, could contribute to the aortic remodelling and stiffening response observed as a consequence of M2 macrophage accumulation in the vessel wall of hypertensive mice (43).

It should be noted that we did not observe any effects of exogenous hydrogen peroxide or co-culture with M2 macrophages on α-SMA expression in our fibroblasts, implying an absence of fibroblast to myofibroblast differentiation. Whilst such a finding was unexpected, it should be noted that a large degree of variability in α-SMA protein expression was observed. Indeed α-SMA expression *per se* can increase with cell passage and it is possible that fibroblasts were already differentiated to myofibroblasts prior to treatment with exogenous hydrogen peroxide or co-culture with macrophages. It is important to note that we also observed an increase in aortic fibroblast collagen expression following co-culture with M1 macrophages, albeit the response tended to be less than that with M2 macrophages. Given we also found that TGF-β expression was modestly upregulated in M1 THP-1 macrophages, this pro-fibrotic chemokine, together with hydrogen peroxide, could be enhancing collagen I expression. Furthermore, the presented results are only preliminary and require additional experiments to confirm the trends observed.

This study has revealed an important role of ROS in M2 macrophage function. Although previously considered a key mediator of M1 macrophage function, we have shown for the first time that increased NOX2-derived superoxide generation also occurs following IL-4-stimulated M2 polarisation. Furthermore, we show that M2 macrophages produce increased amounts of hydrogen peroxide, which has potential pro-fibrotic effects on adventitial fibroblasts. Our findings suggest that the pro-fibrotic actions of M2 macrophages in the vessel wall may be, at least in part, through the generation of hydrogen peroxide, highlighting M2-derived ROS as a potential therapeutic target for fibrotic diseases and aortic stiffening during hypertension.

References

1. Anrather J, Racchumi G, and Iadecola C. NF-kappa B regulates phagocytic NADPH oxidase by inducing the expression of gp91(phox). *Journal of Biological Chemistry* 281: 5657-5667, 2006.

2. Ardanaz N, and Pagano PJ. Hydrogen peroxide as a paracrine vascular mediator: regulation and signaling leading to dysfunction. *Experimental biology and medicine (Maywood, NJ)* 231: 237-251, 2006.

3. Barman SA, Chen F, Su Y, Dimitropoulou C, Wang Y, Catravas JD, Han W, Orfi L, Szantai-Kis C, Keri G, Szabadkai I, Barabutis N, Rafikova O, Rafikov R, Black SM, Jonigk D, Giannis A, Asmis R, Stepp DW, Ramesh G, and Fulton DJ. NADPH oxidase 4 is expressed in pulmonary artery adventitia and contributes to hypertensive vascular remodeling. *Arterioscler Thromb Vasc Biol* 34: 1704-1715, 2014.

4. Bhaskaran G, Nii A, Sone S, and Ogura T. DIFFERENTIAL-EFFECTS OF INTERLEUKIN-4 ON SUPEROXIDE ANION PRODUCTION BY HUMAN ALVEOLAR MACROPHAGES STIMULATED WITH LIPOPOLYSACCHARIDE AND INTERFERON-GAMMA. *Journal of Leukocyte Biology* 52: 218-223, 1992.

5. Bhattacharjee A, Shukla M, Yakubenko VP, Mulya A, Kundu S, and Cathcart MK. IL-4 and IL-13 employ discrete signaling pathways for target gene expression in alternatively activated monocytes/macrophages. *Free radical biology & medicine* 54: 1-16, 2013.

6. Brown DI, and Griendling KK. Regulation of signal transduction by reactive oxygen species in the cardiovascular system. *Circ Res* 116: 531-549, 2015.

7. Brune B, Dehne N, Grossmann N, Jung M, Namgaladze D, Schmid T, von Knethen A, and Weigert A. Redox control of inflammation in macrophages. *Antioxidants & redox signaling* 19: 595-637, 2013.

8. Cai H. NAD(P)H oxidase-dependent self-propagation of hydrogen peroxide and vascular disease. *Circ Res* 96: 818-822, 2005.

9. Calderon B, Suri A, and Unanue ER. In CD4+ T-cell-induced diabetes, macrophages are the final effector cells that mediate islet beta-cell killing: studies from an acute model. *The American journal of pathology* 169: 2137-2147, 2006.

10. Chen C, Yang S, Zhang M, Zhang Z, Hong J, Han D, Ma J, Zhang SB, Okunieff P, and Zhang L. Triptolide mitigates radiation-induced pulmonary fibrosis via inhibition of axis of alveolar macrophages-NOXes-ROS-myofibroblasts. *Cancer biology & therapy* 17: 381-389, 2016.

11. Chen F, Yu Y, Haigh S, Johnson J, Lucas R, Stepp DW, and Fulton DJ. Regulation of NADPH oxidase 5 by protein kinase C isoforms. *PLoS One* 9: e88405, 2014.

12. El Kasmi KC, and Stenmark KR. Contribution of metabolic reprogramming to macrophage plasticity and function. *Seminars in immunology* 27: 267-275, 2015.

13. Ferrer-Sueta G, and Radi R. Chemical biology of peroxynitrite: kinetics, diffusion, and radicals. *ACS chemical biology* 4: 161-177, 2009.

14. Fu X, Beer DG, Behar J, Wands J, Lambeth D, and Cao W. cAMP-response element-binding protein mediates acid-induced NADPH oxidase NOX5-S expression in Barrett esophageal adenocarcinoma cells. *Journal of Biological Chemistry* 281: 20368-20382, 2006.

15. Gauss KA, Nelson-Overton LK, Siemsen DW, Gao Y, DeLeo FR, and Quinn MT. Role of NF-kappaB in transcriptional regulation of the phagocyte NADPH oxidase by tumor necrosis factor-alpha. *J Leukoc Biol* 82: 729-741, 2007.

16. Glim JE, Niessen FB, Everts V, van Egmond M, and Beelen RH. Platelet derived growth factor-CC secreted by M2 macrophages induces alpha-smooth muscle actin expression by dermal and gingival fibroblasts. *Immunobiology* 218: 924-929, 2013.

17. Gordon S, and Martinez FO. Alternative Activation of Macrophages: Mechanism and Functions. *Immunity* 32: 593-604, 2010.

18. Guimaraes DA, Rizzi E, Ceron CS, Martins-Oliveira A, Gerlach RF, Shiva S, and Tanus-Santos JE. Atorvastatin and sildenafil decrease vascular TGF-beta levels and MMP-2 activity and ameliorate arterial remodeling in a model of renovascular hypertension. *Redox biology* 6: 386-395, 2015.

19. Han W, Li H, Cai J, Gleaves LA, Polosukhin VV, Segal BH, Yull FE, and Blackwell TS. NADPH oxidase limits lipopolysaccharide-induced lung inflammation and injury in mice through reduction-oxidation regulation of NF-kappaB activity. *J Immunol* 190: 4786-4794, 2013.

20. Haurani MJ, and Pagano PJ. Adventitial fibroblast reactive oxygen species as autacrine and paracrine mediators of remodeling: bellwether for vascular disease? *Cardiovasc Res* 75: 679-689, 2007.

21. He C, Ryan AJ, Murthy S, and Carter AB. Accelerated development of pulmonary fibrosis via Cu,Zn-superoxide dismutase-induced alternative activation of macrophages. *J Biol Chem* 288: 20745-20757, 2013.

22. Hultqvist M, Olofsson P, Wallner FK, and Holmdahl R. Pharmacological Potential of NOX2 Agonists in Inflammatory Conditions. *Antioxidants & redox signaling* 2014.

23. Hultqvist M, Olsson LM, Gelderman KA, and Holmdahl R. The protective role of ROS in autoimmune disease. *Trends in immunology* 30: 201-208, 2009.

24. Jang YS, Kim HA, Park SR, Lee MR, Park JB, and Kim PH. IL-4 stimulates mouse macrophages to express APRIL through p38MAPK and two different downstream molecules, CREB and Stat6. *Cytokine* 47: 43-47, 2009.

25. Kaess BM, Rong J, Larson MG, and et al. Aortic stiffness, blood pressure progression, and incident hypertension. *JAMA* 308: 875-881, 2012.

26. Kang H, Zhang J, Wang B, Liu M, Zhao J, Yang M, and Li Y. Puerarin inhibits M2 polarization and metastasis of tumor-associated macrophages from NSCLC xenograft model via inactivating MEK/ERK 1/2 pathway. *Int J Oncol* 50: 545-554, 2017.

27. Kossmann S, Hu H, Steven S, Schonfelder T, Fraccarollo D, Mikhed Y, Brahler M, Knorr M, Brandt M, Karbach SH, Becker C, Oelze M, Bauersachs J, Widder J, Munzel T, Daiber A, and Wenzel P. Inflammatory monocytes determine endothelial nitric-oxide synthase uncoupling and nitro-oxidative stress induced by angiotensin II. *J Biol Chem* 289: 27540-27550, 2014.

28. Kraaij MD, Koekkoek KM, van der Kooij SW, Gelderman KA, and van Kooten C. Subsets of human type 2 macrophages show differential capacity to produce reactive oxygen species. *Cell Immunol* 284: 1-8, 2013.

29. Kraaij MD, Savage ND, van der Kooij SW, Koekkoek K, Wang J, van den Berg JM, Ottenhoff TH, Kuijpers TW, Holmdahl R, van Kooten C, and Gelderman KA. Induction of

regulatory T cells by macrophages is dependent on production of reactive oxygen species. *Proc Natl Acad Sci U S A* 107: 17686-17691, 2010.

30. Kumatori A, Yang D, Suzuki S, and Nakamura M. Cooperation of STAT-1 and IRF-1 in interferon-gamma-induced transcription of the gp91(phox) gene. *J Biol Chem* 277: 9103-9111, 2002.

31. Lee CF, Qiao M, Schroder K, Zhao Q, and Asmis R. Nox4 is a novel inducible source of reactive oxygen species in monocytes and macrophages and mediates oxidized low density lipoprotein-induced macrophage death. *Circ Res* 106: 1489-1497, 2010.

32. Lee S, Huen S, Nishio H, Nishio S, Lee HK, Choi BS, Ruhrberg C, and Cantley LG. Distinct macrophage phenotypes contribute to kidney injury and repair. *Journal of the American Society of Nephrology : JASN* 22: 317-326, 2011.

33. Liao TD, Yang XP, Liu YH, Shesely EG, Cavasin MA, Kuziel WA, Pagano PJ, and Carretero OA. Role of inflammation in the development of renal damage and dysfunction in angiotensin II-induced hypertension. *Hypertension* 52: 256-263, 2008.

34. Lin DA, and Boyce JA. IL-4 regulates MEK expression required for lysophosphatidic acid-mediated chemokine generation by human mast cells. *J Immunol* 175: 5430-5438, 2005.

35. Liu J, Ormsby A, Oja-Tebbe N, and Pagano PJ. Gene transfer of NAD(P)H oxidase inhibitor to the vascular adventitia attenuates medial smooth muscle hypertrophy. *Circ Res* 95: 587-594, 2004.

36. Manea A, Manea SA, Gan AM, Constantin A, Fenyo IM, Raicu M, Muresian H, and Simionescu M. Human monocytes and macrophages express NADPH oxidase 5; a potential

source of reactive oxygen species in atherosclerosis. *Biochem Biophys Res Commun* 461: 172-179, 2015.

37. Manea A, Tanase LI, Raicu M, and Simionescu M. Jak/STAT signaling pathway regulates nox1 and nox4-based NADPH oxidase in human aortic smooth muscle cells. *Arterioscler Thromb Vasc Biol* 30: 105-112, 2010.

38. Mantovani A, Sica A, Sozzani S, Allavena P, Vecchi A, and Locati M. The chemokine system in diverse forms of macrophage activation and polarization. *Trends in immunology* 25: 677-686, 2004.

39. Martinez FO, Gordon S, Locati M, and Mantovani A. Transcriptional profiling of the human monocyte-to-macrophage differentiation and polarization: New molecules and patterns of gene expression. *Journal of Immunology* 177: 7303-7311, 2006.

40. Marzaioli V, Hurtado-Nedelec M, Pintard C, Tlili A, Marie JC, Monteiro RC, Gougerot-Pocidalo MA, Dang PM, and El-Benna J. NOX5 and p22phox are 2 novel regulators of human monocytic differentiation into dendritic cells. *Blood* 130: 1734-1745, 2017.

41. Mitchell GF, Hwang SJ, Vasan RS, Larson MG, Pencina MJ, Hamburg NM, Vita JA, Levy D, and Benjamin EJ. Arterial stiffness and cardiovascular events: the Framingham Heart Study. *Circulation* 121: 505-511, 2010.

42. Moon JS, Nakahira K, Chung KP, DeNicola GM, Koo MJ, Pabon MA, Rooney KT, Yoon JH, Ryter SW, Stout-Delgado H, and Choi AM. NOX4-dependent fatty acid oxidation promotes NLRP3 inflammasome activation in macrophages. *Nat Med* 22: 1002-1012, 2016.

43. Moore JP, Vinh A, Tuck KL, Sakkal S, Krishnan SM, Chan CT, Lieu M, Samuel CS, Diep H, Kemp-Harper BK, Tare M, Ricardo SD, Guzik TJ, Sobey CG, and Drummond GR. M2 macrophage accumulation in the aortic wall during angiotensin II infusion in mice is associated with fibrosis, elastin loss, and elevated blood pressure. *American journal of physiology Heart and circulatory physiology* 309: H906-917, 2015.

44. Mosser DM, and Edwards JP. Exploring the full spectrum of macrophage activation. *Nature Reviews Immunology* 8: 958-969, 2008.

45. Murray LA, Chen Q, Kramer MS, Hesson DP, Argentieri RL, Peng X, Gulati M, Homer RJ, Russell T, van Rooijen N, Elias JA, Hogaboam CM, and Herzog EL. TGF-beta driven lung fibrosis is macrophage dependent and blocked by Serum amyloid P. *The international journal of biochemistry & cell biology* 43: 154-162, 2011.

46. Newburger PE, Dai Q, and Whitney C. In vitro regulation of human phagocyte cytochrome b heavy and light chain gene expression by bacterial lipopolysaccharide and recombinant human cytokines. *J Biol Chem* 266: 16171-16177, 1991.

47. Newburger PE, Ezekowitz RA, Whitney C, Wright J, and Orkin SH. Induction of phagocyte cytochrome b heavy chain gene expression by interferon gamma. *Proc Natl Acad Sci U S A* 85: 5215-5219, 1988.

48. Olavarria VH, Figueroa JE, and Mulero V. Induction of genes encoding NADPH oxidase components and activation of IFN regulatory factor-1 by prolactin in fish macrophages. *Innate immunity* 19: 644-654, 2013.

49. Peterman EM, Sullivan C, Goody MF, Rodriguez-Nunez I, Yoder JA, and Kim CH. Neutralization of mitochondrial superoxide by superoxide dismutase 2 promotes bacterial

clearance and regulates phagocyte numbers in zebrafish. *Infection and immunity* 83: 430-440, 2015.

50. Prolo C, Alvarez MN, and Radi R. Peroxynitrite, a potent macrophage-derived oxidizing cytotoxin to combat invading pathogens. *BioFactors (Oxford, England)* 40: 215-225, 2014.

51. Rakkola R, Matikainen S, and Nyman TA. Proteome analysis of human macrophages reveals the upregulation of manganese-containing superoxide dismutase after toll-like receptor activation. *Proteomics* 7: 378-384, 2007.

52. Rosen GM, Pou S, Ramos CL, Cohen MS, and Britigan BE. Free radicals and phagocytic cells. *FASEB journal : official publication of the Federation of American Societies for Experimental Biology* 9: 200-209, 1995.

53. Schenten V, Melchior C, Steinckwich N, Tschirhart EJ, and Brechard S. Sphingosine kinases regulate NOX2 activity via p38 MAPK-dependent translocation of S100A8/A9. *J Leukoc Biol* 89: 587-596, 2011.

54. Schmittgen TD, and Livak KJ. Analyzing real-time PCR data by the comparative C-T method. *Nature Protocols* 3: 1101-1108, 2008.

55. Serrander L, Jaquet V, Bedard K, Plastre O, Hartley O, Arnaudeau S, Demaurex N, Schlegel W, and Krause K-H. NOX5 is expressed at the plasma membrane and generates superoxide in response to protein kinase C activation. *Biochimie* 89: 1159-1167, 2007.

56. Sica A, and Mantovani A. Macrophage plasticity and polarization: in vivo veritas. *J Clin Invest* 122: 787-795, 2012.

57. Siow YL, Au-Yeung KK, Woo CW, and O K. Homocysteine stimulates phosphorylation of NADPH oxidase p47phox and p67phox subunits in monocytes via protein kinase Cbeta activation. *Biochem J* 398: 73-82, 2006.

58. Sudan B, Wacker MA, Wilson ME, and Graff JW. A Systematic Approach to Identify Markers of Distinctly Activated Human Macrophages. *Frontiers in immunology* 6: 253, 2015.

59. Vidal B, Serrano AL, Tjwa M, Suelves M, Ardite E, De Mori R, Baeza-Raja B, Martinez de Lagran M, Lafuste P, Ruiz-Bonilla V, Jardi M, Gherardi R, Christov C, Dierssen M, Carmeliet P, Degen JL, Dewerchin M, and Munoz-Canoves P. Fibrinogen drives dystrophic muscle fibrosis via a TGFbeta/alternative macrophage activation pathway. *Genes & development* 22: 1747-1752, 2008.

60. Vogel DY, Glim JE, Stavenuiter AW, Breur M, Heijnen P, Amor S, Dijkstra CD, and Beelen RH. Human macrophage polarization in vitro: Maturation and activation methods compared. *Immunobiology* 219: 695-703, 2014.

61. Wang N, Liang H, and Zen K. Molecular mechanisms that influence the macrophage m1-m2 polarization balance. *Frontiers in immunology* 5: 614, 2014.

62. Wang P, Zhou S, Xu L, Lu Y, Yuan X, Zhang H, Li R, Fang J, and Liu P. Hydrogen peroxide-mediated oxidative stress and collagen synthesis in cardiac fibroblasts: blockade by tanshinone IIA. *Journal of ethnopharmacology* 145: 152-161, 2013.

63. Wang X, Liu K, Li B, Li Y, Ye K, Qi J, and Wang Y. Macrophages Aggravate Hypoxia-Induced Cardiac Microvascular Endothelial Cell Injury via Peroxynitrite: Protection by Tongxinluo. *Cell communication & adhesion* 22: 39-47, 2015.

64. Wynn TA, and Vannella KM. Macrophages in Tissue Repair, Regeneration, and Fibrosis. *Immunity* 44: 450-462, 2016.

65. Xu Q, Choksi S, Qu J, Jang J, Choe M, Banfi B, Engelhardt JF, and Liu ZG. NADPH Oxidases Are Essential for Macrophage Differentiation. *J Biol Chem* 291: 20030-20041, 2016.

66. Zhang Y, Choksi S, Chen K, Pobezinskaya Y, Linnoila I, and Liu ZG. ROS play a critical role in the differentiation of alternatively activated macrophages and the occurrence of tumor-associated macrophages. *Cell research* 23: 898-914, 2013.

CHAPTER 5:

THE ROLE OF IL-4 AND IL-13 IN THE MODULATION OF MACROPHAGE PHENOTYPE AND REACTIVE OXYGEN SPECIES GENERATION

The role of IL-4 and IL-13 in the modulation of macrophage phenotype and reactive oxygen species generation

Caitlin Lewis[‖], Tara McConaghy[‖], May Zhu[‖], Chao Wang[‖], Chrishan Samuel[‖], Grant Drummond[¶], Barbara Kemp-Harper[‖]

Affiliations

[‖] Cardiovascular Disease Program, Biomedicine Discovery Institute & Department of Pharmacology, Monash University, VIC 3800, Australia

[¶] Department of Physiology, Anatomy & Microbiology, School of Life Sciences, La Trobe University, VIC 3086, Australia

Abstract

In the setting of atherosclerosis, the closely-related Th2 cytokines, IL-4 and IL-13, have been reported to have pathophysiological and protective properties, respectively. Given that macrophages play a central role in atherogenesis, and express both the type I and type II IL-4 receptors, we hypothesised that these contrasting roles may occur through differential effects on M2 macrophage function. Human primary macrophages were treated with IL-4 or IL-13 (0.005-50 ng/ml, 24 hours) and the expression of M2 markers (MRC-1, CCL18, CCL22) assessed via RT-PCR. A maximum effective concentration (50 ng/ml) was used to compare the ability of IL-4 and IL-13 to modulate reactive oxygen species (ROS) and matrix metalloproteinase (MMP) generation, as well as M1 macrophage function. We observed equivalent potency (0.2-0.8 ng/ml) and efficacy of IL-4 and IL-13 to induce M2 marker expression. Both cytokines enhanced PDBu (10μM)-stimulated superoxide generation as detected by L-012 (100 μM)-enhanced chemiluminescence, an effect that was 20% greater in IL-4-treated, as compared to IL-13-treated, macrophages. Whilst no effect was observed for either cytokine on MMP9 generation, IL-13 reduced MMP2 expression by 20% relative to untreated macrophages. Despite demonstrating enhanced type I IL-4 receptor expression on M1 macrophages, we did not observe any differences in the ability of IL-4 and IL-13 to attenuate M1 macrophage-derived superoxide generation. Overall our findings suggest that the opposing roles identified for these two cytokines in atherosclerosis, are likely to be through actions on cell types other than macrophages. Future studies should directly compare IL-4 and IL-13 in atherogenesis *in vivo* and investigate their effects on vascular cells to confirm the therapeutic validity of selective targeting of one cytokine over the other.

Introduction

The Th2 cytokines, interleukin-4 (IL-4) and interleukin-13 (IL-13), are well recognised for their roles in allergic diseases, such as asthma. In addition, they exhibit anti-inflammatory properties, inhibiting type I inflammation (i.e. IFN-γ induced) and promoting polarisation of macrophages towards the reparative, M2 phenotype (18, 44). This alternative activation of macrophages by IL-4 and IL-13 is of particular interest in cardiovascular pathologies, such as atherosclerosis, where M2 macrophages promote the stabilisation of atherosclerotic plaques (9, 30). Interestingly, although IL-4 and IL-13 share many similar biological activities and both promote M2 polarisation, opposing roles of these Th2 cytokines has been reported in atherosclerosis. Thus, pro- and anti-atherogenic properties of IL-4 and IL-13, respectively are evident.

Support for a pro-atherogenic action of IL-4 comes from a growing body of evidence. Thus, King *et al.*(33), demonstrated a reduction in atherosclerotic lesion area in the aortic arch and thoracic aorta of female $LDLR^{-/-}$ mice following IL-$4^{-/-}$ bone marrow transplantation. Moreover, a reduction in aortic lesion area has been reported in $ApoE^{-/-}$ mice with global deficiency in IL-4 (12). Fatty streak formation is also reduced in IL-4 deficient mice placed on a high fat diet and immunised against heat shock protein (HSP)-65 or *mycobacterium tuberculosis* to induce atherosclerosis (17). In addition, a recent study, in mice with allergic asthma, found that increased IL-4 and IL-17 expression was associated with accelerated development of atherosclerosis. Importantly, treatment with monoclonal antibodies against IL-4 reduced this effect (59). Of note, one study has reported no impact of IL-4 deficiency on atherosclerotic lesion development in hypercholesterolaemic or Ang-II treated $ApoE^{-/-}$ or $LDL^{-/-}$ mice (32) and another demonstrated that IL-4 treatment was atheroprotective in $ApoE^{-/-}$ mice fed a high fat

diet and treated with ox-LDL (62). These opposing findings, with regard to IL-4, may be indicative of the nature of the murine model of atherosclerosis used. Collectively however, the evidence to date suggests that IL-4 promotes atherosclerosis.

Although investigation of the effects of IL-13 in the context of atherosclerosis has been limited, atheroprotective actions of IL-13 have been demonstrated. In one study of $LDLR^{-/-}$ mice, the protective effects of malon-dialdehyde-modified LDL immunisation to reduce lesion size were associated with increased production of IL-5 and IL-13, with minimal impact on IL-4 (5). More recently, direct evidence for an atheroprotective role of IL-13 has come to light whereby bone marrow-specific deletion of IL-13 was shown to increase aortic lesion size, whilst IL-13 administration to mice with established atherosclerosis resulted in increased collagen content, reduced M1:M2 marker expression and an overall reduction in macrophage content, consistent with a plaque stabilising response (9).

Taken together these findings suggest that IL-4 and IL-13 may play opposing roles in atherosclerosis. The underlying causes of these opposing actions remain unknown, but may reflect differential effects of these Th2 cytokines on M2 macrophage function. Indeed an ability of IL-4 and IL-13 to target distinct receptors and downstream signalling pathways, and modulate the production of effector molecules such as reactive oxygen species (ROS) and matrix metalloproteinases (MMPs) may contribute to their contrasting actions.

On macrophages, IL-4 can activate two different heterodimeric receptor complexes, known as the type I and type II IL-4 receptors, whilst IL-13 can only activate the type II IL-4 receptor. Common to both receptors is the IL-4Rα subunit, which complexes with either the IL-2Rγ or IL-13Rα1 subunit to form type I or type II receptors, respectively. Of note, IL-13 also exhibits high affinity for a ‘decoy’ cell surface receptor IL-13Rα2 (41) however, its constitutive

expression in macrophages has not been reported. Thus IL-4 has an additional target on macrophages, as compared to IL-13, which may confer differential modulation of macrophage function. Although levels of expression can differ between cell lines, it is reported, at least in murine macrophages, that the type I receptor is more predominant than the type II receptor (28). The involvement of different downstream signalling pathways in response to these cytokines is also evident. Common to IL-4 and IL-13 is the recruitment of STAT6 and STAT3, which occur via the activation of either receptor (4, 22). In particular, STAT6 is considered a key transcription factor downstream of IL-4 receptor activation and plays a central role in driving IL-4 and IL-13 responses (4, 22, 63). Moreover, STAT6 deficiency limits the activation of M2 macrophages (45). Whilst STAT1 recruitment was shown to be exclusive for IL-13 in monocytes (4), this is due to IL-4 preferentially signalling through the type I receptor and hence IL-4 also has the ability to activate STAT1 where the type II receptor is predominant (58). Of note, despite potential to recruit STAT1, both cytokines attenuate IFN-γ stimulated STAT1 phosphorylation in macrophages (53) to inhibit type I inflammation (44). Key differences between IL-4 and IL-13 signalling derive from pathways associated with the IL-2Rγ subunit, specific for IL-4 activation of the type I receptor. These pathways recruit insulin receptor substrate 2 (IRS2) (22), which leads to activation of PI3K/Akt and CREB (22, 26). Interestingly, PI3K inhibition is protective against plaque rupture (61) and as such an ability of IL-4 to activate this pathway may contribute to its pro-atherogenic actions. In addition, CREB signalling can regulate NADPH oxidase activity (16), a key driver of ROS production. Although ROS production has generally been regarded as a function of M1 macrophages, IL-4 has previously been shown to promote vascular oxidative stress (37) and it is tempting to speculate that this property may also be evident in macrophages and promote atherosclerosis. Furthermore, an ability of IL-4 treatment to increase MMP9 production from

macrophages has been demonstrated (29, 40), which could contribute to ECM degradation and plaque destabilisation.

Given the central role of macrophages to atherogenesis and that macrophages express both type I and type II receptors, we hypothesised that the opposing effects of IL-4 and IL-13 in this setting may be through their influences on M2 macrophage function. It was predicted that these cytokines may differ in their ability to promote the production and release of ROS and MMPs from M2 macrophages and thus IL-4 may stimulate a more inflammatory and less atheroprotective M2 phenotype. This study aimed to characterise the effect of IL-4 and IL-13 on the expression of M2 markers, MMPs and NADPH oxidase enzymes, and ROS generating capacity in human primary macrophages. These studies have the potential to inform on more selective targeting of IL-4 and IL-13 and their downstream effector molecules in atherosclerosis.

Materials and Methods

Monocyte isolation

Primary human monocytes were isolated from healthy blood donor buffy coats (Australian Red Cross Blood Service, Melbourne, Australia). Buffy coats were mixed with phosphate buffered saline (PBS; without Ca^{2+}or Mg^{2+}; Sigma-Aldrich) supplemented with 0.5% fetal bovine serum (FBS; Sigma-Aldrich) and 2 mM ethylenediaminetetraacetic acid (EDTA; Sigma-Aldrich) and layered onto Ficoll-Paque PLUS (GE Healthcare no. 17-144) for density gradient centrifugation (400 g, 40 min, acceleration=1, deceleration=0). The peripheral blood mononuclear cell (PBMCs) layer was collected and monocytes isolated using a human pan monocyte isolation kit (Miltenyi Biotec no. 130-096-537), according to the manufacturer's instructions. The purity of the monocyte population was confirmed to be at least 85% as determined by Flow cytometry using $CD14^+$ /$CD16^+$ expression.

Monocyte to macrophage differentiation and macrophage polarisation

Isolated donor blood-derived primary monocytes were seeded into 6-well plates (2 x 10^6 cells/well; RNA and protein extraction) or 96-well plates (2 x 10^5 cells/well; L012-enhanced chemiluminescence) and maintained in a humidified incubator (Sanyo MCO-18AIC CO_2 incubator, Quantum Scientific, USA) at 37°C with 5% CO_2. Monocytes were differentiated to macrophages by culturing for 7 days in RPMI 1640 Glutamax medium (Gibco Life Technologies), supplemented with 10% FBS, 1x antibiotic/antimycotic (Gibco Life Technologies, USA), 1 mM sodium pyruvate (Sigma-Aldrich), 1 x non-essential amino acids (NEAA; Gibco Life Technologies) and 50 ng/ml macrophage colony stimulating factor (M-CSF; Miltenyi Biotec no. 130-096-491). Following 7 day macrophage differentiation, culture media was replaced in the absence of M-CSF and macrophages were either left untreated (MΦ),

treated with 20 ng/ml interferon-γ (IFN-γ; Sigma-Aldrich no. I3265) and 100 ng/ml lipopolysaccharide (LPS; Sigma-Aldrich no. L2630, E.coli 0111:B4 strain) for M1 polarisation, or with either interleukin-4 (IL-4; Sigma-Aldrich no. I4269) or interleukin-13 (IL-13; Sigma-Aldrich no. I1771) at concentrations ranging from 0.005 ng/ml to 50 ng/ml for 24 hours. A number of signal transduction inhibitors were employed to investigate IL-4 and IL-13 signalling pathways. These included; Fludarabine (100 μM; STAT1 inhibitor; Selleckchem), Stattic (10 μM; STAT3 inhibitor; Selleckchem), AS1517499 (100 nM; STAT6 inhibitor; Axon MedChem) and SB203580 (1 μM; p38 MAPK inhibitor; InvivoGen). All inhibitors were reconstituted in dimethyl sulfoxide (DMSO) with the final DMSO concentration in the cell culture media not exceeding 0.1%. Inhibitors were added 30 minutes prior to 24 hour treatment with a submaximal concentration of IL-4 or IL-13 (2.5 ng/ml).

In a separate set of experiments, M1-polarised macrophages (20 ng/ml IFN-γ and 100 ng/ml LPS, 18 hours) were treated with 50 ng/ml IL-4 or IL-13 for 6 hours and superoxide generation detected via L-012 chemiluminescence. Supernatants were also collected to assess MMP expression.

RNA extraction and real time-PCR

Total RNA was extracted from macrophages using the RNeasy Mini Kit (Qiagen) according to the manufacturer's instructions. RNase-free DNase (Qiagen) was used to remove any contaminating DNA. The amount of RNA in each sample was quantified using the Nanodrop 1000D spectrophotometer (ThermoScientific), which measures absorbance at 260 nm and 280 nm. An A_{260}:A_{280} ratio of 2 or more was considered sufficiently pure. 0.5 μg of RNA from each sample was reverse transcribed into cDNA using the High Capacity cDNA Reverse Transcription Kit (Applied Biosystems) with the reaction run in a thermal cycler (BioRad

MyCycler, BioRad Laboratories). The resultant cDNA was used as a template for real time PCR with Taqman® primers and probes for IL-13Rα1, IL-4Rα, IL-2Rγ, MRC-1, CCL22, CCL18, CYBB (NOX2), NCF1 (p47phox), NCF2 (p67phox) (Applied Biosystems). 18S (Applied Biosystems) was used as a housekeeping gene. Real-time PCR was run in triplicate on the CFX96 Touch™ Real-Time PCR Detection Machine (BioRad Laboratories). Gene expression was normalised to 18S and expressed relative to the average MΦ value using the comparative cycle threshold (Ct) method with the formula: Fold change= $2^{-\Delta\Delta Ct}$ (52).

Protein extraction and Western blotting

Total protein from macrophage lysates was collected in 1.5 x Laemmli buffer (7.5% glycerol; 3.75% β-mercaptoethanol; 2.25% SDS; 75 mM Tris-HCl pH 6.8; 0.004% bromophenol blue), cell debris was cleared by centrifugation (13,000 rpm, 10 min, 4°C) and supernatants were collected. Protein concentrations were determined using a modified Lowry protocol (RCDC colorimetric protein assay kit; BioRad Laboratories). 20 µg of protein in 1.5 x Laemmli buffer was loaded into 7.5% or 10% polyacrylamide gels and proteins were separated by SDS-PAGE and transferred onto low fluorescence polyvinylidene fluoride (LF PVDF) membranes using the Bio-Rad Trans Blot Turbo transfer system (Bio-Rad Laboratories). Membranes were blocked with 5% skim milk in Tris-Buffered Saline (TBS; 200 mM Tris, 150 mM NaCl, pH 7.5) with 0.1 % tween-20 for 1 hour and subsequently probed with primary antibodies against NOX2 (1:500; Santa-Cruz no. sc-130549 (CL5)), p47phox (1: 1000; BD Transduction Laboratories no. 610354), p67phox (1:2000; EMD Millipore no. 07-002), IL-4Rα (1:500; Abcam no. ab131058), IL-13Rα1 (1:200; Abcam no. ab140367), IL-2Rγ (1:500; Abcam no. ab180698) and GAPDH (1: 20000; Abcam no. ab8245) overnight at 4 °C. 1 hour incubation with horseradish peroxidase(HRP)-conjugated anti-rabbit (1:10000; Dako) or anti-mouse (1:10000;

Jackson ImmunoResearch Laboratories) secondary antibodies was then performed and protein bands visualised using Clarity ECL substrate (BioRad Laboratories) and the ChemiDoc MP system (BioRad Laboratories). Densitometries of protein bands were quantified using Image Lab Software (BioRad Laboratories) and normalised to GAPDH. Fold change in protein expression was expressed relative to the average MΦ value.

Superoxide detection via L-012-enhanced chemiluminescence

Primary macrophages were seeded and treated on white 96-well tissue culture plates (Perkin Elmer) at 2 x 10^5 cells/well. Groups were set up in quintuplicate with a cell free control group, comprising media alone, included to provide a background reference. On the day of experimentation, culture medium was removed and cells were washed and incubated in warmed Krebs-HEPES buffer (in mM: NaCl 118; KCl 4.7; KH_2PO_4 1.2; $MgSO_4 \cdot 7H_2O$ 1.2; $CaCl_2$ 2.5; $NaHCO_3$ 25; glucose 11.7; HEPES 20, pH 7.4) and background chemiluminescence measured for 30 minutes. Chemiluminescence was measured using a Chameleon Luminescence Plate Reader (Hidex Ltd, Turku, Finland) and data acquired using the MicroWin (Mikrotek, Overath, Germany) data acquisition system. 100 µM L-012 (Wako Pure Chemical Industries) was then added to each well and basal superoxide levels were monitored for 30 minutes. Finally, the protein kinase C (PKC) activator, PDBu (10 µM) was added to each well and superoxide production was then measured for a further 60 minutes. Peak PDBu-stimulated superoxide production was quantified as the average of 5 cycles at the peak of the signal for each group with the basal signal (average of the final 5 basal readings) subtracted.

Gelatin Zymography

Expression of latent (L) MMP2 and MMP9 in the macrophage culture media following 24 hour treatment was assessed using gelatin zymography as previously described (11). 7.5% acrylamide gels containing 1 mg/ml gelatin were loaded with equivalent sample volumes, with samples from three or four independent experiments from each group run on the same gel. Gelatinolytic activity was indicated by clear bands and the densitometries assessed on the ChemiDoc MP system (BioRad Laboratories) using Image Lab Software (BioRad Laboratories). MMP densitometry was determined and expressed as the relative ratio of the values in the untreated control group (MΦ), which was expressed as 1.

Statistical analysis

All data are expressed as mean ± SEM with n=5-9. Comparisons of multiple treatment groups were made using an ordinary one-way analysis of variance (ANOVA) with a Dunnett's (comparison vs MΦ), Sidak's (selected comparisons) or Tukey's (comparison between all groups) post hoc test. For L-012 chemiluminescence experiments, comparisons were made using a repeated measures one-way ANOVA with Sidak's or Tukey's post hoc tests. Concentration response curves to IL-4 and IL-13 were fitted to a sigmoidal logistic equation and EC_{50} values determined based on fitted curves for the group data. $P<0.05$ was considered to be statistically significant and data were graphed and analysed using GraphPad Prism 7.02 software.

Results

Primary human macrophages express equivalent levels of type I and type II IL-4 receptors

To investigate the relative expression of type I and type II receptors in primary human macrophages, mRNA expression was first assessed for the shared IL-4 receptor subunit IL-4Rα, the type I subunit, IL-2Rγ, the type II subunit IL-13Rα1, and the decoy receptor, IL-13Rα2. RT-PCR analysis revealed very similar mRNA expression levels of the type I and type II receptor subunits in untreated M-CSF-differentiated macrophages (Ct values= 25-27) and, as expected, no detectable expression of IL-13Rα2 (Table 1). We then sought to elucidate whether IL-4 and IL-13 treatment (24 hours) altered receptor expression. A 40% decrease in the mRNA expression of IL-13Rα1 was observed with IL-13 treatment, with a trend for a similar reduction following IL-4 treatment (Figure 1A). However, IL-13Rα1 protein expression remained unchanged (Figure 1D). By contrast, whilst no IL-4Rα mRNA changes were observed, IL-4Rα protein expression was modestly increased by 1.5-fold following IL-4 treatment, an effect not observed following IL-13 treatment (Figure 1E). No change in the expression of the type I receptor subunit, IL-2Rγ was detected (Figure 1C and F).

IL-4 and IL-13 upregulate M2 marker expression in primary human macrophages with equivalent potency and efficacy and through similar signalling pathways

Despite increased IL-4Rα protein expression in IL-4-treated cells, and the potential for signalling through both receptor complexes by IL-4, no differences in the induction of M2 marker expression were observed between IL-4 and IL-13. Treatment of M-CSF differentiated human primary macrophages with 50 ng/ml of either IL-4 or IL-13 for 24 hours, lead to approximately 4-, 400-, and 6-fold increases in the M2 markers mannose receptor C type-1 (MRC-1; Figure 2A), chemokine C-C motif ligand 18 (CCL18; Figure 2C) and CCL22 (Figure 2E).

No significant effect on TGFβ1 expression was observed for either cytokine (Supplementary Figure 1A). Both cytokines decreased the expression of IL-10 by approximately 40% but increased the expression of IL-6 by approximately 20-fold (Supplementary Figures 1B and C) As concentration-dependent effects were not observed between 5, 25 and 50 ng/ml treatments, further experiments were performed using lower concentrations of IL-4 or IL-13 (0.005-5 ng/ml, Figures 2B, D and F). The potencies of IL-4 and IL-13 appeared to be similar for the increased expression of all three M2 markers with EC_{50} values ranging from 0.2 to 0.8 ng/ml (Table 2). IL-4 and IL-13 also appeared to increase all three markers with similar efficacy with a maximum response reached at 5 ng/ml (Table 2).

A range of signalling inhibitors were employed to investigate any potential differences in IL-4 and IL-13 signalling to induce M2 marker expression. While signal transducer and activator of transcription 1 (STAT1), STAT3, p38 mitogen-activated protein kinase (p38 MAPK) or STAT6 inhibition had no effect on MRC-1 expression for either cytokine (Figure 3A and B), STAT3 was found to be required for increases in CCL18 and CCL22 expression following treatment with both IL-4 and IL-13 (Figure 3C-F). p38 MAPK inhibition also attenuated CCL18 expression following IL-13 treatment (Figure 3D, P=0.0513), with a trend for a similar effect following IL-4 treatment (Figure 3C).

IL-4 and IL-13 have similar effects on NADPH oxidase expression, superoxide generation and MMP production

To investigate a potential pro-atherogenic function of IL-4, we compared the ROS generating capacities of IL-4- and IL-13-treated macrophages. Whilst IL-4 and IL-13 treatment did not alter basal superoxide levels, a significant 97% and 65% increase in PDBu-stimulated superoxide production, respectively, was observed (Figure 4C). As NOX2 oxidase is the

primary source of ROS in macrophages, expression of its catalytic (NOX2), activator (p67phox), and organiser (p47phox) subunits were assessed by RT-PCR and western blotting. Although differences in protein expression were not detected, NOX2 mRNA was decreased by 80%, whilst 3-fold and 2-fold increases in p47phox and p67phox mRNA, respectively, were observed following treatment with both IL-4 and IL-13 (Figure 4D-I). No effects on the expression of the p22phox subunit or the NOX5 isoform were observed for either cytokine (Supplementary Figure 2). Neither NOX1 nor NOX4 mRNA was detected (Ct>40).

Given that macrophages are a source of MMPs which can contribute to plaque instability, MMP levels in the culture supernatants were also compared using gelatin zymography. Neither IL-4 nor IL-13 altered MMP9 expression. However a 20% decrease in MMP2 expression was observed in the IL-13 treated as compared to untreated macrophages (Figure 5).

Increased type I IL-4 receptor expression in M1 macrophages is not associated with differential effects of IL-4 or IL-13 on macrophage superoxide or MMP generation

It is unknown whether macrophage subsets differentially express type I and type II IL-4 receptors. We investigated whether there were any differences between M1 and M2 macrophage expression of these receptor subunits. Interestingly, the mRNA and protein levels of both subunits of the type I receptor (IL-4Rα and IL-2Rγ) were up to 3-fold higher in M1 as compared to M2 or unpolarised macrophages (Figure 6). We hence hypothesised that IL-4 may have more potent effects on M1 macrophages than IL-13 and compared the effects of IL-4 and IL-13 on M1 macrophage superoxide generation and MMP release.

Although IL-4 and IL-13 alone promote macrophage superoxide generation (Figure 4), both cytokines attenuated PDBu-stimulated superoxide production in M1 macrophages when added for the final 6 hours of the 24 hour M1 polarisation treatment (Figure 7A-C). M1 macrophages are thought to produce more MMPs than other subsets of macrophages, however in this study neither MMP9 nor MMP2 levels were altered by M1 polarisation. MMP levels in M1 macrophages were unchanged following treatment with IL-4 or IL-13 (Figure 7F and G). A summary of all findings comparing the actions of IL-4 and IL-13 on macrophages is provided in Table 3.

Figures and tables

Table 1. mRNA expression of type I and II receptor subunits in untreated human primary macrophages.

Type I and II IL-4 receptor subunit	**Ct (cycle threshold)**
IL-2Rγ (type I)	27.3 ± 0.3 (moderate)
IL-4Rα (type I & II)	26.1 ± 0.4 (moderate)
IL-13Rα1 (type II)	25.8 ± 0.3 (moderate)
IL-13Rα2 (decoy)	Not detected

Cts determined using RT-PCR with equivalent cDNA loading for each gene, n=7, mean ± SEM.

Figure 1. Type I and II IL-4 receptor subunits are expressed in human primary macrophages treated with IL-4 and IL-13. M-CSF-differentiated primary macrophages were left untreated (MΦ) or treated with 50 ng/ml IL-4 or IL-13 for 24h. mRNA levels of IL-2Rγ (A), IL-4Rα (B) and IL-13Rα1 (C) were determined by RT-PCR and expressed relative to the average MΦ value, n=5-8. Protein levels of IL-2Rγ (D), IL-4Rα (E) and IL-13Rα1 (F) were determined by western blotting and expressed relative to the average MΦ value, n=6-8. Representative blots depicting n=4 shown beneath each graph with GAPDH used as a loading control. Note very low expression of IL-2Rγ was observed in the fourth set of samples and this was excluded from the analysis. The structure of the type I and II IL-4 receptor complexes are shown above data. Results presented as mean ± SEM and expressed relative MΦ. ns, not significant ($P>0.05$), *$P<0.05$, ***$P<0.001$ (1-way ANOVA followed by Tukey's post hoc test).

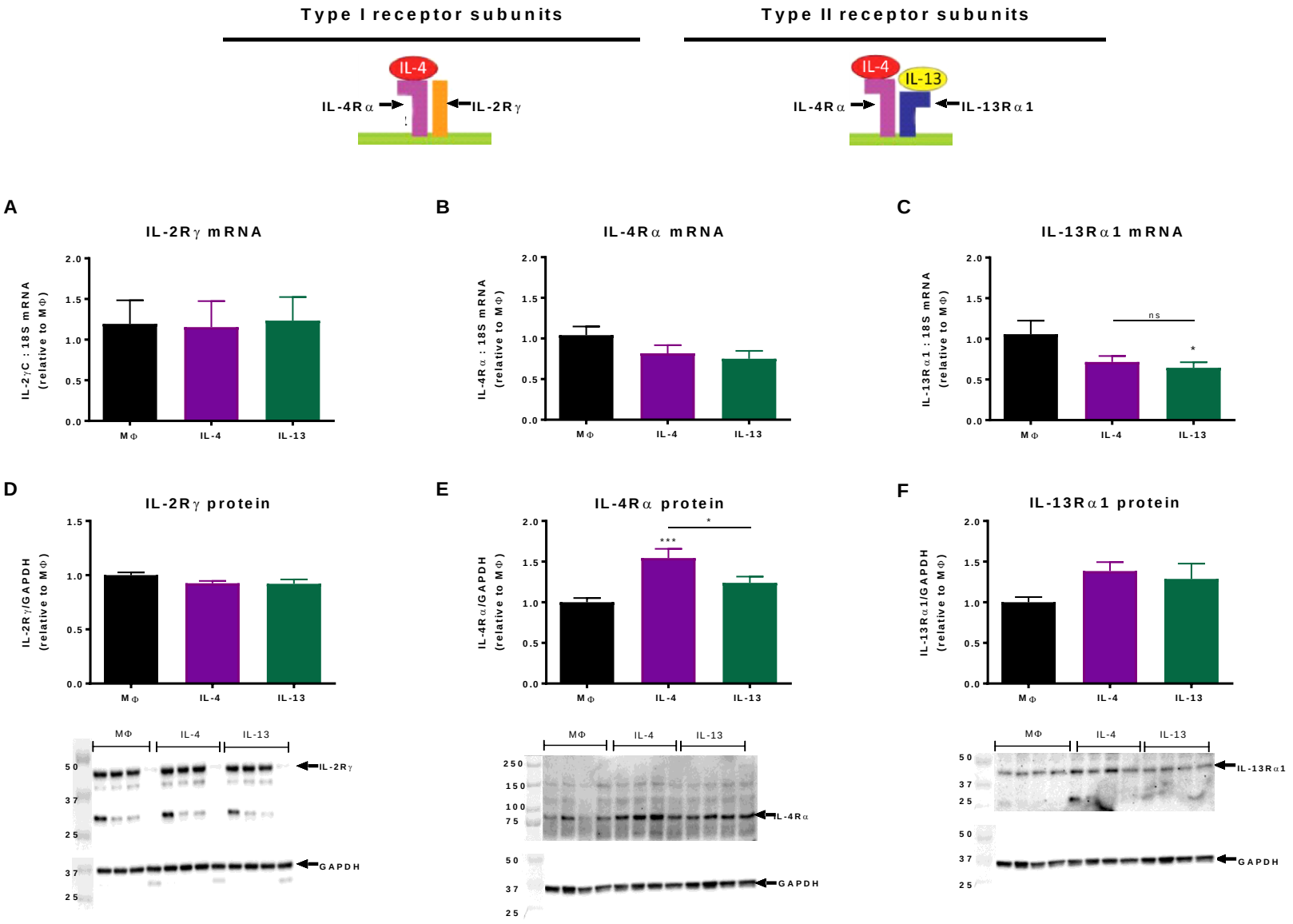
Type I receptor subunits
Type II receptor subunits
IL-4
IL-4Rα
IL-2Rγ
IL-13
IL-13Rα1
A
IL-2Rγ mRNA
IL-2γC : 18S mRNA (relative to MΦ)
B
IL-4Rα mRNA
IL-4Rα : 18S mRNA (relative to MΦ)
C
IL-13Rα1 mRNA
IL-13Rα1 : 18S mRNA (relative to MΦ)
ns
*
D
IL-2Rγ protein
IL-2Rγ/GAPDH (relative to MΦ)
E
IL-4Rα protein
IL-4Rα/GAPDH (relative to MΦ)
***
F
IL-13Rα1 protein
IL-13Rα1/GAPDH (relative to MΦ)
MΦ
IL-4
IL-13
GAPDH

Figure 2. Potency and efficacy of IL-4 and IL-13 induction of M2 marker expression in human primary macrophages M-CSF-differentiated human primary macrophages were left untreated (MΦ) or treated with either IL-4 or IL-13 for 24h. Left panel: Fold changes in mRNA expression of MRC-1 (A), CCL18 (C) and CCL22 (E) treated with 5, 25 or 50 ng/ml IL-4 or IL-13, n=6-8. Right panel: untreated (control) and concentration-dependent fold-changes in mRNA expression of MRC-1 (B), CCL18 (D), and CCL22 (F) following treatment with IL-4 or IL-13 (0.005-5 ng/ml, 24h), n=6-7. Results presented as mean ± SEM and expressed relative to the average MΦ value. *P<0.05, **P<0.01 vs MΦ (1-way ANOVA followed by Dunnett's post hoc test).

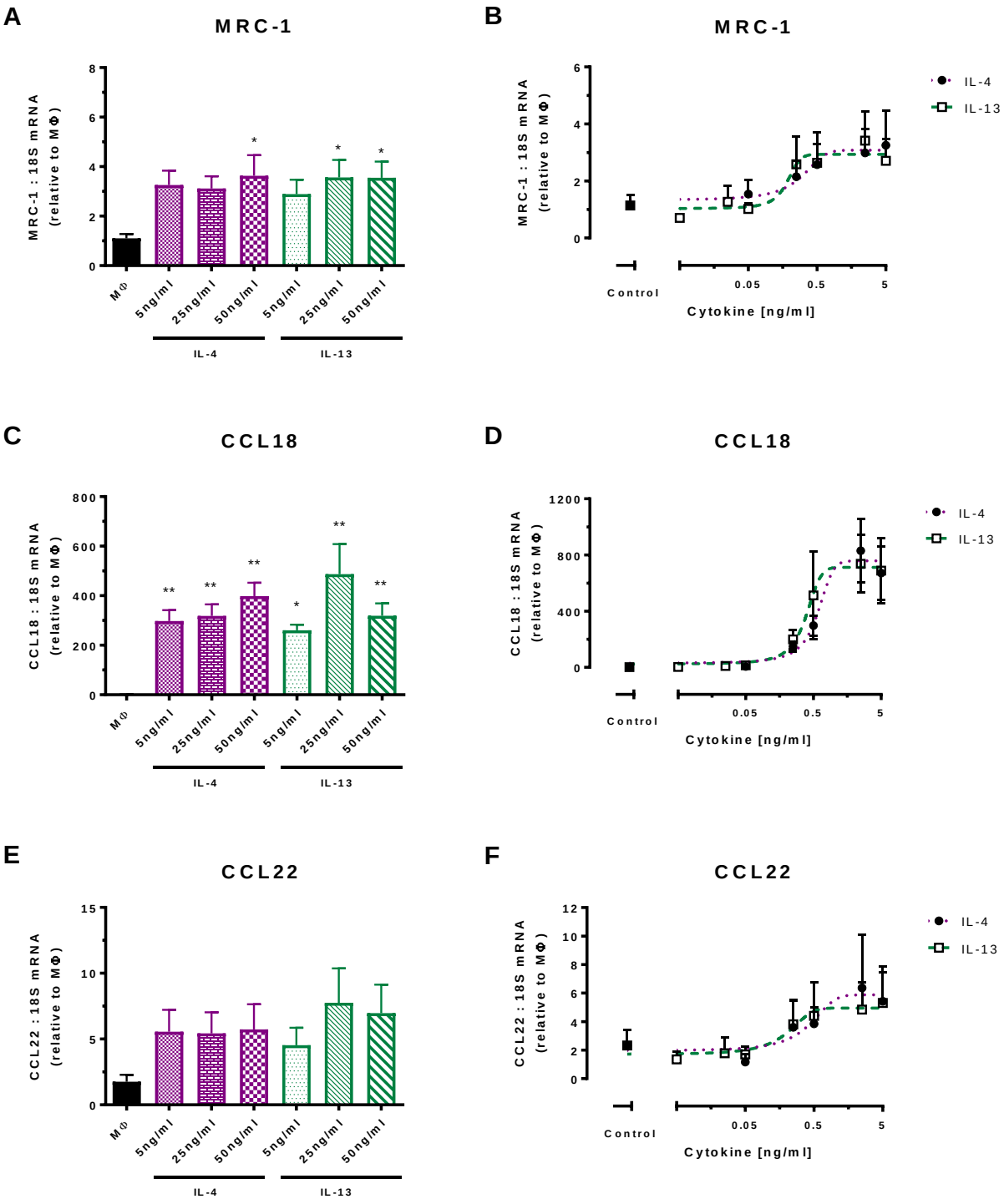
A
MRC-1
MRC-1 : 18S mRNA (relative to MΦ)
8
6
4
2
0
*
*
*
MΦ
5ng/ml
25ng/ml
50ng/ml
5ng/ml
25ng/ml
50ng/ml
IL-4
IL-13
B
MRC-1
MRC-1 : 18S mRNA (relative to MΦ)
6
4
2
0
IL-4
IL-13
Control
0.05
0.5
5
Cytokine [ng/ml]
C
CCL18
CCL18 : 18S mRNA (relative to MΦ)
800
600
400
200
0
**
**
**
*
**
**
MΦ
5ng/ml
25ng/ml
50ng/ml
5ng/ml
25ng/ml
50ng/ml
IL-4
IL-13
D
CCL18
CCL18 : 18S mRNA (relative to MΦ)
1200
800
400
0
IL-4
IL-13
Control
0.05
0.5
5
Cytokine [ng/ml]
E
CCL22
CCL22 : 18S mRNA (relative to MΦ)
15
10
5
0
MΦ
5ng/ml
25ng/ml
50ng/ml
5ng/ml
25ng/ml
50ng/ml
IL-4
IL-13
F
CCL22
CCL22 : 18S mRNA (relative to MΦ)
12
10
8
6
4
2
0
IL-4
IL-13
Control
0.05
0.5
5
Cytokine [ng/ml]

Table 2. Potency and efficacy of IL-4 and IL-13 induction of M2 marker expression in human primary macrophages.

M2 Marker	IL-4		IL-13	
	EC_{50} (ng/ml)	**Maximum** (Fold-change relative to MΦ)	**EC_{50} (ng/ml)**	**Maximum** (Fold-change relative to MΦ)
MRC-1	0.27 ± 0.41	3.3 ± 1.2	0.16 ± 0.22	3.4 ± 1
CCL18	0.83 ± 0.63	831 ± 226	0.43 ± 0.35	737 ± 207
CCL22	0.52 ± 1.04	6.4 ± 3.7	0.25 ± 0.41	5.3 ± 2.2

EC_{50} values determined based on the fitted curve for group data, n=8, mean ± SEM.

Figure 3. Effect of signal transduction inhibitors on the expression of M2 markers in human primary macrophages. Fold changes in mRNA expression of MRC-1 (A, B), CCL18 (C, D) and CCL22 (E, F) in M-CSF-differentiated human primary macrophages treated with 2.5 ng/ml IL-4 (LHS) or IL-13 (RHS) in the absence (control) or presence of inhibitors of either STAT 1 (Fludarabine, 100μM), STAT3 (Stattic, 10μM), STAT6 (AS1517499 (100nM or 1uM) or p38 MAPK (SB203580, 1μM). Signal transduction inhibitors were added 30min prior to the addition of cytokines and maintained for the 24h treatment period. Results presented as mean ± SEM and expressed relative to the average MΦ value, n= 5-8. *P<0.05, **P<0.01 vs IL-4 or IL-13 control (1-way ANOVA followed by Dunnett's post hoc test).

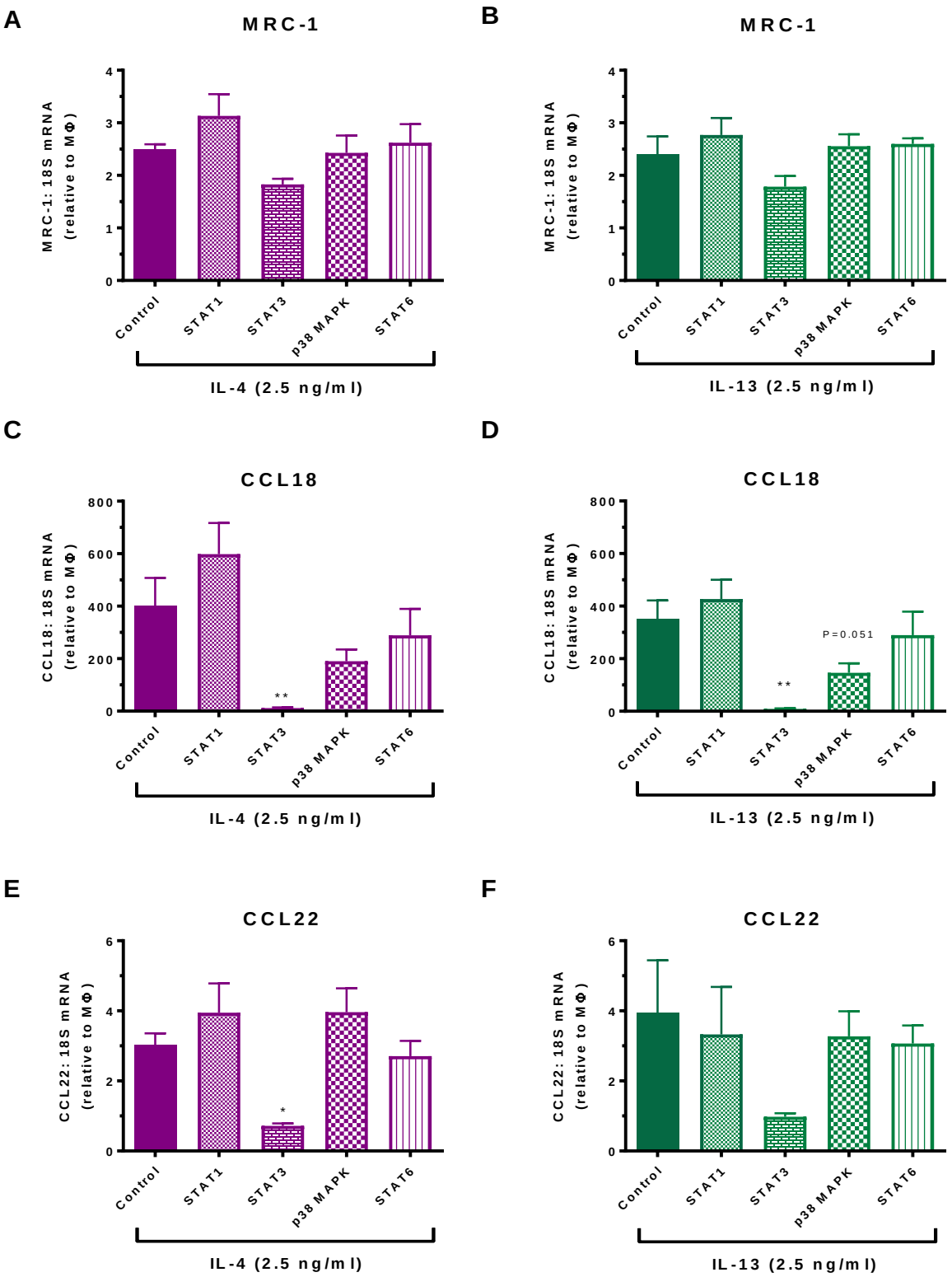
A
MRC-1
MRC-1: 18S mRNA (relative to MΦ)
Control
STAT1
STAT3
p38 MAPK
STAT6
IL-4 (2.5 ng/ml)
B
MRC-1
MRC-1: 18S mRNA (relative to MΦ)
Control
STAT1
STAT3
p38 MAPK
STAT6
IL-13 (2.5 ng/ml)
C
CCL18
CCL18: 18S mRNA (relative to MΦ)
**
Control
STAT1
STAT3
p38 MAPK
STAT6
IL-4 (2.5 ng/ml)
D
CCL18
CCL18: 18S mRNA (relative to MΦ)
P=0.051
**
Control
STAT1
STAT3
p38 MAPK
STAT6
IL-13 (2.5 ng/ml)
E
CCL22
CCL22: 18S mRNA (relative to MΦ)
*
Control
STAT1
STAT3
p38 MAPK
STAT6
IL-4 (2.5 ng/ml)
F
CCL22
CCL22: 18S mRNA (relative to MΦ)
Control
STAT1
STAT3
p38 MAPK
STAT6
IL-13 (2.5 ng/ml)

Figure 4. Effect of IL-4 and IL-13 on superoxide generation and NOX2 expression in M-CSF differentiated human primary macrophages. M-CSF-differentiated human primary macrophages were left untreated (MΦ) or treated with IL-4 or IL-13 (50 ng/ml, 24h) and superoxide levels detected by L-012-enhanced chemiluminescence. A) Average recording demonstrating initial background readings (1-30 minutes), basal superoxide as detected following L-012 (100µM) addition (31-60 minutes) and PDBu (10 µM)-stimulated superoxide generation (61-120 minutes) measured in relative light units (RLU, counts/sec). B) Peak basal (background signal subtract) and C) PDBu-stimulated (basal signal subtracted) superoxide generation. Results presented as mean ± SEM, n= 9. *P<0.05 (Repeated measures 1-way ANOVA followed by Tukey's post hoc test). mRNA (D-F) and protein (G-I) expression of NOX2, p47phox and p67phox. Representative blots, depicting n=4, are shown below each graph with GAPDH used as a loading control. Note low expression of NOX2 was observed in the fourth set of samples but was still included in the analysis. Results presented as mean ± SEM and expressed relative to MΦ, n=6-8. *P<0.05, **P<0.01 (1-way ANOVA followed by Tukey's post hoc test).

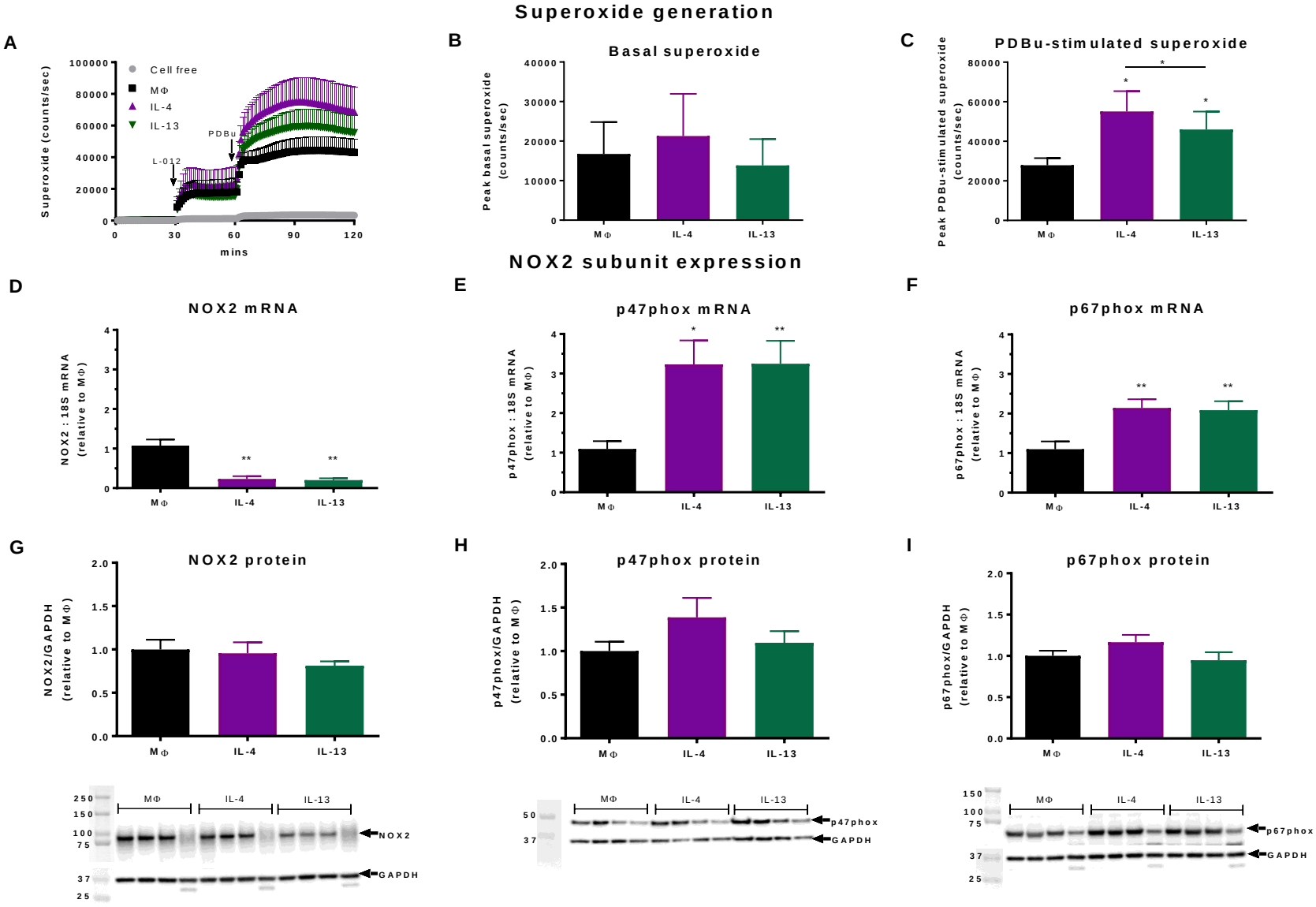
Superoxide generation
A
Superoxide (counts/sec)
Cell free
MΦ
IL-4
IL-13
PDBu
L-012
mins
B
Basal superoxide
Peak basal superoxide (counts/sec)
C
PDBu-stimulated superoxide
Peak PDBu-stimulated superoxide (counts/sec)
NOX2 subunit expression
D
NOX2 mRNA
NOX2 : 18S mRNA (relative to MΦ)
E
p47phox mRNA
p47phox : 18S mRNA (relative to MΦ)
F
p67phox mRNA
p67phox : 18S mRNA (relative to MΦ)
G
NOX2 protein
NOX2/GAPDH (relative to MΦ)
NOX2
GAPDH
H
p47phox protein
p47phox/GAPDH (relative to MΦ)
p47phox
GAPDH
I
p67phox protein
p67phox/GAPDH (relative to MΦ)
p67phox
GAPDH

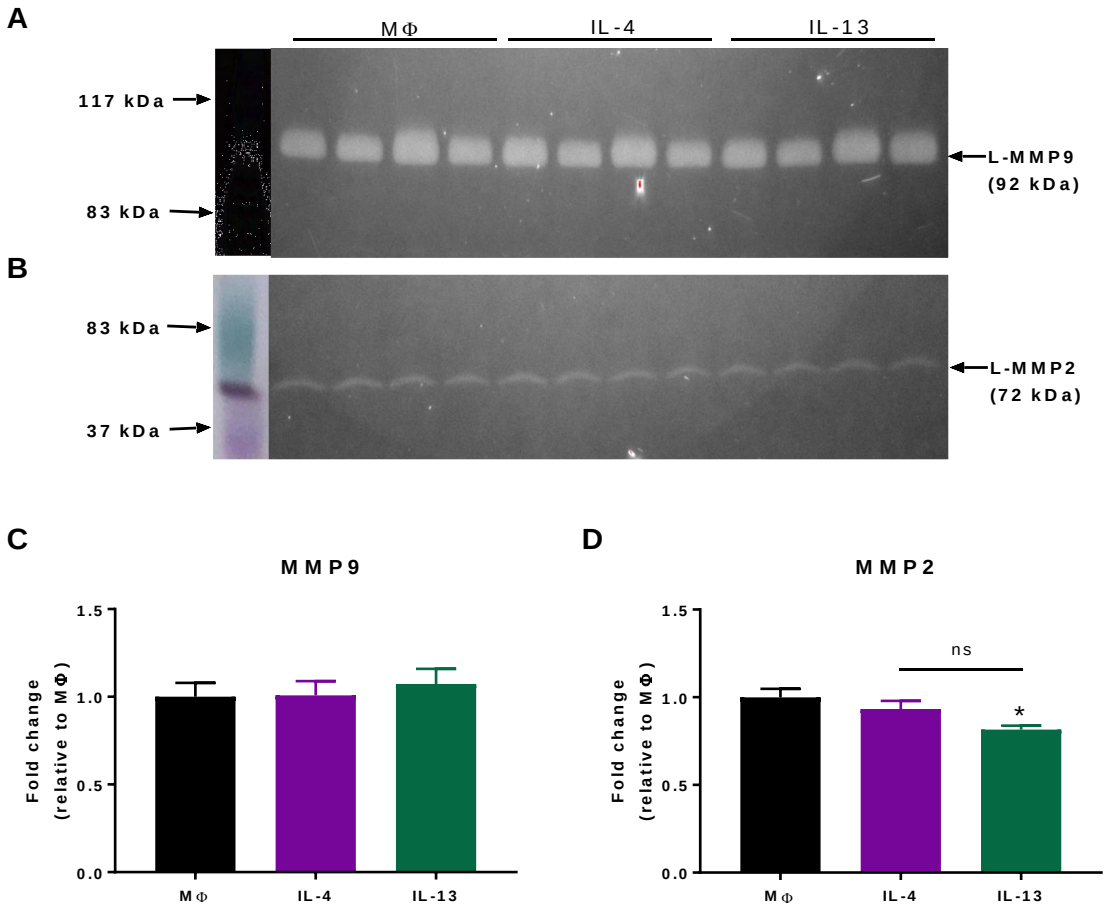

Figure 5. Effects of IL-4 or IL-13 on MMP expression in human primary macrophages. M-CSF-differentiated human primary macrophages were either untreated (MΦ) or treated with IL-4 (50ng/ml) or IL-13 (50ng/ml) for 24 hours and the culture media was collected for gelatin zymography. (A-B) Representative gel shows latent (L)-MMP9 (gelatinase B) and L-MMP2 (gelatinase A) levels for n=4. C) 10µg of total protein loaded in each well, for quantification of MMP9. D) 20µg of total protein loaded in each well, for the quantification of MMP2. All data presented as mean ± SEM, n=8. ns, not significant (P>0.05), *P<0.05, (1-way ANOVA, Tukey's post hot test).

Figure 6. Effects of M1 polarisation on type I and II IL-4 receptor expression. M-CSF-differentiated primary macrophages were left untreated (MΦ) or treated with 20 ng/ml IFN-γ and 100 ng/ml LPS (M1) or 25 ng/ml IL-4 (M2) for 24h. mRNA levels of IL-2Rγ (A), IL-4Rα (B) and IL-13Rα1 (C) were determined by RT-PCR, n=6. Protein levels of IL-2Rγ (D), IL-4Rα (E) and IL-13Rα1 (F) were determined by western blotting, n=5-6. Representative blots, depicting n=2 or 3, are shown beneath each graph with GAPDH included as a loading control. The structure of the type I and II IL-4 receptor complexes are shown above data. Results presented as mean ± SEM and expressed relative to the average MΦ value. *P<0.05, **P<0.01, ***P<0.001, (1-way ANOVA followed by Tukey's post hoc test).

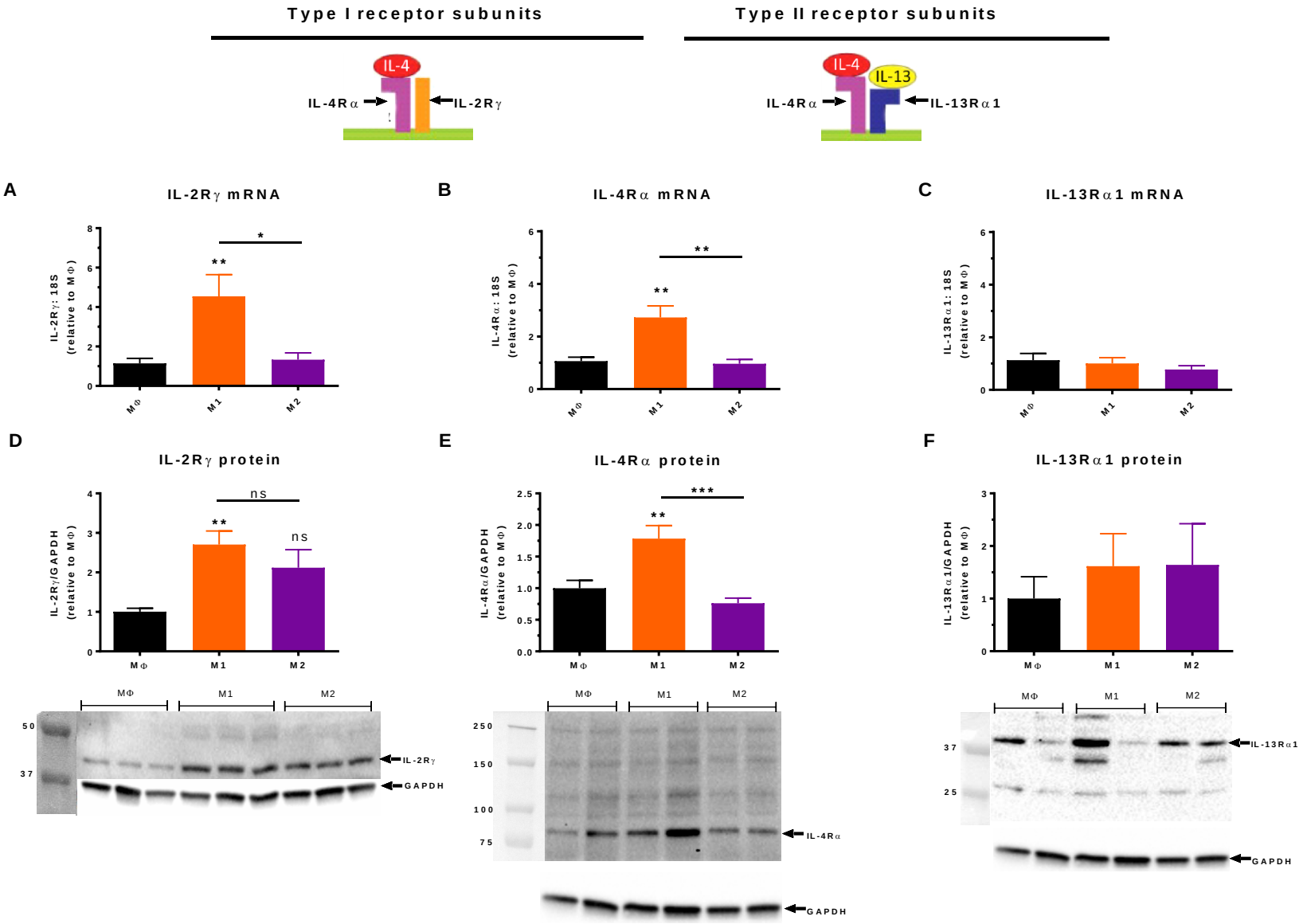
Type I receptor subunits
Type II receptor subunits
IL-4
IL-4Rα
IL-2Rγ
IL-13
IL-13Rα1
A
IL-2Rγ mRNA
IL-2Rγ: 18S (relative to MΦ)
B
IL-4Rα mRNA
IL-4Rα: 18S (relative to MΦ)
C
IL-13Rα1 mRNA
IL-13Rα1: 18S (relative to MΦ)
D
IL-2Rγ protein
IL-2Rγ/GAPDH (relative to MΦ)
E
IL-4Rα protein
IL-4Rα/GAPDH (relative to MΦ)
F
IL-13Rα1 protein
IL-13Rα1/GAPDH (relative to MΦ)
MΦ
M1
M2
ns
GAPDH

Figure 7. Effects of IL-4 or IL-13 on superoxide generation and MMP expression in M1-polarised human primary macrophages. M-CSF-differentiated human primary macrophages were polarised to the M1 phenotype for 18 hours prior to the addition of IL-4 or IL-13 (50 ng/ml) for a further 6 hours. Subsequently, superoxide and MMP levels were measured by L-012-enhanced chemiluminescnece and gelatin zymography, respectively. A) Average recording demonstrating initial background readings (1-30 minutes), basal superoxide as detected following L-012 (100 μM) addition (31-60 minutes) and PDBu(10 μM)-stimulated superoxide generation (61-120 minutes) measured in relative light units (RLU, counts/sec). B) Peak basal (background subtracted) and C) PDBu-stimulated (basal subtracted) superoxide generation. Results presented as mean ± SEM, n= 5. **P<0.01 (Repeated measures 1-way ANOVA followed by Sidak's post hoc test). Representative images of latent (L)-MMP9 (D) and L-MMP2 (E) gelatin zymography, depicting n=3, with 5 μg and 10 μg of total protein loaded in each well for quantification of MMP9 (F) and MMP2 (G), respectively, n=6. Results presented as mean ± SEM. ns, not significant, P>0.05 for all comparisons (1-way ANOVA, Dunnett's post hot test).

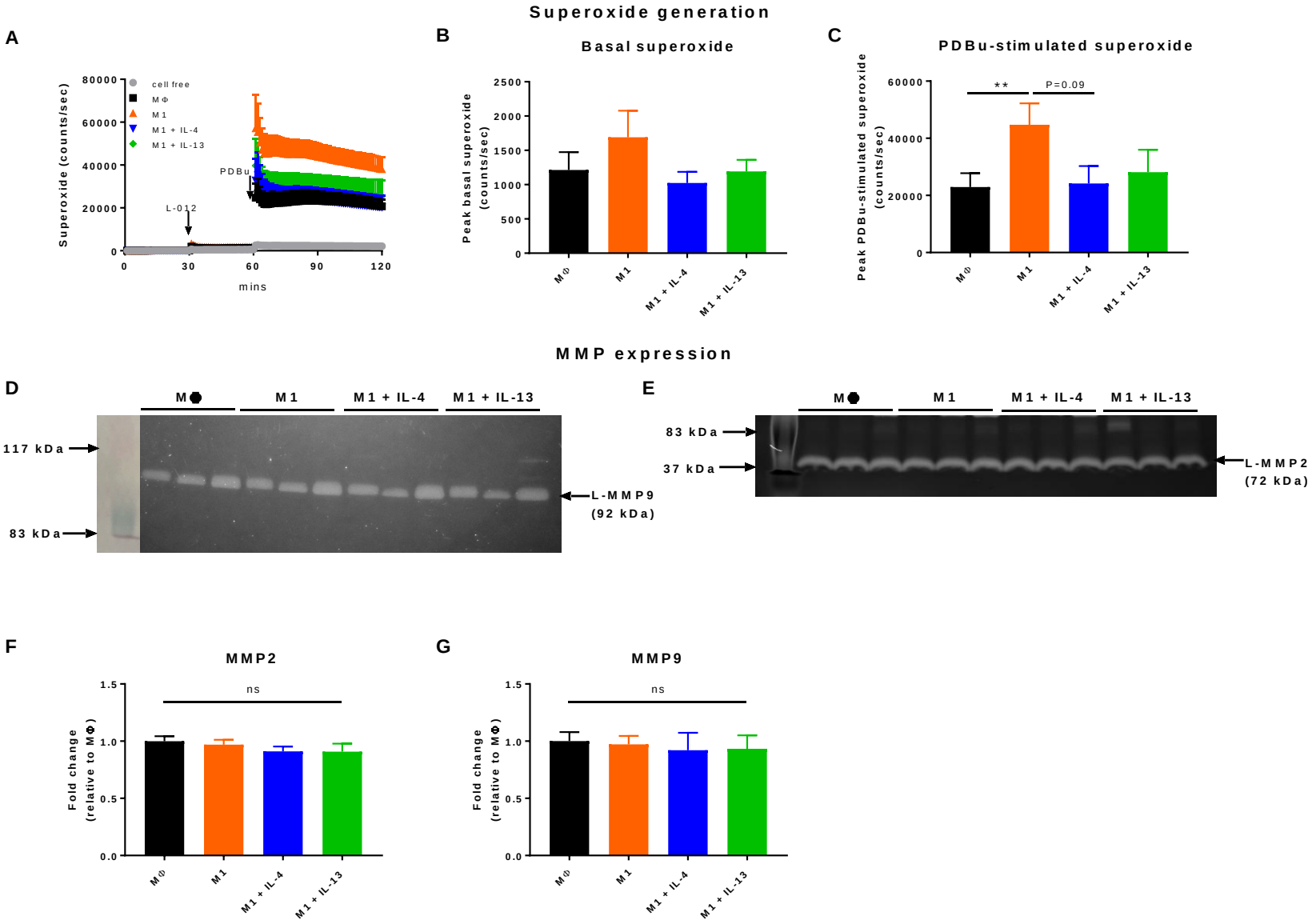
Superoxide generation
A
Superoxide (counts/sec)
cell free
MΦ
M1
M1 + IL-4
M1 + IL-13
PDBu
L-012
mins
B
Basal superoxide
Peak basal superoxide (counts/sec)
C
PDBu-stimulated superoxide
Peak PDBu-stimulated superoxide (counts/sec)
**
P=0.09
MMP expression
D
117 kDa
83 kDa
L-MMP9 (92 kDa)
E
83 kDa
37 kDa
L-MMP2 (72 kDa)
F
MMP2
Fold change (relative to MΦ)
ns
G
MMP9

Table 3. Comparison of the effects of IL-4 and IL-13 on human primary macrophage polarisation and function.

	IL-4	IL-13
Receptors	• Targets type I and type II IL-4 receptors • Upregulates IL-4Rα (subunit of both type I and type II receptors)	• Targets the type II IL-4 receptor • No effect on receptor expression
M2 polarisation	• Increases M2 marker (MRC-1, CCL18, CCL22) expression with similar efficacy and potency to IL-13 • CCL18 and CCL22 upregulation requires STAT3	• Increases M2 marker (MRC-1, CCL18, CCL22) expression with similar efficacy and potency to IL-4 • CCL18 and CCL22 upregulation requires STAT3
ROS generation	• Increases superoxide generation from M2 macrophages (efficacy increased 20% compared to IL-13)	• Increases superoxide generation from M2 macrophages (efficacy decreased 20% compared to IL-4)
MMP expression	• No effect on MMP9 or MMP2 expression	• Decreases MMP2 expression by 20%
Actions on M1 macrophages	• Attenuates increase in superoxide generation • No effect on MMP expression	• Attenuates increase in superoxide generation • No effect on MMP expression

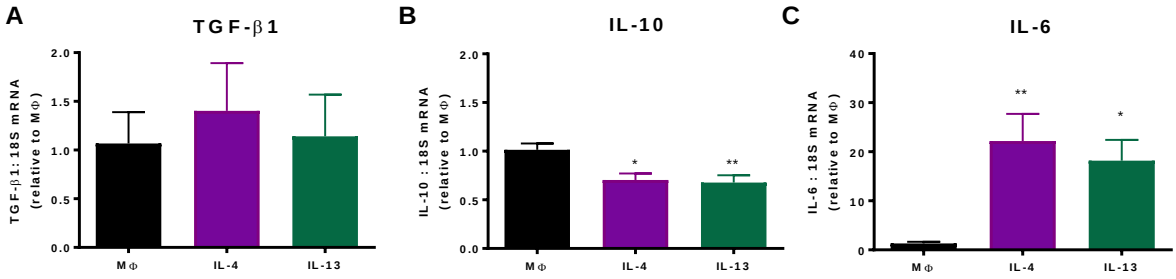

Supplementary Figure 1. Effect of IL-4 and IL-13 on mRNA expression of additional cytokines. M-CSF-differentiated primary macrophages were left untreated (MΦ) or treated with 50 ng/ml IL-4 or IL-13 for 24h. mRNA levels of TGF-β1 (A), IL-10 (B) and IL-6 (C) were determined by RT-PCR, n=5-8. Results presented as mean ± SEM and expressed relative to the average MΦ value. **P<0.01, *P<0.05 (1-way ANOVA followed by Tukey's post hoc test).

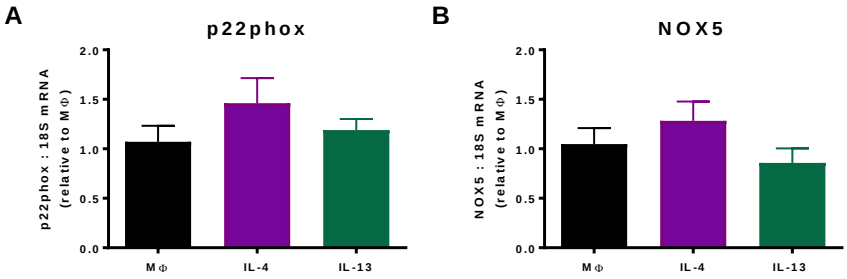

Supplementary Figure 2. Effect of IL-4 and IL-13 on mRNA expression of additional NOX isoforms and subunits. M-CSF-differentiated primary macrophages were left untreated (MΦ) or treated with 50 ng/ml IL-4 or IL-13 for 24h. mRNA levels of p22phox (A), NOX5 (B), NOX1 and NOX4 were determined by RT-PCR, n=5-8. NOX1 and NOX4 isoforms were not detected in any treatment group (Ct value = >40). Results presented as mean ± SEM and expressed relative to the average MΦ value.

Discussion

As closely related Th2 cytokines which can act through a shared receptor, IL-4 and IL-13 are together implicated in allergic inflammation and fibrotic diseases (44). Interestingly, an opposing role for these cytokines in the development of atherosclerosis is evident with pathological and protective properties demonstrated *in vivo* for IL-4 (12, 33) and IL-13 (5, 9), respectively. Given that macrophages are one of just a few cell types reported to express both the type I (activated by IL-4) and type II (activated by IL-4 or IL-13) IL-4 receptors (28), we investigated whether these differential roles in atherosclerosis may be through distinct effects on macrophage function. Despite confirming the expression of both type I and type II IL-4 receptors in primary human macrophages, we found that IL-4 and IL-13 exhibited equivalent potency for the induction of M2 marker expression and only subtle differences in the generation of ROS and MMPs. These small changes are unlikely to explain such contrasting roles in atherosclerosis.

Whilst expression and activity of both the type I and type II IL-4 receptors has been reported in human peripheral blood monocytes (4, 20, 28), there has been limited assessment of their expression following differentiation to macrophages. Here we show clearly that human macrophages express both the type I and II IL-4 receptors at equivalent levels, but lack expression of the decoy receptor, IL-13Rα2, findings which are consistent with those in human peripheral blood monocytes (28). Furthermore, signalling through both receptors has been demonstrated in mouse bone marrow derived macrophages (BMDMs) differentiated with M-CSF (28, 53). Although expression of both IL-2Rγ (type I receptor subunit) and IL-13Rα1 (type II receptor subunit) *per se* may decrease when monocytes are differentiated to macrophages with M-CSF (6, 20), the body of literature showing that IL-4 and IL-13 treatment

of differentiated macrophages induces M2 polarisation (23, 43, 46) provides evidence of functional receptor expression. We were also able to demonstrate protein expression of each subunit via western blotting. Although we did not investigate cell surface expression, as could be assessed via flow cytometry in future studies to confirm functionality of receptors, our findings suggest that both receptors are expressed on human primary macrophages.

Previous investigations have shown enhanced potency of IL-4, as compared to IL-13, to promote STAT6 phosphorylation and increase M2 marker expression in murine macrophages (28, 53) and human monocytes (28), attributed to signalling through the type I receptor (53). Therefore we predicted that IL-4 would more potently induce M2 polarisation in human primary macrophages. However, we demonstrated equivalent potency and efficacy for upregulation of the well-established M2 marker, MRC-1 (also known as CD206) (43, 54, 57), as well as two more recently identified human M2 markers, CCL18 (43, 56) and CCL22 (25, 55). Given the type II IL-4 receptor is common to both cytokines, our observations suggest that signalling to induce M2 polarisation in human primary macrophages is predominantly via this receptor. It is possible that human macrophages lack, or have low cell surface expression of, the type I receptor and future investigations with siRNA to knockdown each receptor would be required to confirm this.

The use of signalling inhibitors revealed STAT3 activity was required for increased CCL18 and CCL22 expression in response to both IL-4 and IL-13, with no clear effects of inhibiting STAT1 or, surprisingly, STAT6. Indeed the role for STAT3 signalling through the shared type I and type II receptor subunit, IL-4Rα, is supported by previous studies in human monocytes (3, 4). However, STAT6 involvement in IL-4 and IL-13 signalling pathways is well recognised and is considered a central M2 transcription factor (44, 45, 63). While many studies demonstrate

the induction of STAT6 phosphorylation in monocytes and macrophages by both cytokines (4, 28, 53), only one study has investigated the impact of its inhibition in monocytes *in vitro.* Here the authors utilised decoy oligonucleotides (ODNs) for STAT6, to prevent its binding to target genes, and observed a reduced ability of IL-4 and IL-13 to elevate several M2 markers (4). The lack of effect of STAT6 inhibition observed in our study could reflect redundancy for STAT6 in human macrophages, but more likely demonstrates the difficulty in inhibiting IL-4 and IL-13 recruitment of STAT6 due to such high levels of STAT6 expression and phosphorylation in these cells (53). Future studies should investigate the potency and efficacy of the inhibitor we have utilised, by assessing its effects on IL-4- and IL-13-induced STAT6 phosphorylation. Alternatively, a similar strategy with decoy ODNs could be adopted to ensure lack of STAT6 activity. Furthermore, a potential limitation of this study was that it lacked any confirmation experiments to validate the chosen signalling inhibitors. Hence we have assumed that signalling via STAT1, STAT3, p38 MAPK and STAT6 pathways were effectively attenuated following these treatments. It will be important for future studies to perform these experiments to assess the efficacy of these compounds in our macrophage culture. Nonetheless, having established equivalent effects of the two cytokines on M2 polarisation, we then wanted to characterise their effects on ROS and MMP production; two mediators that would be detrimental in the setting of atherosclerosis.

NOX2 oxidase is the major source of ROS in macrophages (7) and although more commonly associated with M1 macrophage function, its activity is also observed in alternatively activated macrophages (34) (Chapter 4). Although not investigated in this study, IL-4 signalling is associated with p38 MAPK and CREB activation, both with the capacity to regulate ROS (16, 26, 27, 51). We hypothesised that NOX2-derived ROS may be involved in the pro-atherogenic

actions of M2 macrophages polarised with IL-4, but not IL-13. We found that while both cytokines increased PDBu-stimulated superoxide production, as compared to untreated macrophages, IL-4 treatment resulted in approximately 20% greater superoxide generation than IL-13. Somewhat surprisingly however, both cytokines regulated NOX2 gene expression identically, reducing the expression of the NOX2 catalytic subunit while increasing both p47phox and p67phox. Although such changes were not detected at the protein level, there is evidence to suggest that the up-regulation of both p47phox and p67phox could occur via STAT3 (42). The mechanisms underlying the ability of IL-4 to increase superoxide to a slightly greater extent than IL-13 are unclear, but may be related to additional targeting of the type I receptor. Nevertheless, it is unlikely that such a small difference in ROS production could account for the differential roles of IL-4 and IL-13 observed in atherosclerosis.

In addition to ROS, we assessed the potential for IL-4 and IL-13 to regulate MMP production. Both MMP9 and MMP2 are gelatinase enzymes which target basement membrane collagen (collagen IV) as well as denatured collagens (39). Due to their involvement in degrading the extracellular matrix, MMPs are thought to promote plaque destabilisation. Indeed both MMP9 and MMP2 have been identified in atherosclerotic plaques and implicated in atherogenesis, MMP9 being more predominant in macrophages (1, 39, 47). MMP9, in particular, is identified as a marker of vulnerable plaques (48) and major cardiovascular events (10, 49). We identified expression of both MMP9 and MMP2 in primary macrophage culture supernatants via gelatin zymography. Whilst we did not detect any differences in MMP9 levels between untreated and IL-4- or IL-13-treated macrophages we did observe a 20% decrease in MMP2 expression with IL-13 treatment. Our observation of unchanged MMP9 levels following IL-4 treatment is in agreement with a previous study in human M-CSF-differentiated

macrophages (60). By contrast, other investigators have reported IL-4-mediated upregulation of MMP-9 in both mouse and human macrophages (29, 40), and downregulation in human alveolar (35) and M-CSF-differentiated macrophages (50). It is also possible that IL-4 and IL-13 may enhance, or reduce, MMP9 activity without affecting MMP9 expression levels, namely via regulation of the expression of the MMP9 inhibitor, tissue inhibitor of metalloproteinase-1 (TIMP-1) (50, 60). This hypothesis remains to be investigated. Unchanged MMP2 expression following IL-4 treatment is consistent with the literature (29, 40), however to our knowledge this is the first investigation of the effect of IL-13 on macrophage MMP2 levels. Although reduced MMP2 activity could be beneficial in the setting of atherosclerosis, as with the moderately reduced ROS signal, this is unlikely to explain the atheroprotective effects of IL-13.

It is important to note that, in contrast to our controlled *in vitro* experiments, the microenvironment within atherosclerotic plaques and the *in vivo* environment *per se* are highly complex. Whilst we didn't observe any major differences between IL-4 and IL-13 stimulated macrophages in our experiments, the potential for interaction with other stimuli or targets remain. For example, although macrophages don't constitutively express IL-13Rα2, an environment in which both Th1 and Th2 cytokines are present could induce its expression (2, 15). Cell surface IL-13Rα2 binds IL-13 with extremely high affinity (41) and has been shown to initiate its own signalling pathways, which could be observed in macrophages under inflammatory conditions (8, 15, 21). In THP-1 macrophages, TNFα treatment, in combination with IL-13 or IL-4, was shown to induce IL-13Rα2 and subsequently stimulate TGF-β1 expression and lung fibrosis following activation with IL-13 (15). Importantly this pathway of IL-13-IL-13Rα2-TGF-β1-mediated fibrosis was also observed in a recent study of allograft

fibrosis (8). Hence some of the protective effects of IL-13 in atherosclerosis could be mediated by enhanced TGF-β1 expression, through the IL-13Rα2 receptor, which would increase collagen deposition and have plaque-stabilising effects. This is an area which warrants further investigation.

Another potential point of difference between IL-4 and IL-13 is in their actions on M1 macrophages. Interestingly, we found that M1 macrophages have increased expression of both the IL-4Rα and IL-2Rγ subunits of the type I receptor, suggesting potential for additional, or more potent, effects of IL-4, as compared with IL-13, on these cells. LPS-stimulated increases in IL-2Rγ (24) and IL-4Rα (14) have previously been reported on monocytes and microglia, respectively. Importantly however, this is the first demonstration of enhanced type I IL-4 receptor expression on M1 macrophages and could have implications in a range of inflammatory diseases. However, both IL-4 and IL-13 prevented the increase in PDBu-stimulated superoxide production from M1 macrophages and therefore these Th2 cytokines may serve to attenuate the damaging effects of M1 macrophage-derived ROS in atherosclerosis. Additionally, IL-4 and IL-13 each had no effect on M1 macrophage MMP production, again demonstrating a strong similarity in their actions on macrophages. Whilst modulation of M1 macrophage-derived ROS and MMP generation by these cytokines did not differ, this does not preclude differential actions on other M1 functions not investigated in this study, such as pro-inflammatory cytokine release.

A lack of differential actions on macrophages suggests that the opposing roles of IL-4 and IL-13 in atherosclerosis may be through their effects on other cell types. Although closely related, IL-4 and IL-13 are recognised as playing predominant roles in immunoregulatory and effector functions, respectively, as the type I receptor is only expressed on immune cells (13,

19, 31). As such, IL-4 may more potently induce type II inflammation whist IL-13 is more strongly implicated in fibrosis and TGF-β1 signalling through its actions on non-immune cells (36). IL-13 may therefore have more potent effects on vascular cells that could promote plaque stabilisation. By contrast IL-4 may favour inflammatory responses as it has been shown to promote oxidative stress and adhesion molecule expression in endothelial cells which would contribute to atherogenesis (37, 38). Alternatively, the pro- and anti-atherogenic properties of IL-4 and IL-13 reported in the literature (9, 33) may have arisen due to differences in the experimental design of the investigations. Thus, to date, no study has directly compared the effects of IL-13 and IL-4 deficiency, or treatment, in the same cohort of atherosclerotic animals. Such an approach in addition to comparing the effects of IL-4 and IL-13 on vascular cells, is required to provide definitive evidence for differential effects of these cytokines in atherosclerosis.

In conclusion, we have confirmed the expression of both the type I and type II IL-4 receptor on primary human macrophages but observed no substantial differences in the effects of IL-4 and IL-13 on macrophage function, in the context of polarisation, superoxide generation or MMP expression. Although IL-13 treatment was associated with modestly less superoxide generation than IL-4 treatment, and reduced MMP2 expression as compared with unpolarised macrophages, these subtle differences are unlikely to have a major physiological impact that would explain opposing roles in atherosclerosis. Although, we identified a potential mechanism by which IL-4 could have additional actions on M1 macrophages, its regulation of M1 macrophage ROS and MMP production was identical to that for IL-13. Taken together, our findings suggest that the potentially opposing roles of IL-4 and IL-13 in atherosclerosis are not through direct actions on macrophages, rather they may reflect

differential modulation of other cell types, such as endothelial or vascular smooth muscle cells. Future studies should focus on a direct comparison of IL-4 and IL-13 in the context of atherosclerosis to validate the therapeutic potential of targeting one cytokine over the other.

References

1. Albini PT, Segura AM, Liu G, Minard CG, Coselli JS, Milewicz DM, Shen YH, and LeMaire SA. Advanced atherosclerosis is associated with increased medial degeneration in sporadic ascending aortic aneurysms. *Atherosclerosis* 232: 361-368, 2014.

2. Badalyan V, Thompson R, Addo K, Borthwick LA, Fisher AJ, Ort T, Myers TG, Wynn TA, and Ramalingam TR. TNF-alpha/IL-17 synergy inhibits IL-13 bioactivity via IL-13Ralpha2 induction. *The Journal of allergy and clinical immunology* 134: 975-978.e975, 2014.

3. Bhattacharjee A, Pal S, Feldman GM, and Cathcart MK. Hck is a key regulator of gene expression in alternatively activated human monocytes. *J Biol Chem* 286: 36709-36723, 2011.

4. Bhattacharjee A, Shukla M, Yakubenko VP, Mulya A, Kundu S, and Cathcart MK. IL-4 and IL-13 employ discrete signaling pathways for target gene expression in alternatively activated monocytes/macrophages. *Free radical biology & medicine* 54: 1-16, 2013.

5. Binder CJ, Hartvigsen K, Chang MK, Miller M, Broide D, Palinski W, Curtiss LK, Corr M, and Witztum JL. IL-5 links adaptive and natural immunity specific for epitopes of oxidized LDL and protects from atherosclerosis. *J Clin Invest* 114: 427-437, 2004.

6. Bonder CS, Dickensheets HL, Finlay-Jones JJ, Donnelly RP, and Hart PH. Involvement of the IL-2 receptor gamma-chain (gammac) in the control by IL-4 of human monocyte and macrophage proinflammatory mediator production. *J Immunol* 160: 4048-4056, 1998.

7. Brune B, Dehne N, Grossmann N, Jung M, Namgaladze D, Schmid T, von Knethen A, and Weigert A. Redox control of inflammation in macrophages. *Antioxidants & redox signaling* 19: 595-637, 2013.

8. Brunner SM, Schiechl G, Kesselring R, Martin M, Balam S, Schlitt HJ, Geissler EK, and Fichtner-Feigl S. IL-13 signaling via IL-13Ralpha2 triggers TGF-beta1-dependent allograft fibrosis. *Transplantation research* 2: 16, 2013.

9. Cardilo-Reis L, Gruber S, Schreier SM, Drechsler M, Papac-Milicevic N, Weber C, Wagner O, Stangl H, Soehnlein O, and Binder CJ. Interleukin-13 protects from atherosclerosis and modulates plaque composition by skewing the macrophage phenotype. *EMBO molecular medicine* 4: 1072-1086, 2012.

10. Chan CP, Jiang HL, Leung LY, Wan WM, Cheng NM, Ip WS, Cheung KY, Chan RW, Wong LK, Graham CA, Renneberg R, and Rainer TH. Multiple atherosclerosis-related biomarkers associated with short- and long-term mortality after stroke. *Clinical biochemistry* 45: 1308-1315, 2012.

11. Chow BS, Chew EG, Zhao C, Bathgate RA, Hewitson TD, and Samuel CS. Relaxin signals through a RXFP1-pERK-nNOS-NO-cGMP-dependent pathway to up-regulate matrix metalloproteinases: the additional involvement of iNOS. *PLoS One* 7: e42714, 2012.

12. Davenport P, and Tipping PG. The role of interleukin-4 and interleukin-12 in the progression of atherosclerosis in apolipoprotein E-deficient mice. *The American journal of pathology* 163: 1117-1125, 2003.

13. Fallon PG, Richardson EJ, McKenzie GJ, and McKenzie AN. Schistosome infection of transgenic mice defines distinct and contrasting pathogenic roles for IL-4 and IL-13: IL-13 is a profibrotic agent. *J Immunol* 164: 2585-2591, 2000.

14. Fenn AM, Henry CJ, Huang Y, Dugan A, and Godbout JP. Lipopolysaccharide-induced interleukin (IL)-4 receptor-alpha expression and corresponding sensitivity to the M2

promoting effects of IL-4 are impaired in microglia of aged mice. *Brain, behavior, and immunity* 26: 766-777, 2012.

15. Fichtner-Feigl S, Strober W, Kawakami K, Puri RK, and Kitani A. IL-13 signaling through the IL-13alpha2 receptor is involved in induction of TGF-beta1 production and fibrosis. *Nat Med* 12: 99-106, 2006.

16. Fu X, Beer DG, Behar J, Wands J, Lambeth D, and Cao W. cAMP-response element-binding protein mediates acid-induced NADPH oxidase NOX5-S expression in Barrett esophageal adenocarcinoma cells. *Journal of Biological Chemistry* 281: 20368-20382, 2006.

17. George J, Shoenfeld Y, Gilburd B, Afek A, Shaish A, and Harats D. Requisite role for interleukin-4 in the acceleration of fatty streaks induced by heat shock protein 65 or Mycobacterium tuberculosis. *Circ Res* 86: 1203-1210, 2000.

18. Gordon S, and Martinez FO. Alternative Activation of Macrophages: Mechanism and Functions. *Immunity* 32: 593-604, 2010.

19. Grunig G, Warnock M, Wakil AE, Venkayya R, Brombacher F, Rennick DM, Sheppard D, Mohrs M, Donaldson DD, Locksley RM, and Corry DB. Requirement for IL-13 independently of IL-4 in experimental asthma. *Science* 282: 2261-2263, 1998.

20. Hart PH, Bonder CS, Balogh J, Dickensheets HL, Vazquez N, Davies KV, Finlay-Jones JJ, and Donnelly RP. Diminished responses to IL-13 by human monocytes differentiated in vitro: role of the IL-13Ralpha1 chain and STAT6. *Eur J Immunol* 29: 2087-2097, 1999.

21. He CH, Lee CG, Dela Cruz CS, Lee CM, Zhou Y, Ahangari F, Ma B, Herzog EL, Rosenberg SA, Li Y, Nour AM, Parikh CR, Schmidt I, Modis Y, Cantley L, and Elias JA. Chitinase 3-like 1 regulates cellular and tissue responses via IL-13 receptor alpha2. *Cell reports* 4: 830-841, 2013.

22. Heller NM, Qi X, Junttila IS, Shirey KA, Vogel SN, Paul WE, and Keegan AD. Type I IL-4Rs Selectively Activate IRS-2 to Induce Target Gene Expression in Macrophages. *Science Signaling* 1: 2008.

23. Isa SA, Ruffino JS, Ahluwalia M, Thomas AW, Morris K, and Webb R. M2 macrophages exhibit higher sensitivity to oxLDL-induced lipotoxicity than other monocyte/macrophage subtypes. *Lipids in Health and Disease* 10: 2011.

24. Ishii N, Takeshita T, Kimura Y, Tada K, Kondo M, Nakamura M, and Sugamura K. Expression of the IL-2 receptor gamma chain on various populations in human peripheral blood. *Int Immunol* 6: 1273-1277, 1994.

25. Jaguin M, Houlbert N, Fardel O, and Lecureur V. Polarization profiles of human M-CSF-generated macrophages and comparison of M1-markers in classically activated macrophages from GM-CSF and M-CSF origin. *Cell Immunol* 281: 51-61, 2013.

26. Jang YS, Kim HA, Park SR, Lee MR, Park JB, and Kim PH. IL-4 stimulates mouse macrophages to express APRIL through p38MAPK and two different downstream molecules, CREB and Stat6. *Cytokine* 47: 43-47, 2009.

27. Jimenez-Garcia L, Herranz S, Luque A, and Hortelano S. Critical role of p38 MAPK in IL-4-induced alternative activation of peritoneal macrophages. *Eur J Immunol* 45: 273-286, 2015.

28. Junttila IS, Mizukami K, Dickensheets H, Meier-Schellersheim M, Yamane H, Donnelly RP, and Paul WE. Tuning sensitivity to IL-4 and IL-13: differential expression of IL-4Ralpha, IL-13Ralpha1, and gammac regulates relative cytokine sensitivity. *J Exp Med* 205: 2595-2608, 2008.

29. Khabbazi S, Goumon Y, and Parat MO. Morphine Modulates Interleukin-4- or Breast Cancer Cell-induced Pro-metastatic Activation of Macrophages. *Scientific reports* 5: 11389, 2015.

30. Khallou-Laschet J, Varthaman A, Fornasa G, Compain C, Gaston A-T, Clement M, Dussiot M, Levillain O, Graff-Dubois S, Nicoletti A, and Caligiuri G. Macrophage plasticity in experimental atherosclerosis. *PLoS ONE [Electronic Resource]* 5: e8852, 2010.

31. King IL, and Mohrs M. IL-4-producing CD4+ T cells in reactive lymph nodes during helminth infection are T follicular helper cells. *J Exp Med* 206: 1001-1007, 2009.

32. King VL, Cassis LA, and Daugherty A. Interleukin-4 does not influence development of hypercholesterolemia or angiotensin II-induced atherosclerotic lesions in mice. *The American journal of pathology* 171: 2040-2047, 2007.

33. King VL, Szilvassy SJ, and Daugherty A. Interleukin-4 deficiency decreases atherosclerotic lesion formation in a site-specific manner in female LDL receptor-/- mice. *Arterioscler Thromb Vasc Biol* 22: 456-461, 2002.

34. Kraaij MD, Koekkoek KM, van der Kooij SW, Gelderman KA, and van Kooten C. Subsets of human type 2 macrophages show differential capacity to produce reactive oxygen species. *Cell Immunol* 284: 1-8, 2013.

35. Lacraz S, Nicod L, Galve-de Rochemonteix B, Baumberger C, Dayer JM, and Welgus HG. Suppression of metalloproteinase biosynthesis in human alveolar macrophages by interleukin-4. *J Clin Invest* 90: 382-388, 1992.

36. Lee CG, Homer RJ, Zhu Z, Lanone S, Wang X, Koteliansky V, Shipley JM, Gotwals P, Noble P, Chen Q, Senior RM, and Elias JA. Interleukin-13 induces tissue fibrosis by selectively stimulating and activating transforming growth factor beta(1). *J Exp Med* 194: 809-821, 2001.

37. Lee YW, Kim PH, Lee WH, and Hirani AA. Interleukin-4, Oxidative Stress, Vascular Inflammation and Atherosclerosis. *Biomolecules & therapeutics* 18: 135-144, 2010.

38. Lee YW, Kuhn H, Hennig B, Neish AS, and Toborek M. IL-4-induced oxidative stress upregulates VCAM-1 gene expression in human endothelial cells. *Journal of molecular and cellular cardiology* 33: 83-94, 2001.

39. Lin J, Kakkar V, and Lu X. Impact of matrix metalloproteinases on atherosclerosis. *Curr Drug Targets* 15: 442-453, 2014.

40. Lolmede K, Campana L, Vezzoli M, Bosurgi L, Tonlorenzi R, Clementi E, Bianchi ME, Cossu G, Manfredi AA, Brunelli S, and Rovere-Querini P. Inflammatory and alternatively activated human macrophages attract vessel-associated stem cells, relying on separate HMGB1- and MMP-9-dependent pathways. *J Leukoc Biol* 85: 779-787, 2009.

41. Lupardus PJ, Birnbaum ME, and Garcia KC. Molecular basis for shared cytokine recognition revealed in the structure of an unusually high affinity complex between IL-13 and IL-13Ralpha2. *Structure (London, England : 1993)* 18: 332-342, 2010.

42. Manea A, Tanase LI, Raicu M, and Simionescu M. Jak/STAT signaling pathway regulates nox1 and nox4-based NADPH oxidase in human aortic smooth muscle cells. *Arterioscler Thromb Vasc Biol* 30: 105-112, 2010.

43. Martinez FO, Gordon S, Locati M, and Mantovani A. Transcriptional profiling of the human monocyte-to-macrophage differentiation and polarization: New molecules and patterns of gene expression. *Journal of Immunology* 177: 7303-7311, 2006.

44. McCormick SM, and Heller NM. Commentary: IL-4 and IL-13 receptors and signaling. *Cytokine* 75: 38-50, 2015.

45. Mishra BB, Gundra UM, and Teale JM. STAT6-/- mice exhibit decreased cells with alternatively activated macrophage phenotypes and enhanced disease severity in murine neurocysticercosis. *Journal of Neuroimmunology* 232: 26-34.

46. Murray PJ, Allen JE, Biswas SK, Fisher EA, Gilroy DW, Goerdt S, Gordon S, Hamilton JA, Ivashkiv LB, Lawrence T, Locati M, Mantovani A, Martinez FO, Mege JL, Mosser DM, Natoli G, Saeij JP, Schultze JL, Shirey KA, Sica A, Suttles J, Udalova I, van Ginderachter JA, Vogel SN, and Wynn TA. Macrophage activation and polarization: nomenclature and experimental guidelines. *Immunity* 41: 14-20, 2014.

47. Newby AC. Metalloproteinase expression in monocytes and macrophages and its relationship to atherosclerotic plaque instability. *Arterioscler Thromb Vasc Biol* 28: 2108-2114, 2008.

48. Papaspyridonos M, Smith A, Burnand KG, Taylor P, Padayachee S, Suckling KE, James CH, Greaves DR, and Patel L. Novel candidate genes in unstable areas of human atherosclerotic plaques. *Arterioscler Thromb Vasc Biol* 26: 1837-1844, 2006.

49. Ramos-Fernandez M, Bellolio MF, and Stead LG. Matrix metalloproteinase-9 as a marker for acute ischemic stroke: a systematic review. *Journal of stroke and cerebrovascular diseases : the official journal of National Stroke Association* 20: 47-54, 2011.

50. Roma-Lavisse C, Tagzirt M, Zawadzki C, Lorenzi R, Vincentelli A, Haulon S, Juthier F, Rauch A, Corseaux D, Staels B, Jude B, Van Belle E, Susen S, Chinetti-Gbaguidi G, and Dupont A. M1 and M2 macrophage proteolytic and angiogenic profile analysis in atherosclerotic patients reveals a distinctive profile in type 2 diabetes. *Diabetes & vascular disease research* 12: 279-289, 2015.

51. Schenten V, Melchior C, Steinckwich N, Tschirhart EJ, and Brechard S. Sphingosine kinases regulate NOX2 activity via p38 MAPK-dependent translocation of S100A8/A9. *J Leukoc Biol* 89: 587-596, 2011.

52. Schmittgen TD, and Livak KJ. Analyzing real-time PCR data by the comparative C-T method. *Nature Protocols* 3: 1101-1108, 2008.

53. Sheikh F, Dickensheets H, Pedras-Vasconcelos J, Ramalingam T, Helming L, Gordon S, and Donnelly RP. The Interleukin-13 Receptor-alpha1 Chain Is Essential for Induction of the Alternative Macrophage Activation Pathway by IL-13 but Not IL-4. *Journal of innate immunity* 2015.

54. Stein M, Keshav S, Harris N, and Gordon S. INTERLEUKIN-4 POTENTLY ENHANCES MURINE MACROPHAGE MANNOSE RECEPTOR ACTIVITY - A MARKER OF ALTERNATIVE IMMUNOLOGICAL MACROPHAGE ACTIVATION. *Journal of Experimental Medicine* 176: 287-292, 1992.

55. Sudan B, Wacker MA, Wilson ME, and Graff JW. A Systematic Approach to Identify Markers of Distinctly Activated Human Macrophages. *Frontiers in immunology* 6: 253, 2015.

56. Tarique AA, Logan J, Thomas E, Holt PG, Sly PD, and Fantino E. Phenotypic, functional, and plasticity features of classical and alternatively activated human macrophages. *Am J Respir Cell Mol Biol* 53: 676-688, 2015.

57. Vogel DY, Glim JE, Stavenuiter AW, Breur M, Heijnen P, Amor S, Dijkstra CD, and Beelen RH. Human macrophage polarization in vitro: Maturation and activation methods compared. *Immunobiology* 219: 695-703, 2014.

58. Wang IM, Lin H, Goldman SJ, and Kobayashi M. STAT-1 is activated by IL-4 and IL-13 in multiple cell types. *Molecular immunology* 41: 873-884, 2004.

59. Wang L, Gao S, Xu W, Zhao S, Zhou J, Wang N, and Yuan Z. Allergic asthma accelerates atherosclerosis dependent on Th2 and Th17 in apolipoprotein E deficient mice. *Journal of molecular and cellular cardiology* 72: 20-27, 2014.

60. Zajac E, Schweighofer B, Kupriyanova TA, Juncker-Jensen A, Minder P, Quigley JP, and Deryugina EI. Angiogenic capacity of M1- and M2-polarized macrophages is determined by the levels of TIMP-1 complexed with their secreted proMMP-9. *Blood* 122: 4054-4067, 2013.

61. Zhai C, Cheng J, Mujahid H, Wang H, Kong J, Yin Y, Li J, Zhang Y, Ji X, and Chen W. Selective inhibition of PI3K/Akt/mTOR signaling pathway regulates autophagy of macrophage and vulnerability of atherosclerotic plaque. *PLoS One* 9: e90563, 2014.

62. Zhao XN, Li YN, and Wang YT. Interleukin-4 regulates macrophage polarization via the MAPK signaling pathway to protect against atherosclerosis. *Genetics and molecular research : GMR* 15: 2016.

63. Zhu J, Guo L, Watson CJ, Hu-Li J, and Paul WE. Stat6 is necessary and sufficient for IL-4's role in Th2 differentiation and cell expansion. *J Immunol* 166: 7276-7281, 2001.

CHAPTER 6:

CCL18 AS A POTENTIAL MEDIATOR OF THE PRO-FIBROTIC ACTIONS OF M2 MACROPHAGES IN THE VESSEL WALL DURING HYPERTENSION

CCL18 as a potential mediator of the pro-fibrotic actions of M2 macrophages in the vessel wall during hypertension

Caitlin Lewis[‖], May Zhu[‖], Maggie Lieu[‖,¶], Yan Wang[‖], Robert Widdop[‖], Chrishan Samuel[‖], Grant Drummond[¶], Barbara Kemp-Harper[‖]

Affiliations

[‖] Cardiovascular Disease Program, Biomedicine Discovery Institute & Department of Pharmacology, Monash University, VIC 3800, Australia

[¶] Department of Physiology, Anatomy & Microbiology, School of Life Sciences, La Trobe University, VIC 3086, Australia

Abstract

Aortic stiffening often precedes the development of hypertension and is strongly correlated with the incidence of major cardiovascular events. M2 macrophages accumulate in the aorta during hypertension and are implicated in aortic stiffening, however the mechanisms underlying these effects remain unknown. A potential mediator of these actions is the M2 macrophage-derived pro-fibrotic chemokine, CCL18, however its roles in hypertension and aortic stiffening have not been investigated. We aimed to determine whether CCL18 expression from M2 macrophages may be elevated in the presence of the hypertensive stimulus, angiotensin II, and whether CCL18 has pro-fibrotic effects on vascular cells. We also wished to investigate the expression and localisation of its receptor (CCR8) and murine function analogue (CCL8) in the vessel wall of angiotensin II (0.7 mg/kg/d, 28 day)-infused hypertensive mice. Polarisation of human primary M2 macrophages, in the presence of angiotensin II (0.1 nM), augmented CCL18 protein release into the culture supernatant by ~43% and CCL18 treatment enhanced collagen I protein expression in aortic adventitial fibroblasts by up to 4-fold. Angiotensin II-induced hypertension in mice was associated with a 50% increase in M2 macrophages in the aortic wall and increased CCL8 aortic mRNA expression (~3-fold). CCL8 was predominantly co-localised with M2 macrophages, and its receptor, CCR8, was found to be expressed on the endothelium as well as additional cells in the adventitia and perivascular fat. Taken together our findings support a role for M2 macrophages in the pathophysiology of hypertension and reveal CCL18 and CCR8 as potential therapeutic targets to reduce aortic stiffening during hypertension and thus limit the incidence of cardiovascular events.

Introduction

Chronic hypertension is a major risk factor for cardiovascular events such as myocardial infarction, stroke and kidney disease (5). Approximately one third of the Western population suffers from hypertension and its prevalence increases with age (14). In addition to elevated blood pressure (BP), a major complication of the disease is stiffening of central elastic arteries such as the aorta. Interestingly, aortic stiffening often precedes the development of hypertension (21), and in the established disease it can contribute to end organ damage. As such, pulse wave velocity (PWV), a measure of aortic stiffening, is strongly correlated with the incidence of major cardiovascular events (3, 27, 32, 34). To date, most anti-hypertensive therapies have focussed on symptomatic relief (lowering of BP) but have not sought to directly reduce aortic stiffening. Importantly, up to 25% of patients remain at risk of a cardiovascular event, despite adequate control of BP (1, 13, 22). Hence it is important to understand the mechanisms underlying aortic stiffening during hypertension, to identify new potential targets for the disease and reduce cardiovascular morbidity and mortality.

Vascular inflammation occurs during hypertension and is believed to contribute to both end organ damage and aortic stiffening (33). Indeed, macrophages are key contributors to the pathophysiology of hypertension (9, 23, 44, 47) with a major role for the M2 subset of macrophages in aortic stiffening and elevated BP, recently identified in our laboratory. Specifically, in a preclinical murine model of hypertension, 14 days of angiotensin II infusion lead to an increase in M2 macrophages in the aortic wall and this was associated with enhanced collagen deposition, vascular remodelling, and aortic stiffening (35). However, the mechanisms by which M2 macrophages promote vascular fibrosis remain to be fully elucidated. In addition to the production of traditional pro-fibrotic factors such as platelet-

derived growth factor (PDGF) and transforming growth factor-β (TGF-β), M2 macrophages generate large amounts of a pro-fibrotic chemokine CCL18 (42) (Chapter 4), which may also contribute to vascular stiffening.

A role for CCL18 in tissue remodelling is evident in the lung, such that CCL18 stimulates collagen production in lung fibroblasts. In addition, CCL18 is increased in the lungs of patients with pulmonary disease, and this is associated with increased collagen (37, 41). Whilst a role for CCL18 in hypertension has not been directly investigated, there is growing evidence implicating this chemokine in cardiovascular disease. Plasma levels of CCL18 are elevated in patients with obstructive coronary artery disease (46), CCL18 is co-localised with macrophages in human carotid atherosclerotic lesions (16, 38), and a 3-fold increased risk of a fatal cardiovascular event was reported in acute coronary syndrome patients with high serum CCL18 (10). In addition, CCL18 is transiently raised in patients with unstable angina pectoris (24) and was identified as a biomarker for aortic aneurysm rupture risk (8). Interestingly, Gunther *et al.* observed increased CCL18 expression from peripheral blood mononuclear cells (PBMCs) following activation of the angiotensin receptor type 1 (AT_1R) and endothelin receptor type A (ET_A) by autoantibodies from patients with systemic sclerosis; such an observation correlated with the incidence of vascular complications (15). Given that autoantibodies are also evident in hypertension (50), and that the AT_1 and ET_A receptors are implicated in the hypertensive response (26, 43), this may represent a mechanism by which CCL18 generation could be elevated in a hypertensive environment. Further evidence for a potential role of CCL18 in hypertension-associated fibrosis comes from the finding that the vascular expression of its murine analogue, CCL8, is elevated in the murine angiotensin II-infusion model of hypertension (35). Moreover, its recently identified, cognate receptor CCR8

(19) is expressed on vascular cells including fibroblasts, endothelial and vascular smooth muscle cells (VSMCs) (4, 17). Collectively these data suggest CCL18 may serve as a biomarker for adverse cardiovascular events and play a pathophysiological role in these diseases. To date, however, CCL18 has not been studied in the context of hypertension and vascular fibrosis.

Given the key role M2 macrophages play in hypertension-associated aortic stiffening and their ability to generate large quantities of the pro-fibrotic chemokine, CCL18, we hypothesised that M2 macrophage-derived CCL18 contributes to aortic fibrosis and the pathogenesis of hypertension. This study aimed to identify whether CCL18 levels in macrophages were upregulated by hypertensive stimuli and whether this may promote fibrosis in the vasculature. To further investigate a potential role for CCL18 in hypertension, we also investigated the expression and localisation of its murine functional analogue CCL8, and its receptor CCR8, in the vessel wall of hypertensive mice.

Materials and Methods

Monocyte isolation

Primary human monocytes were isolated from healthy blood donor buffy coats (Australian Red Cross Blood Service, Melbourne, Australia). Buffy coats were mixed with phosphate buffered saline (PBS; without Ca^{2+}or Mg^{2+}; Sigma-Aldrich) supplemented with 0.5% fetal bovine serum (FBS; Sigma-Aldrich) and 2 mM ethylenediaminetetraacetic acid (EDTA; Sigma-Aldrich) and layered onto Ficoll-Paque PLUS (GE Healthcare no. 17-144) for density gradient centrifugation (400 g, 40 min, acceleration=1, deceleration=0). The peripheral blood mononuclear cell (PBMCs) layer was collected and monocytes isolated using a human pan monocyte isolation kit (Miltenyi Biotec no. 130-096-537), according to the manufacturer's instructions. The purity of the monocyte population was confirmed to be at least 85% as determined by Flow cytometry using $CD14^+$ /$CD16^+$ expression.

Monocyte to macrophage differentiation and macrophage treatment

Monocytes were seeded into 6-well plates (2 x 10^6 cells/well) and maintained in a humidified incubator (Sanyo MCO-18AIC CO_2 incubator, Quantum Scientific, USA) at 37°C with 5% CO_2. Macrophage differentiation was stimulated by culturing for 7 days in RPMI 1640 Glutamax medium (Gibco Life Technologies), supplemented with 10% FBS, 1x antibiotic/antimycotic (Gibco Life Technologies, USA), 1 mM sodium pyruvate (Sigma-Aldrich), 1 x non-essential amino acids (NEAA; Gibco Life Technologies) and 50 ng/ml macrophage colony stimulating factor (M-CSF; Miltenyi Biotec no. 130-096-491). Following 7 days of macrophage differentiation, the culture media was replaced in the absence of M-CSF and macrophages were either left untreated (MΦ), or treated with angiotensin II (0.1-1000 nM; AusPep) or interleukin-4 (IL-4; 5 ng/ml; Sigma-Aldrich) for 48 hours. In a separate set of experiments, the

effects of angiotensin II on IL-4 polarized M2 macrophages were investigated. For these experiments, macrophages were initially polarized to the M2 phenotype with a submaximal concentration of IL-4 (0.5 ng/ml) for 24 hours, followed by treatment with 0.1 or 10 nM angiotensin II (concentrations chosen from mRNA and protein data) for a further 24 or 48 hours in the absence or presence of candesartan (1 μM; 30 minutes pre-treatment; AstraZeneca). Angiotensin II was refreshed twice per day. Cell lysates were harvested for RNA and subsequent real-time PCR analysis, whilst cell culture supernatants were collected for CCL18 detection via ELISA.

Fibroblast culture and treatment

Human cardiac fibroblasts (HCF; ScienCell, USA) were cultured from passages 1 to 6 in Medium 199 (Life Technologies, USA) supplemented with 10% heat inactivated FBS (Life Technologies, USA), 5% penicillin streptomycin (Life Technologies, USA) and 5% fibroblast growth supplement (ScienCell, USA). Human aortic adventitial fibroblasts (AoAF; Lonza no. CC-7014; Lonza) were grown in Stromal Cell Growth Medium (SCGM; Lonza no. CC-3205), containing 5% FBS and used from passages 2 to 8. All fibroblasts were grown in T-75 flasks in a humidified incubator (Sanyo MCO-18AIC CO2 incubator, Quantum Scientific, USA), maintained at 37°C with 5% CO_2 and passaged using Trypsin-EDTA solution (Lonza no. CC-5012) for cell detachment. HCF and AoAF were seeded on 12-well and 6-well plates, respectively, at 1x 10^5 cells/well. Cells were either left untreated (negative control) or treated with TGF-β (10 ng/ml; R & D Systems, USA) or CCL18 (3-300 ng/ml; R&D systems, USA) for 3, 6, 24, 48 or 72 hours. Cell lysates were harvested for RNA and subsequent real-time PCR analysis (3-24 hours) or protein and subsequent western blotting (24-48 hours).

Animals

Male 10-12 week-old C57BL6/J mice were obtained from Monash Animal Services and housed in the Animal Research Laboratories (Clayton, Australia). Mice were housed under specific pathogen free conditions, on a 12 hour light-dark cycle with free access to chow diet and drinking water. This study was approved by the Monash University Animal Research Platform Animal Ethics Committee (Monash University, Clayton, Australia) and conducted in accordance with the Australian Code for the Care and Use of Animals for Scientific Purposes.

Angiotensin II infusion model of hypertension in mice

Mice were placed under general anaesthesia by isoflurane inhalation (0.4 L/min, 2.5%, Baxter, USA) and a small incision was made at the nape of the neck. Blunt dissection was then performed to make a subcutaneous pouch for insertion of micro-osmotic minipumps (Model 1004, flow rate 0.11 µl/hr, Alzet, USA) containing either vehicle (0.9% saline) or Ang II (0.7 mg/kg/day) (See General Methods, Section 2.2). Following surgery, mice were maintained on drinking water and normal chow for 28 days with blood pressure measured, by tail-cuff plethysmography, on days 5, 14, 21 and 28. The thoracic aorta was then harvested with the perivascular fat intact, the top third section snap frozen in liquid nitrogen for mRNA measurements, and the bottom third frozen in Optimal Cutting Temperature compound (OCT; Sakura Finetek, USA) for immunohistochemistry.

Tail-cuff plethysmography

Systolic blood pressure was measured prior to surgeries (day 0), and on days 5, 14, 21 and 28, using tail cuff plethysmography (MC4000 multi-channel blood pressure analysis system; Hatteras Instruments, USA). In brief, mice were place in a restraint on a heated pad (40°C) and a small inflatable cuff positioned around the base of the tail. BP was determined as the

cuff inflation pressure at which blood flow to the tail becomes completely occluded (25). BP was recorded every day for 3 days before surgery to acclimatise mice to the procedure (See General Methods, Section 2.2).

RNA extraction and Real-time PCR

Total RNA was extracted from macrophages and thoracic aorta using the RNeasy Mini Kit and Micro Kit (Qiagen), respectively, according to the manufacturer's instructions. RNase-free DNase (Qiagen) was used to remove any contaminating DNA. The amount of RNA in each sample was quantified using the Nanodrop 1000D spectrophotometer (ThermoScientific), which measures absorbance at 260 nm and 280 nm. An A_{260}:A_{280} ratio of 2 or more was considered sufficiently pure. 1 µg of RNA from each sample was reverse transcribed into cDNA using the High Capacity cDNA Reverse Transcription Kit (Applied Biosystems) with the reaction run in a thermal cycler (BioRad MyCycler, BioRad Laboratories). The resultant cDNA was used as a template for real time PCR with Taqman® primers and probes for CCR8, CCL8, CCL18, COL1A1, COL3A1, COL5A1 and ACTA2 (Applied Biosystems). GAPDH and 18S were used as housekeeping genes. Real-time PCR was run in triplicate on the CFX96 Touch™ Real-Time PCR Detection Machine (BioRad Laboratories). Gene expression was normalised to the housekeeping gene and expressed relative to the average control value using the comparative cycle threshold (Ct) method with the formula: Fold change= $2^{-\Delta\Delta Ct}$ (40).

Measurement of CCL18 by ELISA

CCL18 levels in the conditioned media of IL-4 and/or Ang II-treated primary macrophages was measured via an ELISA (R & D Systems no. DY394). The assay was performed according to the manufacturer's instructions in microtiter plates coated with antibodies specific for CCL18. The

amount of CCL18 in the samples was estimated by calibrating the optical density (OD) values of the samples with the OD values of serially diluted protein standards.

Protein extraction and Western blotting

Total protein from fibroblast cell lysates were collected in 1x RIPA Lysis and extraction buffer (Cell Signalling Technology, USA). Cell debris was cleared by centrifugation (13,000 rpm, 10 min, 4°C) and supernatants collected. Protein concentrations were determined using a Bicinchonic acid (BCA) based colorimetric quantification assay (Pierce™ BCA Protein Assay, ThermoScientific). Equivalent volumes of protein in 1.5 x Laemmli buffer were loaded into 7.5%, 10% or 4-15% polyacrylamide gels. Proteins were separated by SDS-PAGE and transferred onto low fluorescence polyvinylidene fluoride (LF PVDF) membranes using the Bio-Rad Trans Blot Turbo transfer system (Bio-Rad Laboratories). Membranes were blocked with 5% skim milk in Tris-Buffered Saline (TBS; 200 mM Tris, 150 mM NaCl, pH 7.5) with 0.1 % tween-20 for 1 hour and subsequently probed with primary antibodies against α-SMA (1:2500; Abcam no. ab5694), collagen I (1:1000; Abcam no. ab34710) and GAPDH (1:20000; Abcam no. ab8245) overnight at 4°C. 1 hour incubation with horseradish peroxidase(HRP)-conjugated anti-rabbit (1:10000; Dako) or anti-mouse (1:10000; Jackson ImmunoResearch Laboratories) secondary antibodies was then performed and protein bands visualised using Clarity ECL substrate (BioRad Laboratories) and the ChemiDoc MP system (BioRad Laboratories). Densitometries of protein bands were quantified using Image Lab Software (BioRad Laboratories). Results were normalised to GAPDH and expressed relative to control (untreated) samples.

Immunohistochemistry

Frozen mouse aortae were cut into 10 µm sections and mounted on Poly-L-Lysine coated glass slides. Sections were fixed in 4% paraformaldehyde (PFA; Sigma) for 15 minutes and washed with PBS. Fixed sections were blocked with 2% bovine serum albumin (BSA; Sigma) in PBS with 0.2% Triton X-100 (TX; Sigma) for 30 minutes and subsequently incubated with primary antibodies against mCCL8 (1:150 dilution; R and D systems), mCCR8 (1:200 dilution; Abcam), M2 macrophage marker CD206 (1:500 dilution; Abcam) and endothelial cell marker Von Willebrand factor (vWF; 1:500 dilution; Abcam) at room temperature for 2 hours. Sections were then washed and incubated with secondary antibodies in the dark, at room temperature for 2 hours. Finally, slides were washed, and Vectashield mounting medium with diamidino-2-phenylindole (DAPI) added (Vector Laboratories, USA). Sections were imaged using a Nikon C1 upright confocal fluorescence microscope (x 40 objective lens; Monash Micro Imaging, Monash University, Clayton, Australia). CD206 and CCL8 positive cells were quantified using Image J (FIJI image analysis software, USA) in a blinded manner.

Statistical analysis

All data are expressed as mean ± SEM with n=4-8. Comparisons of multiple treatment groups were made using a 1-Way ANOVA. Groups were compared using either a Sidak's or Dunnett's post hoc test for selected comparisons and comparisons with control, respectively. Systolic BP data were analysed with a 2-way ANOVA followed by Bonferroni's post hoc test. Aortic mRNA expression of CCL8 and CCR8, and quantified immunohistochemistry results, were analysed using a student's unpaired t-test. $P<0.05$ was considered to be statistically significant and data were graphed and analysed using GraphPad Prism 7.02 software.

Results

Angiotensin II stimulates CCL18 generation from M2 macrophages

Polarisation of primary human macrophages towards an M2 phenotype with IL-4 resulted in concentration- (Figure 1A) and time- (Figure 1B) dependent increases in CCL18 mRNA, and time-dependent increases in CCL18 protein (Figure 1C). Following 24 hours of treatment, CCL18 mRNA expression was increased ~800-fold with IL-4 at concentrations of 2.5 and 5 ng/ml. CCL18 mRNA expression was increased further over time, such that 5 ng/ml IL-4 resulted in a 1500-fold increase at 48 and 72 hours (Figure 1B). CCL18 protein levels secreted into the cell culture supernatants were assessed by ELISA and found to increase from 1 ng/ml (untreated macrophages; MØ) to 500 ng/ml following 72 hours treatment with IL-4 (5 ng/ml); Figure 1C). To elucidate whether hypertensive stimuli may also increase macrophage CCL18 generation, primary macrophages were treated with increasing concentrations of angiotensin II for 48 hours and the effects on CCL18 expression compared to 5 ng/ml IL-4. Whilst IL-4 treatment again robustly increased CCL18 mRNA and protein expression, 0.1-1000 nM angiotensin II alone had no effect (Figure 1D).

Given resident macrophages in hypertensive vessels are predominantly of the M2 phenotype, we also examined the effects of angiotensin II on M2 macrophage CCL18 generation. Primary macrophages were first polarised to M2 with a submaximal concentration of IL-4 (0.5 ng/ml, 24 hours), and then treated with 0.1 nM angiotensin II for a further 24 or 48 hours in the absence or presence of the AT_1 receptor antagonist, candesartan (1 μM) (Figure 1E). Whilst, 24 hour treatment of M2 macrophages with angiotensin II did not alter CCL18 mRNA there was a trend to increase CCL18 protein concentration in the supernatant from 91 ng/ml to 125 ng/ml ($P=0.12$). This effect was attenuated by candesartan ($P<0.05$, Figure 1F). Treatment of M2 macrophages with angiotensin II for 48 hours also failed to alter CCL18 mRNA but was

associated with a 43% increase (P<0.05) in CCL18 protein release. Of note, candesartan did not appear to attenuate this effect (Figure 1G). The effect of a higher concentration of angiotensin II (10 nM) on M2 macrophages was also investigated but appeared to have a reduced effect compared to the 0.1 nM treatment (Supplementary Figure 1).

CCL18 increases collagen 1 expression in human aortic adventitial fibroblasts

To determine whether CCL18 may promote fibrosis in the vessel wall, human aortic adventitial fibroblasts were treated with increasing concentrations of CCL18 (3-300 ng/ml), over a period of 3 to 72 hours, and collagen (types I, III and V) and alpha smooth muscle actin (α-SMA) mRNA and protein levels determined. The established pro-fibrotic stimulus, TGF-β was used as a positive control. Neither TGF-β, nor CCL18, altered collagen or α-SMA mRNA expression following 3 or 6 hours treatment (Figure 2). 24 hours treatment with TGF-β (10 ng/ml), but not CCL18, increased collagen I (1.7-fold), collagen V (2.5-fold) and α-SMA (5.7-fold) mRNA expression (Figure 2). These effects of TGF-β on mRNA corresponded with increased α-SMA protein by up to 3-fold after 24, 48 and 72 hours of treatment (Figure 3). For TGF-β-stimulated collagen I expression, there was a trend for increased pro-collagen up to 1.5-fold (doublet at ~235 and 215 kDa) and a significant 2-fold increase in the mature collagen I bands (doublet at ~130 and 115 kDa) at 24 hours. However, collagen levels appeared to decrease in the TGF-β group at 48 and 72 hours (Figure 4). Consistent with the mRNA data, CCL18 had no effect on α-SMA protein expression (Figure 3). However, CCL18 treatment did increase protein levels of pro-collagen I up to 2-fold at 24 hours and resulted in a trend for increased mature collagen protein in a concentration-dependent manner, up to 2- and 4-fold at 48 and 72 hours, respectively (Figure 4). An ability of CCL18 to increase collagen I protein

expression was also demonstrated in human cardiac fibroblasts (see Supplementary Figure 2).

Angiotensin II-induced hypertension is associated with accumulation of CCL8-expressing M2 macrophages in the vessel wall

Angiotensin II infusion significantly elevated systolic BP from day 5, as compared to saline treated mice. By day 28, systolic BP reached 151 ± 5 mmHg in angiotensin II-treated versus 111 ± 5 mmHg in saline-treated mice (Figure 6A). This increase in blood pressure was associated with a 3-fold increase in aortic mRNA expression of CCL8 (functional analogue of human CCL18; Figure 6B) but no change in the expression of its receptor, CCR8 (Figure 6C). To elucidate whether M2 macrophages were the main source of increased aortic CCL8, we used immunohistochemical techniques to localise expression of CCL8 and the M2 macrophage marker, CD206 in aortic sections from saline and angiotensin II-treated mice. We observed increased M2 macrophage staining in hypertensive mice, predominantly located in the adventitia (Figure 6A). Blinded quantification of CD206 positive cells revealed a 50% increase in M2 macrophages in angiotensin-II treated hypertensive mice (Figure 6B). Double staining with CCL8 showed co-localisation of CD206 with CCL8 in both saline and angiotensin II-treated mice. The total number of CD206+/CCL8+ cells was increased by 50% in angiotensin II-treated mice, consistent with the increase in the M2 macrophage population (Figure 6C).

CCR8 is expressed in the vessel wall

To investigate which cell types CCL8 may target within the vessel wall, localisation of it receptor, CCR8 was assessed via immunofluorescent staining. CCR8 staining was most predominant in the adventitia and perivascular adipose tissue with some CCR8 positive cells also observed in the media, likely to be vascular smooth muscle cells (Figure 7). As endothelial

staining was also evident, we assessed co-localisation of CCR8 with the endothelial marker vWF (Figure 7). Co-localisation was shown in both saline- and angiotensin II-treated mice (Figure 7). Consistent with our findings with regard to aortic CCR8 mRNA levels in these mice, no clear differences in CCR8 staining were observed between the two groups.

Figures

Figure 1. Effects of IL-4 and angiotensin II on CCL18 expression in human primary macrophages. Concentration-dependent changes in CCL18 mRNA at 24 h (A) and time-dependent (6 to 72 h) changes in CCL18 mRNA (B) and protein (C) expression following treatment of M-CSF (50 ng/ml)-differentiated human primary macrophages with IL-4, n=4-7, * P<0.05 vs. MΦ (at the same time point); $^{\#}$P<0.05 vs. 6 h and 24 h; $^{\$}$P<0.05 vs. 6h, 24h and 48h (1-way ANOVA, Sidak's post hoc test). Please note concentration response curve in A is reproduced from Chapter 5, Figure 2D, n=6. D) Effect of 48 h angiotensin II treatment on CCL18 mRNA and protein expression in unpolarised macrophages, n=3-7. E) Schema of treatment protocol for angiotensin II treatment of M2-polarised macrophages. M-CSF (50 ng/ml)-differentiated human primary macrophages (MΦ) were polarised to the M2 phenotype (by 0.5 ng/ml IL-4, 24 h) prior to the addition of 0.1 nM angiotensin II in the absence, or presence, of candesartan (1 μM) for 24 h (F) or 48 h (G) and mRNA and protein CCL18 levels measured, n=4-5 , *P<0.05, **P<0.01, (Repeated measure 1-way ANOVA, Sidak's post hoc test). C = candesartan (AT_1 receptor antagonist; 0.5 h pre-treatment). All data presented as mean ± SEM. mRNA expressed relative to the average MΦ (untreated) value.

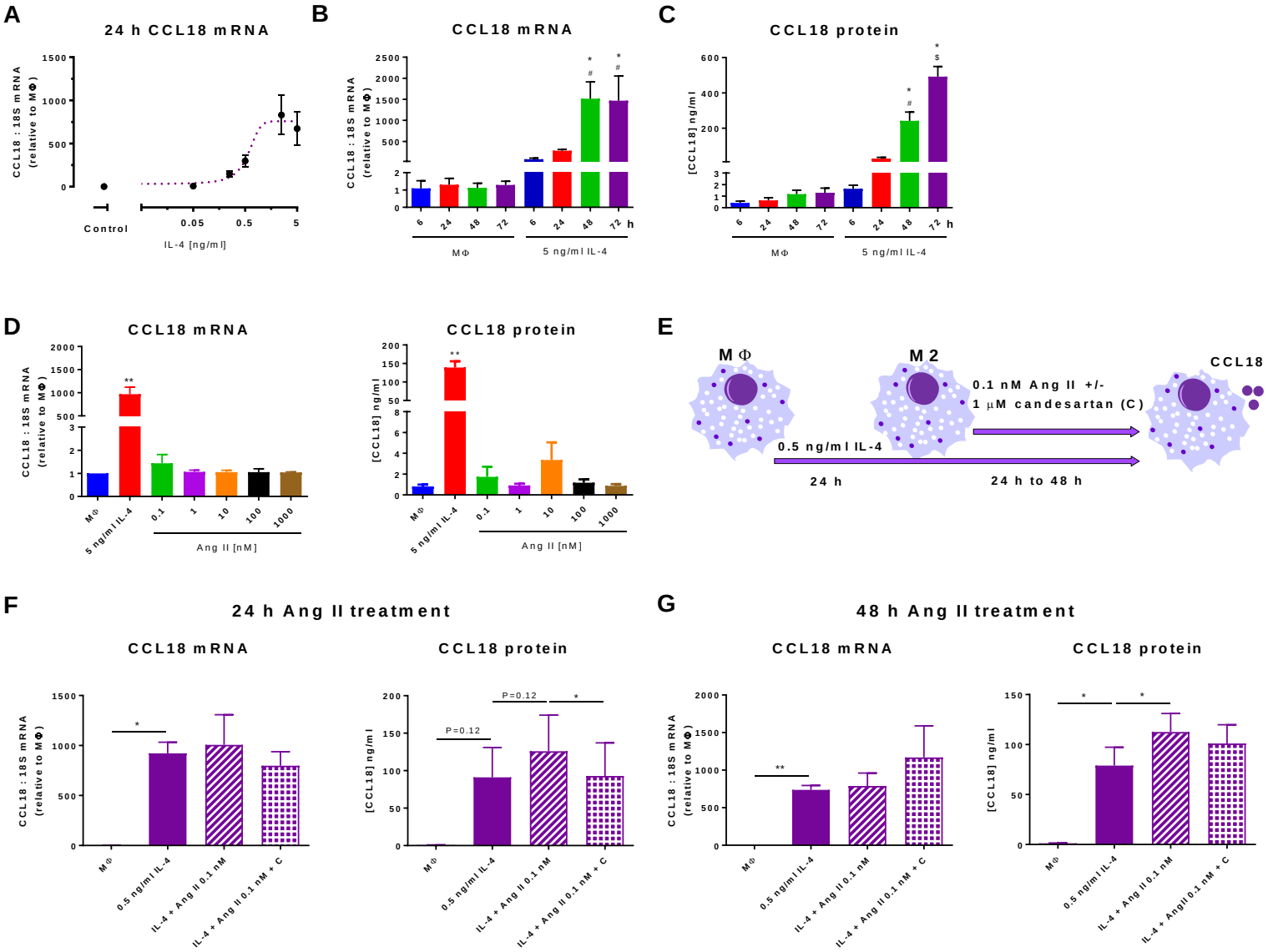
A
24 h CCL18 mRNA
CCL18 : 18S mRNA (relative to MΦ)
Control
0.05
0.5
5
IL-4 [ng/ml]
B
CCL18 mRNA
CCL18 : 18S mRNA (relative to MΦ)
MΦ
5 ng/ml IL-4
C
CCL18 protein
[CCL18] ng/ml
D
CCL18 mRNA
CCL18 protein
Ang II [nM]
E
MΦ
M2
CCL18
0.1 nM Ang II +/-
1 µM candesartan (C)
0.5 ng/ml IL-4
24 h
24 h to 48 h
F
24 h Ang II treatment
CCL18 mRNA
CCL18 protein
P=0.12
0.5 ng/ml IL-4
IL-4 + Ang II 0.1 nM
IL-4 + Ang II 0.1 nM + C
G
48 h Ang II treatment
CCL18 mRNA
CCL18 protein

Figure 2. Effects of CCL18 on collagen and α-smooth muscle actin mRNA expression in human aortic adventitial fibroblasts. Concentration- and time-dependent changes in the mRNA expression of COL1A1 (A), COL3A1 (B), COL5A1 (C) and ACTA2 (α-SMA, D) following 3, 6 or 24 hours treatment with CCL18 (3-300 ng/ml) or TGF-β1 (10 ng/ml). All data presented as mean ± SEM and expressed relative to the average control (untreated) value, n=4-6.*P<0.05 vs control (1-way ANOVA, Dunnett's post hoc test).

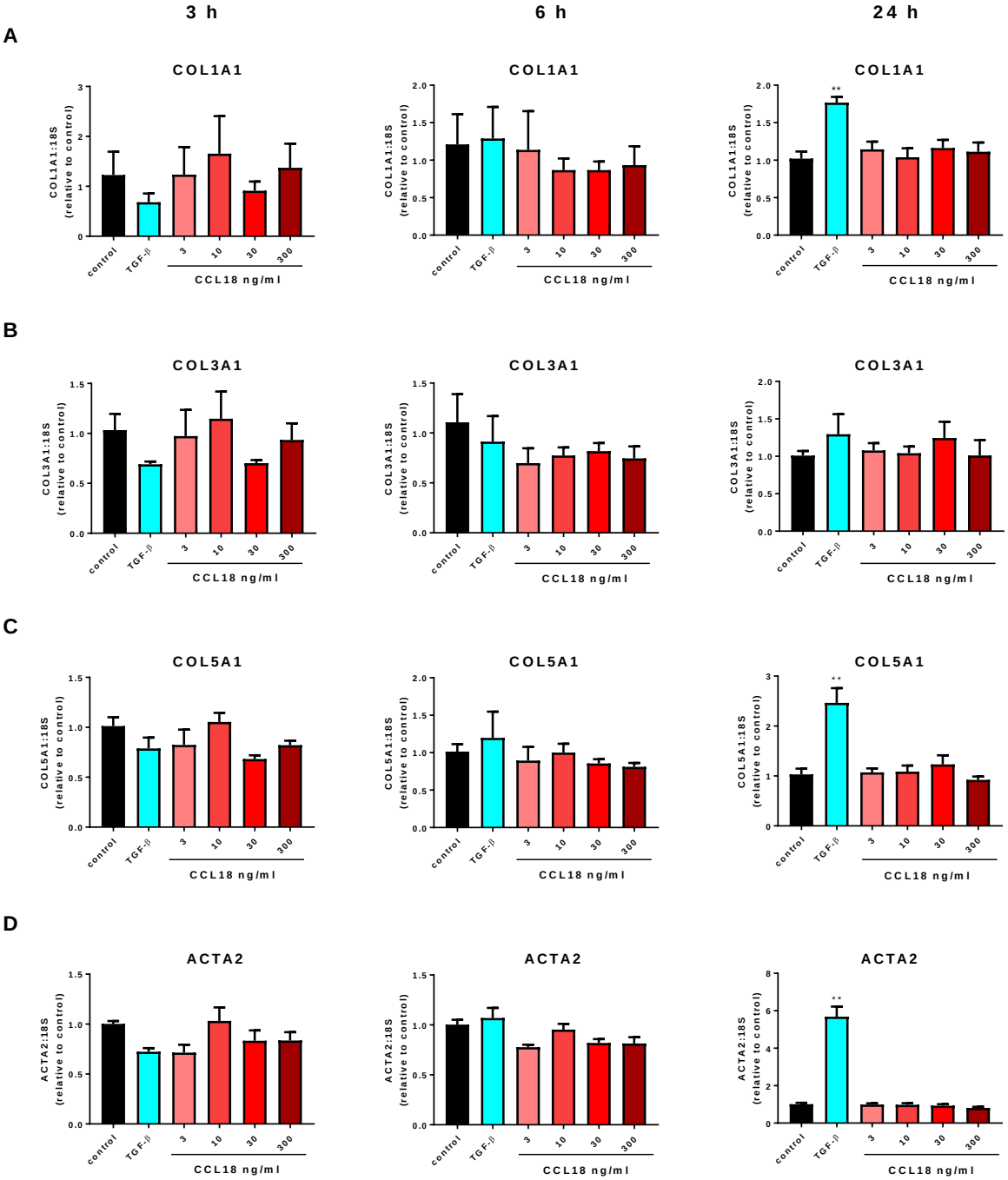
3 h
6 h
24 h
A
COL1A1
COL1A1:18S (relative to control)
B
COL3A1
COL3A1:18S (relative to control)
C
COL5A1
COL5A1:18S (relative to control)
D
ACTA2
ACTA2:18S (relative to control)
control
TGF-β
3
10
30
300
CCL18 ng/ml
**

Figure 3. Effects of CCL18 on α-smooth muscle actin protein expression in human aortic adventitial fibroblasts. Concentration-dependent changes in α-SMA protein following 24 (A), 48 (C), and 72 (E) hours treatment with CCL18 (3-300 ng/ml) or TGF-β (10 ng/ml). All data presented as mean ± SEM and expressed relative to the average control (untreated) value, n=7-8. Representative blots for 24 (B), 48 (D) and 72 (F) hours treatment depicting n=1, run in duplicate, shown to the right hand side of data with GAPDH used as a loading control. **P<0.01, ***P<0.001 vs control (1-way ANOVA, Dunnett's post hoc test).

24 h

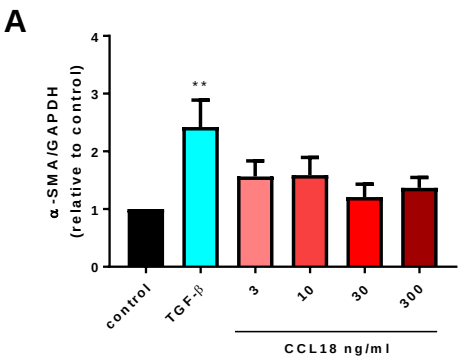
A
α-SMA/GAPDH (relative to control)
**
control
TGF-β
3
10
30
300
CCL18 ng/ml

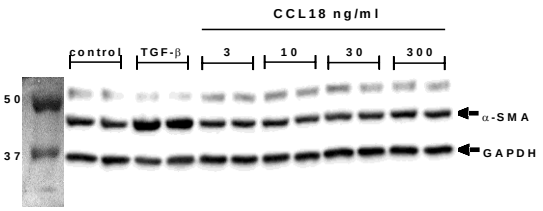
B
CCL18 ng/ml
control
TGF-β
3
10
30
300
50
37
α-SMA
GAPDH

48 h

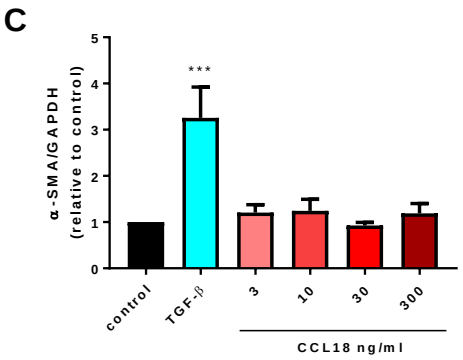
C
α-SMA/GAPDH (relative to control)
***
control
TGF-β
3
10
30
300
CCL18 ng/ml

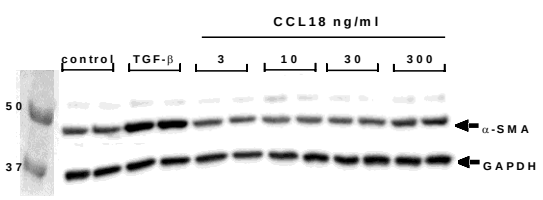
D
CCL18 ng/ml
control
TGF-β
3
10
30
300
50
37
α-SMA
GAPDH

72 h

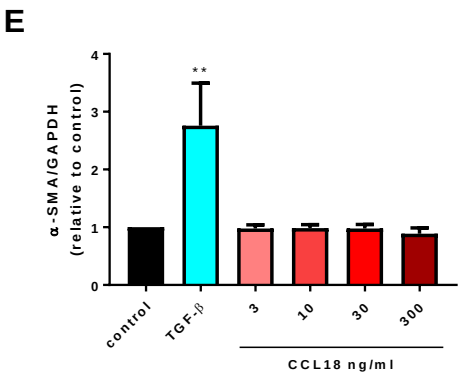
E
α-SMA/GAPDH (relative to control)
**
control
TGF-β
3
10
30
300
CCL18 ng/ml

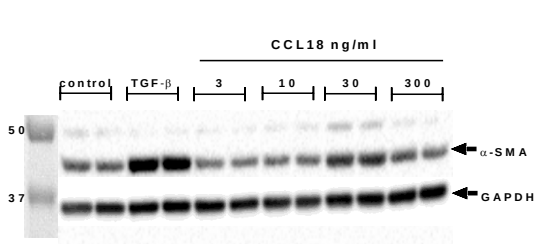
F
CCL18 ng/ml
control
TGF-β
3
10
30
300
50
37
α-SMA
GAPDH

Figure 4. Effects of CCL18 on collagen I protein expression in human aortic adventitial fibroblasts. Concentration-dependent changes in pro collagen I (A, D, G) and collagen I protein (B, E, H) following 24, 48, and 72 hours treatment with CCL18 (3-300 ng/ml) or TGF-β (10 ng/ml). All data presented as mean ± SEM and expressed relative to the average control (untreated) value, n=4-7. Representative blots for 24 (C), 48 (F) and 72 (I) hours treatment depicting n=1, run in duplicate, shown to the right hand side of data with GAPDH used as a loading control. **P<0.01, ***P<0.001 vs control (1-way ANOVA, Dunnett's post hoc test).

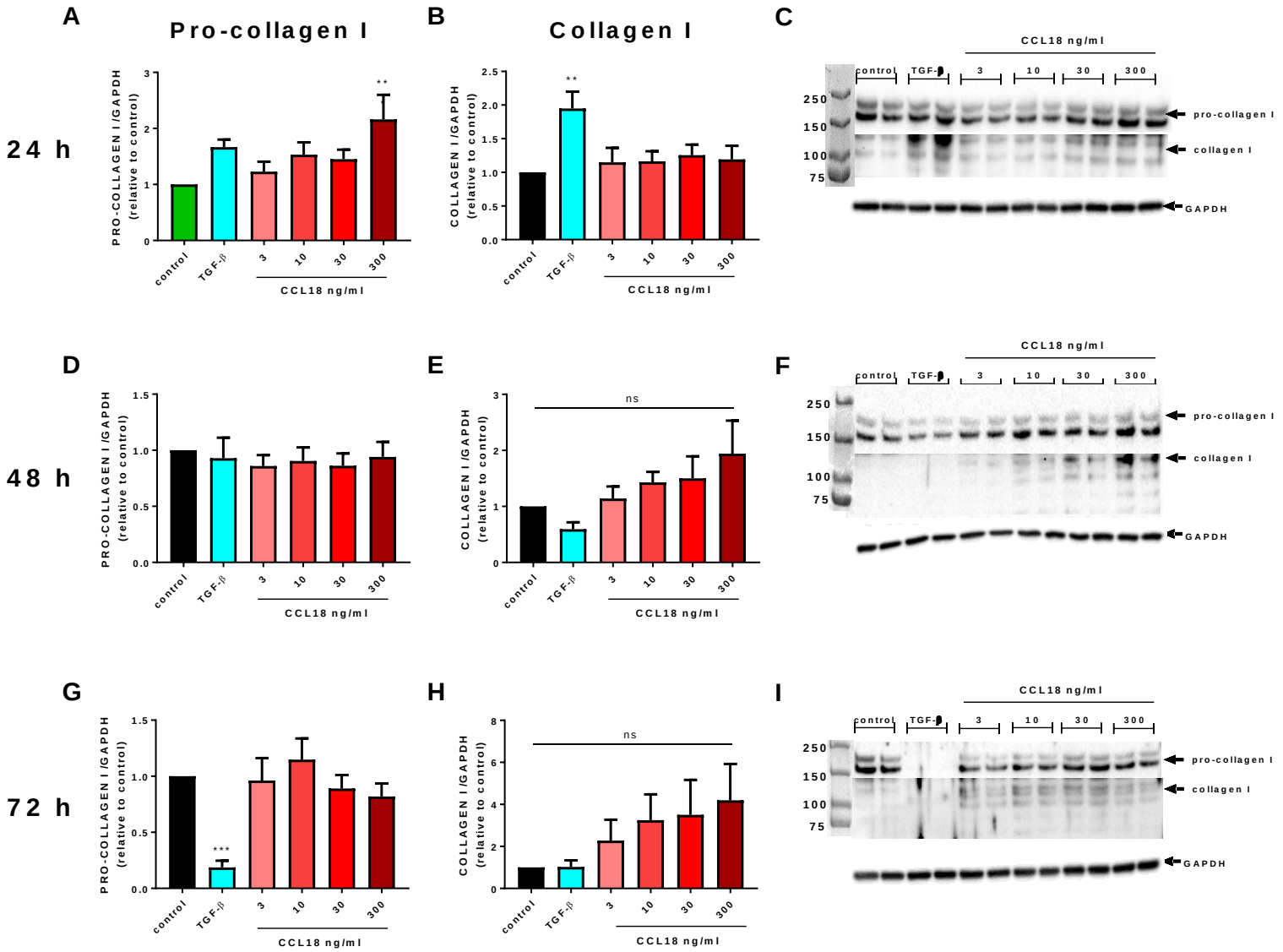
A
Pro-collagen I
24 h
PRO-COLLAGEN I /GAPDH (relative to control)
control
TGF-β
3
10
30
300
CCL18 ng/ml
**
B
Collagen I
COLLAGEN I /GAPDH (relative to control)
C
CCL18 ng/ml
250
150
100
75
pro-collagen I
collagen I
GAPDH
D
48 h
E
ns
F
G
72 h
***
H
I

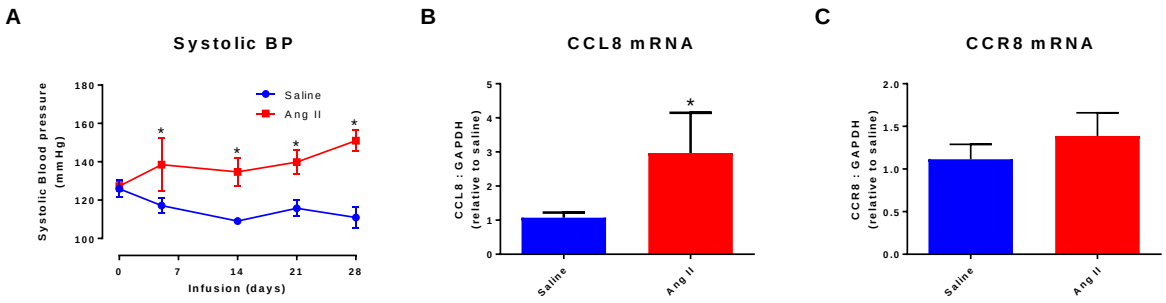

Figure 5. Effects of chronic angiotensin II treatment on systolic blood pressure (BP) and aortic expression of CCL8 and CCR8 in mice. A) Systolic BP in mice after infusion of either saline or angiotensin II (Ang II; 0.7 mg/kg/d) over 28 days. BP was measured by tail cuff plethysmography. Aortic mRNA expression of CCL8 (B) and CCR8 (C) following 28 day treatment with either saline or angiotensin II. Fold changes in mRNA expressed relative to the average control (saline) value. Data presented as mean ± SEM, n=8 (saline treatment) or n=4 (Ang II treatment). *P<0.05 vs. saline; (A) 2-way ANOVA, Bonferroni's post hoc test; (B-C) Student's unpaired t-test.

Figure 6. Localisation of M2 macrophages and CCL8 in the aorta of normotensive (saline treated) and Ang II-induced hypertensive mice. A) Immunohistochemical staining for CD206 (M2 marker; green), CCL8 (red), and DAPI (nucleated cells; blue) in aortic sections, from 28 day saline (top panels) or Ang II (0.7 mg/kg/d; bottom panels) treated mice. Images were taken at a magnification of X40. Representative images from n=6 are shown. Vessel lumen (L), media (M), adventitia (A) and perivascular fat (P) are indicated on each image, scale bars show 50 µm. Yellow cells indicate co-localisation of CCL8 with CD206 (CD206+ CCL8 +) and are highlighted by white arrows. Quantification of M2 macrophages (B; DAPI+ CD206+) and CCL8-expressing M2 macrophages (C; DAPI+ CD206+ CCL8+) was performed using ImageJ in a blinded manner and normalized to area (mm^2). Values are expressed as mean ± SEM, n=5-6. *P<0.05 vs. saline (Student's unpaired t-test).

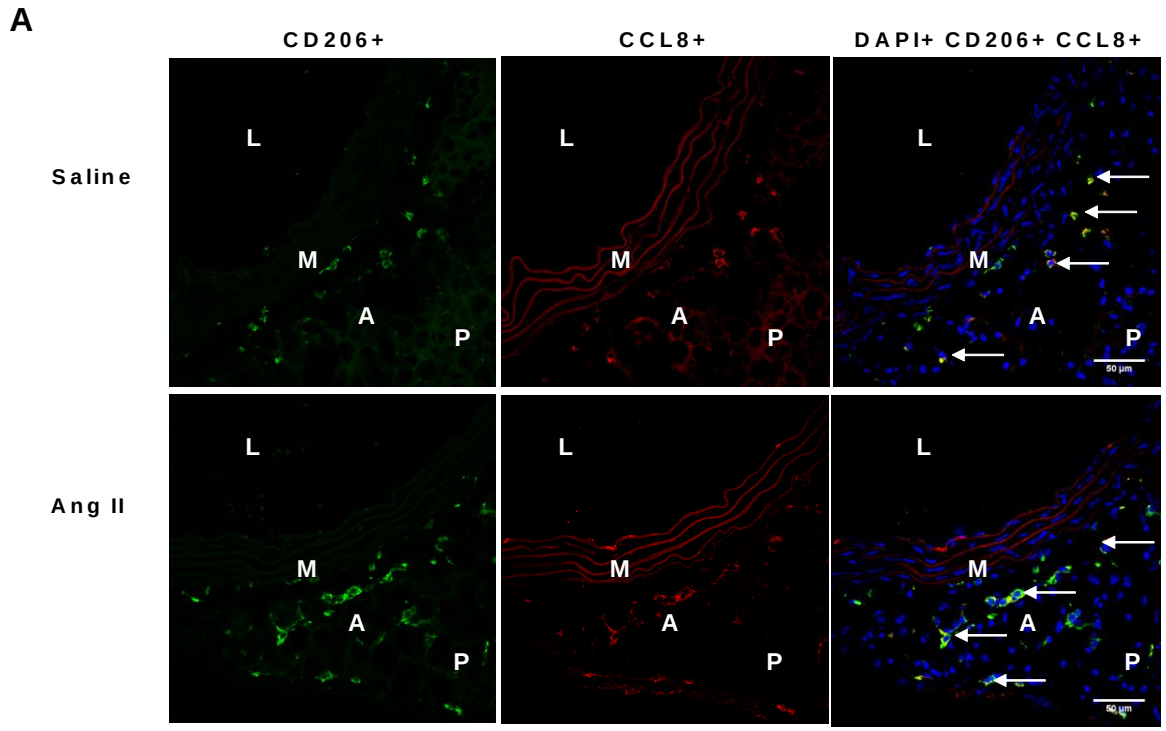
A
CD206+
CCL8+
DAPI+ CD206+ CCL8+
Saline
Ang II
L
M
A
P
50 µm

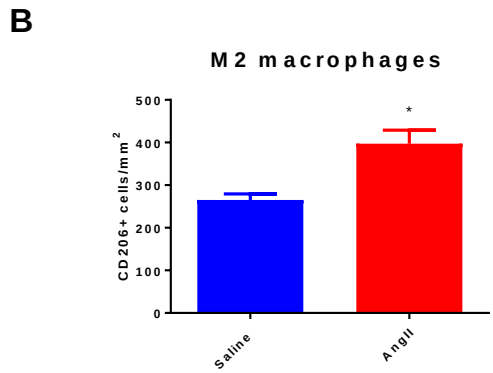
B
M2 macrophages
CD206+ cells/mm2
500
400
300
200
100
0
*
Saline
AngII

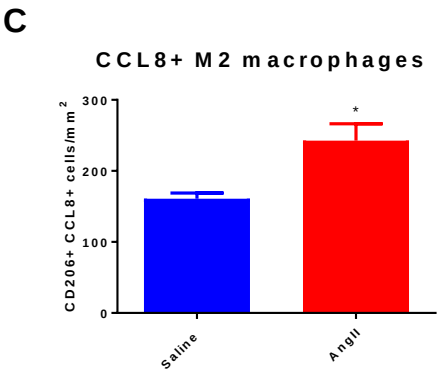
C
CCL8+ M2 macrophages
CD206+ CCL8+ cells/mm2
300
200
100
0
*
Saline
AngII

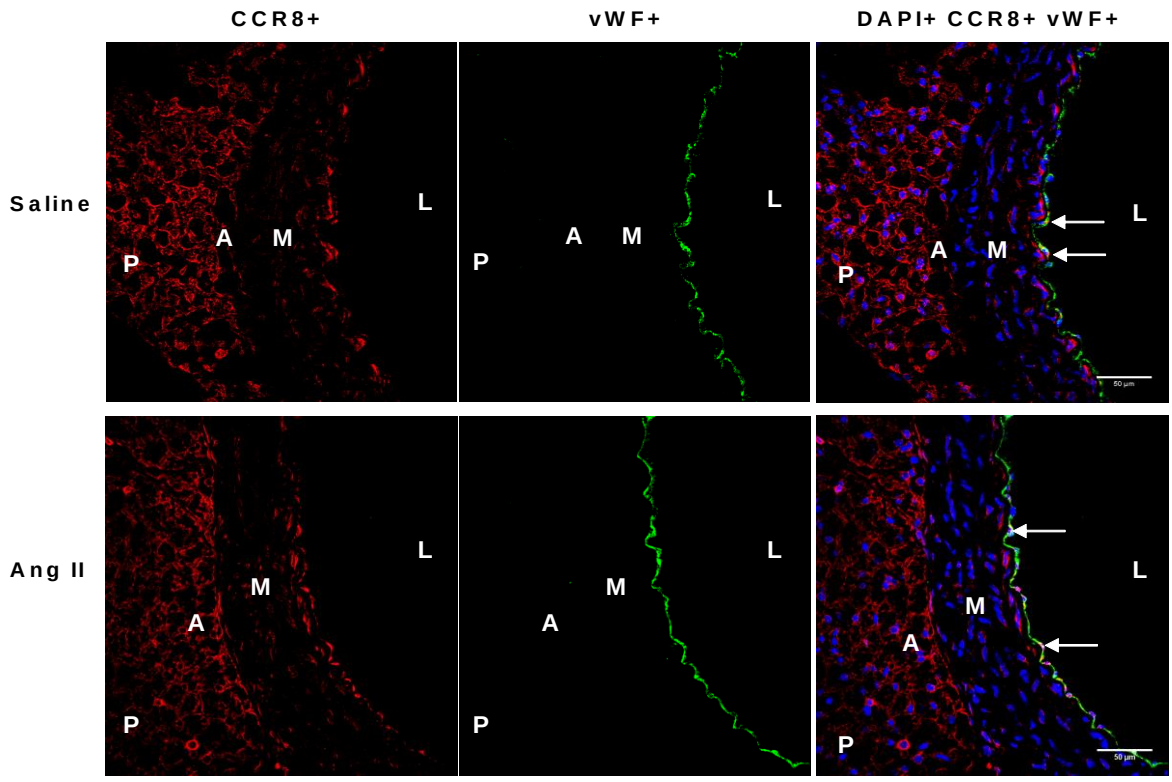

Figure 7. Localization of CCR8 to aortic endothelial cells and other vascular cell types in the aorta of normotensive (saline treated) and Ang II-induced hypertensive mice. Representative immunohistochemical staining for CCR8 (red), von Willebrand Factor (vWF; endothelial cells; green), and DAPI (nucleated cells; blue) in aortic sections from 28 day saline (top panels) or Ang II (0.7 mg/kg/d; bottom panels) treated mice. Images were taken at a magnification of X40. Representative images from n=6 are shown. Vessel lumen (L), media (M), adventitia (A) and perivascular fat (P) are indicated on each image, scale bars show 50 µm. Yellow cells indicate co-localisation of CCR8 with vWF (CCR8+ vWF+) and are highlighted by white arrows.

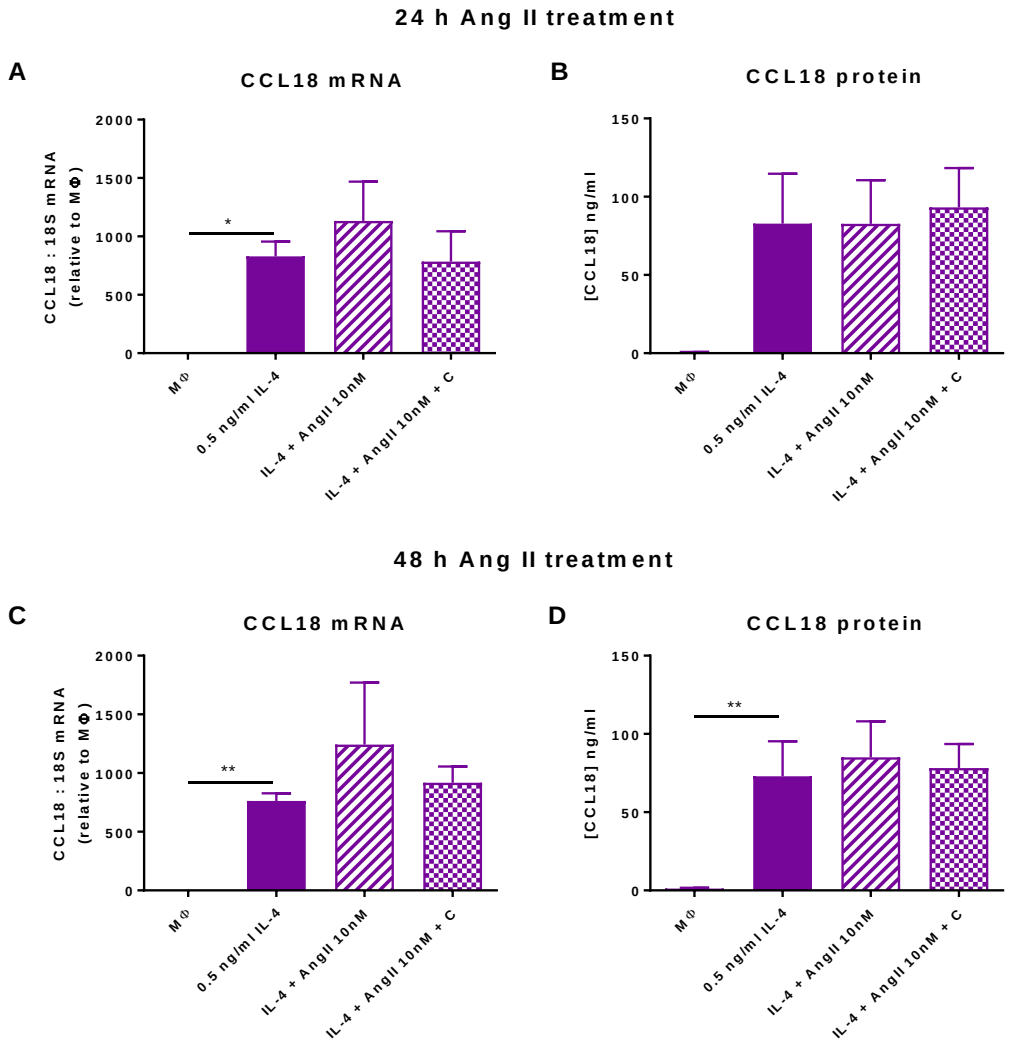

Supplementary Figure 1. Effects of 10 nM angiotensin II on CCL18 expression in human primary M2 macrophages. M-CSF (50 ng/ml)-differentiated human primary macrophages (MΦ) were polarised to the M2 phenotype (by 0.5 ng/ml IL-4, 24 h) prior to the addition of 10 nM angiotensin II in the absence, or presence, of candesartan (1 μM) for 24 (A, B) or 48 hours (C, D) and mRNA and protein CCL18 levels were measured, n=3-4. C = candesartan (AT_1 receptor antagonist; 0.5 h pre-treatment). All data presented as mean ± SEM. mRNA expressed relative to the average MΦ (untreated) value. *P<0.05, **P<0.01, (Repeated measure 1-way ANOVA, Sidak's post hoc test).

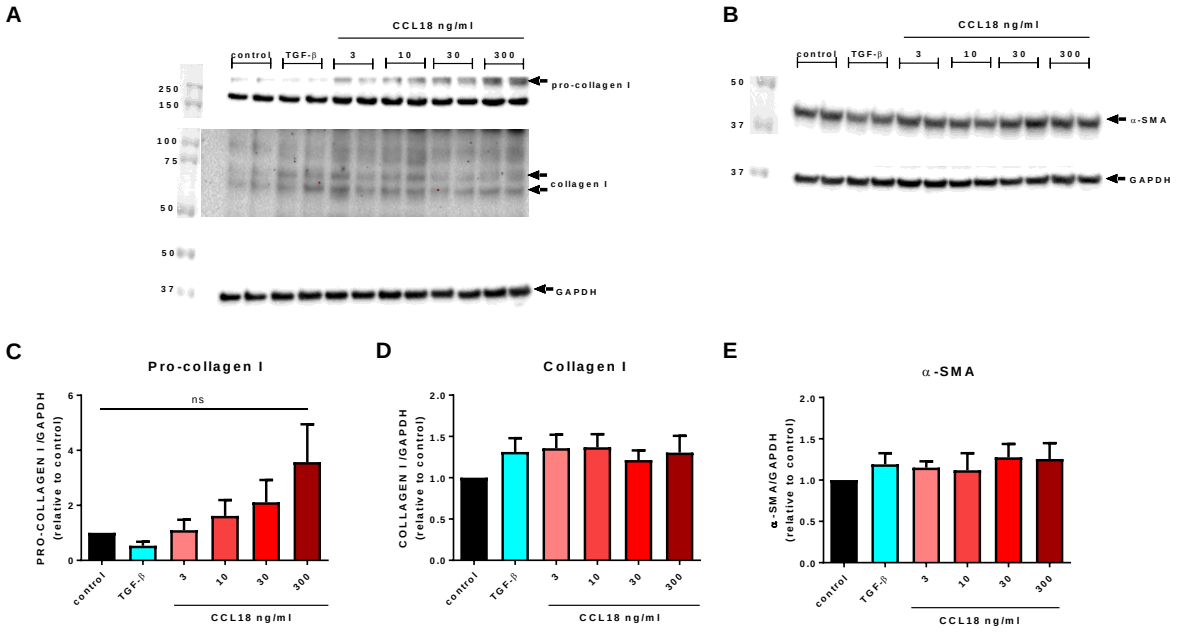

Supplementary Figure 2. Effects of CCL18 on collagen I and α-smooth muscle actin protein expression in human cardiac fibroblasts. Concentration-dependent changes in pro-collagen 1 (A, C), collagen 1 (A, D) and α-SMA (B, E) protein following 72 hours treatment with CCL18 (3-300 ng/ml) or TGF-β (10 ng/ml). All data presented as mean ± SEM and expressed relative to the average control (untreated) value, n=4-5. Representative blot depicting n=1, loaded in duplicate, shown above data with GAPDH used as a loading control. ns, not significant (P>0.05).

Discussion

Human CCL18 (hCCL18) and mouse CCL8 (mCCL8, functional analogue of hCCL18) are pro-fibrotic chemokines which have been shown to exert effects through activation of CCR8 (17-19). These chemokines are abundantly expressed by M2 macrophages *in vitro* (19, 31). Given that a role for M2 macrophages in aortic stiffening during hypertension has emerged (35), this study investigated the potential role of hCCL18/mCCL8 and CCR8 in this setting. We have provided the first evidence that the hypertensive stimulus, angiotensin II can increase CCL18 generation from human primary M2 macrophages. We also showed increased mCCL8-expressing M2 macrophages in the aortae of hypertensive mice and expression of CCR8 in the vessel wall, revealing CCL18 and CCR8 as potential therapeutic targets for hypertension.

Treatment of M-CSF-differentiated human primary macrophages with IL-4 to induce M2 polarisation resulted in robust increases in CCL18 mRNA and protein in a time-dependent manner. Given the magnitude of this upregulation, CCL18 appears to be an important pro-fibrotic mediator released by M2 macrophages. A previous study found that autoantibodies, from patients with systemic sclerosis, activated AT_1 receptors expressed on human peripheral blood mononuclear cells (PBMCs) to increase CCL18 protein (15). We were therefore interested in whether the hypertensive stimulus, angiotensin II promoted CCL18 generation from macrophages. Whilst angiotensin II did not have any clear effects on CCL18 expression in unpolarised macrophages, it did increase the CCL18 protein produced by M2 macrophages by 43% following 48 hours of treatment. A lack of effect on unpolarised macrophages is perhaps not surprising as there is indirect evidence to suggest angiotensin II can promote an M1 phenotype, with an increased M2 population observed *in vivo* in the absence of AT_1 receptor signalling (30, 49). Investigating the effects of angiotensin II on polarised, M2

macrophages may also be more representative of the macrophage population found in the hypertensive vasculature (35).

Our findings suggest that angiotensin II can target M2-polarised macrophages to further augment the release of the pro-fibrotic chemokine, CCL18. Perhaps 'priming' for CCL18 production, with IL-4 or other M2-polarising stimuli, is required for an effect of angiotensin II on CCL18 release to be observed. It is also possible that angiotensin II promotes the proliferation of M2 macrophages to increase the total amount of CCL18 released into the supernatant as we did not investigate relative cell numbers. Given AT_1R activation, albeit via IgG, has been previously shown to lead to CCL18 generation from PBMCs (15), we proposed angiotensin II mediated its effects via the AT_1 receptor. This concept was supported by our finding that the AT_1R antagonist, candesartan attenuated the angiotensin-II mediated increase CCL18 protein observed at 24 hours. However, such an effect of candesartan was not observed at a later time point (48 hours) and re-addition of the antagonist may be required for the final 24 hours of the treatment period. An ability of angiotensin II to modulate M2 macrophage function, requires further interrogation as our investigation was limited to the study of only two concentrations of angiotensin II and conclusive evidence for a role of the AT_1 receptor in mediating the response is lacking. Interestingly, we have previously reported marked IgG deposition in the aorta after 28 days of angiotensin II infusion (7) and this may represent another stimulus of CCL18 in hypertension (possibly via targeting AT_1R). Future work should investigate the effects of a range of angiotensin II concentrations and other stimuli, such as IgG, on CCL18 expression in M2 macrophages, together with re-addition of candesartan or use of AT_1R siRNA to negate the effects of the AT_1 receptor. Nonetheless, our findings reflect the potential for CCL18 to be increased in a hypertensive environment in

which the renin angiotensin aldosterone system (RAAS) is upregulated, consistent with the elevated CCL18 levels observed is several cardiovascular pathologies such as unstable angina (24), aneurysm (8) and coronary artery disease (10, 11). To our knowledge the plasma levels of CCL18 from hypertensive patients have not been reported and would be a valuable measure to evaluate the usefulness of CCL18 as a biomarker for aortic stiffening and hypertension.

With the potential for increased CCL18 in the hypertensive vasculature, we wanted to investigate whether it exerted pro-fibrotic effects on aortic adventitial fibroblasts (AoAF), a relevant vascular cell. Indeed, AoAF play an important role in aortic stiffening and readily interact with, and respond to, monocytes to generate collagen and promote fibrosis (45). Although we assessed mRNA expression of 3 collagen types, collagen I, collagen III and collagen V, we were particularly interested in collagen I as it is the most abundantly expressed collagen in the aortic adventitia and is known to contribute to vessel stiffening (36). Collagen processing in fibroblasts is a complex process first involving the synthesis of pro-collagen chains which, in the case of collagen I, form a procollagen trimer consisting of two pro-COL1A1 and one pro-COL1A2 chain folded together into a triple-helical domain, with N- and C-propeptides at either end. These propeptides are cleaved by specific N- or C-proteinases to form collagen fibrils (6). Hence there are many levels of regulation of collagen synthesis and processing which could lead to enhanced fibroblast secretion. In this study we focussed on the expression of both pro-collagen, and the cleaved collagen fibrils, in fibroblast lysates using western blotting.

The effects of CCL18 on collagen and α-SMA expression were examined over a concentration range of 3-300 ng/ml. This concentration range has previously been shown to increase

collagen generation from lung fibroblasts (2), represents levels observed in our M2 macrophage supernatants, and are relevant to measurements of plasma CCL18 levels in patients suffering from cardiovascular diseases (eg. 104 ng/ml in patients with refractory angina) (24). To validate our assay conditions, the effects of CCL18 were compared to the pro-fibrotic cytokine, TGF-β. As anticipated, TGF-β increased α-SMA mRNA and protein levels in AoAF, indicating myofibroblast differentiation, a well-documented effect of the pro-fibrotic cytokine (12, 20, 28). TGF-β also increased collagen I and V mRNA which was associated with increased collagen I protein at 24 hours. Interestingly, its modulation of collagen I protein expression appeared to be time-dependent, with its effects lost at 48 and 72 hours. A possible explanation to account for these observations is that collagen I is rapidly released into the culture supernatant and, as a result, less protein is detected in the cell lysate at these later time points. A reduced effect of TGF-β on these cells, over time, can be discounted as robust increases in α-SMA protein in response to TGF-β were still observed. Future studies will evaluate collagen protein levels in the culture supernatants.

In contrast to TGF-β, pro-fibrotic effects of CCL18 were not evident following 24 hours treatment, with no change in either collagen I or α-SMA mRNA or protein. This lack of effect of CCL18 on collagen I mRNA levels was unexpected given that CCL18 has been shown to increase collagen I mRNA expression in lung fibroblasts following 3 and 6 hours treatment. Of note, this previous study in lung fibroblasts only examined COL1A2 mRNA (2), whereas we investigated COL1A1. Although it would be predicted that both collagen I chains would increase together, it remains possible that a larger effect is observed for COL1A2, which we did not investigate. Furthermore, the reported effects in lung fibroblasts at the mRNA level were modest and only convincingly observed in one out of two fibroblast cell lines, despite

robust increases in collagen I protein throughout the study. This supports a greater ability of CCL18 to enhance protein levels, as we observed. Indeed, in AoAF, we demonstrated increased pro-collagen I protein expression at 24 hours, and this preceded an elevation in mature collagen I levels at 48 and 72 hours. Therefore we provide the first evidence that CCL18 can promote collagen production in vascular cells. The mechanisms by which CCL18 drives fibroblast collagen synthesis remain to be elucidated, but we speculate CCL18 targets its cognate receptor, CCR8 to promote fibrosis. Moreover, in addition to direct stimulation of collagen synthesis, CCL18 may elevate collagen I levels via enhancing tissue inhibitor of metalloproteinase (TIMP), or reducing matrix metalloproteinase, expression and activity. These concepts remain to be investigated.

It is important to note however, that our results with regard to α-SMA expression suggest that CCL18 does not promote myofibroblast differentiation. To our knowledge, an ability of CCL18 to modulate myofibroblast differentiation has not previously been reported, with studies utilising lung fibroblasts only assessing the effects of CCL18 on collagen expression. Given that TGF-β is also released by M2 macrophages, and plays a role in vascular remodelling, it would be interesting to determine if TGF-β and CCL18 have synergistic actions. Furthermore, whether CCL18 has additional effects on other important cell types involved in aortic fibrosis, such as fibrocytes and endothelial cells (48) or vascular smooth muscle cells (39), will be explored in future studies. Nonetheless, we provide preliminary evidence for CCL18 as a potential pro-fibrotic mediator which could enhance collagen deposition from vascular cells.

To translate our *in vitro* findings to a hypertensive setting *in vivo*, we investigated the expression of the murine functional analogue for hCCL18 (mCCL8), and its receptor CCR8, in

the aortae of normotensive (saline-treated) and hypertensive (angiotensin II-treated) mice. We have previously reported that aortic mCCL8 expression is increased following 14 days of angiotensin II infusion in mice (35). Here we extend these findings, demonstrating an approximate 3-fold increase in aortic mCCL8 mRNA expression after 28 days of angiotensin II infusion. Immunohistochemistry revealed that CCL8 expression in the vessel wall was predominantly localised to M2 macrophages, present in the adventitia and to a lesser extent in the perivascular fat. Importantly we observed a 50% increase in the number of mCCL8+CD206+ double positive cells in hypertensive, as compared to normotensive, mice. This observation concurs with our previous findings that hypertension is associated with an increase in M2 macrophages in the vessel wall (35). We now identify an ability of these cells to generate CCL8, consistent with our demonstration of enhanced M2 macrophage CCL18 expression with angiotensin II treatment *in vitro.* Although not studied here, enhanced collagen deposition and stiffening of the aorta is evident in these angiotensin II-infused mice and such remodelling is prevented by the depletion of macrophages (35). Thus CCL8 may well be contributing to M2 macrophage-mediated aortic stiffening in these mice. Future studies will utilise other models of hypertension, such as the one kidney/deoxycorticosterone acetate (DOCA)/salt model, to determine if the elevation in CCL8 is related to the stimuli used or an increase in blood pressure *per se*.

Having identified M2 macrophages as a major source of CCL8 in the hypertensive vasculature, we next sought to examine the presence of its main target, CCR8. Previous studies have reported CCR8 expression in cultured human umbilical vein endothelial cells (HUVECS) (17). Consistent with these findings, we observed CCR8 expression on endothelial cells as determined by co-localisation with vWF. To our knowledge, this is the first evidence of

endothelial cell CCR8 expression in the intact aorta. Based on these findings, it is tempting to speculate that hCCL18/mCCL8 could promote endothelial-mesenchymal transition (EndMT) to increase vessel wall collagen in addition to its actions on resident fibroblasts. This concept is supported by a study examining the role of CCL18 in tumour development, which demonstrated an ability of CCL18 to promote EndMT (29). We also found evidence of CCR8 expression in VSMCs together with numerous cells in the adventitia and perivascular fat. The identity of these cells remains to be confirmed, but they may represent T-cells and fibroblasts, given that CCR8 is known to be expressed on T cells (18) and we have shown effects of CCL18 on fibroblasts. It will be important to co-localise CCR8 with relevant cell markers and confirm antibody specificity with CCR8 deficient tissue in the future. It should also be noted that hypertension *per se* did not appear to alter the level of expression of CCR8 or its vascular localisation. Nonetheless, our findings suggest that hCCL18/mCCL8 may mediate the pro-fibrotic actions of M2 macrophages in hypertensive vasculature, potentially through CCR8. Future studies will investigate the effects of hCCL18/mCCL8 on other potential CCR8-expressing cell types such as endothelial and vascular smooth muscle cells, T cells and fibrocytes, both *in vitro* and *in vivo*. The effects of genetic deletion, or pharmacological inhibition, of the CCL18-CCR8 axis will also be investigated to further confirm their roles in hypertension.

In conclusion, this study provides the first evidence that angiotensin II promotes enhanced CCL18 generation from M2 macrophages and that CCL18 can have pro-fibrotic effects on aortic fibroblasts. We also demonstrate that chronic angiotensin II infusion in mice is associated with an increase in the population of mCCL8-expressing M2 macrophages in the adventitia and that its receptor, CCR8, is expressed on endothelial and other vascular cells.

Collectively, our findings in the angiotensin II infusion model of hypertension suggest that M2 macrophages can synthesise CCL8, which may target CCR8-expressing endothelial cells and fibroblasts to stimulate collagen production. The increased number of CCL8-expressing M2 macrophages in the vessel wall may contribute to the vascular stiffening associated with hypertension. Thus we provide further support for the key role of M2 macrophages in the pathophysiology of hypertension and targeting the CCL18/CCR8 pathway may be an effective approach to reduce aortic stiffening and cardiovascular events.

References

1. Achelrod D, Wenzel U, and Frey S. Systematic review and meta-analysis of the prevalence of resistant hypertension in treated hypertensive populations. *American journal of hypertension* 28: 355-361, 2015.

2. Atamas SP, Luzina IG, Choi J, Tsymbalyuk N, Carbonetti NH, Singh IS, Trojanowska M, Jimenez SA, and White B. Pulmonary and activation-regulated chemokine stimulates collagen production in lung fibroblasts. *Am J Respir Cell Mol Biol* 29: 743-749, 2003.

3. Blacher J, Asmar R, Djane S, London GM, and Safar ME. Aortic pulse wave velocity as a marker of cardiovascular risk in hypertensive patients. *Hypertension* 33: 1111-1117, 1999.

4. Brix SR, Stege G, Disteldorf E, Hoxha E, Krebs C, Krohn S, Otto B, Klatschke K, Herden E, Heymann F, Lira SA, Tacke F, Wolf G, Busch M, Jabs WJ, Ozcan F, Keller F, Beige J, Wagner K, Helmchen U, Noriega M, Wiech T, Panzer U, and Stahl RA. CC Chemokine Ligand 18 in ANCA-Associated Crescentic GN. *Journal of the American Society of Nephrology : JASN* 26: 2105-2117, 2015.

5. Bromfield S, and Muntner P. High blood pressure: the leading global burden of disease risk factor and the need for worldwide prevention programs. *Curr Hypertens Rep* 15: 134-136, 2013.

6. Canty EG, and Kadler KE. Procollagen trafficking, processing and fibrillogenesis. *Journal of cell science* 118: 1341-1353, 2005.

7. Chan CT, Sobey CG, Lieu M, Ferens D, Kett MM, Diep H, Kim HA, Krishnan SM, Lewis CV, Salimova E, Tipping P, Vinh A, Samuel CS, Peter K, Guzik TJ, Kyaw TS, Toh BH, Bobik A, and Drummond GR. Obligatory Role for B Cells in the Development of Angiotensin II-Dependent Hypertension. *Hypertension* 66: 1023-1033, 2015.

8. Courtois A, Nusgens BV, Hustinx R, Namur G, Gomez P, Kuivaniemi H, Defraigne JO, Colige AC, and Sakalihasan N. Gene expression study in positron emission tomography-positive abdominal aortic aneurysms identifies CCL18 as a potential biomarker for rupture risk. *Molecular medicine (Cambridge, Mass)* 20: 697-706, 2014.

9. De Ciuceis C, Amiri F, Brassard P, Endemann DH, Touyz RM, and Schiffrin EL. Reduced Vascular Remodeling, Endothelial Dysfunction, and Oxidative Stress in Resistance Arteries of Angiotensin II–Infused Macrophage Colony-Stimulating Factor–Deficient Mice. *Ateriosl cerosis, Thrombosis and Vascular Biology* 25: 2106-2113, 2005.

10. de Jager SC, Bongaerts BW, Weber M, Kraaijeveld AO, Rousch M, Dimmeler S, van Dieijen-Visser MP, Cleutjens KB, Nelemans PJ, van Berkel TJ, and Biessen EA. Chemokines CCL3/MIP1alpha, CCL5/RANTES and CCL18/PARC are independent risk predictors of short-term mortality in patients with acute coronary syndromes. *PLoS One* 7: e45804, 2012.

11. De Sutter J, Struyf S, Van de Veire NR, Philippe J, De Buyzere M, and Van Damme J. Cardiovascular determinants and prognostic significance of CC Chemokine Ligand-18 (CCL18/PARC) in patients with stable coronary artery disease. *Journal of molecular and cellular cardiology* 49: 894-896, 2010.

12. Desmouliere A, Geinoz A, Gabbiani F, and Gabbiani G. Transforming growth factor-beta 1 induces alpha-smooth muscle actin expression in granulation tissue myofibroblasts and in quiescent and growing cultured fibroblasts. *The Journal of cell biology* 122: 103-111, 1993.

13. Egan BM, Zhao Y, Axon RN, Brzezinski WA, and Ferdinand KC. Uncontrolled and apparent treatment resistant hypertension in the United States, 1988 to 2008. *Circulation* 124: 1046-1058, 2011.

14. Franklin SS, Gustin Wt, Wong ND, Larson MG, Weber MA, Kannel WB, and Levy D. Hemodynamic patterns of age-related changes in blood pressure. The Framingham Heart Study. *Circulation* 96: 308-315, 1997.

15. Gunther J, Kill A, Becker MO, Heidecke H, Rademacher J, Siegert E, Radic M, Burmester GR, Dragun D, and Riemekasten G. Angiotensin receptor type 1 and endothelin receptor type A on immune cells mediate migration and the expression of IL-8 and CCL18 when stimulated by autoantibodies from systemic sclerosis patients. *Arthritis research & therapy* 16: R65, 2014.

16. Hagg DA, Olson FJ, Kjelldahl J, Jernas M, Thelle DS, Carlsson LM, Fagerberg B, and Svensson PA. Expression of chemokine (C-C motif) ligand 18 in human macrophages and atherosclerotic plaques. *Atherosclerosis* 204: e15-20, 2009.

17. Haque NS, Fallon JT, Pan JJ, Taubman MB, and Harpel PC. Chemokine receptor-8 (CCR8) mediates human vascular smooth muscle cell chemotaxis and metalloproteinase-2 secretion. *Blood* 103: 1296-1304, 2004.

18. Islam SA, Chang DS, Colvin RA, Byrne MH, McCully ML, Moser B, Lira SA, Charo IF, and Luster AD. Mouse CCL8, a CCR8 agonist, promotes atopic dermatitis by recruiting IL-5+ T(H)2 cells. *Nat Immunol* 12: 167-177, 2011.

19. Islam SA, Ling MF, Leung J, Shreffler WG, and Luster AD. Identification of human CCR8 as a CCL18 receptor. *J Exp Med* 210: 1889-1898, 2013.

20. Jester JV, Barry-Lane PA, Cavanagh HD, and Petroll WM. Induction of alpha-smooth muscle actin expression and myofibroblast transformation in cultured corneal keratocytes. *Cornea* 15: 505-516, 1996.

21. Kaess BM, Rong J, Larson MG, and et al. Aortic stiffness, blood pressure progression, and incident hypertension. *JAMA* 308: 875-881, 2012.

22. Kannel WB. Hypertension: reflections on risks and prognostication. *The Medical clinics of North America* 93: 541-558, Table of Contents, 2009.

23. Ko EA, Amiri F, Pandey NR, Javeshghani D, Leibovitz E, Touyz RM, and Schiffrin EL. Resistance artery remodeling in deoxycorticosterone acetate-salt hypertension is dependent on vascular inflammation: evidence from m-CSF-deficient mice. *American journal of physiology Heart and circulatory physiology* 292: H1789-1795, 2007.

24. Kraaijeveld AO, de Jager SC, de Jager WJ, Prakken BJ, McColl SR, Haspels I, Putter H, van Berkel TJ, Nagelkerken L, Jukema JW, and Biessen EA. CC chemokine ligand-5 (CCL5/RANTES) and CC chemokine ligand-18 (CCL18/PARC) are specific markers of refractory unstable angina pectoris and are transiently raised during severe ischemic symptoms. *Circulation* 116: 1931-1941, 2007.

25. Krege JH, Hodgin JB, Hagaman JR, and Smithies O. A noninvasive computerized tail-cuff system for measuring blood pressure in mice. *Hypertension* 25: 1111-1115, 1995.

26. Laffin LJ, and Bakris GL. Endothelin antagonism and hypertension: an evolving target. *Seminars in nephrology* 35: 168-175, 2015.

27. Laurent S, Boutouyrie P, Asmar R, Gautier I, Laloux B, Guize L, Ducimetiere P, and Benetos A. Aortic Stiffness Is an Independent Predictor of All-Cause and Cardiovascular Mortality in Hypertensive Patients. *Hypertension* 37: 1236-1241, 2001.

28. Lijnen P, and Petrov V. Transforming growth factor-beta 1-induced collagen production in cultures of cardiac fibroblasts is the result of the appearance of myofibroblasts. *Methods and findings in experimental and clinical pharmacology* 24: 333-344, 2002.

29. Lin L, Chen YS, Yao YD, Chen JQ, Chen JN, Huang SY, Zeng YJ, Yao HR, Zeng SH, Fu YS, and Song EW. CCL18 from tumor-associated macrophages promotes angiogenesis in breast cancer. *Oncotarget* 6: 34758-34773, 2015.

30. Ma LJ, Corsa BA, Zhou J, Yang H, Li H, Tang YW, Babaev VR, Major AS, Linton MF, Fazio S, Hunley TE, Kon V, and Fogo AB. Angiotensin type 1 receptor modulates macrophage polarization and renal injury in obesity. *American journal of physiology Renal physiology* 300: F1203-1213, 2011.

31. Martinez FO, Gordon S, Locati M, and Mantovani A. Transcriptional profiling of the human monocyte-to-macrophage differentiation and polarization: New molecules and patterns of gene expression. *Journal of Immunology* 177: 7303-7311, 2006.

32. Meaume S, Benetos A, Henry OF, Rudnichi A, and Safar ME. Aortic pulse wave velocity predicts cardiovascular mortality in subjects >70 years of age. *Arterioscler Thromb Vasc Biol* 21: 2046-2050, 2001.

33. Mian MO, Paradis P, and Schiffrin EL. Innate immunity in hypertension. *Curr Hypertens Rep* 16: 413, 2014.

34. Mitchell GF, Hwang SJ, Vasan RS, Larson MG, Pencina MJ, Hamburg NM, Vita JA, Levy D, and Benjamin EJ. Arterial stiffness and cardiovascular events: the Framingham Heart Study. *Circulation* 121: 505-511, 2010.

35. Moore JP, Vinh A, Tuck KL, Sakkal S, Krishnan SM, Chan CT, Lieu M, Samuel CS, Diep H, Kemp-Harper BK, Tare M, Ricardo SD, Guzik TJ, Sobey CG, and Drummond GR. M2 macrophage accumulation in the aortic wall during angiotensin II infusion in mice is associated with fibrosis, elastin loss, and elevated blood pressure. *American journal of physiology Heart and circulatory physiology* 309: H906-917, 2015.

36. Osidak MS, Osidak EO, Akhmanova MA, Domogatsky SP, and Domogatskaya AS. Fibrillar, fibril-associated and basement membrane collagens of the arterial wall: architecture, elasticity and remodeling under stress. *Current pharmaceutical design* 21: 1124-1133, 2015.

37. Pochetuhen K, Luzina IG, Lockatell V, Choi J, Todd NW, and Atamas SP. Complex regulation of pulmonary inflammation and fibrosis by CCL18. *The American journal of pathology* 171: 428-437, 2007.

38. Reape TJ, Rayner K, Manning CD, Gee AN, Barnette MS, Burnand KG, and Groot PH. Expression and cellular localization of the CC chemokines PARC and ELC in human atherosclerotic plaques. *The American journal of pathology* 154: 365-374, 1999.

39. Rocnik EF, Chan BM, and Pickering JG. Evidence for a role of collagen synthesis in arterial smooth muscle cell migration. *J Clin Invest* 101: 1889-1898, 1998.

40. Schmittgen TD, and Livak KJ. Analyzing real-time PCR data by the comparative C-T method. *Nature Protocols* 3: 1101-1108, 2008.

41. Schutyser E, Richmond A, and Van Damme J. Involvement of CC chemokine ligand 18 (CCL18) in normal and pathological processes. *J Leukoc Biol* 78: 14-26, 2005.

42. Tarique AA, Logan J, Thomas E, Holt PG, Sly PD, and Fantino E. Phenotypic, functional, and plasticity features of classical and alternatively activated human macrophages. *Am J Respir Cell Mol Biol* 53: 676-688, 2015.

43. Te Riet L, van Esch JH, Roks AJ, van den Meiracker AH, and Danser AH. Hypertension: renin-angiotensin-aldosterone system alterations. *Circ Res* 116: 960-975, 2015.

44. Thang LV, Demel SL, Crawford R, Kaminski NE, Swain GM, Van Rooijen N, and Galligan JJ. Macrophage depletion lowers blood pressure and restores sympathetic nerve alpha2-adrenergic receptor function in mesenteric arteries of DOCA-salt hypertensive rats. *American journal of physiology Heart and circulatory physiology* 309: H1186-1197, 2015.

45. Tieu BC, Ju X, Lee C, Sun H, Lejeune W, Recinos A, 3rd, Brasier AR, and Tilton RG. Aortic adventitial fibroblasts participate in angiotensin-induced vascular wall inflammation and remodeling. *Journal of vascular research* 48: 261-272, 2011.

46. Versteylen MO, Manca M, Joosen IA, Schmidt DE, Das M, Hofstra L, Crijns HJ, Biessen EA, and Kietselaer BL. CC chemokine ligands in patients presenting with stable chest pain: association with atherosclerosis and future cardiovascular events. *Netherlands heart journal : monthly journal of the Netherlands Society of Cardiology and the Netherlands Heart Foundation* 24: 722-729, 2016.

47. Wenzel P, Knorr M, Kossmann S, Stratmann J, Hausding M, Schuhmacher S, Karbach SH, Schwenk M, Yogev N, Schulz E, Oelze M, Grabbe S, Jonuleit H, Becker C, Daiber A, Waisman A, and Munzel T. Lysozyme M-positive monocytes mediate angiotensin II-induced arterial hypertension and vascular dysfunction. *Circulation* 124: 1370-1381, 2011.

48. Wu J, Montaniel KR, Saleh MA, Xiao L, Chen W, Owens GK, Humphrey JD, Majesky MW, Paik DT, Hatzopoulos AK, Madhur MS, and Harrison DG. Origin of Matrix-Producing Cells That Contribute to Aortic Fibrosis in Hypertension. *Hypertension* 67: 461-468, 2016.

49. Yamamoto S, Yancey PG, Zuo Y, Ma LJ, Kaseda R, Fogo AB, Ichikawa I, Linton MF, Fazio S, and Kon V. Macrophage polarization by angiotensin II-type 1 receptor aggravates renal injury-acceleration of atherosclerosis. *Arterioscler Thromb Vasc Biol* 31: 2856-2864, 2011.

50. Yang S, Zhong Q, Qiu Z, Chen X, Chen F, Mustafa K, Ding D, Zhou Y, Lin J, Yan S, Deng Y, Wang M, Zhou Y, Liao Y, and Zhou Z. Angiotensin II receptor type 1 autoantibodies promote endothelial microparticles formation through activating p38 MAPK pathway. *J Hypertens* 32: 762-770, 2014.

CHAPTER 7:

GENERAL DISCUSSION

7.1 Summary of key findings

Macrophages play crucial roles in the development of cardiovascular diseases such as atherosclerosis and hypertension (19, 107). It is well known that these immune cells can adopt multiple phenotypes in response to local stimuli, including, but not limited to, the pro-inflammatory M1 (classically activated) and the wound healing M2 (alternatively activated) macrophage (110). However, there remains a lack of robust markers for the identification of distinct macrophage subsets that can be translated from *in vitro* culture to an *in vivo* setting and to human disease. Furthermore, while M2 macrophages are often thought to be protective in cardiovascular settings, potential pathogenic roles in the development of both atherosclerosis and hypertension have emerged (58, 87, 90). In this thesis we identified novel markers of macrophage polarisation and validated IFIT1 as a potential M1 biomarker in atherosclerosis (Chapter 3). Exploration of NAPDH oxidase expression and activity revealed that, contrary to the generally accepted dogma, enhanced ROS generation is not necessarily indicative of an M1 phenotype but appears to also be involved in M2 macrophage function (Chapter 4). Given that opposing roles of the M2 polarising stimuli IL-4 and IL-13 in the pathogenesis of atherosclerosis have been reported (13, 58), we investigated whether this was related to differing effects on M2 macrophage function. We suggest that their differential roles may be through actions on other cell types involved in atherogenesis, as no major differences in their effects on macrophage function were observed (Chapter 5). Finally, we demonstrated that the M2 macrophage-derived pro-fibrotic chemokine, CCL18 could be an important mediator of aortic stiffening during hypertension and hence holds promise as a potential therapeutic target for cardiovascular disease (Chapter 6).

7.2 Identifying M1 and M2 macrophages in disease settings

Although there are a number of markers and functions commonly associated with M1 and M2 macrophages, characterisation of these phenotypes is ongoing. Additionally, some currently used markers may require reassessment as they can be common to multiple macrophages phenotypes, exhibit only low expression in *in vivo* models of disease or lack translation into humans (79, 88, 104). In Chapter 3 we adopted a global quantitative proteomic approach to identify key markers of M1 and M2 polarisation, stimulated by combination treatment with IFN-γ and LPS, or IL-4, respectively. We identified a large number of proteins that were differentially expressed between unpolarised, M1 or M2 phenotypes in THP-1 macrophages. Importantly, in addition to confirming a number of currently used markers such as STAT1, CD14, NFκB and CCL5 for M1 (22, 79, 99), and CD209, TGM2 and F13A1 for M2 (25, 79, 80), we observed striking upregulation of a family of related proteins (IFIT1, IFIT2 and IFIT3) in M1 macrophages. These findings were confirmed in human primary macrophages, a more clinically relevant cell line. We also demonstrated IFIT1 staining in a subset of macrophages (F4/80+ cells) within the plaques of $ApoE^{-/-}$ mice, suggesting that it could be used as an M1 marker in this setting. Future experiments should compare this staining with currently used M1 markers as well as confirming these findings in human atherosclerotic plaques and in other diseases involving M1 macrophages.

A large proportion of the identified proteins upregulated under M1 conditions in Chapter 3 were related to IFN-γ signalling through the transcription factor IRF-1. As such it cannot be ruled out that some of these identified proteins are specific for IFN-γ treatment and comparison with additional M1 stimuli such as TNFα and IL-1β will be important in further validating their use as markers. Interestingly however, while the type I interferons, IFN-α and IFN-β, are known to strongly induce IFIT expression (27, 30), IFN-γ was previously reported as

only a weak stimulus for IFIT upregulation (27), suggesting synergistic effects with LPS in our study. IFIT1 proteins play critical roles in fighting viral infection and hence a role in M1 macrophage function is expected (30).

Interestingly, there is a large body of evidence pointing to the involvement of viral and bacterial infections in the pathogenesis of atherosclerosis (12). In particular, clinical and epidemiological studies of influenza demonstrate increased rates of cardiovascular mortality and myocardial infarction during epidemics (3, 113). Influenza virus has also been detected within human atherosclerotic lesions and increased influenza antibody levels were observed in patients with ischemic heart disease as compared to asymptomatic controls (37). Moreover, several large scale clinical trials have found reductions in cardiovascular morbidity and mortality in patients vaccinated against influenza (17, 74, 108). Similar associations with atherosclerosis are reported for other viral infections such as herpes simplex virus (60), human cytomegalovirus (15, 34, 120) and human immunodeficiency virus (43) pointing to a role for viral infection *per se* in atherogenesis. Taken together, these findings suggest that IFIT1, and other related anti-viral proteins identified in Chapter 3, may not only be valid M1 markers but could also serve as early biomarkers for the development of coronary artery disease.

Our proteomic analysis revealed a much smaller group of proteins associated with M2, as compared with M1, polarisation. It is interesting to note that throughout the current thesis, the traditional 'M2 markers' IL-10 and TGF-β are not strongly induced by IL-4 or IL-13 in either THP-1 or primary macrophages (Chapters 3-5). Thus in Chapters 3 and 4, TGF-β mRNA and protein expression was modestly increased in M1 (~1.5-fold) and M2 (~1.8-fold) THP-1 macrophages. Moreover, there was no clear effect of macrophage polarisation on TGF-β

expression in human primary macrophages (Chapter 4 and 5). These observations are in agreement with a previous study in THP-1 macrophages in which IL-4 and IL-13 had little impact on TGF-β generation (10). Collectively, these findings suggest that TGF-β is not a strong marker of M2a polarisation (induced with IL-4). Additionally, we observed either no effect (THP-1 macrophages) or down regulation (primary macrophages) of IL-10 expression following IL-4 treatment, consistent with a previous study of human primary macrophages (61). Furthermore, we and others (61), have demonstrated increased IL-6 expression in IL-4-treated macrophages (Chapter 4 and 5). These findings highlight that the M2a macrophage subset is not necessarily anti-inflammatory and hence markers related to immunosuppression are unlikely to identify this phenotype. Going forward it will be important to distinguish between this subset and the 'resolving' (M2c) phenotype induced by IL-10 and other anti-inflammatory stimuli. Importantly, we found that the chemokine, CCL18 was a much stronger marker of M2 polarisation than any other M2 marker investigated. This was particularly true in human primary macrophages where increases in CCL18 expression, of up to 800-fold, were observed after 24 hours of polarisation (Chapter 4). Having also co-localised its murine counterpart, CCL8 with the M2 marker, CD206 *in vivo* (Chapter 6), we have revealed that CCL18 may be a more robust and valid marker of the M2a phenotype.

Finally, while ROS generation has previously been considered a hallmark of M1 polarisation, our findings in Chapter 4 challenge this notion. Given NOX2 oxidase-derived superoxide was enhanced in both M1 (IFN-y/LPS-polarised) and M2 (IL-4-polarised) macrophages, staining for, or measurement of, macrophage ROS is unlikely to distinguish between these phenotypes. Interestingly, enhanced NOX2 oxidase activity, in M1 and M2 macrophages, appeared to occur through upregulation of the p47phox and p67phox subunits, respectively. This raises the interesting concept that these subunits may serve as additional markers of

macrophage polarisation in the future. Of note, although similar observations were made in human primary macrophages at the mRNA level, we did not detect changes in p47phox or p67phox subunit protein in these cells, suggesting these effects may be specific to the THP-1 macrophage cell line. It should also be acknowledged that much of the work in this thesis focused on the characterisation of macrophage phenotypes *in vitro*. It will be important to validate these findings in the more complex *in vivo* disease setting in the future, particularly in human tissue.

7.3 M2 macrophages: friend or foe?

The label 'M2' defines a broad category of macrophages, including those polarised with any 'alternative' (i.e not typically pro-inflammatory) stimulus. Hence we, and others, have highlighted the importance of the precise stimulus in dictating the properties of M2 macrophages which could contribute to, or protect against, disease. Whilst a capacity to reduce inflammation is likely to be protective in cardiovascular disease, we have shown that this is not necessarily a characteristic of all M2 macrophages. Additionally, given their roles in the wound healing response, M2a macrophages can promote fibrosis when over-activated. Indeed their ability to enhance ECM generation and promote vessel remodelling may aid in the stabilisation of atherosclerotic plaques (23), but is also likely to contribute to the pathogenesis of hypertension, promoting aortic fibrosis and vascular stiffening (87). Thus while a reduction in the M1 macrophage population is certainly protective in both atherosclerosis and hypertension (41, 114), and M1 macrophages are crucially involved in the initial inflammatory response, the contribution of the M2 macrophage is likely to depend on both the stage, and nature of, the disease itself. In this thesis we identified the potential roles of ROS, particularly hydrogen peroxide, and the chemokine, CCL18 in the pro-fibrotic actions of M2a macrophages and highlighted that these, and other effector molecules generated by

macrophages, may be more valuable therapeutic targets than attempting to alter macrophage polarisation itself.

7.3.1 Oxidative stress and inflammation

Many reviews of macrophage polarisation and function state that the M1 macrophage is distinguishable by its ability to generate large amounts of reactive oxygen and nitrogen species and promote inflammation. In contrast, the M2 phenotype is considered to be anti-inflammatory and generate limited ROS (78, 104, 110). However, while we showed that M1 macrophages do indeed express much higher levels of the pro-inflammatory cytokines IL-1β, TNFα, and IL-6 than M2 (IL-4-polarised) macrophages, as discussed above, the M2a subset was not found to be an anti-inflammatory phenotype. Furthermore, both M1 and M2a macrophages demonstrated enhanced generation of ROS as compared to unpolarised macrophages (Chapter 4). This increase in superoxide generation was also observed when M2 macrophages were polarised with IL-13 (Chapter 5), suggesting an action common to M2a macrophages as part of the Th2 response. In THP-1 macrophages, we showed that the primary source of superoxide is NOX2 oxidase, and that M1 polarisation enhanced the expression of the NOX2 catalytic and p47phox subunits, whilst M2 polarisation increased p67phox expression. Several pro-inflammatory signalling pathways, which are involved in M1 polarisation, can lead to upregulation of these subunits. In particular, the transcription factors NFκB (1) and STAT1 (64) have both been shown to induce NOX2 oxidase subunit expression. Furthermore, STAT1 and IRF-1 pathways (91), as well as activation of TLR2 and induction of apoptosis-related signalling kinase 1 (ASK1) pathways (117), can induce p47phox expression in M1 macrophages.

With regard to M2 macrophages, the signalling that may lead to enhanced NOX2 oxidase activity is less well known. Given that we showed STAT3 involvement in M2 polarisation in Chapter 5, and STAT3 activation can induce p67phox expression in human smooth muscle cells (77), this is one potential mechanism by which NOX2 oxidase activity could be enhanced. Furthermore p38 MAPK pathways can also be induced by IL-4 and regulate NOX expression and activity (50, 100). Interestingly, we observed NOX5 expression in macrophages which was upregulated following IL-4 treatment in the THP-1 cell line. NOX5 upregulation via CREB has been previously reported (32) and is downstream of p38 MAPK. Although the superoxide signal was shown to be predominantly NOX2-derived, a contribution of NOX5 to this, and the hydrogen peroxide signal, cannot be discounted and NOX5 siRNA treatment could be utilised in the future investigate this. Finally, to comprehensively elucidate the signalling pathways implicated in increasing macrophage ROS generation following macrophage polarisation in our studies, future experiments should investigate the expression and phosphorylation of these transcription factors and their potential involvement in enhancing NOX activity. Considering our findings for STAT3 in Chapter 5, it would be particularly interesting to investigate whether STAT3 inhibition could attenuate NOX2 activity in M2 macrophages and thus reduce the superoxide and hydrogen peroxide signals observed in these cells.

Importantly, we identified in Chapter 4 that enhanced hydrogen peroxide production was a characteristic of M2, but not M1, macrophages. This could be a key point of difference between M1 and M2 macrophages, and we suggest that in M1 macrophages superoxide is not necessarily dismutated to hydrogen peroxide. Rather, superoxide may react with nitric oxide, derived from iNOS, to generate the highly damaging peroxynitrite molecule (94, 112). Whilst we were unable to confirm peroxynitrite generation in M1 macrophages, it remains a focus of future studies. Our finding of greater hydrogen peroxide generation in M2, versus

M1, macrophages is of interest. Although we did not confirm the source of hydrogen peroxide, we proposed that it was generated via the dismutation of NOX2-derived superoxide by SOD3, which was upregulated at the mRNA level in M2 macrophages. It is possible, however, that hydrogen peroxide may be derived from a NOX2 oxidase-independent source. Thus PDBu did not stimulate hydrogen peroxide generation above basal levels, as it did for superoxide generation (Chapter 4). In addition, although we did not detect NOX4 mRNA in either THP-1 or human primary macrophages, others have reported its expression in human macrophages (67, 86). As such this constitutively active enzyme, which predominantly produces hydrogen peroxide, may serve as an important source of hydrogen peroxide in M2 macrophages. This concept is further supported by the finding that ox-LDL upregulates NOX4 expression in macrophages via the MEK/ERK pathway (67), which is also involved in IL-4-stimulated M2 polarisation (54). Hence there is potential for IL-4 to upregulate NOX4 in macrophages. Future experiments could utilise NOX2, NOX4 and NOX5 siRNA to elucidate the major source of hydrogen peroxide in M2 macrophages and investigate the role of these potential signalling pathways.

In this thesis we have shown that the regulation of ROS in macrophages, with distinct polarisation states, is complex but importantly we highlight that superoxide generation is associated with both M1 and M2a polarisation. Thus in addition to M1 macrophages, M2a macrophages could contribute to the oxidative stress and inflammation, which is characteristic of both atherosclerosis and hypertension. Overall these findings suggest that a reduction in the infiltrating macrophage population per se is likely to confer protection via reducing inflammation and oxidative stress in the vessel wall. Interestingly, we also suggested that the nature of the downstream ROS generated by M1 and M2 macrophages may also differ, favouring peroxynitrite and hydrogen peroxide, respectively. With regard to M1

macrophages, peroxynitrite may contribute to their ability to cause tissue damage, particularly endothelial injury which can initiate atherosclerosis (112). Considering M2 macrophages, hydrogen peroxide could play a role in intracellular or paracrine signalling (2, 98) and in atherogenic or pro-fibrotic responses (67, 111), which will be discussed below.

7.3.2 Roles in atherosclerosis

Although increasing the proportion of M2 macrophages is commonly associated with reduced lesion size and stabilised plaques (41, 55), debate remains as to whether these macrophages also contribute to the pathogenesis of atherosclerosis (90). Indeed it is difficult to ascertain whether the protective effects of reducing the M1:M2 ratio are simply through attenuating the M1 macrophage population or through increasing the number of M2 macrophages in plaques. An atheroprotective role of M2 macrophages has been proposed as M2 macrophages are found in more stable areas of plaque (16, 105), are associated with enhanced collagen and TGF-β expression in lesions (13, 33) and can themselves be a source of collagen within plaques (82). However, some pro-atherogenic characteristics, such as enhanced foam cell formation and contribution to the necrotic core have also been identified (45, 90). Furthermore, expression of the M2 marker, CD163 was shown to be increased in symptomatic carotid plaques and was strongly correlated with iron deposits, suggesting a potential role in intraplaque haemorrhage and plaque destabilisation (44). Overall our studies of the M2a macrophage phenotype point to a range of roles in atherosclerosis, with potential contributions to oxidative stress and inflammation but also stabilisation through pro-fibrotic actions.

In Chapter 5, we found that both the M2a stimuli, IL-4 and IL-13, increased macrophage NOX2 oxidase-mediated superoxide generation. Given NOX2 oxidase is strongly associated with the

development of atherosclerosis (52), this function of M2 macrophages could further promote inflammatory responses in the vessel wall (85). In contrast to superoxide, the role that M2 macrophage-derived hydrogen peroxide may play in atherogenesis is less clear, though as a potential pro-fibrotic factor, it may contribute to plaque stabilisation through enhanced collagen deposition. In support of an atheroprotective role of hydrogen peroxide, genetic deletion of the hydrogen peroxide-producing NOX isoform, NOX4, was shown to exacerbate inflammation, vascular remodelling and atherosclerotic lesion development in mouse models of the disease (28, 65, 102). However a pro-atherogenic role of hydrogen peroxide has also been reported. As such, enhanced hydrogen peroxide production in the vessel wall was found to increase atheroma formation (56) and overexpression of the hydrogen peroxide scavenger, catalase reduced atherogenesis (118). Therefore, in addition to its potential to confer protection in this setting, enhanced hydrogen peroxide generation could further implicate M2 macrophages in the progression of atherosclerosis.

In Chapter 5 we sought to identify a mechanism which could explain the protective and pathogenic roles reported for IL-13 and IL-4 respectively, in the setting of atherosclerosis. We proposed that this may be through differing effects on macrophage function as IL-4 can activate both type I (IL-4Rα/IL-2Rγ) and type II (IL-4Rα/IL-13Rα1) receptors on macrophages, where IL-13 exclusively activates the type II receptor. We compared IL-4 and IL-13 in terms of their potency to promote M2 polarisation and their effects on macrophage ROS and MMP generation. Though we predicted that IL-4 may promote a more inflammatory, ROS-generating phenotype than IL-13, we didn't observe any substantial differences which could explain their distinct roles in this disease state. However, the parameters of our study were somewhat limited, mostly focussed on ROS and MMP production, and a more thorough investigation of the effects of IL-4 and IL-13 on macrophage function should assess additional

characteristics relevant to atherosclerosis such as the expression of a panel of cytokines, chemokines and stress-related factors, lipid uptake, and apoptosis. Nonetheless, our finding of similar potency and efficacy of IL-4 and IL-13 to promote M2 polarisation would suggest that both cytokines signal predominantly through the type II receptor in M-CSF-differentiated human primary macrophages. Future studies knocking down components of the type I and II receptor complexes will provide definitive evidence of the main target of IL-4 vs IL-13 on macrophages. It should be acknowledged that our findings are at odds with a study in human monocytes and murine macrophages, where IL-4 was shown to act more potently through the type I receptor to enhance STAT6 phosphorylation and downstream M2 marker expression (53). However, based upon our findings in human primary macrophages we propose that the differential effects of IL-4 and IL-13 in atherosclerosis are most likely through actions on other cell types.

Although IL-4 and IL-13 are closely related cytokines with similar functions, IL-4 has been proposed as a more dominant 'immunoregulatory' cytokine. Indeed, some Th2 functions such as IgE production require IL-4, but not IL-13 (18, 57). By contrast, IL-13 has a potentially more limited impact on immune cells, rather targeting non-immune cells to modulate effector functions (29, 35). Such differences arise as the type I, rather than type II, receptor is the predominant IL-4 receptor expressed on T and B cells. This is of particular relevance in mice where the type II receptor is reportedly absent (53). Moreover, non-immune cells exclusively express the type II receptor and not the IL-4-specific type I receptor (53, 81, 116). Taking the differential expression of the type I and type II receptors into consideration, it is anticipated that in the setting of atherosclerosis IL-13 may have more potent effects on vascular cells rather than macrophages and other immune cells. Indeed this may underlie IL-13's well-documented roles in fibrosis and TGF-β1 signalling (68, 116), potentially leading to plaque

stabilisation. This protective, pro-fibrotic response to IL-13 may be further enhanced via its ability to activate IL-13Rα2, a cell surface 'decoy' receptor, on macrophages or other cell types such as fibroblasts (10, 31, 39). Indeed IL-13 exhibits exceptionally high affinity for IL-13Rα2 yet IL-4 does not activate this receptor (75). Furthermore, the effects of IL-4 on non-immune cells appear to be more inflammatory in nature, with IL-4 promoting oxidative stress and adhesion molecule expression on endothelial and vascular smooth muscle cells (69-72). Thus, despite our finding of similar effects of IL-4 and IL-13 on macrophage function, the actions of IL-4 and IL-13 on other cell types to promote inflammation and fibrosis, respectively, could explain their opposing roles in the development of atherosclerosis. Nonetheless it remains possible that the opposing effects of IL-4 and IL-13 deficiency observed in the setting of atherosclerosis, are due to differences in the nature of the studies themselves. To date, no single study has directly compared the impact of IL-4 and IL-13 inhibition, or treatment, on atherogenesis. Future studies should explore these concepts by contrasting the actions of IL-4 and IL-13, in parallel, during atherosclerosis *in vivo.*

Importantly, we also identified an ability of both IL-4 and IL-13 to cause a striking increase in the generation of the pro-fibrotic chemokine, CCL18 from human primary macrophages. As such, CCL18 represents a highly expressed marker of M2a macrophages. Interestingly, recent studies have observed CCL18 expression in human carotid plaques, and report co-localisation with plaque macrophages (38, 93, 97). Although the phenotype of these macrophages was not investigated, our findings suggest they are likely to be of the M2a subset. Of note, CCL18 itself also promotes M2 polarisation (101). Interestingly, one study has reported upregulated CCL18 expression in unstable sections of human carotid plaques as compared to stable areas (93), suggesting that this chemokine may serve as a biomarker of future cardiovascular events. Indeed, this concept is supported by a growing body of evidence in which elevated

plasma CCL18 levels have been correlated with cardiovascular mortality in patients with stable coronary artery disease (CAD) (26) and acute coronary syndromes (24), and CCL18 levels are raised in unstable angina pectoris (62) and aortic aneurysm rupture (21). Of note, one study in patients with obstructive CAD reported elevated plasma CCL18 levels in patients as compared to healthy controls, but did not find the chemokine to be predictive of future cardiovascular events (109).

The majority of the data obtained to date, suggests that CCL18 serves as a biomarker for adverse cardiovascular outcomes in patients with CAD. Whether elevated CCL18 levels contribute to the pathophysiology of the disease or arise as a compensatory mechanism to limit atherogenesis, remains to be determined. Indeed the pro-fibrotic (4) and angiogenic (73) actions of CCL18 could aid in the stabilisation of atherosclerotic plaques. Regardless of the role of CCL18 in atherosclerosis, this chemokine is emerging as a key marker of human cardiovascular disease.

7.3.3 Roles in hypertension and aortic fibrosis

Although M1 macrophages are present in the early stages of hypertension and can contribute to endothelial dysfunction (59), M2 macrophages have recently been identified as the dominant macrophage phenotype in the vessel wall at the later stages of hypertension where they are implicated in vascular remodelling and aortic stiffening (87). In this thesis we identified two potential novel, M2 macrophage-derived mediators of this pro-fibrotic response in the vessel wall, namely hydrogen peroxide and CCL18.

In Chapter 4 we showed that M2 macrophages have an enhanced capacity to generate hydrogen peroxide and suggested that this ROS could promote collagen expression in aortic fibroblasts. Moreover, we provided preliminary data to suggest that co-culture of aortic

fibroblasts with M2 macrophages increased fibroblast collagen expression to a greater extent than co-culture with unpolarised or M1-polarised macrophages. This effect of M2 macrophages was attenuated by treatment with the hydrogen peroxide scavenger, PEG-catalase. Although additional experiments are required to confirm these observations, our findings are supported by previously identified pro-fibrotic actions of hydrogen peroxide in both cardiac and adventitial fibroblasts (36, 111). Furthermore, catalase overexpression in renal proximal tubular cells has been shown to reduce interstitial fibrosis and prevent hypertension in diabetic mice (8, 103) and the hypertensive stimulus angiotensin II downregulates catalase expression in adventitial fibroblasts (119), suggesting increased hydrogen peroxide may be present in a hypertensive environment.

In addition to highlighting the potential pro-fibrotic actions of M2 macrophage-derived hydrogen peroxide generation, in Chapter 6, we provided the first evidence that the chemokine, CCL18 may also serve as an important contributor to M2 macrophage-mediated aortic stiffening in hypertension. We showed that the hypertensive stimulus, angiotensin II augments CCL18 generation from human primary M2 macrophages and that the expression of CCL8, the murine functional analogue of CCL18 (47, 48), is upregulated in the aortae of hypertensive mice. Furthermore, we suggested that M2 macrophages serve as the predominant source of this increased vascular CCL8 expression as there was an accumulation of CCL8+/CD206+ cells in hypertensive aortae. Our hypothesis that CCL18 may promote vascular fibrosis was further strengthened by our findings that exogenous CCL18 increased collagen expression in both cardiac and aortic adventitial fibroblasts and that its cognate receptor, CCR8 was expressed on endothelial cells and throughout the vessel wall.

As discussed with regards to atherosclerosis, CCL18 expression has emerged as a candidate biomarker for major cardiovascular events (21, 24, 26, 62). Aortic pulse wave velocity, a measure of aortic fibrosis, can predict the development of hypertension and cardiovascular morbidity and mortality (66, 84). Given the potential role of CCL18 in these processes, we propose that it may represent a pre-hypertensive marker and future studies in hypertensive patients is of great interest. Preclinical studies in animal models of hypertension are also imperative to fully interrogate the role of CCL18 and CCR8 in this disease state. As such, we plan to investigate whether monoclonal antibodies against CCL18 and pharmacological blockade or genetic deficiency of its receptor, CCR8, could prevents and/or reverses the development of hypertension and aortic stiffening in mice. If this proves effective, we would propose the use of CCL18 monoclonal antibodies or CCR8 antagonists as an adjunct therapy with currently used anti-hypertensives such as ACE inhibitors or AT_1R blockers, to directly target fibrosis in addition to lowering blood pressure.

It should be acknowledged that our results with regard to the roles of both hydrogen peroxide and CCL18 in fibrosis and hypertension are only preliminary and remain to be fully characterised *in vivo*. There are likely additional effector molecules secreted by M2 macrophages that could further contribute to these responses. IGF-1 for example, is secreted by M2 macrophages (5) and directly stimulates collagen production from vascular smooth muscle cells and fibroblasts (7, 42), but was not investigated in our studies. Furthermore, to date we have only investigated the effects of CCL18 or hydrogen peroxide on fibroblasts, yet they may also modulate other vascular cells which could contribute to collagen deposition in the vessel wall such as endothelial cells and VSMCs. Of particular interest, CCL18 stimulation of endothelial cells promotes endothelial-mesenchymal transition (EndMT) (73) but this has not yet been investigated in the context of hypertension. Interestingly, Wu *et al*. recently

suggested that, rather than resident fibroblasts, collagen-producing leukocytes known as 'fibrocytes' are the predominant source of collagen in the aortic wall during hypertension (115). Thus there is potential for CCL18 to additionally target fibrocytes to enhance their infiltration into the vessel wall and/or generation of collagen. Furthermore fibrocytes themselves may be a source of CCL18. These concepts would be interesting to investigate in future studies in order to identify the key vascular targets of M2 macrophage-derived CCL18 and their role in mediate aortic stiffening.

7.4 Limitations and future directions

Whilst we have provided new insights into M1 and M2 polarisation, a number of limitations to our research, and within the field, need to be considered. In terms of markers of macrophage polarisation, there are two major limitations which make translation between studies difficult and may account for conflicting findings between research groups. The first is inconsistencies between markers identified using different cell lines, treatment protocols and species. In our studies, some differences were evident in the profiles of macrophages derived from the immortalised THP-1 line as compared to primary macrophages derived from donor blood monocytes, highlighting the importance of confirming findings in primary cell lines. Furthermore the monocyte-macrophage differentiation stimulus (49) and the nature of the macrophage polarisation stimuli (106) can also alter expression profiles and thus it is important for investigators to clearly specify *in vitro* conditions. The second major limitation to *in vitro* identification of M1 and M2 macrophage markers is its application and relevance to *in vivo* disease settings. The challenges in translation are mostly related to the more complex environment where a combination of stimuli can act together *in vivo*, potentially producing mixed macrophage phenotypes (104). This highlights the need to validate findings *in vivo.* Towards this goal, we were able to confirm IFIT1 expression in macrophages within

atherosclerotic lesions in ApoE$^{-/-}$ mice and identified mCCL8-expressing M2 macrophages in aortae from hypertensive mice, however our findings for ROS generation require confirmation *in vivo*.

The study of macrophage-derived ROS *in vivo* is currently hampered by the limited availability of selective NOX inhibitors. Additionally, given the recognised roles for NOX enzymes in the function of multiple cell types both in disease and homeostasis (6, 85), including effective immune function (40), inhibition of these enzymes could have widespread and unwanted effects. To this end, therapies to inhibit NOX would need to be specifically targeted to macrophages within diseased tissue, such as the atherosclerotic plaque itself or the vessel wall. Theoretically, there is potential in targeting the downstream macrophage derived-ROS implicated in disease, such as peroxynitrite (from M1 macrophages) and hydrogen peroxide (from M2 macrophages). Furthermore, mitochondrial production of ROS may also play a role in the contribution of each macrophage phenotype to cardiovascular disease, particularly given the differences in the metabolic profiles associated with these polarisation states. Future studies could assess mitochondrial function and mitochondrial ROS production following M1 and M2 polarisation and may reveal mitochondrial ROS as an additional disease target. However, the utility of limiting ROS remains to be proven, given the failure of antioxidant therapies to protect against cardiovascular disease in multiple clinical trials (89).

Whilst we were interested in reports of differing roles of the M2 macrophage stimuli, IL-4 and IL-13 in pre-clinical models of atherosclerosis, our consideration of the literature highlighted that there has been limited investigation, and mixed evidence, of the expression of these cytokines in patients with cardiovascular disease. In fact circulating and local plaque levels of these cytokines appear to be mostly low with expression increased in some studies of CAD

(51, 83, 96), but reduced in others (11, 76, 95). This raises questions as to whether these cytokines truly do play important roles in human atherosclerosis and furthermore whether they are indeed the major stimuli for M2 macrophages within plaques.

Perhaps most interesting were our findings for CCL18, particularly compelling due to much association of its expression with human cardiovascular disease and mortality. However, until recently, its receptor had not been identified. Thus although CCL18 has now been shown to activate CCR8 (48), the role of this receptor in the pro-fibrotic actions of CCL18 has not been confirmed. While a small molecule CCR8 inhibitor, R243, is commercially available it lacks selectivity, also inhibiting CCR2 (92). Given the protective effects of CCR2 inhibition demonstrated in mouse models of hypertension (14, 46), this dual-action of R243 could provide additional benefit, yet at the same time conferring difficulty when trying to identify CCR8-specific mechanisms. Importantly, more selective CCR8 inhibitors are currently being developed (i.e AstraZeneca, AZ084) (20) and future testing of these in pre-clinical models of hypertension will be insightful. It should also be noted that CCL18 can serve as an antagonist at CCR3 (63), which may limit its inflammatory and fibrotic effects where both receptors are present. Furthermore, whilst we, and others (9), examined CCL8 in mice (mCCL8), as the functional analogue of CCL18 (hCCL18), it should be noted that CCL18 does not have a true equivalent in the rodent genome. Thus whilst mCCL8 may act on the same receptor and elicit similar responses (47, 48), subtle differences between the actions of mCCL8 and hCCL18 could be revealed. As such, caution should be taken in translating findings with regard to hCCL18/mCCL8 between the two species. Nonetheless, future studies negating the CCL18-CCR8 axis will be valuable in elucidating the therapeutic utility of targeting this pathway in the treatment of human cardiovascular disease.

7.5 Conclusions and therapeutic implications

This thesis has contributed to the growing characterisation of M1 and M2 macrophages in cardiovascular diseases. Importantly, we have identified that M2 macrophages, or at least the M2a subset, are implicated in hypertension and have characteristics that could also contribute to atherosclerosis. Thus it appears that M2 macrophages may not be as protective as earlier studies have suggested. We demonstrate that M2 macrophage polarisation is associated with robust increases in the generation of ROS and the chemokine CCL18, which could serve as important effector molecules in the detrimental actions of these M2 macrophages. We propose that rather than seeking therapeutics which may skew macrophage polarisation towards an M2 phenotype, targeting effector molecules released by pathogenic macrophage subsets would be more effective. Although there are potential complications associated with NOX inhibition, targeting CCL18, and/or its receptor, may prove effective in the treatment of hypertension and in the prevention of major cardiovascular events. Specifically, with a potential ability to limit vascular fibrosis, CCL18/CCR8 inhibitors may represent an adjunct therapy to standard antihypertensive treatments, leading to a reduction in blood pressure and targeting of the underlying disease mechanisms, such as aortic stiffening. Overall, the findings of this thesis advance our understanding of the biological function of M1 and M2 macrophages and demonstrate the potential roles or their effector molecules as both therapeutic targets and biomarkers of cardiovascular disease.

References

1. Anrather J, Racchumi G, and Iadecola C. NF-kappa B regulates phagocytic NADPH oxidase by inducing the expression of gp91(phox). *Journal of Biological Chemistry* 281: 5657-5667, 2006.

2. Ardanaz N, and Pagano PJ. Hydrogen peroxide as a paracrine vascular mediator: regulation and signaling leading to dysfunction. *Experimental biology and medicine (Maywood, NJ)* 231: 237-251, 2006.

3. Armstrong BG, Mangtani P, Fletcher A, Kovats S, McMichael A, Pattenden S, and Wilkinson P. Effect of influenza vaccination on excess deaths occurring during periods of high circulation of influenza: cohort study in elderly people. *BMJ (Clinical research ed)* 329: 660, 2004.

4. Atamas SP, Luzina IG, Choi J, Tsymbalyuk N, Carbonetti NH, Singh IS, Trojanowska M, Jimenez SA, and White B. Pulmonary and activation-regulated chemokine stimulates collagen production in lung fibroblasts. *Am J Respir Cell Mol Biol* 29: 743-749, 2003.

5. Barrett JP, Minogue AM, Falvey A, and Lynch MA. Involvement of IGF-1 and Akt in M1/M2 activation state in bone marrow-derived macrophages. *Exp Cell Res* 335: 258-268, 2015.

6. Bedard K, and Krause K-H. The NOX family of ROS-generating NADPH oxidases: Physiology and pathophysiology. *Physiological Reviews* 87: 245-313, 2007.

7. Blackstock CD, Higashi Y, Sukhanov S, Shai SY, Stefanovic B, Tabony AM, Yoshida T, and Delafontaine P. Insulin-like growth factor-1 increases synthesis of collagen type I via induction

of the mRNA-binding protein LARP6 expression and binding to the 5' stem-loop of COL1a1 and COL1a2 mRNA. *J Biol Chem* 289: 7264-7274, 2014.

8. Brezniceanu ML, Liu F, Wei CC, Chenier I, Godin N, Zhang SL, Filep JG, Ingelfinger JR, and Chan JS. Attenuation of interstitial fibrosis and tubular apoptosis in db/db transgenic mice overexpressing catalase in renal proximal tubular cells. *Diabetes* 57: 451-459, 2008.

9. Brix SR, Stege G, Disteldorf E, Hoxha E, Krebs C, Krohn S, Otto B, Klatschke K, Herden E, Heymann F, Lira SA, Tacke F, Wolf G, Busch M, Jabs WJ, Ozcan F, Keller F, Beige J, Wagner K, Helmchen U, Noriega M, Wiech T, Panzer U, and Stahl RA. CC Chemokine Ligand 18 in ANCA-Associated Crescentic GN. *Journal of the American Society of Nephrology : JASN* 26: 2105-2117, 2015.

10. Brunner SM, Schiechl G, Kesselring R, Martin M, Balam S, Schlitt HJ, Geissler EK, and Fichtner-Feigl S. IL-13 signaling via IL-13Ralpha2 triggers TGF-beta1-dependent allograft fibrosis. *Transplantation research* 2: 16, 2013.

11. Buhlin K, Hultin M, Norderyd O, Persson L, Pockley AG, Rabe P, Klinge B, and Gustafsson A. Risk factors for atherosclerosis in cases with severe periodontitis. *Journal of clinical periodontology* 36: 541-549, 2009.

12. Campbell LA, and Rosenfeld ME. Infection and Atherosclerosis Development. *Archives of medical research* 46: 339-350, 2015.

13. Cardilo-Reis L, Gruber S, Schreier SM, Drechsler M, Papac-Milicevic N, Weber C, Wagner O, Stangl H, Soehnlein O, and Binder CJ. Interleukin-13 protects from atherosclerosis and modulates plaque composition by skewing the macrophage phenotype. *EMBO molecular medicine* 4: 1072-1086, 2012.

14. Chan CT, Moore JP, Budzyn K, Guida E, Diep H, Vinh A, Jones ES, Widdop RE, Armitage JA, Sakkal S, Ricardo SD, Sobey CG, and Drummond GR. Reversal of vascular macrophage accumulation and hypertension by a CCR2 antagonist in deoxycorticosterone/salt-treated mice. *Hypertension* 60: 1207-1212, 2012.

15. Chen R, Xiong S, Yang Y, Fu W, Wang Y, and Ge J. The relationship between human cytomegalovirus infection and atherosclerosis development. *Molecular and cellular biochemistry* 249: 91-96, 2003.

16. Chinetti-Gbaguidi G, Baron M, Bouhlel MA, Vanhoutte J, Copin C, Sebti Y, Derudas B, Mayi T, Bories G, Tailleux A, Haulon S, Zawadzki C, Jude B, and Staels B. Human Atherosclerotic Plaque Alternative Macrophages Display Low Cholesterol Handling but High Phagocytosis Because of Distinct Activities of the PPAR gamma and LXR alpha Pathways. *Circulation Research* 108: 985-995, 2011.

17. Ciszewski A, Bilinska ZT, Brydak LB, Kepka C, Kruk M, Romanowska M, Ksiezycka E, Przyluski J, Piotrowski W, Maczynska R, and Ruzyllo W. Influenza vaccination in secondary prevention from coronary ischaemic events in coronary artery disease: FLUCAD study. *Eur Heart J* 29: 1350-1358, 2008.

18. Coffman RL, Ohara J, Bond MW, Carty J, Zlotnik A, and Paul WE. B cell stimulatory factor-1 enhances the IgE response of lipopolysaccharide-activated B cells. *J Immunol* 136: 4538-4541, 1986.

19. Colin S, Chinetti-Gbaguidi G, and Staels B. Macrophage phenotypes in atherosclerosis. *Immunological reviews* 262: 153-166, 2014.

20. Connolly S, Skrinjar M, and Rosendahl A. Orally bioavailable allosteric CCR8 antagonists inhibit dendritic cell, T cell and eosinophil migration. *Biochemical pharmacology* 83: 778-787, 2012.

21. Courtois A, Nusgens BV, Hustinx R, Namur G, Gomez P, Kuivaniemi H, Defraigne JO, Colige AC, and Sakalihasan N. Gene expression study in positron emission tomography-positive abdominal aortic aneurysms identifies CCL18 as a potential biomarker for rupture risk. *Molecular medicine (Cambridge, Mass)* 20: 697-706, 2014.

22. Darnell JE, Kerr IM, and Stark GR. JAK-STAT PATHWAYS AND TRANSCRIPTIONAL ACTIVATION IN RESPONSE TO IFNS AND OTHER EXTRACELLULAR SIGNALING PROTEINS. *Science* 264: 1415-1421, 1994.

23. de Gaetano M, Crean D, Barry M, and Belton O. M1- and M2-Type Macrophage Responses Are Predictive of Adverse Outcomes in Human Atherosclerosis. *Frontiers in immunology* 7: 275, 2016.

24. de Jager SC, Bongaerts BW, Weber M, Kraaijeveld AO, Rousch M, Dimmeler S, van Dieijen-Visser MP, Cleutjens KB, Nelemans PJ, van Berkel TJ, and Biessen EA. Chemokines CCL3/MIP1alpha, CCL5/RANTES and CCL18/PARC are independent risk predictors of short-term mortality in patients with acute coronary syndromes. *PLoS One* 7: e45804, 2012.

25. De Paoli F, Eeckhoute J, Copin C, Vanhoutte J, Duhem C, Derudas B, Dubois-Chevalier J, Colin S, Zawadzki C, Jude B, Haulon S, Lefebvre P, Staels B, and Chinetti-Gbaguidi G. The neuron-derived orphan receptor 1 (NOR1) is induced upon human alternative macrophage polarization and stimulates the expression of markers of the M2 phenotype. *Atherosclerosis* 241: 18-26, 2015.

26. De Sutter J, Struyf S, Van de Veire NR, Philippe J, De Buyzere M, and Van Damme J. Cardiovascular determinants and prognostic significance of CC Chemokine Ligand-18 (CCL18/PARC) in patients with stable coronary artery disease. *Journal of molecular and cellular cardiology* 49: 894-896, 2010.

27. Der SD, Zhou A, Williams BR, and Silverman RH. Identification of genes differentially regulated by interferon alpha, beta, or gamma using oligonucleotide arrays. *Proc Natl Acad Sci U S A* 95: 15623-15628, 1998.

28. Di Marco E, Gray SP, Kennedy K, Szyndralewiez C, Lyle AN, Lassegue B, Griendling KK, Cooper ME, Schmidt H, and Jandeleit-Dahm KAM. NOX4-derived reactive oxygen species limit fibrosis and inhibit proliferation of vascular smooth muscle cells in diabetic atherosclerosis. *Free radical biology & medicine* 97: 556-567, 2016.

29. Fallon PG, Richardson EJ, McKenzie GJ, and McKenzie AN. Schistosome infection of transgenic mice defines distinct and contrasting pathogenic roles for IL-4 and IL-13: IL-13 is a profibrotic agent. *J Immunol* 164: 2585-2591, 2000.

30. Fensterl V, and Sen GC. Interferon-induced Ifit proteins: their role in viral pathogenesis. *Journal of virology* 89: 2462-2468, 2015.

31. Fichtner-Feigl S, Strober W, Kawakami K, Puri RK, and Kitani A. IL-13 signaling through the IL-13alpha2 receptor is involved in induction of TGF-beta1 production and fibrosis. *Nat Med* 12: 99-106, 2006.

32. Fu X, Beer DG, Behar J, Wands J, Lambeth D, and Cao W. cAMP-response element-binding protein mediates acid-induced NADPH oxidase NOX5-S expression in Barrett esophageal adenocarcinoma cells. *Journal of Biological Chemistry* 281: 20368-20382, 2006.

33. Gong M, Zhuo X, and Ma A. STAT6 Upregulation Promotes M2 Macrophage Polarization to Suppress Atherosclerosis. *Medical science monitor basic research* 23: 240-249, 2017.

34. Grattan MT, Moreno-Cabral CE, Starnes VA, Oyer PE, Stinson EB, and Shumway NE. Cytomegalovirus infection is associated with cardiac allograft rejection and atherosclerosis. *Jama* 261: 3561-3566, 1989.

35. Grunig G, Warnock M, Wakil AE, Venkayya R, Brombacher F, Rennick DM, Sheppard D, Mohrs M, Donaldson DD, Locksley RM, and Corry DB. Requirement for IL-13 independently of IL-4 in experimental asthma. *Science* 282: 2261-2263, 1998.

36. Guo JL, Yu Y, Jia YY, Ma YZ, Zhang BY, Liu PQ, Chen SR, and Jiang JM. Transient receptor potential melastatin 7 (TRPM7) contributes to H2O2-induced cardiac fibrosis via mediating Ca(2+) influx and extracellular signal-regulated kinase 1/2 (ERK1/2) activation in cardiac fibroblasts. *Journal of pharmacological sciences* 125: 184-192, 2014.

37. Gurevich VS, Pleskov VM, Levaia MV, Bannikov AI, Mitrofanova LB, and Urazgil'deeva SA. [Influenza virus infection in progressing atherosclerosis]. *Kardiologiia* 42: 21-24, 2002.

38. Hagg DA, Olson FJ, Kjelldahl J, Jernas M, Thelle DS, Carlsson LM, Fagerberg B, and Svensson PA. Expression of chemokine (C-C motif) ligand 18 in human macrophages and atherosclerotic plaques. *Atherosclerosis* 204: e15-20, 2009.

39. He CH, Lee CG, Dela Cruz CS, Lee CM, Zhou Y, Ahangari F, Ma B, Herzog EL, Rosenberg SA, Li Y, Nour AM, Parikh CR, Schmidt I, Modis Y, Cantley L, and Elias JA. Chitinase 3-like 1 regulates cellular and tissue responses via IL-13 receptor alpha2. *Cell reports* 4: 830-841, 2013.

40. Heyworth PG, Cross AR, and Curnutte JT. Chronic granulomatous disease. *Curr Opin Immunol* 15: 578-584, 2003.

41. Hirata Y, Tabata M, Kurobe H, Motoki T, Akaike M, Nishio C, Higashida M, Mikasa H, Nakaya Y, Takanashi S, Igarashi T, Kitagawa T, and Sata M. Coronary Atherosclerosis Is Associated With Macrophage Polarization in Epicardial Adipose Tissue. *Journal of the American College of Cardiology* 58: 248-255, 2011.

42. Horio T, Maki T, Kishimoto I, Tokudome T, Okumura H, Yoshihara F, Suga S, Takeo S, Kawano Y, and Kangawa K. Production and autocrine/paracrine effects of endogenous insulin-like growth factor-1 in rat cardiac fibroblasts. *Regulatory peptides* 124: 65-72, 2005.

43. Hsue PY, Hunt PW, Schnell A, Kalapus SC, Hoh R, Ganz P, Martin JN, and Deeks SG. Role of viral replication, antiretroviral therapy, and immunodeficiency in HIV-associated atherosclerosis. *AIDS (London, England)* 23: 1059-1067, 2009.

44. Ijas P, Nuotio K, Saksi J, Soinne L, Saimanen E, Karjalainen-Lindsberg ML, Salonen O, Sarna S, Tuimala J, Kovanen PT, Kaste M, and Lindsberg PJ. Microarray analysis reveals overexpression of CD163 and HO-1 in symptomatic carotid plaques. *Arterioscler Thromb Vasc Biol* 27: 154-160, 2007.

45. Isa SA, Ruffino JS, Ahluwalia M, Thomas AW, Morris K, and Webb R. M2 macrophages exhibit higher sensitivity to oxLDL-induced lipotoxicity than other monocyte/macrophage subtypes. *Lipids in Health and Disease* 10: 2011.

46. Ishibashi M, Hiasa K, Zhao Q, Inoue S, Ohtani K, Kitamoto S, Tsuchihashi M, Sugaya T, Charo IF, Kura S, Tsuzuki T, Ishibashi T, Takeshita A, and Egashira K. Critical role of monocyte

chemoattractant protein-1 receptor CCR2 on monocytes in hypertension-induced vascular inflammation and remodeling. *Circ Res* 94: 1203-1210, 2004.

47. Islam SA, Chang DS, Colvin RA, Byrne MH, McCully ML, Moser B, Lira SA, Charo IF, and Luster AD. Mouse CCL8, a CCR8 agonist, promotes atopic dermatitis by recruiting IL-5+ T(H)2 cells. *Nat Immunol* 12: 167-177, 2011.

48. Islam SA, Ling MF, Leung J, Shreffler WG, and Luster AD. Identification of human CCR8 as a CCL18 receptor. *J Exp Med* 210: 1889-1898, 2013.

49. Jaguin M, Houlbert N, Fardel O, and Lecureur V. Polarization profiles of human M-CSF-generated macrophages and comparison of M1-markers in classically activated macrophages from GM-CSF and M-CSF origin. *Cell Immunol* 281: 51-61, 2013.

50. Jang YS, Kim HA, Park SR, Lee MR, Park JB, and Kim PH. IL-4 stimulates mouse macrophages to express APRIL through p38MAPK and two different downstream molecules, CREB and Stat6. *Cytokine* 47: 43-47, 2009.

51. Jha HC, Divya A, Prasad J, and Mittal A. Plasma circulatory markers in male and female patients with coronary artery disease. *Heart & lung : the journal of critical care* 39: 296-303, 2010.

52. Judkins CP, Diep H, Broughton BRS, Mast AE, Hooker EU, Miller AA, Selemidis S, Dusting GJ, Sobey CG, and Drummond GR. Direct evidence of a role for Nox2 in superoxide production, reduced nitric oxide bioavailability, and early atherosclerotic plaque formation in ApoE(-/-) mice. *American Journal of Physiology-Heart and Circulatory Physiology* 298: H24-H32, 2010.

53. Junttila IS, Mizukami K, Dickensheets H, Meier-Schellersheim M, Yamane H, Donnelly RP, and Paul WE. Tuning sensitivity to IL-4 and IL-13: differential expression of IL-4Ralpha, IL-13Ralpha1, and gammac regulates relative cytokine sensitivity. *J Exp Med* 205: 2595-2608, 2008.

54. Kang H, Zhang J, Wang B, Liu M, Zhao J, Yang M, and Li Y. Puerarin inhibits M2 polarization and metastasis of tumor-associated macrophages from NSCLC xenograft model via inactivating MEK/ERK 1/2 pathway. *Int J Oncol* 50: 545-554, 2017.

55. Khallou-Laschet J, Varthaman A, Fornasa G, Compain C, Gaston A-T, Clement M, Dussiot M, Levillain O, Graff-Dubois S, Nicoletti A, and Caligiuri G. Macrophage plasticity in experimental atherosclerosis. *PLoS ONE [Electronic Resource]* 5: e8852, 2010.

56. Khatri JJ, Johnson C, Magid R, Lessner SM, Laude KM, Dikalov SI, Harrison DG, Sung HJ, Rong Y, and Galis ZS. Vascular oxidant stress enhances progression and angiogenesis of experimental atheroma. *Circulation* 109: 520-525, 2004.

57. King IL, and Mohrs M. IL-4-producing CD4+ T cells in reactive lymph nodes during helminth infection are T follicular helper cells. *J Exp Med* 206: 1001-1007, 2009.

58. King VL, Szilvassy SJ, and Daugherty A. Interleukin-4 deficiency decreases atherosclerotic lesion formation in a site-specific manner in female LDL receptor-/- mice. *Arterioscler Thromb Vasc Biol* 22: 456-461, 2002.

59. Kossmann S, Hu H, Steven S, Schonfelder T, Fraccarollo D, Mikhed Y, Brahler M, Knorr M, Brandt M, Karbach SH, Becker C, Oelze M, Bauersachs J, Widder J, Munzel T, Daiber A, and Wenzel P. Inflammatory monocytes determine endothelial nitric-oxide synthase uncoupling and nitro-oxidative stress induced by angiotensin II. *J Biol Chem* 289: 27540-27550, 2014.

60. Kotronias D, and Kapranos N. Herpes simplex virus as a determinant risk factor for coronary artery atherosclerosis and myocardial infarction. *In vivo (Athens, Greece)* 19: 351-357, 2005.

61. Kraaij MD, Koekkoek KM, van der Kooij SW, Gelderman KA, and van Kooten C. Subsets of human type 2 macrophages show differential capacity to produce reactive oxygen species. *Cell Immunol* 284: 1-8, 2013.

62. Kraaijeveld AO, de Jager SC, de Jager WJ, Prakken BJ, McColl SR, Haspels I, Putter H, van Berkel TJ, Nagelkerken L, Jukema JW, and Biessen EA. CC chemokine ligand-5 (CCL5/RANTES) and CC chemokine ligand-18 (CCL18/PARC) are specific markers of refractory unstable angina pectoris and are transiently raised during severe ischemic symptoms. *Circulation* 116: 1931-1941, 2007.

63. Krohn SC, Bonvin P, and Proudfoot AE. CCL18 exhibits a regulatory role through inhibition of receptor and glycosaminoglycan binding. *PLoS One* 8: e72321, 2013.

64. Kumatori A, Yang D, Suzuki S, and Nakamura M. Cooperation of STAT-1 and IRF-1 in interferon-gamma-induced transcription of the gp91(phox) gene. *J Biol Chem* 277: 9103-9111, 2002.

65. Langbein H, Brunssen C, Hofmann A, Cimalla P, Brux M, Bornstein SR, Deussen A, Koch E, and Morawietz H. NADPH oxidase 4 protects against development of endothelial dysfunction and atherosclerosis in LDL receptor deficient mice. *Eur Heart J* 37: 1753-1761, 2016.

66. Laurent S, Boutouyrie P, Asmar R, Gautier I, Laloux B, Guize L, Ducimetiere P, and Benetos A. Aortic Stiffness Is an Independent Predictor of All-Cause and Cardiovascular Mortality in Hypertensive Patients. *Hypertension* 37: 1236-1241, 2001.

67. Lee CF, Qiao M, Schroder K, Zhao Q, and Asmis R. Nox4 is a novel inducible source of reactive oxygen species in monocytes and macrophages and mediates oxidized low density lipoprotein-induced macrophage death. *Circ Res* 106: 1489-1497, 2010.

68. Lee CG, Homer RJ, Zhu Z, Lanone S, Wang X, Koteliansky V, Shipley JM, Gotwals P, Noble P, Chen Q, Senior RM, and Elias JA. Interleukin-13 induces tissue fibrosis by selectively stimulating and activating transforming growth factor beta(1). *J Exp Med* 194: 809-821, 2001.

69. Lee YW, Kim PH, Lee WH, and Hirani AA. Interleukin-4, Oxidative Stress, Vascular Inflammation and Atherosclerosis. *Biomolecules & therapeutics* 18: 135-144, 2010.

70. Lee YW, Kuhn H, Hennig B, Neish AS, and Toborek M. IL-4-induced oxidative stress upregulates VCAM-1 gene expression in human endothelial cells. *Journal of molecular and cellular cardiology* 33: 83-94, 2001.

71. Lee YW, Kuhn H, Hennig B, and Toborek M. IL-4 induces apoptosis of endothelial cells through the caspase-3-dependent pathway. *FEBS letters* 485: 122-126, 2000.

72. Lee YW, Lee WH, and Kim PH. Role of NADPH oxidase in interleukin-4-induced monocyte chemoattractant protein-1 expression in vascular endothelium. *Inflammation research : official journal of the European Histamine Research Society [et al]* 59: 755-765, 2010.

73. Lin L, Chen YS, Yao YD, Chen JQ, Chen JN, Huang SY, Zeng YJ, Yao HR, Zeng SH, Fu YS, and Song EW. CCL18 from tumor-associated macrophages promotes angiogenesis in breast cancer. *Oncotarget* 6: 34758-34773, 2015.

74. Loomba RS, Aggarwal S, Shah PH, and Arora RR. Influenza vaccination and cardiovascular morbidity and mortality: analysis of 292,383 patients. *Journal of cardiovascular pharmacology and therapeutics* 17: 277-283, 2012.

75. Lupardus PJ, Birnbaum ME, and Garcia KC. Molecular basis for shared cytokine recognition revealed in the structure of an unusually high affinity complex between IL-13 and IL-13Ralpha2. *Structure (London, England : 1993)* 18: 332-342, 2010.

76. Madhumitha H, Mohan V, Deepa M, Babu S, and Aravindhan V. Increased Th1 and suppressed Th2 serum cytokine levels in subjects with diabetic coronary artery disease. *Cardiovascular diabetology* 13: 1, 2014.

77. Manea A, Tanase LI, Raicu M, and Simionescu M. Jak/STAT signaling pathway regulates nox1 and nox4-based NADPH oxidase in human aortic smooth muscle cells. *Arterioscler Thromb Vasc Biol* 30: 105-112, 2010.

78. Mantovani A, Sica A, Sozzani S, Allavena P, Vecchi A, and Locati M. The chemokine system in diverse forms of macrophage activation and polarization. *Trends in immunology* 25: 677-686, 2004.

79. Martinez FO, Gordon S, Locati M, and Mantovani A. Transcriptional profiling of the human monocyte-to-macrophage differentiation and polarization: New molecules and patterns of gene expression. *Journal of Immunology* 177: 7303-7311, 2006.

80. Martinez FO, Helming L, Milde R, Varin A, Melgert BN, Draijer C, Thomas B, Fabbri M, Crawshaw A, Ho LP, Ten Hacken NH, Cobos Jimenez V, Kootstra NA, Hamann J, Greaves DR, Locati M, Mantovani A, and Gordon S. Genetic programs expressed in resting and IL-4 alternatively activated mouse and human macrophages: similarities and differences. *Blood* 121: e57-69, 2013.

81. McCormick SM, and Heller NM. Commentary: IL-4 and IL-13 receptors and signaling. *Cytokine* 75: 38-50, 2015.

82. Medbury HJ, James V, Ngo J, Hitos K, Wang Y, Harris DC, and Fletcher JP. Differing association of macrophage subsets with atherosclerotic plaque stability. *International angiology : a journal of the International Union of Angiology* 32: 74-84, 2013.

83. Mirhafez SR, Zarifian A, Ebrahimi M, Ali RF, Avan A, Tajfard M, Mohebati M, Eslami S, Rahsepar AA, Rahimi HR, Mehrad-Majd H, Ferns GA, and Ghayour-Mobarhan M. Relationship between serum cytokine and growth factor concentrations and coronary artery disease. *Clinical biochemistry* 48: 575-580, 2015.

84. Mitchell GF, Hwang SJ, Vasan RS, Larson MG, Pencina MJ, Hamburg NM, Vita JA, Levy D, and Benjamin EJ. Arterial stiffness and cardiovascular events: the Framingham Heart Study. *Circulation* 121: 505-511, 2010.

85. Mittal M, Siddiqui MR, Tran K, Reddy SP, and Malik AB. Reactive oxygen species in inflammation and tissue injury. *Antioxidants & redox signaling* 20: 1126-1167, 2014.

86. Moon JS, Nakahira K, Chung KP, DeNicola GM, Koo MJ, Pabon MA, Rooney KT, Yoon JH, Ryter SW, Stout-Delgado H, and Choi AM. NOX4-dependent fatty acid oxidation promotes NLRP3 inflammasome activation in macrophages. *Nat Med* 22: 1002-1012, 2016.

87. Moore JP, Vinh A, Tuck KL, Sakkal S, Krishnan SM, Chan CT, Lieu M, Samuel CS, Diep H, Kemp-Harper BK, Tare M, Ricardo SD, Guzik TJ, Sobey CG, and Drummond GR. M2 macrophage accumulation in the aortic wall during angiotensin II infusion in mice is associated with fibrosis, elastin loss, and elevated blood pressure. *American journal of physiology Heart and circulatory physiology* 309: H906-917, 2015.

88. Murray PJ, Allen JE, Biswas SK, Fisher EA, Gilroy DW, Goerdt S, Gordon S, Hamilton JA, Ivashkiv LB, Lawrence T, Locati M, Mantovani A, Martinez FO, Mege JL, Mosser DM, Natoli G, Saeij JP, Schultze JL, Shirey KA, Sica A, Suttles J, Udalova I, van Ginderachter JA, Vogel SN, and Wynn TA. Macrophage activation and polarization: nomenclature and experimental guidelines. *Immunity* 41: 14-20, 2014.

89. Myung SK, Ju W, Cho B, Oh SW, Park SM, Koo BK, and Park BJ. Efficacy of vitamin and antioxidant supplements in prevention of cardiovascular disease: systematic review and meta-analysis of randomised controlled trials. *BMJ (Clinical research ed)* 346: f10, 2013.

90. Oh J, Riek AE, Weng S, Petty M, Kim D, Colonna M, Cella M, and Bernal-Mizrachi C. Endoplasmic reticulum stress controls M2 macrophage differentiation and foam cell formation. *J Biol Chem* 287: 11629-11641, 2012.

91. Olavarria VH, Figueroa JE, and Mulero V. Induction of genes encoding NADPH oxidase components and activation of IFN regulatory factor-1 by prolactin in fish macrophages. *Innate immunity* 19: 644-654, 2013.

92. Oshio T, Kawashima R, Kawamura YI, Hagiwara T, Mizutani N, Okada T, Otsubo T, Inagaki-Ohara K, Matsukawa A, Haga T, Kakuta S, Iwakura Y, Hosokawa S, and Dohi T.

Chemokine receptor CCR8 is required for lipopolysaccharide-triggered cytokine production in mouse peritoneal macrophages. *PLoS One* 9: e94445, 2014.

93. Papaspyridonos M, Smith A, Burnand KG, Taylor P, Padayachee S, Suckling KE, James CH, Greaves DR, and Patel L. Novel candidate genes in unstable areas of human atherosclerotic plaques. *Arterioscler Thromb Vasc Biol* 26: 1837-1844, 2006.

94. Prolo C, Alvarez MN, and Radi R. Peroxynitrite, a potent macrophage-derived oxidizing cytotoxin to combat invading pathogens. *BioFactors (Oxford, England)* 40: 215-225, 2014.

95. Raaz-Schrauder D, Klinghammer L, Baum C, Frank T, Lewczuk P, Achenbach S, Cicha I, Stumpf C, Wiltfang J, Kornhuber J, Daniel WG, and Garlichs CD. Association of systemic inflammation markers with the presence and extent of coronary artery calcification. *Cytokine* 57: 251-257, 2012.

96. Raaz-Schrauder D, Schrauder MG, Stumpf C, Lewczuk P, Kilian T, Dietel B, Garlichs CD, Schlundt C, Achenbach S, and Klinghammer L. Plasma levels of sRANKL and OPG are associated with atherogenic cytokines in patients with intermediate cardiovascular risk. *Heart and vessels* 32: 1304-1313, 2017.

97. Reape TJ, Rayner K, Manning CD, Gee AN, Barnette MS, Burnand KG, and Groot PH. Expression and cellular localization of the CC chemokines PARC and ELC in human atherosclerotic plaques. *The American journal of pathology* 154: 365-374, 1999.

98. Rhee SG, Kang SW, Jeong W, Chang TS, Yang KS, and Woo HA. Intracellular messenger function of hydrogen peroxide and its regulation by peroxiredoxins. *Current opinion in cell biology* 17: 183-189, 2005.

99. Sanjabi S, Hoffmann A, Liou HC, Baltimore D, and Smale ST. Selective requirement for c-Rel during IL-12 P40 gene induction in macrophages. *Proc Natl Acad Sci U S A* 97: 12705-12710, 2000.

100. Schenten V, Melchior C, Steinckwich N, Tschirhart EJ, and Brechard S. Sphingosine kinases regulate NOX2 activity via p38 MAPK-dependent translocation of S100A8/A9. *J Leukoc Biol* 89: 587-596, 2011.

101. Schraufstatter IU, Zhao M, Khaldoyanidi SK, and Discipio RG. The chemokine CCL18 causes maturation of cultured monocytes to macrophages in the M2 spectrum. *Immunology* 135: 287-298, 2012.

102. Schurmann C, Rezende F, Kruse C, Yasar Y, Lowe O, Fork C, van de Sluis B, Bremer R, Weissmann N, Shah AM, Jo H, Brandes RP, and Schroder K. The NADPH oxidase Nox4 has anti-atherosclerotic functions. *Eur Heart J* 36: 3447-3456, 2015.

103. Shi Y, Lo CS, Chenier I, Maachi H, Filep JG, Ingelfinger JR, Zhang SL, and Chan JS. Overexpression of catalase prevents hypertension and tubulointerstitial fibrosis and normalization of renal angiotensin-converting enzyme-2 expression in Akita mice. *American journal of physiology Renal physiology* 304: F1335-1346, 2013.

104. Sica A, and Mantovani A. Macrophage plasticity and polarization: in vivo veritas. *J Clin Invest* 122: 787-795, 2012.

105. Stoger JL, Gijbels MJ, van der Velden S, Manca M, van der Loos CM, Biessen EA, Daemen MJ, Lutgens E, and de Winther MP. Distribution of macrophage polarization markers in human atherosclerosis. *Atherosclerosis* 225: 461-468, 2012.

106. Sudan B, Wacker MA, Wilson ME, and Graff JW. A Systematic Approach to Identify Markers of Distinctly Activated Human Macrophages. *Frontiers in immunology* 6: 253, 2015.

107. Thang LV, Demel SL, Crawford R, Kaminski NE, Swain GM, Van Rooijen N, and Galligan JJ. Macrophage depletion lowers blood pressure and restores sympathetic nerve alpha2-adrenergic receptor function in mesenteric arteries of DOCA-salt hypertensive rats. *American journal of physiology Heart and circulatory physiology* 309: H1186-1197, 2015.

108. Udell JA, Zawi R, Bhatt DL, Keshtkar-Jahromi M, Gaughran F, Phrommintikul A, Ciszewski A, Vakili H, Hoffman EB, Farkouh ME, and Cannon CP. Association between influenza vaccination and cardiovascular outcomes in high-risk patients: a meta-analysis. *Jama* 310: 1711-1720, 2013.

109. Versteylen MO, Manca M, Joosen IA, Schmidt DE, Das M, Hofstra L, Crijns HJ, Biessen EA, and Kietselaer BL. CC chemokine ligands in patients presenting with stable chest pain: association with atherosclerosis and future cardiovascular events. *Netherlands heart journal : monthly journal of the Netherlands Society of Cardiology and the Netherlands Heart Foundation* 24: 722-729, 2016.

110. Wang N, Liang H, and Zen K. Molecular mechanisms that influence the macrophage m1-m2 polarization balance. *Frontiers in immunology* 5: 614, 2014.

111. Wang P, Zhou S, Xu L, Lu Y, Yuan X, Zhang H, Li R, Fang J, and Liu P. Hydrogen peroxide-mediated oxidative stress and collagen synthesis in cardiac fibroblasts: blockade by tanshinone IIA. *Journal of ethnopharmacology* 145: 152-161, 2013.

112. Wang X, Liu K, Li B, Li Y, Ye K, Qi J, and Wang Y. Macrophages Aggravate Hypoxia-Induced Cardiac Microvascular Endothelial Cell Injury via Peroxynitrite: Protection by Tongxinluo. *Cell communication & adhesion* 22: 39-47, 2015.

113. Warren-Gash C, Smeeth L, and Hayward AC. Influenza as a trigger for acute myocardial infarction or death from cardiovascular disease: a systematic review. *The Lancet Infectious diseases* 9: 601-610, 2009.

114. Wenzel P, Knorr M, Kossmann S, Stratmann J, Hausding M, Schuhmacher S, Karbach SH, Schwenk M, Yogev N, Schulz E, Oelze M, Grabbe S, Jonuleit H, Becker C, Daiber A, Waisman A, and Munzel T. Lysozyme M-positive monocytes mediate angiotensin II-induced arterial hypertension and vascular dysfunction. *Circulation* 124: 1370-1381, 2011.

115. Wu J, Montaniel KR, Saleh MA, Xiao L, Chen W, Owens GK, Humphrey JD, Majesky MW, Paik DT, Hatzopoulos AK, Madhur MS, and Harrison DG. Origin of Matrix-Producing Cells That Contribute to Aortic Fibrosis in Hypertension. *Hypertension* 67: 461-468, 2016.

116. Wynn TA. IL-13 effector functions. *Annual review of immunology* 21: 425-456, 2003.

117. Yang CS, Shin DM, Lee HM, Son JW, Lee SJ, Akira S, Gougerot-Pocidalo MA, El-Benna J, Ichijo H, and Jo EK. ASK1-p38 MAPK-p47phox activation is essential for inflammatory responses during tuberculosis via TLR2-ROS signalling. *Cellular microbiology* 10: 741-754, 2008.

118. Yang H, Roberts LJ, Shi MJ, Zhou LC, Ballard BR, Richardson A, and Guo ZM. Retardation of atherosclerosis by overexpression of catalase or both Cu/Zn-superoxide dismutase and catalase in mice lacking apolipoprotein E. *Circ Res* 95: 1075-1081, 2004.

119. Yang W, Zhang J, Wang H, Gao P, Singh M, Shen K, and Fang N. Angiotensin II downregulates catalase expression and activity in vascular adventitial fibroblasts through an AT1R/ERK1/2-dependent pathway. *Molecular and cellular biochemistry* 358: 21-29, 2011.

120. Zhang J, Liu YY, Sun HL, Li S, Xiong HR, Yang ZQ, Xiang GD, and Jiang XJ. High Human Cytomegalovirus IgG Level is Associated with Increased Incidence of Diabetic Atherosclerosis in Type 2 Diabetes Mellitus Patients. *Medical science monitor : international medical journal of experimental and clinical research* 21: 4102-4110, 2015.